

A Mechanistic Approach Towards the Discovery of Catalytic Acylation Reactions

Wanying Zhang

A thesis submitted to the Faculty of Graduate and Postdoctoral Studies in partial
fulfillment of the requirements for the degree of

Masters of Science

in Chemistry

**Department of Chemistry and Biomolecular Sciences
University of Ottawa**

© Wanying Zhang, Ottawa, Canada, 2016

A Mechanistic Approach towards the Discovery of Catalytic Acylation Reactions

Wanying Zhang, Masters of Science

Department of Chemistry and Biomolecular Sciences, University of Ottawa, 2016

Abstract

The development of new, efficient methods for the formation of carbon-carbon bonds using transition metal catalysis has broad applications in the field of organic chemistry and is the key to efficient chemical synthesis. Many efforts had been made to develop efficient ways to make these linkages particularly with the aid of metals such as Rh, Pd, Ni, Ru and Cu. Our group is primarily focused on exploring how these transition metals can activate typically inert functional groups, paving way to new synthetic routes to construct more complex molecules.

Chapter 1 describes attempts that were conducted to achieve hydroacylation between an aldehyde and a non-conjugated alkene via a metal hydride intermediate. The use of $\text{RuHCl}(\text{CO})(\text{PPh}_3)_3$ proved to be the most efficient catalyst for this transformation thus far. Mechanistic investigations were conducted to explore different possibilities to enable this transformation. This chapter also identifies a new self-aldol domino reaction, which consists of a self-aldol condensation of an aldehyde, followed by oxidation and decarbonylation giving rise to a ketone product. Finally, the use of a simple and direct method to access deuterated aldehydes using $\text{RuHCl}(\text{CO})(\text{PPh}_3)_3$ as a catalyst and D_2O as a deuterium source is outlined.

Chapter 2 describes a novel Suzuki-Miyaura system that couples esters and boronic esters to form the corresponding ketone product. It was found that an NHC-based Pd catalyst is crucial

in the transformation wherein it activates the C(acyl)-O bond of the ester. It is notable that this transformation takes place with the absence of decarbonylation. Reactivity under water in the presence of surfactants was also discovered. Results in aqueous media were demonstrated to be milder than in organic conditions, while achieving similar yields. This system was also applied to coupling of esters and anilines.

Acknowledgements

Graduate school is a time of exploration and building of confidence. Throughout these two years, I have learned a considerable amount of useful chemistry skills and knowledge, which complements to my personal growth and development, from my fellow colleagues, friends and family and I would like to extend my thanks to all of them.

For being my primary source of guidance during times of convoluted paths presented by obscure chemical reactions, I like to thank my supervisor, Professor Stephen G. Newman for his continuous support and opportunity to work in his dynamic research group. The diversity in people and research in our group presented an enriching and compassionate environment to learn and grow in. He has dedicated a lot of time and energy to his students to achieve great things and share his knowledge in whatever way possible. He had taught me many advanced lab skills that finds its use in many instances.

I've had the privilege for being one of the group's first students along with Kaylie (Xi Ye) Hua, which I also had the pleasure of becoming fast friends with and share similar experiences and challenges throughout this program. Our mutual support made my transition into graduate school an enjoyable experience. I hope that our futures will cross paths again and the bridge of friendship that we have made will remain forever solid.

I have also had the pleasure to work with a few undergraduate students. Jeanne Masson-Makdissi was the first undergraduate I had the pleasure to work with and contributed considerably to my first project on hydroacylation. I hope she will find success in pursuing her graduate studies. I would like to thank Eric Isbrandt for contributing to pursuing the project

involving ruthenium catalyzed deuteration of aldehydes, and Parsa Jamshidi for starting the project. It was also my pleasure to work with undergraduates Claudia Meloche and Sara Omaiche for their continuous enthusiasm and eagerness in learning always brighten the day. I am also grateful for their unwavering friendship and support throughout my graduate studies. I would also like to thank Ph.D student, Taoufik Ben Halima and visiting Masters Student from France, Imane Yalaoui for their discovery and collaboration in the Suzuki-Miyaura coupling of esters project.

I would also like to express my appreciation to all my teachers at every academic level for giving me the intellectual tools and skills necessary to survive and thrive in a dynamic environment. Thank you to my first research supervisor Dr. Chao-Jun Li at McGill University for giving me the opportunity to work in a research lab as an undergraduate honours student, which pique my interest in this field of organometallic and green chemistry. Special thanks to the former post-doc Dr. Feng Zhou in Li's group for being my direct mentor and patiently teaching me a considerable amount of skills and knowledge that are needed in a research lab environment.

Finally, I like to thank my close friends that have been with me throughout the years that have been there for me and shared many adventures throughout the stages of life and helped shape who I am today. I very much also appreciate my good friend Kshitij Agarwal's support who had the patience to look over and edit my thesis. I also thank my parents for their continuous support and encouragement throughout school and life. They have been a solid rock through my life and have given me the tools to have a good education and just about everything else.

Contents

Abstract	ii
Acknowledgements	iv
List of Tables	viii
List of Figures	viii
List of Schemes	ix
Abbreviations	xiv
Introduction	1
Chapter 1: Ruthenium catalyzed couplings of aldehydes and olefins	2
1.1. Transition metal catalysis for intermolecular olefin aldehydes couplings	2
1.2. Rhodium catalyzed hydroacylation	3
1.3. Iridium catalyzed hydroacylation	5
1.4. Palladium catalyzed hydroacylation	6
1.5. Nickel catalyzed coupling of olefins to aldehydes	7
1.6. Ruthenium catalyzed hydroacylation	9
1.7. Research goals	13
2. Results and discussion	15
2.1. Probing reactivity	15
2.2. Isomerization catalysis	19
2.3. Exploring ruthenium catalysts for hydroacylation	24
2.4. Coupling of aldehydes and alkenes via allylic oxidation	28
2.5. Transition-metal catalyzed oxidative decarbonylation of an aldol adduct	31
2.6. Ruthenium catalyzed deuteration of aldehydes	44
2.6.1.1. Optimization of ruthenium catalyzed deuteration of aldehydes	47
2.6.1.2. Scope, proposed mechanism and limitations	50
3. Summary and future work	52
4. Experimental	54
Chapter 2: Palladium catalyzed cross-coupling reactions of esters	63
5. Transition metal catalysis for cross-coupling reactions	63
5.1. Suzuki-Miyaura cross-coupling reaction	65

5.1.1.	Mechanism of reaction	66
5.1.1.1.	Activation of the catalyst	68
5.2.	Suzuki-Miyaura cross-coupling reaction of carboxylate derivatives	68
5.3.	Using surfactants with Suzuki-Miyaura cross-coupling reactions	74
5.4.	Pd catalysis with NHC Ligands	80
5.5.	Research goals	83
6.	Results and discussion	84
6.1.	Starting material preparation	84
6.2.	Reaction optimization	86
6.3.	Scope	95
6.3.1.	Aqueous conditions for Suzuki-Miyaura coupling reaction	98
6.3.2.	Limitations	104
7.	Robustness studies	108
8.	Electronic influence and proposed mechanism	111
9.	Aqueous conditions for cross-coupling of esters for amidation	114
9.1.	Optimization	116
9.2.	Scope and limitations	119
10.	Summary and future work	121
11.	Experimental	123
11.1.	Synthesis of starting materials	127
11.2.	Reaction development	138
11.3.	Study of substrate and boronic acid electronics	139
11.4.	Study of relative rates of degradation	140
11.5.	Synthesis of final products	142
Appendix 1:	^1H and ^{13}C NMR spectra from Chapter 1	157
Appendix 2:	^1H and ^{13}C NMR spectra from Chapter 2	160

List of Tables

Chapter 1

Table 1. Results from screening of various ruthenium catalysts on hydroacylation	27
Table 2. Testing of different oxidative conditions on aldol adduct	40
Table 3. Catalyst and ligand screen for deuteration of aldehydes	48
Table 4. Optimization of deuterium source	49
Table 5. Scope of deuterated aldehydes.....	50
Table 6. Ligand screening for Suzuki-Miyaura coupling of esters.....	89
Table 7. Catalyst and temperature screening for Suzuki-Miyaura coupling of esters	90
Table 8. Solvent screen for Suzuki-Miyaura coupling of esters.....	91
Table 9. Base screen for Suzuki-Miyaura coupling of esters	93
Table 10. Additive screen for Suzuki-Miyaura coupling of esters	94
Table 11. Synthesis of ketones via Suzuki-Miyaura Coupling of esters	97
Table 12. Surfactant screen for Suzuki-Miyaura coupling of esters.....	100
Table 13. Base screen under aqueous conditions for Suzuki-Miyaura coupling of esters	102
Table 14. Boronic acid scope of Suzuki-Miyaura cross-coupling of esters under aqueous conditions.....	103
Table 15. Substrate and boronic acid screen for Suzuki-Miyaura coupling of esters.....	105
Table 16. Catalyst optimization for amidation of esters under aqueous conditions	117
Table 17. Base optimization for amidation of esters under aqueous conditions	118
Table 18. Surfactant optimization for amidation of esters under aqueous conditions.....	119
Table 19. Synthesis of amides under aqueous conditions.....	120
Table 20. Percentage of substrate degradation over time	141

List of Figures

Chapter 1

Figure 1. Structures of screened ruthenium catalysts	25
Figure 2. Structure of RuHCl(CO)(PPh ₃) ₃ versus RuHCl(CO)(PMePh ₂) ₃	28
Figure 3. Structure of Coazaar	65
Figure 4. Classes of surfactants used in aqueous media	76
Figure 5. Lipshutz's 1 st and 2 nd generation designer surfactants used in cross-coupling reactions in aqueous media.....	77
Figure 6. Electron donation of a typical NHC ligand	81
Figure 7. Structures of Pd-NHC catalysts.....	83
Figure 8. Esters that exhibit low reactivity in the Pd-catalyzed cross-coupling of esters	107
Figure 9: Scale of relative rate of degradation.....	109
Figure 10. Comparative rate of 1 st order degradation	110
Figure 11. Number of esters.....	125
Figure 12. Numbering of boronic acids	126
Figure 13. Comparative rate of degradation	141

List of Schemes

Chapter 1

Scheme 1. General scheme for hydroacylation.....	2
Scheme 2. Traditional oxidative addition pathway of hydroacylation	4
Scheme 3. Obora and Ishii's iridium catalyzed hydroacylation of alkynes with alcohols	5
Scheme 4. Development of palladium catalyzed hydroacylation	6

Scheme 5. Tsuda and Saegusa's nickel catalyzed hydroacylation	7
Scheme 6. Jamison's nickel catalyzed hydroacylation using silyl triflate.....	8
Scheme 7. Jamison's mechanistic hypothesis for nickel catalyzed hydroacylation through oxametallacycle intermediate.....	8
Scheme 8. Development of ruthenium catalyzed hydroacylation	10
Scheme 9. Recent developments of hydroacylation of conjugated dienes	10
Scheme 10. Krische's transfer hydrogenation pathway for ruthenium catalyzed hydroacylation	11
Scheme 11. Strategies for metal catalyzed olefin-aldehyde coupling	14
Scheme 12. Ruthenium catalyzed hydroacylation of styrene and benzaldehyde derivatives	15
Scheme 13. Ruthenium catalyzed hydroacylation of benzaldehydes to terminal alkene	16
Scheme 14. Possible hypotheses for observation of formation of linear ketone product	17
Scheme 15. Ruthenium catalyzed hydroacylation of benzaldehyde and non-conjugated diene ..	17
Scheme 16. Ru-allyl intermediate.....	18
Scheme 17. Hydride mechanism for metal hydride formation to facilitate hydrometallation to perform aldehyde to olefin coupling.....	19
Scheme 18. Skyrstrup's condition for coupling of aldehydes to alkenes via Pd-H intermediate	20
Scheme 19. Activation of dimeric Pd(I) species to hydridopalladium(II) complex for hydropalladiation	21
Scheme 20. Mazet's system for isomerization of allylic and alkenyl alcohols	21
Scheme 21. Scheme for isomerization of allylbenzene using nickel catalysis	22
Scheme 22. Hydroacylation of benzaldehyde and styrene using nickel catalysis	23
Scheme 23. Synthesis of 3-phenylhex-5-enal via Barbier's method followed by anionic oxy-cope rearrangement	23

Scheme 24. Intramolecular hydroacylation using nickel catalysis	24
Scheme 25. Intermolecular hydroacylation of alkene and benzaldehydes with different [Ru] catalysts.....	26
Scheme 26. Proposed mechanism for formation ketones via allylic oxidation	29
Scheme 27. Observed product from high-throughput screening	31
Scheme 28. Proposed mechanistic pathways of formation of ketone product	32
Scheme 29. Synthesis of aldol adduct intermediate.....	33
Scheme 30. Probing of intermediate species under different oxidative conditions.....	34
Scheme 31. General scheme for oxidation of alcohols to ketones or aldehydes	35
Scheme 32. Testing traditional oxidative conditions.....	36
Scheme 33. Sheldon's strategy for ruthenium catalyzed oxidation of secondary alcohols mediated by TEMPO	36
Scheme 34. Waymouth's strategy for oxidation of alcohols using palladium catalyst	37
Scheme 35. Sheldon's strategy for copper catalyzed oxidation of alcohols mediated by TEMPO	38
Scheme 36. William's strategy of oxidation of alcohols into amines via hydrogen transfer	38
Scheme 37. Ajjiou's strategy for oxidation of secondary alcohols using iridium catalysts via hydrogen transfer	39
Scheme 38. Effect of water on equilibrium of catalytic oxidation of aldol adduct	42
Scheme 39. Optimized condition of oxidative decarbonylation of an aldol adduct	42
Scheme 40. Competing pathways of π -bond insertion of metal hydride catalysts.....	44
Scheme 41. Conversion of metal-hydride into metal-deuterium.....	44
Scheme 42. General reaction scheme for catalytic deuteration of aldehydes.....	45

Scheme 43. Traditional methods of aldehyde deuteration.....	46
Scheme 44. Development in metal-catalyzed deuteration.....	47
Scheme 45. Effect of ligands on ruthenium catalyzed deuteration of aldehydes.	48
Scheme 46. Proposed mechanism for ruthenium catalyzed deuteration of aldehyde.....	51
Scheme 47. General scheme for cross-coupling reactions.....	63
Scheme 48. General catalytic cycle for transition metal-catalyzed cross-coupling reactions	64
Scheme 49. General scheme for Suzuki-Miyaura cross-coupling reaction	65
Scheme 50. Oxidative addition and reductive elimination	66
Scheme 51. Representative catalytic cycle for Suzuki-Miyaura cross-coupling reaction	67
Scheme 52. Liebeskind's strategy for cross-coupling of thioesters.....	69
Scheme 53. Formation of ketone via acylpalladium-thiolate species mediated by CuTC	69
Scheme 54. Shi's strategy for coupling of boronic acid with phenolic carboxylates	70
Scheme 55. Shi's catalytic cycle for biaryl synthesis	71
Scheme 56. Garg's scheme for cross-coupling of amides	72
Scheme 57. Szostak's strategy for cross-coupling of amides	72
Scheme 58. Itami's scheme for decarbonylative cross-coupling using nickel catalysis.....	73
Scheme 59. Love's proposed mechanism for decarbonylative cross-coupling of esters and boronic acids	74
Scheme 60. Xin's strategy for Suzuki-Miyaura cross-coupling in aqueous media	78
Scheme 61. Xin's strategy for Suzuki-Miyaura cross-coupling in aqueous media with surfactant	78
Scheme 62. Lipshutz' development of Pd-catalyzed cross-coupling reactions in aqueous media with the aid of surfactants	79

Scheme 63. Arguengo's scheme for synthesis and isolation of NHC ligands.....	80
Scheme 64. Resonance structures of aromatic carbenes.....	81
Scheme 65. Deprotonation of NHC ligand by base.....	82
Scheme 66. Methods of synthesis of esters	85
Scheme 67. Synthesis of phenyl 4-(benzyl(tert-butoxycarbonyl)carbamoyl)benzoate	85
Scheme 68. Results from initial high throughput screening and optimization.....	87
Scheme 69. Role of the base in possible pathways during transmetallation	92
Scheme 70. Intermediate of transmetallation step in Suzuki-Miyaura cross coupling.....	106
Scheme 71. Proposed mechanism for palladium catalyzed cross-coupling of esters.....	112
Scheme 72. Electronic influence of substituents in the Pd-catalyzed cross-coupling of esters..	113
Scheme 73. Development of C-N bond forming reactions.....	115

Abbreviations

aq.	aqueous
Ar	aryl
BINAP	2,2'-Bis(diphenylphosphino)-1,1'-binaphthalene
Bn	benzyl
Boc	tert-butyloxycarbonyl
bpy	bipyridine
Bu	butyl
cat.	catalytic or catalyst
Cp*	tetramethylcyclopentadienyl
COD	1,5-Cyclooctadiene
Tc	thiophene-2-carboxylate
Cy	cyclohexyl
dba	dibenzylideneacetone
D	Deuterium
DBU	1,8-diazabicyclo[5.4.0]undec-7-ene
DCC	N, N'-dicyclohexylcarbodiimide
DCE	1,2-dichloroethane
DCM	dichloromethane
DMAP	4-Dimethylaminopyridine
DMF	N,N-dimethylformamide
DMSO	dimethylsulfoxide
dcpe	1,2-bis(dicyclohexylphosphino)ethane
dppb	1,4 Butanediylbis[diphenylphosphine]
dppf	1,1'-Ferrocenediyl-bis(diphenylphosphine)
dppp	1,3-Bis(diphenylphosphino)propane
dtbpf	1,1'-Bis(di- <i>tert</i> -butylphosphino)ferrocene
equiv.	equivalent(s)
EDC	1-Ethyl-3-(3-dimethylaminopropyl)carbodiimide
ESI	electrospray ionization

Et	ethyl
EtOAc	ethyl acetate
g	gram(s)
GC-MS	gas chromatography coupled with mass spectrometry
hr	hour(s)
IMes	1,3-Bis(2,4,6-trimethylphenyl)-4,5-dihydroimidazol-2-ylidene
IPent	bis(2,6-di(3-pentyl)phenyl)imidazol-2-ylidene
IPr	1,3-Bis(2,4,6-trimethylphenyl)-1,3-dihydro-2 <i>H</i> -imidazol-2-ylidene
J	coupling constant (NMR spectrometry)
L or Ln	generic ligand
m	meta
M	generic metal, or molecular ion, or molar
MeCN	acetonitrile
Me	methyl
MHz	megahertz
min	minute(s)
mL	millilitre(s)
mol	mole(s)
MS	mass spectrometry
NHC	N-heterocyclic carbene
NMR	nuclear magnetic resonance
Nu or Nu-	nucleophile
o	ortho
OAc	acetate
OTf	triflate
p	para
PEG	polyethylene glycol
Ph	phenyl
piv	pivalate

ppm	parts per million
PTS	PEG-600/ α -Tocopherol-based diester of Sebacic acid
Py	pyridyl
R	generic chemical group
r.t.	room temperature
s	Seconds
SIPr	1,3-bis(2,6-diisopropylphenyl)-imidazolidinium
SPGS	β -sitosteryl polyoxoethanylsuccinate
SPhos	2-Dicyclohexylphosphino-2',6'-dimethoxybiphenyl
t-Bu	tert-butyl
T	temperature
TEMPO	(2,2,6,6-Tetramethyl-piperidin-1-yl)oxyl
THF	tetrahydrofuran
TLC	thin-layer chromatography
TMS	tetramethylsilane or trimethylsilyl
tol	tolyl
TPGS	D - α -Tocopherol polyethylene glycol succinate
wt	weight
X	generic halogen/heteroatom

Introduction

Organic chemistry is a fundamental science that surrounds the very environment we live in and structures the fiber of our existence. One of the most important goals that organic chemists strive to achieve is to make carbon-carbon bonds in order to transform simple molecules into more complex molecules for applications in pharmaceuticals, agriculture etc. Many notable Nobel-prize winning chemists from the last 100 years such as Grignard,¹ Diels and Alder² and Brown and Wittig³ developed well known named reactions that give access to a toolbox for simple carbon-carbon bond formation. Although these traditional organic reactions remain very relevant today, synthetic chemists are actively searching to develop new catalytic processes as opposed to stoichiometric ones. The activity of transition metals received particular attention in their ability to participate in small and large scale catalytic synthesis. Therefore, there has been a great surge in the development of homogeneous transition metal catalyzed processes especially near the turn of the 21st century, which have crossed over in the field of organometallic chemistry. Among these discoveries include olefin metathesis and cross-coupling reactions. In the last few decades, chemists have dedicated their work to improve these processes and develop new catalytic transformations. In improving these conditions, synthetic chemists strive to broaden scope, develop milder conditions, and increase catalytic turnover numbers which can find better applications especially in the synthesis of complex molecules. There also has been a particular emphasis on “green chemistry” recently where these goals are put into practice in order to develop more efficient, economical and environmentally friendly processes.

¹ a) Grignard, V., *Compt. Rend. Acad. Sci. Paris.* **1900**, 130, 1322; b) Grignard, V., *Ann. Chim.* **1901**, 24, 433.

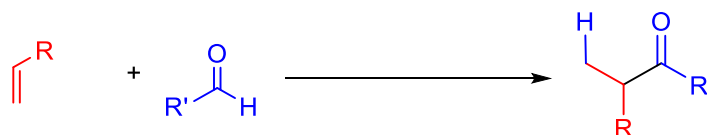
² "The Nobel Prize in Chemistry 1950". *Nobelprize.org*. Nobel Media AB 2014. Web.

³ "The Nobel Prize in Chemistry 1979". *Nobelprize.org*. Nobel Media AB 2014. Web.

Chapter 1: Ruthenium catalyzed couplings of aldehydes and olefins

1.1. Transition metal catalysis for intermolecular olefin aldehydes coupling

Olefin to aldehyde coupling to form carbon-carbon bonds between easily accessible substrates allows for the synthesis of highly functionalized molecules from simple precursors. One of the most common methods for this coupling is known as hydroacylation. This transformation allows efficient production of ketones from the addition of an acyl unit and a hydrogen atom across an alkene or alkyne (**Scheme 1**).



Scheme 1. General scheme for hydroacylation

This reaction has intra- and intermolecular variants. Catalysts based on rhodium, iridium, nickel, palladium, ruthenium, among others have been explored to enable hydroacylation processes.⁴ Most of these transformations rely on a conventional hydroacylation mechanism that involves aldehyde C-H oxidative addition or alkyne-aldehyde oxidative coupling followed by a β -hydride elimination to form the conjugated enone. The challenges with these mechanisms are met by an undesirable decarbonylation pathway. Some require harsh conditions such as high pressure of CO or high temperatures. Other methods may rely on a metal hydride transfer hydrogenation pathway, which use milder conditions. A brief survey of these hydroacylation methods and alternative olefin aldehyde couplings is detailed in the following sections. Efforts have been made to improve conditions for reactivity. Recently, Krische and co-workers developed a unique mode of reactivity for the hydroacylation of conjugated dienes and acyl

⁴ Leung, J. C.; Krische, M. J., *Chemical Science*, **2012**, 3, 2202.

derivatives via hydrometallation, which is the addition of hydrogen and metal across a π -bond. In this case, the hydrometallation is achieved via transfer hydrogenation from a ruthenium hydride catalyst. This work will be the basis of our discussion in the following sections.

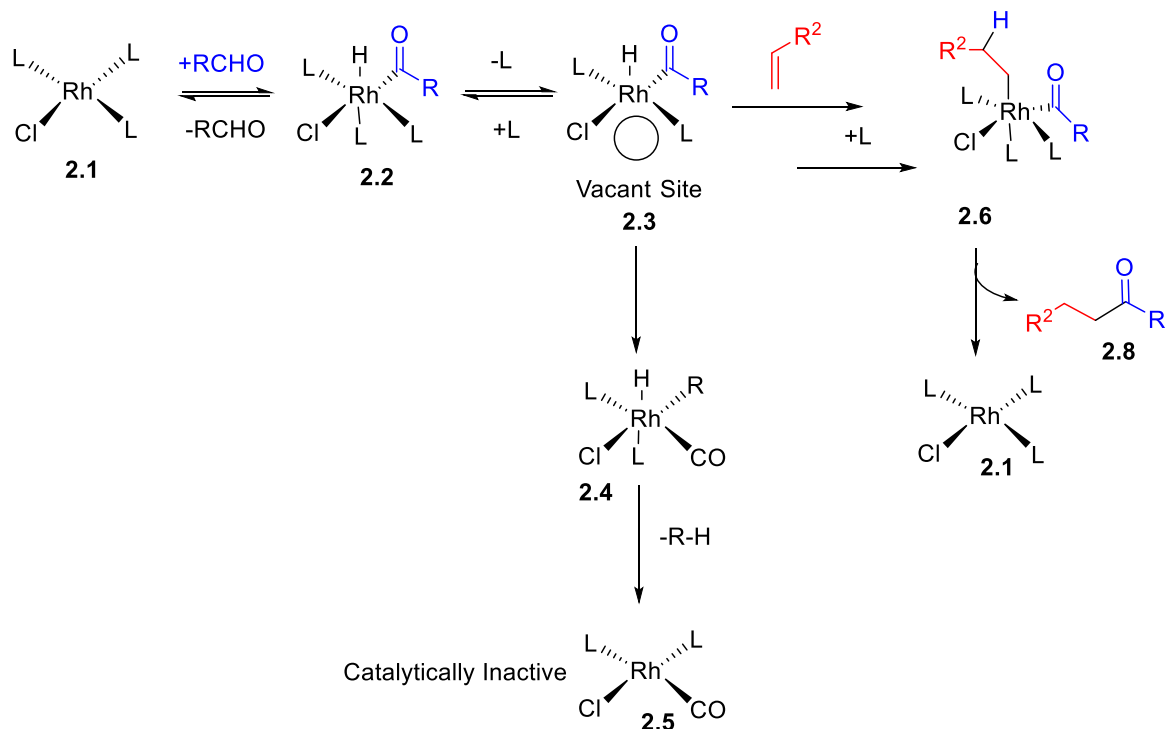
1.2. Rhodium catalyzed hydroacylation

The first alkene hydroacylation was reported by Sakai and co-workers in 1972,⁵ achieving intramolecular hydroacylation to form ketone products. However, intermolecular hydroacylation suffered greatly from the competing decarbonylation pathway, which renders the catalyst inactive (Scheme 2). For example, using the common Wilkinson's complex $\text{Rh}(\text{PPh}_3)_3\text{Cl}$ allows oxidative addition to the catalyst providing the cis-(hydrido)(acyl)rhodium complex **2.2**.⁶ This complex is then subjected to rate-determining dissociation of a ligand that is trans to the hydride to give **2.3**. From this coordinatively unsaturated species, the olefin can either insert into the Ru-H bond to give desired product **2.8**, or it can undergo decarbonylation, which gives intermediate **2.4** and reductively eliminate to **2.5**.⁷

⁵ Sakai, K.; Ide, J.; Oda, O.; Nakamura, N., *Tetrahedron Lett.* **1972**, *13*, 1287.

⁶ (a) Tsuji, J.; Ohno, K., *Tetrahedron Lett.* **1965**, *6*, 3969; (b) Baird, M. C.; Nyman, C. J.; Wilkinson, G., *J. Chem. Soc. A*, **1968**, 348.

⁷ (a) Doughty, D. H.; Pignolet, L. H., *J. Am. Chem. Soc.* **1978**, *100*, 7083; (b) O'Conner, J. M.; Ma, J., *J. Org. Chem.*, **1992**, *57*, 5075. (c) Beck, C.M.; Rathmill, S. E.; Park, Y. J.; Chen J.; Crabtree, R. H., *Organometallics*, **1999**, *18*, 5311.



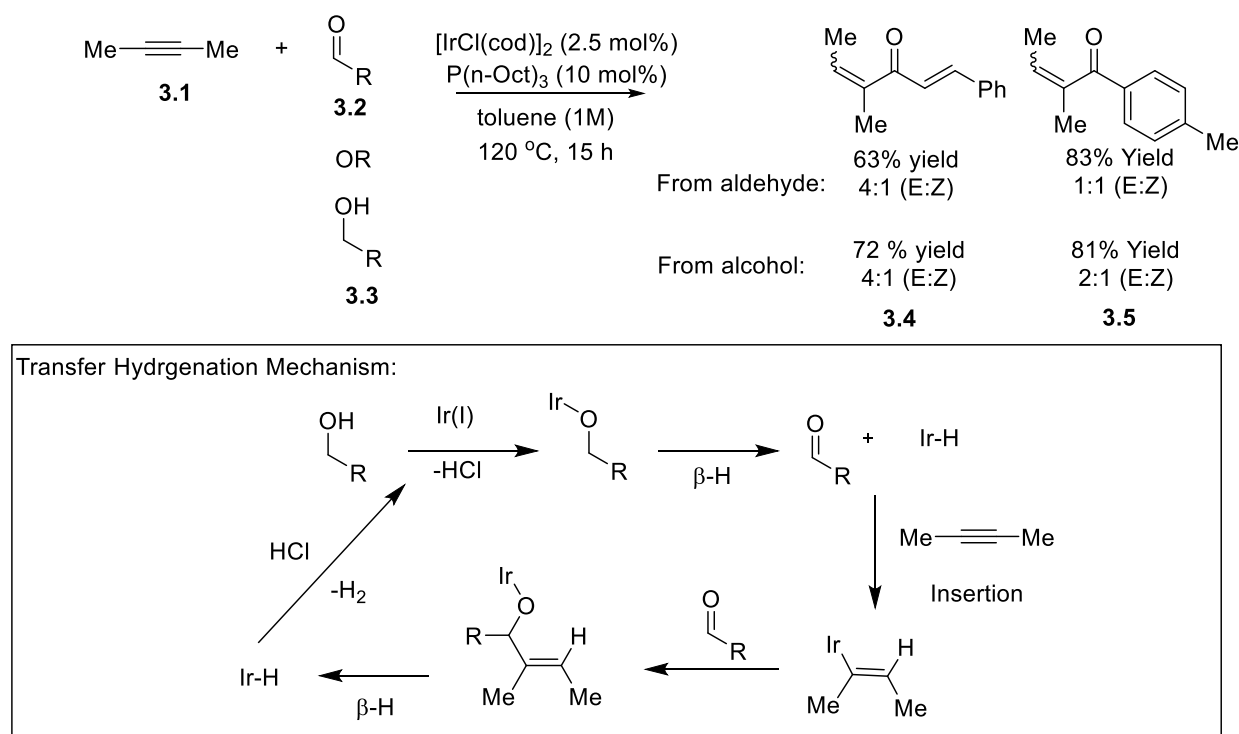
Scheme 2. Traditional oxidative addition pathway of hydroacylation⁸

There exists a few ways to prevent decarbonylation as reviewed by Krische,⁸ in which one of them is the use of β -chelating aldehydes, due to the undesirable formation of the resulting four-membered metallacycle. This requirement poses a great limitation on possible substrates. Second, would be the use of an electron deficient rhodium catalyst, which facilitates the reductive elimination step. This system disfavours the introduction of a π -acidic carbonyl ligand to the metal center, which would be an electrophilic high valent rhodium(III) center. Finally, the use of strongly coordinating olefin partners that better compete for the vacant site of the rhodium intermediate would mediate decarbonylation.

⁸ Leung, J. C.; Krische, M. J., *Chemical Science*, **2012**, 3, 2202.

1.3. Iridium catalyzed hydroacylation

Iridium catalyzed hydroacylation are limited to alkynes coupling with aldehydes through a hydrogen transfer mechanism. An example of this work was done by Obora and Ishii and co-workers in 2010 (Scheme 3). Their mechanistic hypothesis involves the formation of homoallylic alcohols followed by dehydrogenation to β,γ -unsaturated ketones. Then isomerization would lead to hydroacylation products **3.4**, **3.5**. Their pathway is analogous to that of ruthenium catalyzed process and gives high regioselectivity.⁹ Currently, iridium catalyzed hydroacylations via C-H oxidative addition pathway are not successful due to the predominant decarbonylative pathway.¹⁰



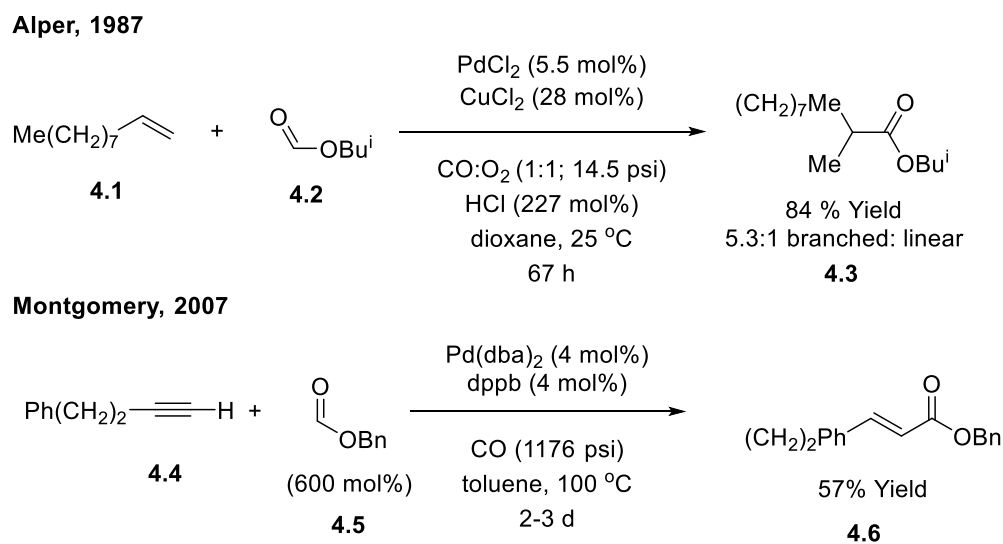
Scheme 3. Obora and Ishii's iridium catalyzed hydroacylation of alkynes with alcohols⁹

⁹ Hatanaka, S.; Obora, Y.; Ishii, Y., *Eur. J. Org. Chem.*, **2010**, 16, 1883.

¹⁰ Iwai, T.; Fujihara, T.; Tsuji, Y., *Chem. Commun.*, **2008**, 6215; (b) Geilen, F. M. A.; vom Stein, T.; Engendahl, B.; Winterle, S.; Liauw, M. A.; Klankermayer, J.; Leitner, W., *Angew. Chem., Int. Ed.* **2011**, 50, 6831; (c) Roa, A. E.; Salazar, V.; Lopez-Serrano, J.; Onate, E.; Paneque, M.; Poveda, M. L., *Organometallics*, **2012**, 31, 716.

1.4. Palladium catalyzed hydroacylation

Palladium catalyzed hydroacylation dates back to 1987 when Alper and co-workers reported coupling between formate esters and alpha olefins.¹¹ This system required the use of carbon monoxide, hydrochloric acid, oxygen and copper chloride, which renders the system quite complex. Palladium (0) species are electron rich and are known to form Pd-H bonds in the presence of acid,¹² which in this case is HCl. Their system is not very regioselective giving a mixture of isomers in moderate yields. Slightly simpler conditions were employed by Montgomery's group achieving hydroacylation of alkynes and substituted styrenes with formate esters (Scheme 4).¹³ However, the requirement of high CO pressure poses limitations and is undesirable.



Scheme 4. Development of palladium catalyzed hydroacylation^{11, 13}

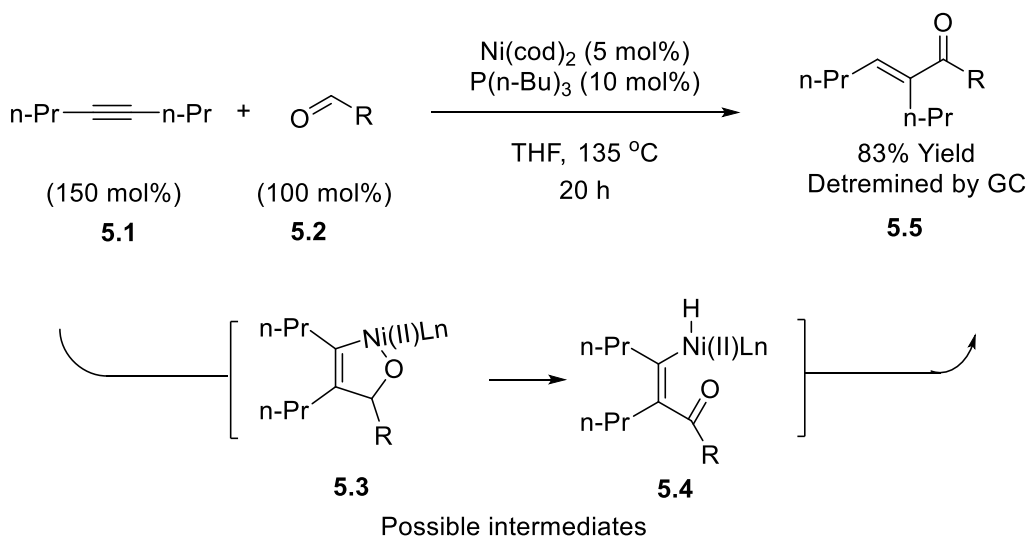
¹¹ Alper, H.; Saldana-Maldonado, M.; Lin, v. J. B., *J. Mol. Catal.* **1988**, *49*, L27-L30.

¹² Zargarian, D.; Alper, H., *Organometallics*. **1993**, *12*, 712.

¹³ Montgomery, J.; Sormunen, G. J., *Top. Curr. Chem.* **2007**, *279*, 1.

1.5. Nickel catalyzed coupling of olefins to aldehydes

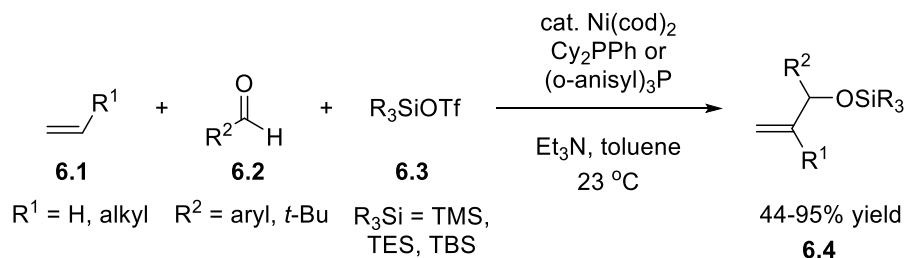
In 1990, Tsuda, Saegusa and co-workers reported nickel catalyzed hydroacylation of alkynes with aliphatic and aromatic aldehydes. In this case, there are two possible reaction pathways. One consisting of the conventional hydroacylation pathway as discussed in Section 1.1 involving C-H aldehyde oxidation, the second is an alkyne-aldehyde oxidative coupling to form an oxametallacyclopentene **5.3**, which β -hydride eliminates to form the conjugated enone (Scheme 5).



Scheme 5. Tsuda and Saegusa's nickel catalyzed hydroacylation¹⁴

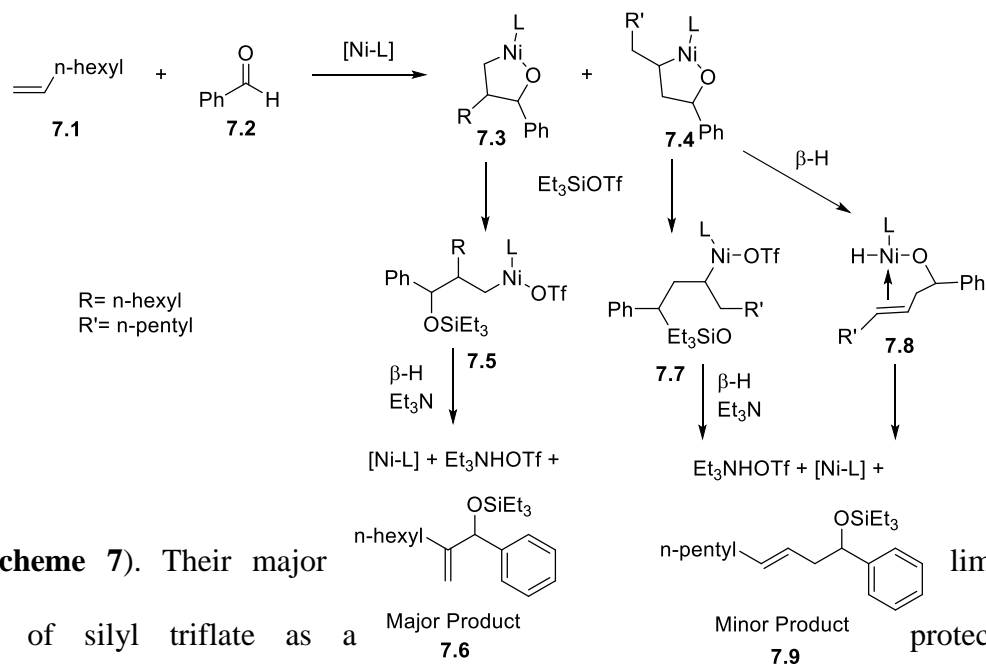
Jamison and co-workers also reported the reactivity of alpha olefins and aldehydes to provide homoallylic alcohols. Using a nickel catalyst and a silyl triflate, allylic alcohol derivatives can be obtained (Scheme 6).¹⁴

¹⁴ Ng, S.-S.; Jamison, T. F., *J. Am. Chem. Soc.* **2005**, *127*, 14194.



Scheme 6. Jamison's nickel catalyzed hydroacylation using silyl triflate¹⁴

They propose that one of the key steps is the formation of an oxametallacycle **7.3**, which would lead to the major observed allylic product **7.6** by reaction with the silyl triflate, cleavage of the Ni-O bond and β -H elimination. **7.9** is a minor byproduct that is likely formed from regioisomer **7.4**, which can subsequently either first react via the same pathway as for **7.6**, or can undergo β -H elimination first, then followed by reaction with silyl triflate. Therefore, the hydroacylation product observed here is the minor product **7.10** (



Scheme 7. Jamison's mechanistic hypothesis for nickel catalyzed hydroacylation through oxametallacycle intermediate¹⁴

1.6. Ruthenium catalyzed hydroacylation

Ruthenium catalyzed hydroacylations generally follow the C-H oxidative addition pathway, but require high reaction temperatures up to 200 °C. Not only it is undesirable to have energy consuming and harsh reaction conditions, but it also potentially gives undesirable side products, such as Tischenko products from the aldehydes. Watanabe and Kondo and co-workers found that Ru₃(CO)₁₂ performs well as a pre-catalyst for the hydroacylation of aromatic aldehydes¹⁵ and formic esters with alkenes.¹⁶ These conditions however require pressure of carbon monoxide with high temperature. Later, their group reported that another ruthenium catalyst, Ru(cod)(cot) and PPh₃ is useful for the hydroacylation of aromatic aldehydes with conjugated dienes.¹⁷ In this

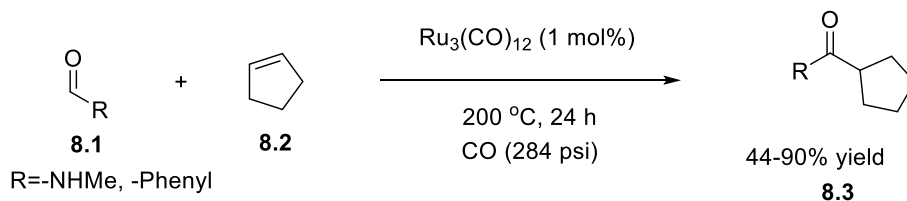
¹⁵ Kondo, T.; Tsuji, Y.; Watanabe, Y., *Tetrahedron Lett.* **1987**, 28, 6229.

¹⁶ Kondo, T.; Akazome, M.; Tsuji, Y.; Watanabe, Y., *J. Org. Chem.* **1990**, 55, 1286.

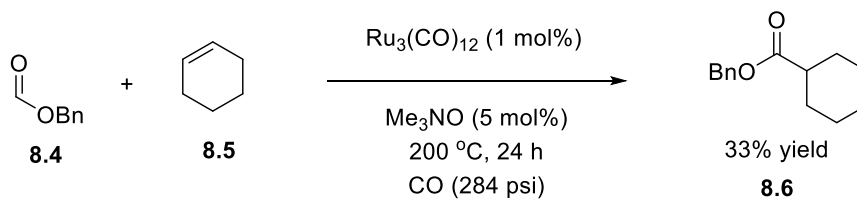
¹⁷ Kondo, T.; Hiraishi, N.; Morisaki Y.; Wada, K.; Watanabe, Y.; Mitsudo, T.-A., *Organometallics*. **1998**, 17, 2131.

case, carbon monoxide pressure was not required, but likely still follows the C-H aldehyde oxidative addition pathway.

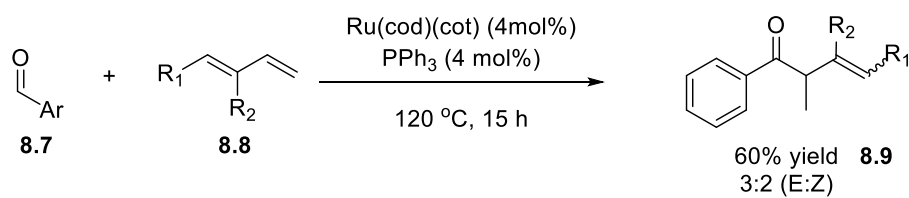
Watanabe, 1987



Watanabe, 1990



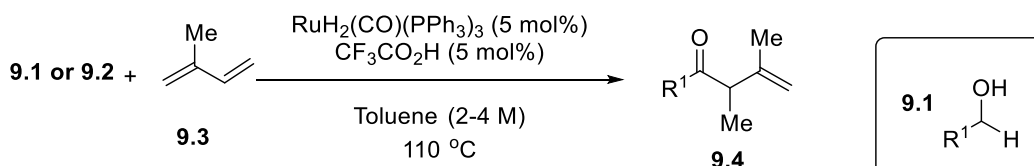
Watanabe, 1998



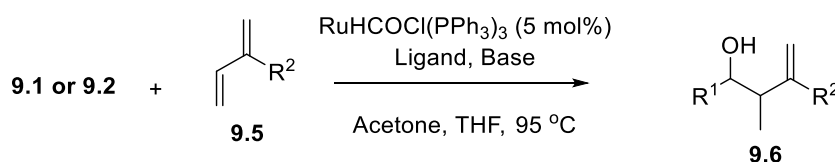
Scheme 8. Development of ruthenium catalyzed hydroacylation^{15, 16, 17}

One of the most important chemists that developed an effective method for hydroacylation of dienes from alcohols or aldehydes is Krische¹⁸ (**Scheme 9**). His group predominately uses ruthenium-hydride catalysis to achieve the desired transformation.

Krische, 2008

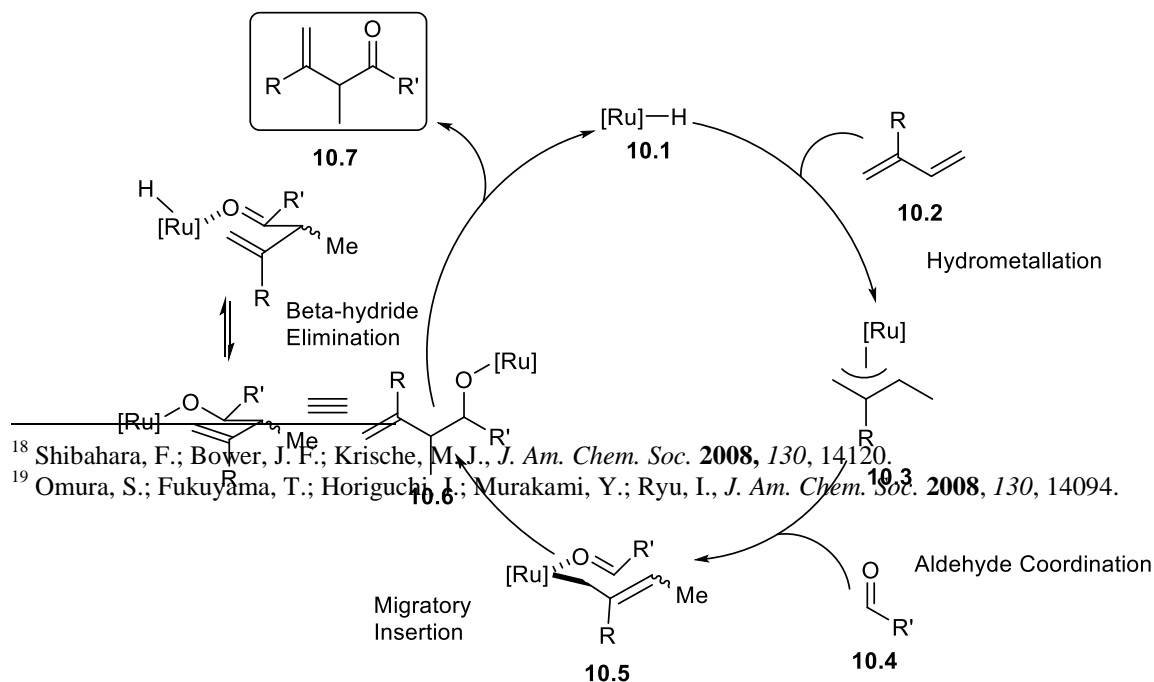


Ryu, 2008



Scheme 9. Recent developments of hydroacylation of conjugated dienes^{18,19}

Krische's mechanism differs from the conventional aldehyde C-H oxidative addition pathways. Starting with the ruthenium hydride **10.1**, it will hydrometalate on the olefin of isoprene **10.2** to give a metal allyl species **10.3**, which can isomerize in the case of a longer carbon chain. An aldehyde **10.4** will then coordinate to the ruthenium center. Migratory insertion of the carbonyl will then occur through a six-membered chair like transition structure **10.5**. The



transition structure will establish the E and Z allylruthenium species, which will translate to a stereospecific aldehyde addition. Dehydrogenation of the resulting ruthenium alkoxide intermediate **10.6** via β -hydride elimination will result in the desired hydroacylation product **10.7** (**Scheme 10**).

Scheme 10. Krische's transfer hydrogenation pathway for ruthenium catalyzed hydroacylation²⁰

Ryu and co-workers also independently reported ruthenium hydrides modified by phosphine ligands can catalyze intermolecular diene hydroacylation via the same reaction pathway (**Scheme 9**).²¹ It is also notable that all oxidation levels of the substrate, aldehyde or alcohol, can give access to the corresponding ketone or alcohol in the presence of a hydrogen acceptor. Although Krische's method of hydroacylation provides a viable alternative to the C-H oxidative addition pathway, the major limitation is the choice of the conjugated diene as a coupling partner. Since the formation of the ketone product relies on the formation of the π -allyl metal intermediate, the scope of the reaction is quite limited. His method also takes place at high reaction temperatures, high concentration and long reactions times.

²⁰ Leung, J. C.; Krische, M. J., *Chemical Science*. **2012**, 3, 2202.

²¹ Omura, S.; Fukuyama, T.; Horiguchi, J.; Murakami, Y.; Ryu, I., *J. Am. Chem. Soc.* **2008**, 130, 14094.

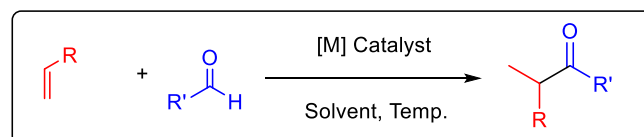
1.7. Research goals

As outlined above, several groups presented different modes of hydroacylation methodologies using various transition metal catalysts. Despite decades of research, it remains a challenge to circumvent the C-H oxidative aldehyde pathways, and some require harsh conditions. As this pathway is limited to specific substrates that are tolerant to the undesirable decarbonylative pathway, we seek an alternative mechanism to alleviate the limitations. Our proposal was to present a mode of reactivity analogous to that of Krische's mechanism for hydroacylation of conjugated dienes to access the carbon-carbon bond formation between aldehydes and olefins. Unconjugated alkenes are more challenging than conjugated dienes due to their inability to form an allyl species with the metal, which would then facilitate the migratory insertion step.

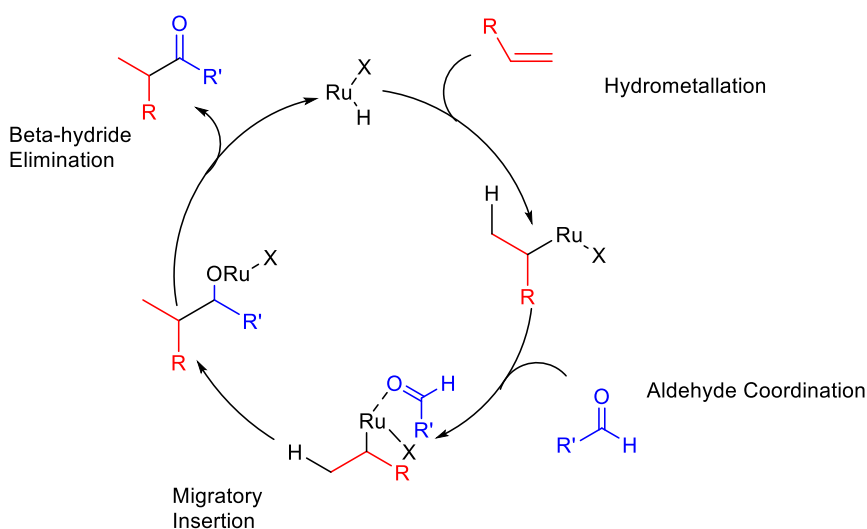
In order to gain access to an efficient catalytic system for this carbon-carbon bond formation between simple substrates (**Scheme 11**), we must examine the challenges met by previous studies. We were particularly interested in exploring metal hydrides for hydrogen transfer coupling. This project was approached from three main directions. First, we borrowed Krische's

hydroacylation conditions using $\text{RuHCl}(\text{CO})(\text{PPh}_3)_3$ as a starting point to test reactivity for non-conjugated dienes and probe the challenging steps of the reaction. Our hypothesis was that the ability to form metal allyl species facilitated the coupling between the aldehyde and the olefin and in its absence, the rate determining step may be the insertion of the olefin into the metal-hydride bond. Initial screening of variables such as ligands, bases, solvent and temperature was done to test the efficiency of the hydrometallation step. This also led to exploration of other Ru-hydride analogue catalysts to investigate the influence of sterics and electronics on the system's reactivity. Second, we sought to explore various isomerization catalysts to enable non-conjugated dienes to isomerize into conjugation to facilitate migratory insertion. Finally, the third approach was to seek catalysts that could selectively oxidize the olefin through a π -allyl species to facilitate the migratory insertion step.

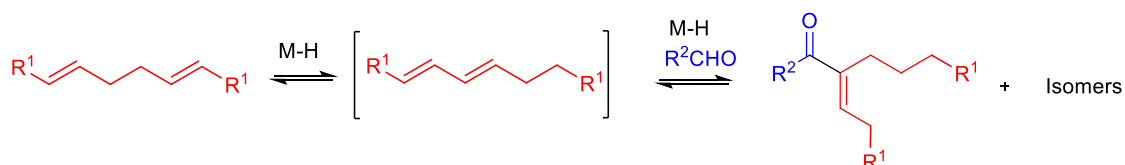
General Scheme:



Strategy 1: Use of Ru-H that are known for hydroacylation of conjugated dienes



Strategy 2: Use of isomerization catalysts to explore coupling of carbonyls to non-conjugated dienes

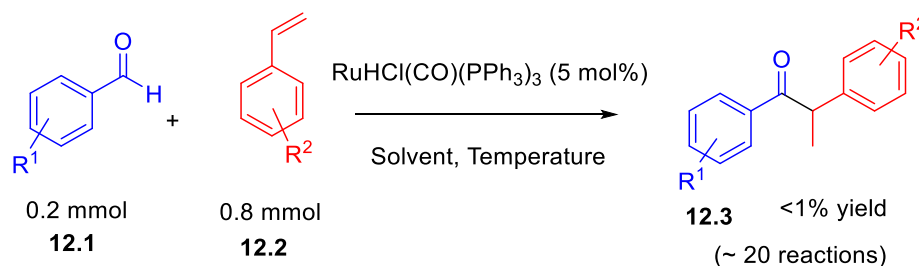


Scheme 11. Strategies for metal catalyzed olefin-aldehyde coupling

2. Results and discussion

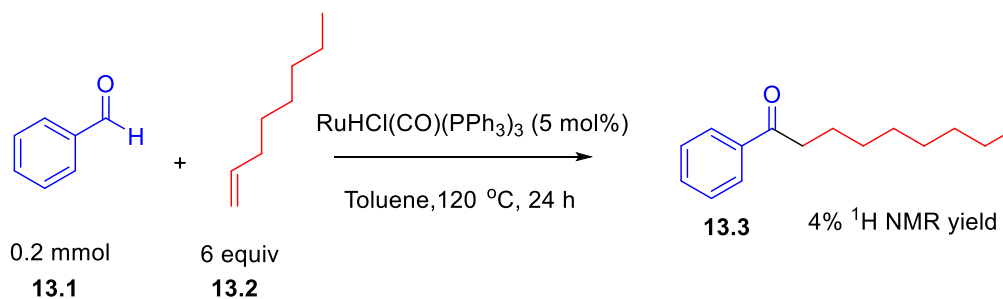
2.1. Probing reactivity

Adapting Krische and Ryu's procedure for hydroacylation of aldehydes to conjugated dienes, we tested the reactivity of the system using terminal alkenes. More specifically, styrene was used as it is most similar to a conjugated diene, but the formation of the allyl species on the terminal alkene could be more challenging due to the aromaticity of the styrene. A number of variables such as solvent, temperature and the use of various electron donating and withdrawing groups on the aldehyde to test reactivity on the starting materials were screened (Scheme 12). Elevation of temperature had no effect on the reactivity. Modifying electronics with different substituents on the aryl group of the benzaldehyde and styrene did not have an influence on the yield of results. Only trace product **12.3** was detected on the GC. Results indicate that Krische's conditions for hydroacylation of aldehydes to conjugated dienes remained optimal for this transformation. Interestingly, changing the alkene coupling partner to a terminal aliphatic alkene provided the coupling product **13.3** with a yield up to 4% (Scheme 13).



Scheme 12. Ruthenium catalyzed hydroacylation of styrene and benzaldehyde derivatives

We hypothesized that the alkyl metal species formed by an aliphatic substrate is more reactive than that of styrene. Therefore, a smaller substrate such as 1-octene in this case showed slightly higher reactivity than styrene as the terminal alkene has a higher chance to coordinate with the ruthenium center, and thus enabling the migratory insertion to occur more effectively to form the final product.

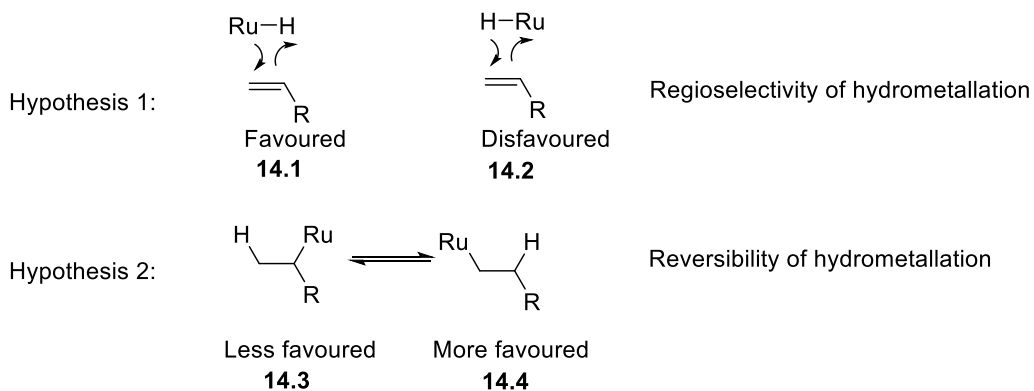


Scheme 13. Ruthenium catalyzed hydroacylation of benzaldehydes to terminal alkene

It is interesting to note that the addition only occurred on the 1 position of the octene rather than the 2 position, as would be predicted with a conjugated diene. This results in forming a linear ketone rather than branched. There are two possible explanations for this observation (**Scheme 14**). The first hypothesis would be that the addition of the Ru-H over the alkene bond is favored when the hydrogen is added on the more substituted side of the alkene **14.1** showing regioselectivity of substrate during hydrometallation. The second possible hypothesis could be

due to the reversibility of the hydrometallation step. Species **14.4** may be favoured over **14.3** for the migratory insertion step to occur. It is possible that carbonyl coordination can occur only when the alkene species is not substituted. Several experiments were also done using cyclohexene substrate as the olefin coupling partner under these conditions, but only trace product was detected on the GC. This result is consistent with the theory that sterics of the olefin

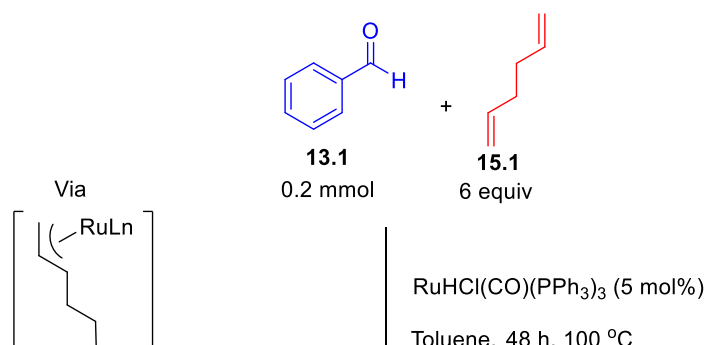
may play a role in the regioselectivity of hydrometallation in the



reactivity.

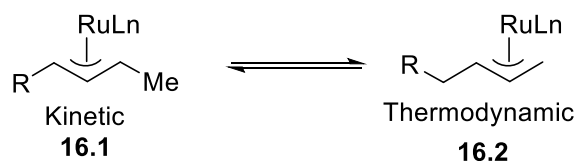
Scheme 14. Possible hypotheses for observation of formation of linear ketone product

Another substrate that was used as the alkene coupling partner for the aldehyde was the non-conjugated diene. Krische's recent publication showed that his hydroacylation conditions using the same catalyst enabled the coupling of an aldehyde with 1,3-pentadiene. Inspired by this reactivity, 1,5 hexadiene substrate **15.1** was chosen as an alternative alkene coupling partner to investigate its extent of reactivity. The results were the most promising thus far in this research giving three different isomers of the hydroacylation product **15.2**, **15.3**, **15.4** (Scheme 15).



Scheme 15. Ruthenium catalyzed hydroacylation of benzaldehyde and non-conjugated diene

(E)-2-ethylidene-1-phenylpentan-1-one **15.4** was shown to be the major product giving a yield of 32%, whereas the (Z) isomer of the product **15.3** gave a yield of 12%. Finally, there was some trace of the 1-phenyl-2-vinylpentan-1-one **15.2**. From the results, we hypothesize that the ruthenium catalyst isomerizes the non-conjugated diene into its conjugated isomer, which then can form the desired π -allyl species. The observed distribution is likely due to a combination of kinetic and thermodynamic bias. According to Krische's studies, hydrometallation at the disubstituted π -allyl species **16.1** is kinetically favoured over monosubstituted complex **16.2** (Scheme 16). However, **16.2** is thermodynamically more favourable and reacts faster during the migratory insertion step than **16.1**, which led to the hypothesis that the former will isomerize to the latter to give access to the observed product **15.2**



Scheme 16. Ru-allyl intermediate²²

From product **15.2**, it is likely that the Ru-H can hydrometallate the olefin bond to give isomers **15.3**, **15.4**, which are likely thermodynamically preferred over **15.2** as an α - β unsaturated ketone. The E isomer **15.4** is preferred over the Z isomer **15.3** likely due to favourable steric distribution. Our results are consistent with Krische's, demonstrating the reversible nature of diene hydrometalation and proven by deuterium labelling studies.²²

2.2. Isomerization catalysis

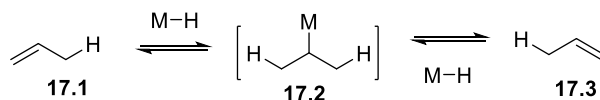
A second approach that was explored was investigating various isomerization catalysts that can perform hydrometallation, where the metal hydride adds across the olefin. The reversibility of this step allows isomerization to occur and may be able to isomerize non-conjugated dienes into conjugation (**Scheme 17**). These catalysts can start either from the metal hydride or generate metal hydride in situ. A few systems have been shown to show reactivity in C-C bond formation in addition to isomerization. For systems that solely perform isomerization via metal-hydrides, the Ru-H was added to the system in hopes to facilitate the migratory insertion step for C-C bond formation. Three different isomerization systems were explored. The first system was inspired by Skrydstrup's²³ catalytic system for isomerization of olefins transforming terminal alkenes to 2-alkenes. The second system is inspired by Gooßen's catalyst which is highly active for double-

²² Chen, T.-Y.; Tsutsumi, R.; Montgomery, T. P.; Volchkov, I.; Krische, M. J., *J. Am. Chem. Soc.* **2015**, *137*, 1798.

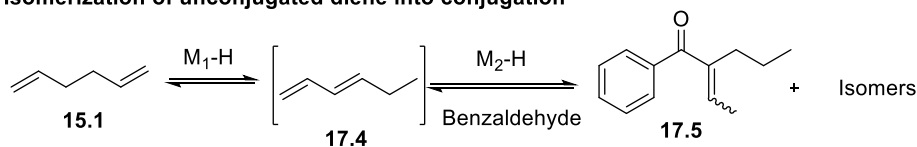
²³ Gauthier, D.; Lindhardt, A. T.; Olsen, E. P. K.; Overgaard, J.; Skrydstrup, T., *J. Am. Chem. Soc.* **2010**, *132*, 7998.

bond migration and known to be efficient in olefin metathesis.²⁴ Finally, the third system was inspired from Mazet's catalyst for isomerization of highly substituted allylic alcohols and alkenyl alcohols.²⁵

Hydride Mechanism

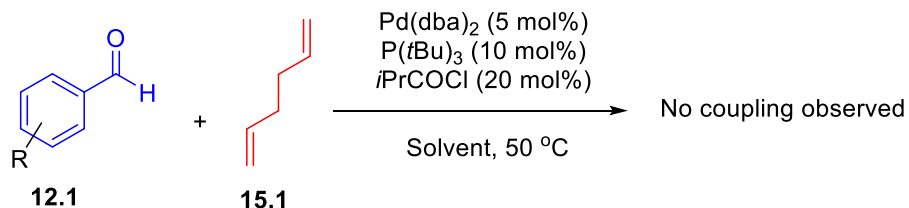


Isomerization of unconjugated diene into conjugation



Scheme 17. Hydride mechanism for metal hydride formation to facilitate hydrometallation to perform aldehyde to olefin coupling

Skyrdstrup's group developed a catalytic system where they generated a palladium (II) hydride catalyst in situ starting with a 1:1:1 ratio of Pd(dba)₂, P(tBu)₃, and isobutyryl chloride. Mechanistic investigations supported the formation of [HPd(Cl)(PtBu₃)₂] complex which is likely employed as the active catalyst to perform hydropalladation and subsequently couple alkynes to alkenes. Inspired by their catalytic system to perform hydropalladation and insertion, we extended their conditions to our substrates to investigate its reactivity in our desired transformation. However, after several reactions, no product was observed whether we used electron-donating or electron-withdrawing groups on the benzaldehyde substrate.

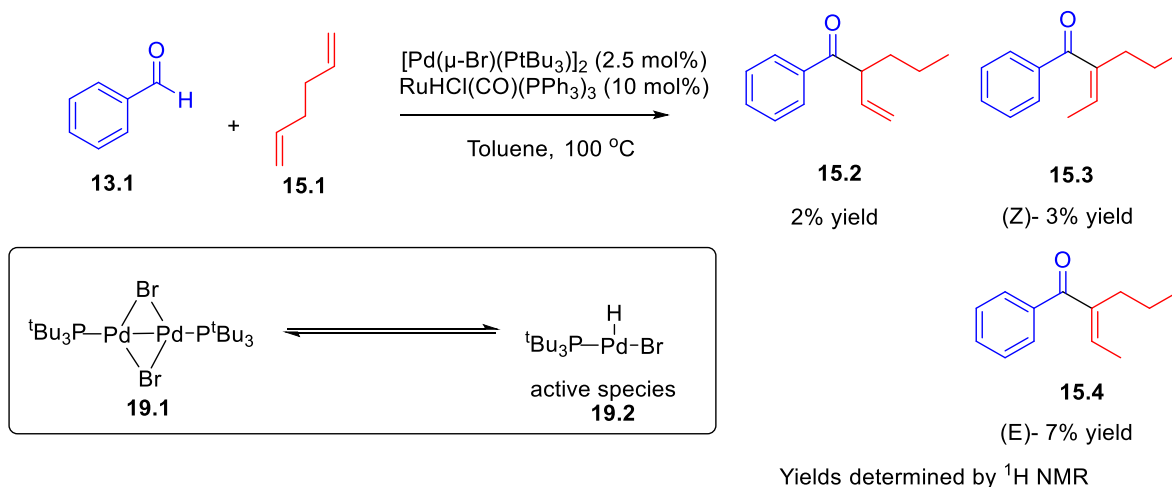


²⁴ Mamone, P.; Grünberg, M. F.; Fromm, A.; Khan, B. A.; Gooßen, L. J., *Org. Lett.* **2012**, *14*, 3716.

²⁵ Larionov, E.; Lin, L.; Guénée, L.; Mazet, C., *J. Am. Chem. Soc.* **2014**, *136*, 16882.

Scheme 18. Skyrdstrup's condition for coupling of aldehydes to alkenes via Pd-H intermediate

Gooßen's system used a Pd (I) dimer **19.1** to enable the formation of Pd-H species **19.2** in situ, in other words performing alkene isomerization via hydrometallation.²⁶ We borrowed his conditions for our system, in hopes to perform hydropalladation using the palladium catalyst and migratory insertion using the RuH catalyst. The same distribution of products was observed with a similar ratio as observed with the Ru-H system described in Section 2.1, but with significantly lower yields (Scheme 19). No reactivity is observed using solely the palladium dimer catalyst.

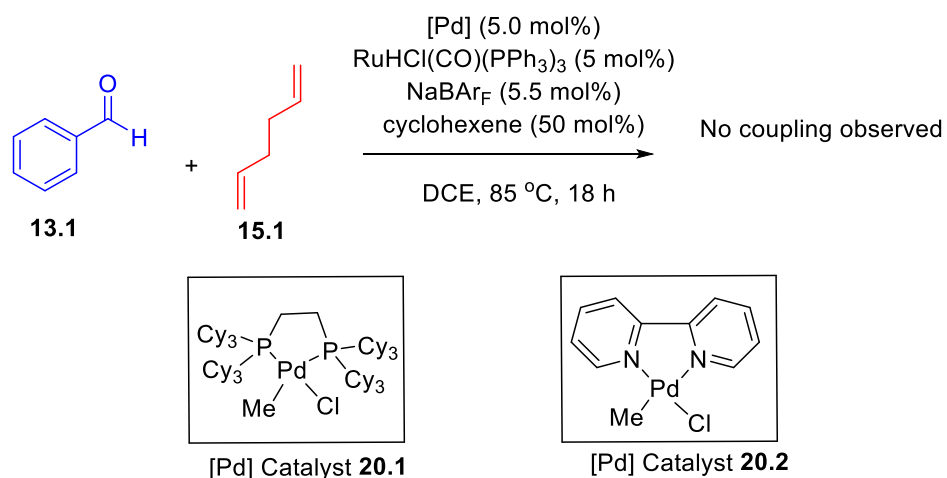


Scheme 19. Activation of dimeric Pd(I) species to hydridopalladium(II) complex for hydropalladiation

Going after a similar concept, we sought another system that can perhaps undergo the desired mechanism. Mazet's²⁷ palladium catalysts allow isomerization of highly substituted allylic alcohols and alkenyl alcohols (Scheme 20).

²⁶ Mamone, P.; Grünberg, M. F.; Fromm, A.; Khan, B. A.; Gooßen, L. J., *Org. Lett.* **2012**, *14*, 3716.

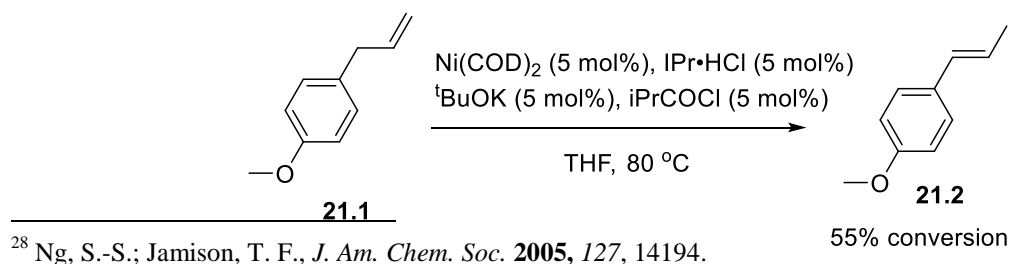
²⁷ Larionov, E.; Lin, L.; Guénée, L.; Mazet, C., *J. Am. Chem. Soc.* **2014**, *136*, 16882.



Scheme 20. Mazet's system for isomerization of allylic and alkenyl alcohols

Adapting their procedure, we synthesized a few palladium complexes with the general formula $[LnPd(Me)(Cl)]$ where Ln is a chelating bidentate ligand (catalyst **20.1** and **20.1**). These species provides in situ access to the corresponding cationic palladium hydride $[Ln(Pd-H)]^+$ species. Again, upon application of their system on our substrates, with or without the ruthenium catalyst, it did not produce the desired results.

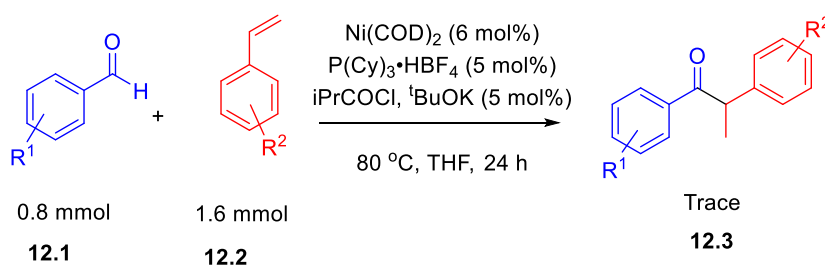
Since Pd catalysts did not enable this transformation to take place, we decided to extend this idea by using a different catalyst. As Jamison²⁸ and co-workers successfully used $Ni(cod)_2$ to perform olefin to aldehyde coupling with the presence silyl triflate or allylic alcohol, we attempted to use this catalyst in our system. To determine the formation of nickel-hydride, we tested the isomerization of an olefinic species under Skyrdrstrup's condition swapping out the palladium catalyst with $Ni(cod)_2$ (Scheme 21).



²⁸ Ng, S.-S.; Jamison, T. F., *J. Am. Chem. Soc.* **2005**, *127*, 14194.

Scheme 21. Scheme for isomerization of allylbenzene using nickel catalysis

The transformation was able to take place with a 55% conversion to **21.2**, showing that this system has potential for isomerization and to perform the desired transformation. However, after several experiments using this system of screening different variables, only trace amount of product **12.3** was detected (Scheme 22). There was also presence of side reactivity such as the presence of products from benzoin condensation, and coupling of styrene, and benzyl benzoate.

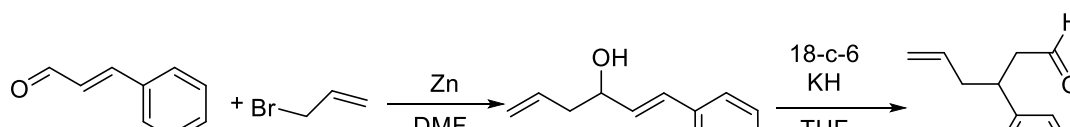


Scheme 22. Hydroacylation of benzaldehyde and styrene using nickel catalysis

An intramolecular hydroacylation reaction was also attempted with substrate 3-phenylhex-5-enal, which possesses a terminal alkene and terminal aldehyde. Synthesis of aliphatic aldehydes with terminal olefins were attempted via the Swern oxidation²⁹ and PCC oxidation³⁰ from the alcohol derivative, but proved to be difficult to isolate due to their instability under air and side-reactivity. To circumvent this issue, a molecule with a phenyl group on the aliphatic back bone was chosen to enhance stability. This molecule was synthesized starting from commercially available cinnamaldehyde **23.1** and allyl bromide **23.2**. Adapting procedure using

²⁹ A) Omura, K.; Swern, D., *Tetrahedron*. **1978**, *34*, 1651. B) Liniger, M.; Neuhaus, C.; Hofmann, T.; Fransioli-Ignazio, L.; Jordi, M.; Drueckes, P.; Trappe, J.; Fabbro, D.; Altmann, K.-H., *ACS Medicinal Chemistry Letters*. **2011**, *2*, 22.

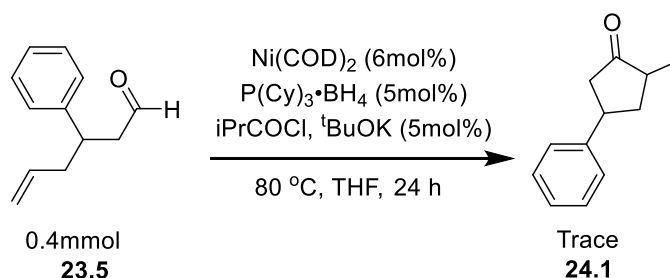
³⁰ Glaros, G., *J. Chem. Educ.* **1978**, *55*, 410.



Barbier's method,³¹ (E)-1-phenylpenta-1,4-dien-3-ol **23.4** was successfully synthesized. To obtain the desired product, a procedure for anionic oxy-cope rearrangement was adapted³² (Scheme 23).

Scheme 23. Synthesis of 3-phenylhex-5-enal via Barbier's method followed by anionic oxy-cope rearrangement

The intramolecular reaction could perhaps be aided by the bulky phenyl group on the backbone of the substrate to orient the two ends of reactivity. Using the above system, the intramolecular hydroacylation yielded only trace amount of product **24.1** (Scheme 24). Not surprisingly, we observed isomers of the starting material as discussed previously in this section, the system enables isomerization via double bond migration. Krische's hydroacylation conditions were also applied to this substrate, but again only isomers were observed.



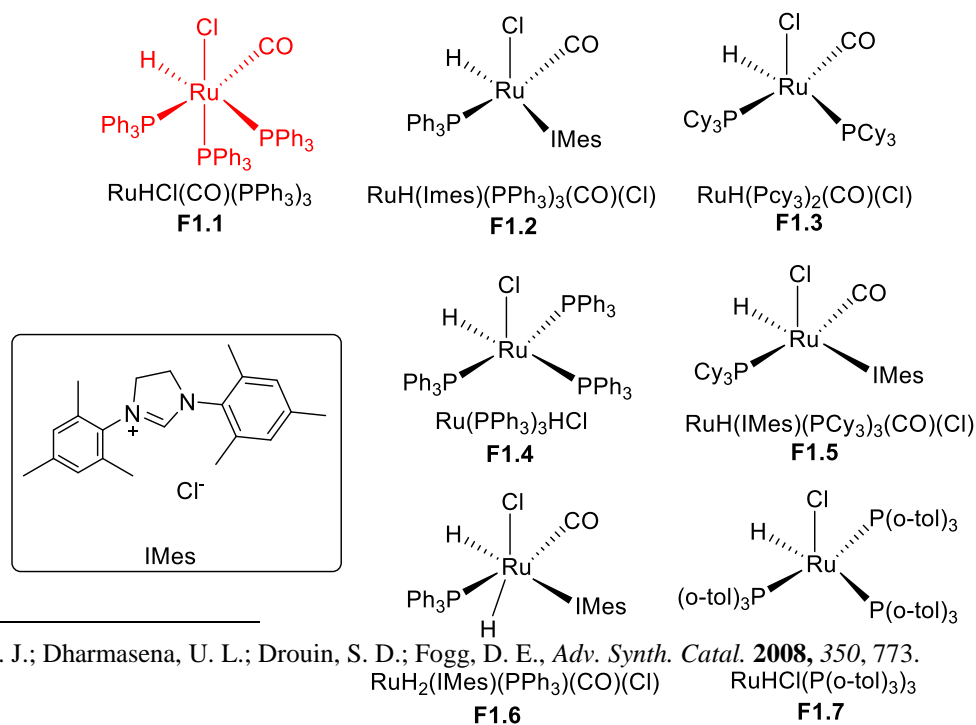
Scheme 24. Intramolecular hydroacylation using nickel catalysis

2.3. Exploring ruthenium catalysts for hydroacylation

³¹ Ranu, B. C.; Majee, A.; Das, A. R., *Tetrahedron Lett.* **1995**, 36, 4885.

³² Lee, E.; Lee, Y. R.; Moon, B.; Kwon, O.; Shim, M. S.; Yun, J. S., *J. Org. Chem.* **1994**, 59, 1444.

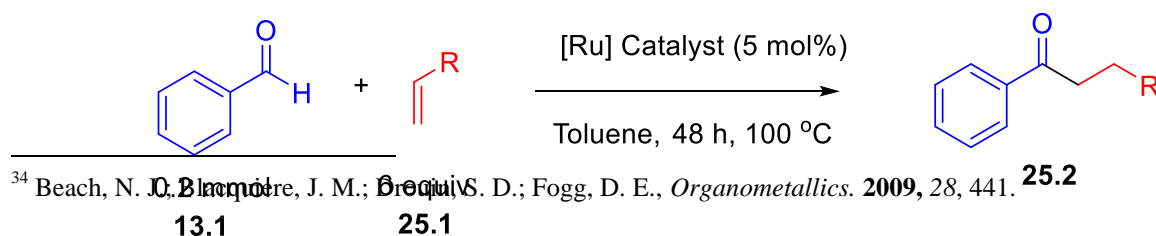
Due to the unsuccessful attempts from other isomerization catalysts, we diverted our attention back to ruthenium catalysis. Thus far, Krische has shown that $\text{RuHCl}(\text{CO})(\text{PPh}_3)_3$ or $\text{RuH}_2(\text{CO})(\text{PPh}_3)_3$, are the best known for hydroacylation via the insertion/insertion/elimination mechanism from **Scheme 11**. The latter dihydrogen analogue can be activated to the former with the addition of an acid HX. Variation of the steric and electronic properties of this ligand may lead to a superior catalyst; however, very few analogs have been reported. Recently, a series of Ruthenium hydride catalysts have been developed by Fogg and co-workers, which have been shown to be effective in applications involving olefin metathesis, polymer hydrogenation and isomerization.³³ Most can be prepared by ligand exchange from the parent catalyst, $\text{RuHCl}(\text{CO})(\text{PPh}_3)_3$ **F1.1**. The PPh_3 substrate can be swapped out for PCy_3 , IMes, $\text{P}(\text{o-tol})_3$ and other phosphines or NHCs. The following catalysts were used under our reaction conditions: $\text{Ru}(\text{PPh}_3)_3\text{HCl}$, $\text{RuH}(\text{IMes})(\text{PCy}_3)_3(\text{CO})(\text{Cl})$, $\text{RuH}_2(\text{IMes})(\text{PPh}_3)(\text{CO})(\text{Cl})$, $\text{RuHCl}(\text{P}(\text{o-tol})_3)_3$, $\text{RuH}(\text{IMes})(\text{PPh}_3)_3(\text{CO})(\text{Cl})$, $\text{RuH}(\text{PCy}_3)_2(\text{CO})(\text{Cl})$ (**Figure 1, F1.2-F1.7**). It was believed that they exhibit similar reactivity as the parent catalyst due to similarities in structure.



³³ Beach, N. J.; Dharmasena, U. L.; Drouin, S. D.; Fogg, D. E., *Adv. Synth. Catal.* **2008**, 350, 773.

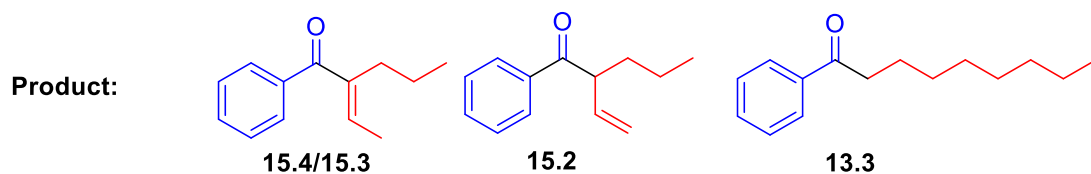
Figure 1. Structures of screened ruthenium catalysts

Electronics can be tuned based on the ligand used. Phosphine ligands such PCy₃, and P(o-tol)₃ are more electron rich than PPh₃, which makes them very good σ-donors to the metal center. In addition, NHCs such as IMes are much more electron rich than the original PPh₃, which also contribute significantly in donating electron density to the ruthenium center. NHC ligands will be discussed in further detail in Section 5.4. Electron rich ligands were thought to perform better as studies have been shown that σ-donating alkylphosphines ligands perform better than arylphosphines in the context of hydrogenation.³⁴ Therefore, it was thought that it would aid in the insertion of the alkene into the ruthenium hydride bond. With the hopes that these slight modifications on the electronics of the catalyst can facilitate the hydroacylation pathway, we applied it to our system (Scheme 25). Unfortunately, these catalysts performed unambiguously worse than the original catalyst with both the cases of octene or 1, 5 hexadiene (Table 1). Ru(PPh₃)₃HCl (entry 4) and RuHCl(P(o-tol)₃)₃ (entry 7) only provided trace amount of product in both cases. Both these catalysts are similar to RuHCl(CO)(PPh₃)₃, in that they were the ones that possessed three phosphine ligands, which may be pertinent to the reactivity. It is also notable that the ligands employed here were all significantly bulkier than PPh₃ which in this case may have hindered reactivity. It was thought the additional steric bulk of the ligand may have interfered with the coordination of the alkene to the ruthenium center.



Scheme 25. Intermolecular hydroacylation of alkene and benzaldehydes with different [Ru] catalysts

Table 1. Results from screening of various ruthenium catalysts on hydroacylation



Entry	[Ru]	(E/Z) ¹ H NMR Yield	¹ H NMR Yield	¹ H NMR Yield
1	RuHCl(CO)(PPh ₃) ₃	32/12%	<1%	4%
2	RuH(IMes)(PPh ₃) ₃ (CO)(Cl)	n.d.	n.d.	n.d.
3	RuH(PCy ₃) ₂ (CO)(Cl)	n.d.	n.d.	n.d.
4	Ru(PPh ₃) ₃ HCl	<1%	<1%	<1%
5	RuH(IMes)(PCy ₃) ₃ (CO)(Cl)	n.d.	n.d.	n.d.
6	RuH ₂ (IMes)(PPh ₃)(CO)(Cl)	n.d.	n.d.	<1%
7	RuHCl(P(o-tol)) ₃	<1%	<1%	<1%

n.d= not determined

Since the above mentioned catalysts were inactive in this transformation, we attempted to modify the parent catalyst to $\text{RuHCl}(\text{CO})(\text{PMePh}_2)_3$ **F2.1**. This catalyst utilizes an alternative phosphine methyldiphenylphosphane (Figure 2) that is smaller than PPh_3 , but yet more electron rich. This modification may favour interaction of the alkene or aldehyde on the ruthenium center with less steric hindrance. This notion may be in line with the theory that less sterics on the substrate also favours reactivity as discussed in Section 2.1. A procedure for synthesis of $\text{RuHCl}(\text{CO})(\text{PPh}_3)_3$ was adapted swapping the PPh_3 with PMePh_2 .³⁵ However, the synthesis of this catalyst was not trivial and attempts to generate the catalyst in situ via ligand exchange of the phosphine ligand were unsuccessful. An alternate synthetic route may be necessary to develop this family of smaller catalysts in order to test our hypothesis.

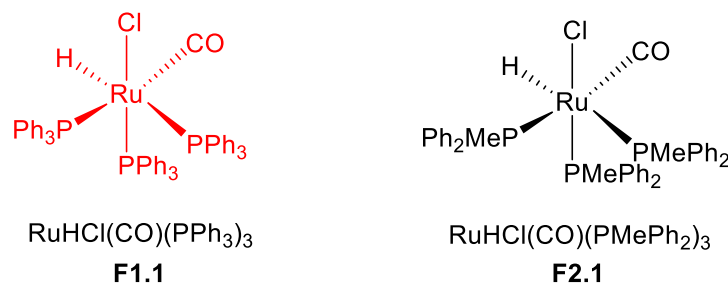


Figure 2. Structure of $\text{RuHCl}(\text{CO})(\text{PPh}_3)_3$ versus $\text{RuHCl}(\text{CO})(\text{PMePh}_2)_3$

2.4. Coupling of aldehydes and alkenes via allylic oxidation

Another method that was investigated was to selectively oxidize the olefin through a π -allyl species to facilitate the addition step. As the migratory insertion step remains a challenge due to the alkene's inability to form an allylic species, this is an important investigation to undertake. Literature precedents have outlined strategies for oxidation of alkenes via π -allyl intermediates.

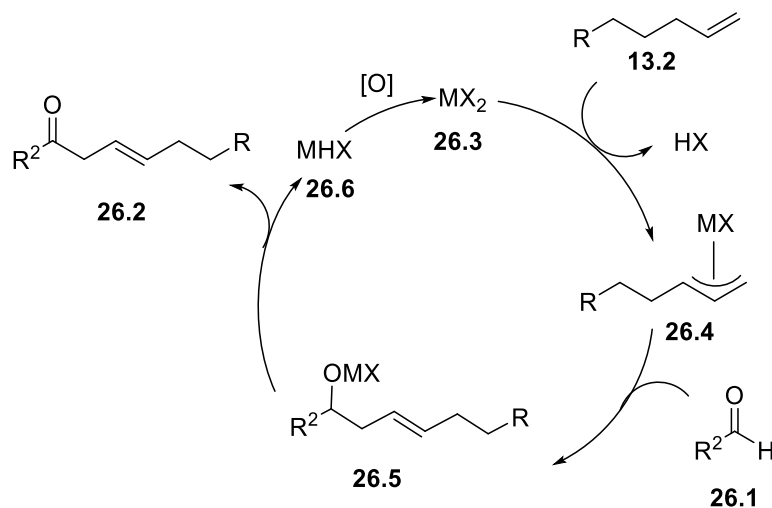
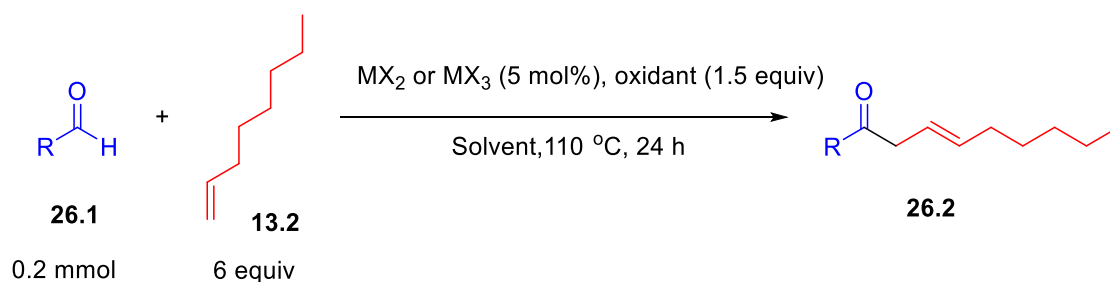
³⁵ Zhu, S.; Lu, X.; Luo, Y.; Zhang, W.; Jiang, H.; Yan, M.; Zeng, W., *Org. Lett.* **2013**, *15*, 1440.

White and co-workers reported a few systems for the oxidation of saturated C-H bond. Their allylic oxidation methods involve the use of palladium (II) salts in acetic acid to transform olefins into mixtures of allylic acetates.³⁶ Notably, these are believed to react via substitution of π -allyl intermediates via allylic C-H cleavage, followed by nucleophilic attack of the acetate.³⁷

Having access to a few methods for oxidative allylation, we hoped to find a catalytic system that can undergo a metal-allylic species to enable the migratory insertion step of a carbonyl. A mechanism to access this is proposed in **Scheme 26**. Starting with a metal **26.3** with an oxidation state of two or three, it will proceed to form a metal-allyl species **26.4** with the alkene **13.2** upon the loss of HX. The carbonyl of the aldehyde will then insert in the allyl species forming metal alkoxide species **26.5**. Upon elimination, the final ketone **26.2** will be generated along with MHX, which will then be oxidized to regenerate the active catalyst **26.3**.

³⁶ Chen, M. S.; White, M. C., *J. Am. Chem. Soc.* **2004**, *126*, 1346.

³⁷ Hansson, S.; Heumann, A.; Rein, T.; Aakermark, B., *J. Org. Chem.* **1990**, *55*, 975.



Scheme 26. Proposed mechanism for formation ketones via allylic oxidation

In order to explore the maximum number of catalytic systems that potentially can undergo this mechanism, the method of high-throughput screening was used. Several variables, in particular the choice of catalysts and oxidants were varied. According to literature, several metals have been used for selective oxidation of olefins apart from $\text{Pd}(\text{OAc})_2$ and PdCl_2 . $\text{RuCl}_2(\text{p-cymene})_2$,³⁸ $\text{Ru}(\text{Me-allyl})_2\text{COD}$,³⁹ RuCl_3 ,⁴⁰ $\text{Ir}(\text{COD})\text{Cl}_2$,⁴¹ and $[\text{Rh}(\text{cod})\text{Cl}]_2$ ⁴² have been shown to either perform allylic oxidation and/or form π -allyl metal species with alkenes. Platinum has no precedents in forming π -allyl intermediates, but rather have been shown to have

³⁸ Graczyk, K.; Ma, W.; Ackermann, L., *Org. Lett.* **2012**, *14*, 4110.

³⁹ Kondo, T.; Ono, H.; Satake, N.; Mitsudo, T.-a.; Watanabe, Y., *Organometallics*. **1995**, *14*, 1945.

⁴⁰ Kondo, T.; Ono, H.; Satake, N.; Mitsudo, T.-a.; Watanabe, Y., *Organometallics*. **1995**, *14*, 1945.

⁴¹ Takeuchi, R. *Synlett*. **2002**, *12*, 1954.

⁴² Mimoun, H.; Perez Machirant, M. M.; Sere de Roch, I., *J. Am. Chem. Soc.* **1978**, *100*, 5437.

reactivity to olefins in olefin metathesis.⁴³ Therefore, PtCl₂, PtCl₄ were selected here. In order to maximize discovery, some other metals that have not been reported in literature for this sort of transformation were used in this screening. These metals include, IrCl₃, AuCl(SMe)₂, and NiCl₂(dppp).

The two most common oxidants found in literature for allylic oxidation are benzoquinone⁴⁴ and copper acetate.⁴⁵ Choice of solvent also followed precedents in literature, using DMSO: acetic acid from White's paper and dioxane as a common organic solvent. Finally the choice of substrates were octanal and benzaldehyde with a terminal alkene, octene. Thus, the screening would explore reactivity between aliphatic aldehydes versus benzylic aldehydes with terminal alkenes. Unfortunately, the results of the screening did not provide any evidence of the carbon-carbon bond formation between an aldehyde and alkene. Further investigations remain to be done to individually probe the challenging steps of the mechanism.

2.5. Transition-metal catalyzed oxidative decarbonylation of an aldol adduct

From the results of the high-throughput screening we observed another interesting product during the analysis on the GC-MS that seems to suggest carbon-carbon formation through another metal-catalyzed mechanism. A ketone product, tridecan-7-one **27.2** was observed in

⁴³ Chianese, A. R.; Lee, S. J.; Gagné, M. R., *Angew. Chem. Int. Ed.* **2007**, *46*, 4042.

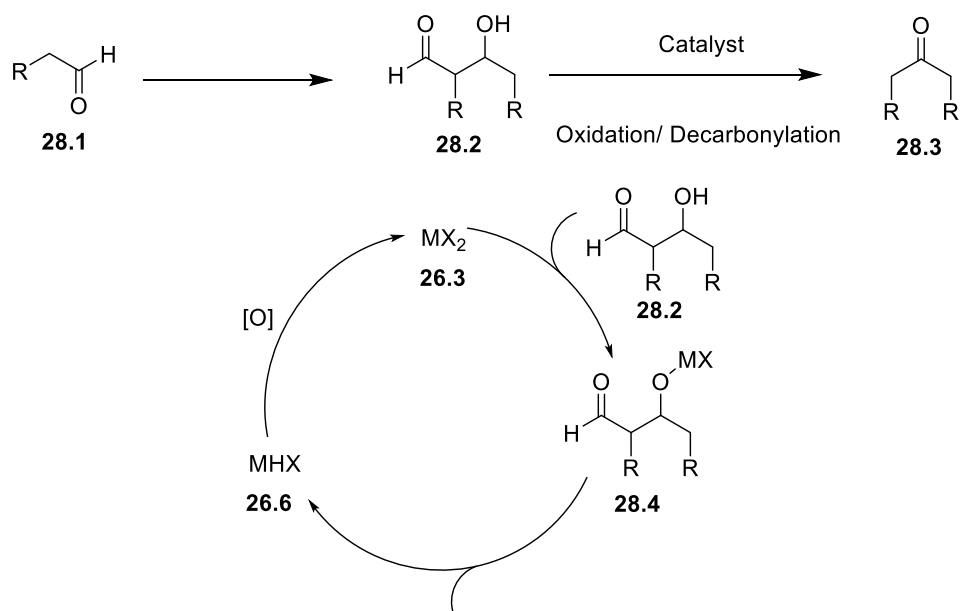
⁴⁴ a) Chen, M. S.; White, M. C., *J. Am. Chem. Soc.* **2004**, *126*, 1346. b) Hull, K. L.; Sanford, M. S., *J. Am. Chem. Soc.* **2009**, *131*, 9651.

⁴⁵ Graczyk, K.; Ma, W.; Ackermann, L., *Org. Lett.* **2012**, *14*, 4110.

some vials that contained the aliphatic aldehyde octanal and 2-octene substrates, with $[\text{RuCl}_2(\text{p-cymene})]_2$ or $[\text{Ir}(\text{COD})_2]\text{Cl}_2$ as the catalyst and $\text{Cu}(\text{OAc})_2$ as the oxidant. By performing a few control experiments on bench, it was concluded that octene did not participate in the reaction. Trace product was observed by GC-MS with only the presence of the catalyst with the aldehyde and the presence of the oxidant seemed to increase the product slightly, suggesting that the role of the oxidant is relevant.

Scheme 27. Observed product from high-throughput screening

From these sets of experiments, we were able to develop a hypothesis for the formation of this ketone product. As the aldehyde is the only substrate participating in the reaction, it likely easily undergoes self-aldol condensation with its enolate form. In order to arrive to the observed product, the condensation is likely followed by an oxidation and decarbonylation (Scheme 28).

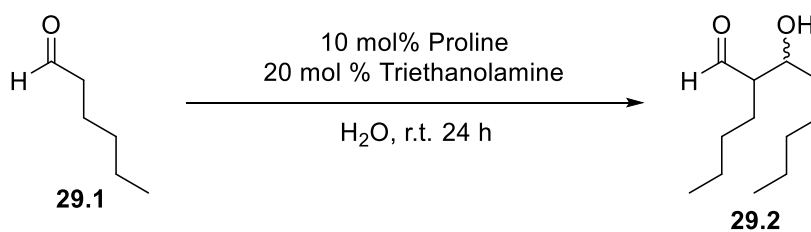


Scheme 28. Proposed mechanistic pathways of formation of ketone product

A mechanism was proposed starting from the aldol adduct intermediate **28.2** (**Scheme 28**). From this intermediate, a transition metal catalyst likely participates in the oxidation of the alcohol of the aldol adduct to a ketone **28.3**, by forming a metal alkoxy species **28.4**. From here, the metal is either reoxidized to the active catalyst or participates further in decarbonylation or decarboxylation step to give the final ketone **28.3**. It is also possible that the catalyst does not participate in the decarbonylation or decarboxylation step. In which case, intermediate **28.5** can undergo Path A or Path B to form the final ketone **28.3**. Further mechanistic studies remain to be done to test the validity of other intermediates.

In order to test the validity of the oxidative hypothesis, 2-butyl-3-hydroxyoctanal **29.2** was synthesized and used as the representative aldol adduct for subsequent reactions. The objective was to subject the aldol adduct to similar oxidative conditions where the new product was observed to see if it can give the same ketone product at a higher yield.

Literature procedures have outlined some methods for the synthesis of an isolated aldol adduct **29.2**, but the isolation of this adduct is challenging as it faces issues for chemo- and regioselectivity. Many side reactions from aldehydes may arise such as dehydration, oligomerization, and Tischenko products.⁴⁶ Most procedures require the protection of the alcohol via silyl enol ethers to prevent side reactivity.⁴⁷ Notably, MacMillan developed a procedure for synthesis of cross-aldol reactions of aldehydes using Proline catalysis that possesses high diastereo- and enantiocontrol.⁴⁸ The procedure adapted from Fréchet and co-workers using proline-catalysis under aqueous conditions was the most efficient synthetic route to access this molecule (**Scheme 29**).⁴⁹ Enantioselectivity is irrelevant in our desired transformation, since we sought to oxidize the corresponding alcohol to a ketone. Therefore, the racemic mixture was isolated.



Scheme 29. Synthesis of aldol adduct intermediate

Using one of the conditions that provided the new product, we replicated the condition on bench with the aliphatic aldehyde (**Scheme 30 A**) and the aldol adduct **29.2** respectively (**Scheme 30 B-C**). The first condition that was applied is using [RuCl₂(p-cymene)]₂ in the presence of dppb as the ligand, Cs₂CO₃ as the base, and acetone as the hydrogen acceptor in dioxane (**Scheme 30 B**). Our hypothesis proved to be correct as when the same catalytic conditions were applied to the aldehyde, it only provided a 4% yield. Whereas when substrate

⁴⁶ Denmark, S. E.; Bui, T., *Proceedings of the National Academy of Sciences of the United States of America*. **2004**, *101*, 5439.

⁴⁷ Denmark, S. E.; Ghosh, S. K., *Angew. Chem. Int. Ed.* **2001**, *40*, 4759.

⁴⁸ Northrup, A. B.; MacMillan, D. W. C., *J. Am. Chem. Soc.* **2002** *124*, 6798.

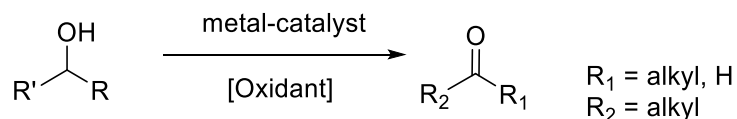
⁴⁹ Chi, Y.; Scroggins, S. T.; Boz, E.; Fréchet, J. M. J., *J. Am. Chem. Soc.* **2008**, *130*, 17287.

29.2 was used, the yield increased to 12%. Another system from the high-throughput screening was also applied to the aldol adduct, which used $[\text{Ir}(\text{COD})]_2$ and $\text{Cu}(\text{OAc})_2$ as the oxidant, which gave a yield of 18% (**Scheme 30 C**). The absence of the oxidants in both cases provided no reaction, which supports the theory that an oxidant is pertinent in the reaction. This provides evidence that **29.2** is shown to be the intermediate of the reaction. The intermediate can be further confirmed if mechanistic studies were done to trap the intermediate from the starting aldehyde.

Scheme 30. Probing of intermediate species under different oxidative conditions

With this prospect, we sought to improve conditions to increase the yield. In order to test if oxidation occurred after aldol condensation, we subjected the **29.2** to traditional non-catalytic oxidative conditions. Many reagents for alcohol oxidations are known, namely hypochlorite, chromium (VI) oxide, dichromate, manganese (IV) oxide, permanganate and

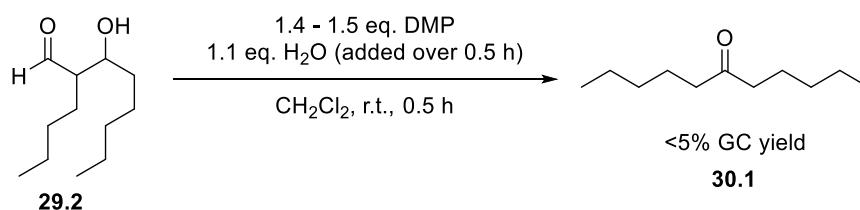
ruthenium (VIII) oxide.⁵⁰ However, these are used stoichiometrically and are often hazardous or toxic, which renders it inefficient from an economic and environmental point of view. In the quest to use more effective catalytic oxidation processes, only a few more “traditional methods” were applied to our system to explore its reactivity (**Scheme 31**).



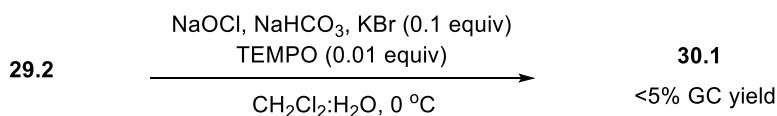
Scheme 31. General scheme for oxidation of alcohols to ketones or aldehydes

The methods selected were relatively mild compared to the ones listed above. Notably the Dess-Martin and TEMPO oxidation were applied to this substrate. Dess-Martin oxidation is known for oxidation of secondary alcohols into ketones.⁵¹ TEMPO oxidation⁵² is another facile way to oxidize primary or secondary alcohols into aldehydes or ketones respectively. Yields from these two oxidations were less than 5% by GC yield (**Scheme 32**).

Dess Martin Oxidation



TEMPO Oxidation



⁵⁰ Dijkman, A.; Marino-González, A.; Mairata i Payeras, A.; Arends, I. W. C. E.; Sheldon, R. A., *J. Am. Chem. Soc.* **2001**, *123*, 6826.

⁵¹ Meyer, S.D.; Schreiber, S.L., *J. Org. Chem.* **1994**, *59*, 7549.

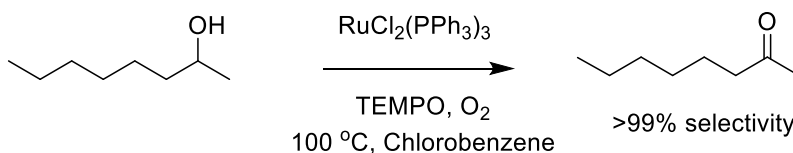
⁵² Lucio Anelli, P.; Biffi, C.; Montanari, F.; Quici, S., *J. Org. Chem.* **1987**, *52*, 2559.

Scheme 32. Testing traditional oxidative conditions

These results show that traditional oxidative conditions were not effective in the oxidation of aldol like adducts. Therefore, it is likely that the oxidation step after the formation of the **29.2** involves the aid of the catalyst. There is precedent that proposed a metal-catalyzed oxidation. Some of the metals involved in these oxidative processes include ruthenium, palladium, copper and iridium.

Ruthenium catalysts in particular, which are widely used in other applications in organic synthesis, have been investigated. Sheldon and co-workers have reported that $\text{RuCl}_2(\text{PPh}_3)_3$, and RuCl_3 are known to perform alcohol oxidation in the presence of stoichiometric oxidants such as iodosobenzene, TEMPO, or peroxides and etc. (

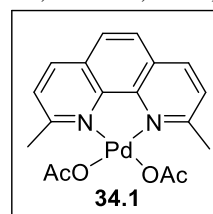
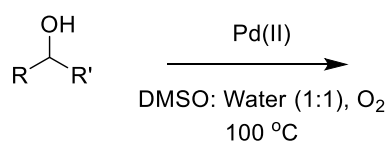
Scheme 33).⁵³



Scheme 33. Sheldon's strategy for ruthenium catalyzed oxidation of secondary alcohols mediated by TEMPO⁵³

Palladium oxidation reactions are known since the breakthrough Pd(II) oxidation known as Wacker process. The challenge using Pd(II) catalysts is the re-oxidation of Pd(0) species by oxygen to the active Pd(II). Rather than the use of co-catalysts to facilitate the re-oxidation process, efforts had been made to develop a single palladium complex with chelating ligands, which allow the tuning of catalytic activity and selectivity. For example, Waymouth and co-workers reported that a $\text{Pd}(\text{OAc})_2/\text{pyridine}$ system, which utilize a uniquely synthesized

⁵³ Dijkman, A.; Marino-González, A.; Mairata i Payeras, A.; Arends, I. W. C. E.; Sheldon, R. A., *J. Am. Chem. Soc.* **2001**, *123*, 6826.



catalyst [(neocuproine)Pd(μ -OAc)]₂-(OTf)₂ **34.1** to mediate oxidative transformations (**Scheme 34**)⁵⁴.

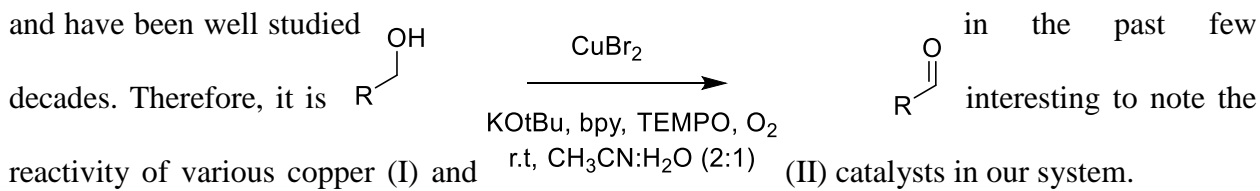
Scheme 34. Waymouth's strategy for oxidation of alcohols using palladium catalyst⁵⁴

Sigman and co-workers reported that Pd-NHC complexes catalyze the oxidation of alcohols under air at room temperature.⁵⁵ Sigman attributes the success of these systems to the dual role acetate can play as an anionic ligand and as a base for intramolecular deprotonation of the palladium-bound alcohol species. As palladium is a convenient metal used in oxidation, we proceeded to screen a few palladium-ligated complexes in our system.

⁵⁴ Conley, N. R.; Labios, L. A.; Pearson, D. M.; McCrory, C. C. L.; Waymouth, R. M., *Organometallics*. **2007**, *26*, 5447.

⁵⁵ Schultz, M. J.; Hamilton, S. S.; Jensen, D. R.; Sigman, M. S., *J. Org. Chem.* **2005**, *70*, 3343.

Copper catalysts are also particularly advantageous and highly selective in aerobic oxidation transformations. Recently, Sheldon and co-workers reported a copper (II) catalyzed aerobic oxidation of alcohols using a $\text{CuBr}_2(\text{Bipy})$ -TEMPO catalyst (Scheme 35).⁵⁶ Stahl and co-workers later reported (Bpy)Cu(I)/TEMPO system in the presence of that can selectively oxidize primary alcohols to aldehydes.⁵⁷ Copper catalysts offer a cheap and facile method of oxidation and have been well studied in the past few decades. Therefore, it is interesting to note the reactivity of various copper (I) and (II) catalysts in our system.



Scheme 35. Sheldon's strategy for copper catalyzed oxidation of alcohols mediated by TEMPO⁵⁶

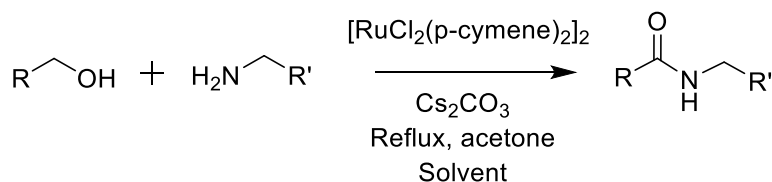
Other than using stoichiometric oxidant as the oxidizing agent, hydrogen acceptors can also be employed for the transformation of alcohols into ketones or aldehydes, such as Oppenauer-type oxidation.⁵⁸ More recently, Williams and co-workers reported ruthenium catalyzed oxidation of alcohols into amides via a coupling of primary alcohols and amines, using acetone as the hydrogen acceptor (**Scheme 36**).⁵⁹

⁵⁶ Gamez, P.; Arends, I. W. C. E.; Sheldon, R. A.; Reedijk, J., *Adv. Synth. Catal.* **2004**, 346, 805.

⁵⁷ Hoover, J. M.; Stahl, S. S., *J. Am. Chem. Soc.* **2011**, 133, 16901.

⁵⁸ Oppenauer, R. V., *Recl. Trav. Chim. Pays-Bas.* **1937**, 56, 137.

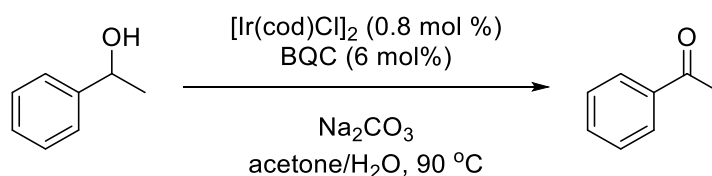
⁵⁹ Watson, A. J. A.; Maxwell, A. C.; Williams, J. M. J., *Org. Lett.* **2009**, 11, 2667.



Scheme 36. William's strategy of oxidation of alcohols into amines via hydrogen transfer⁵⁹

Other hydrogen acceptors that could potentially work under these oxidative conditions can include, but not limited to simple alkenes such as styrene, cyclohexene, and norbornene, ketones such as 2-butanone and cyclohexanone.

In addition, Ajjiou reported the selective oxidation of benzylic and aliphatic secondary alcohols using $[\text{Ir}(\text{cod})\text{Cl}]_2$, 2,2'-biquinoline-4,4'-dicarboxylic acid dipotassium salt (BQC), and acetone as the hydrogen acceptor (**Scheme 37**).⁶⁰ Hydrogen transfer methods of oxidation offer a milder catalytic system than using stoichiometric amounts of oxidants. Therefore, we also applied this alternative oxidative pathway to our system.



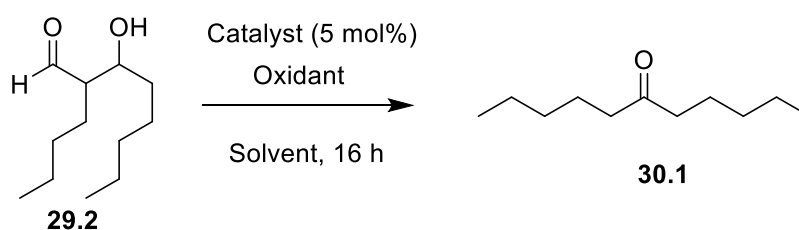
Scheme 37. Ajjiou's strategy for oxidation of secondary alcohols using iridium catalysts via hydrogen transfer⁶⁰

It is interesting to note that the systems reported in literature for oxidation of alcohol does not encompass the selective oxidation of an aldol intermediate. Perhaps the lacking in literature in this area is due to the difficulty in isolating the intermediate and the competing

⁶⁰ Nait Ajjiou, A., *Tetrahedron Lett.* **2001**, 42, 13.

dehydration pathway to form an α,β conjugated carbonyl compound. Having a good inventory of oxidative conditions that could be applied to our system, some experiments with these conditions inspired from these literature studies were conducted. A summary of results is presented in **Table 2**.

Table 2. Testing of different oxidative conditions on aldol adduct



Entry	Catalyst	Temp °C	Base	Solvent	Oxidant	¹ H NMR Yield
1	RuCl ₂ (PPh ₃) ₃	56	--	acetone	NMO (2 equiv)	6%
2	RuCl ₂ (PPh ₃) ₃	100	--	toluene	TEMPO (6 mol%), O ₂	3%
3	RuCl ₂ (PPh ₃) ₃	90	Na ₂ CO ₃ (4 mol%)	toluene	hexanal (3 equiv)	7%
4	RuCl ₂ (PPh ₃) ₃	90	Na ₂ CO ₃ (4 mol%)	toluene	benzaldehyde (3 equiv)	5%
5	[RuCl ₂ (p-cymene)] ₂	100	Cs ₂ CO ₃ (10 mol%)	dioxane	acetone (2.5 equiv)	12%
6	Ir(COD)Cl ₂	56	KOH (10 mol%)	acetone	acetone (solvent)	6%
7	Ir(COD)Cl ₂	110	--	dioxane	Cu(OAc) ₂ (1.5 equiv)	18%
8	Pd(OAc) ₂	100	K ₂ CO ₃ (1.3 equiv)	DMF	bromobenzene (1 equiv)	8%
9	Cu(OTf) ₂	80	---	toluene	TEMPO (5 mol%), O ₂	10%

We found that the original two catalytic systems that gave hits in our first screening still gave the most promising results. Other oxidative conditions provided significantly lower yields of less than 10%.

Applying these oxidative conditions on bench was quite limited in screening of variables to find the desired combination of metal and oxidant. Therefore, we decided to use the high-throughput method to screen selected variables in order to optimize conditions. From the commonly used metals for aerobic oxidation, Cu(OTf)₂,⁶¹ CuCl,⁶² [RuCl₂(p-cymene)]₂,⁶³ RuCl₂(PPh₃)₃,⁶⁴ Ir(COD)Cl₂,⁶⁵ IrCl₃,⁶⁶ Pd(OAc)₂⁶⁷ were selected as the metals of choice. A few oxidants that seem promising from the preceding results were also selected. TEMPO/PhI (OAc)₂, Cu(OAc)₂, and NMO were used as oxidants. Similar to the first screening, the atmosphere in which the screening would be conducted would be under oxygen. A few ligands that were found to be compatible with the selected metals in literature were used. The ligands include, 1, 10 phenanthroline, dppb, BINAP and SIPr•HCl. The NHC ligand SIPr•HCl was also used as different class of ligands than typical phosphine or pyridine derived ligands. Their electron donating ability could perhaps increase nucleophilicity on the metal center as will be discussed further in Section 5.4. Typical solvents used in oxidative reaction conditions such as toluene, dioxane, water, acetonitrile: DMSO were selected.

Not surprisingly, the original two metals that gave the desired product **30.1** in the first screening produced relatively good results in this second screening. [RuCl₂(p-cymene)]₂ in the presence of acetone as the hydrogen acceptor and Xantphos as the chelating ligand gave promising results. As the main side product of the reaction was the dehydrated aldol adduct **30.2**,

⁶¹ Hoover, J. M.; Stahl, S. S., *J. Am. Chem. Soc.* **2011**, *133*, 16901.

⁶² Semmelhack, M. F.; Schmid, C. R.; Cortes, D. A.; Chou, C. S., *J. Am. Chem. Soc.* **1984**, *106*, 3374.

⁶³ Watson, A. J. A.; Maxwell, A. C.; Williams, J. M. J., *Org. Lett.* **2009**, *11*, 2667.

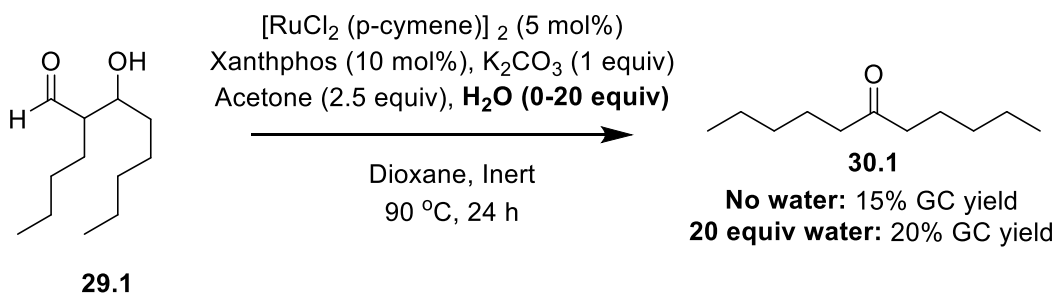
⁶⁴ (a) Wang, G. Z.; Backvall, J.-E., *J. Chem. Soc., Chem. Commun.* **1992**, 337, (b) Dijkman, A.; Marino-González, A.; Mairata i Payaras, A.; Arends, I. W. C. E.; Sheldon, R. A., *J. Am. Chem. Soc.* **2001**, *123*, 6826.

⁶⁵ Nait Ajjou, A., *Tetrahedron Lett.* **2001**, *42*, 13.

⁶⁶ Suzuki, T. *Chem. Rev.*, **2011**, *111*, 1825.

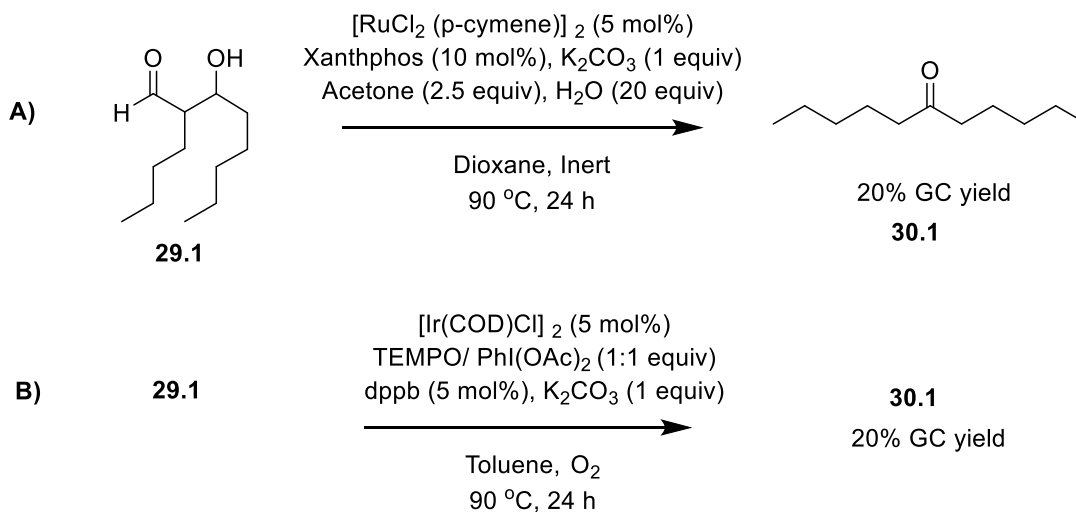
⁶⁷ Conley, N. R.; Labios, L. A.; Pearson, D. M.; McCrory, C. C. L.; Waymouth, R. M., *Organometallics* **2007**, *26*, 5447.

20 equivalents of water were added to push the equilibrium towards the desired product (**Scheme 38**). Several experiments were done to determine the optimal amount of water.



Scheme 38. Effect of water on equilibrium of catalytic oxidation of aldol adduct

The same system applied to $\text{Ir}(\text{COD})\text{Cl}_2$ failed as the catalyst in this case may be water or moisture sensitive. This metal works the best with TEMPO/ $\text{PhI}(\text{OAc})_2$ system that yielded a comparable result with $[\text{RuCl}_2(\text{p-cymene})]_2$. In this case, this system works best under aerobic conditions (**Scheme 39B**). Control experiments were conducted to validate the relevancy of each component.



Scheme 39. Optimized condition of oxidative decarbonylation of an aldol adduct

Studies to support the decarbonylation step have not been done. However, there is evidence in literature that supports transition metal-catalyzed decarbonylation⁶⁸ or decarboxylation⁶⁹ in the case if the aldehyde is oxidized into a carboxylic acid moiety.

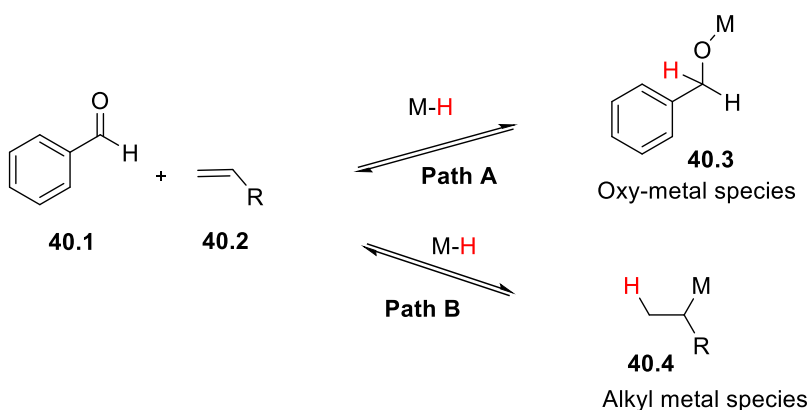
The scope of this study is limited to self-condensation of aldehydes and the competing dehydrated pathway as shown in **Scheme 38**. More investigations of mechanistic problems in this reaction must be done in order to resolve the competing side reactions and potential degradation of starting material.

⁶⁸ a) Fristrup, P.; Kreis, M.; Palmelund, A.; Norrby, P.-O.; Madsen, R., *J. Am. Chem. Soc.* **2008**, *130*, 5206. b) O'Connor, J. M.; Ma, J., *J. Org. Chem.* **1992**, *57*, 5075.

⁶⁹ a) Magdziak, D.; Lalic, G.; Lee, H. M.; Fortner, K. C.; Aloise, A. D.; Shair, M. D., *J. Am. Chem. Soc.* **2005**, *127*, 7284. b) Tunge, J. A.; Burger, E. C., *Eur. J. Org. Chem.* **2005**, *2005*, 1715.

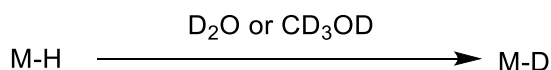
2.6. Ruthenium catalyzed deuteration of aldehydes⁷⁰

One proposed reason for the modest reactivity of the various metal hydride catalysts examined is the potential competition between π -bond insertion of the olefin (path B) and aldehyde starting material (**Scheme 40**). If the metal hydride shows preferred reaction with the aldehyde to form an oxy-metal species **40.3** (path A), the metal may spend a significant amount of time in this off-cycle intermediate.



Scheme 40. Competing pathways of π -bond insertion of metal hydride catalysts

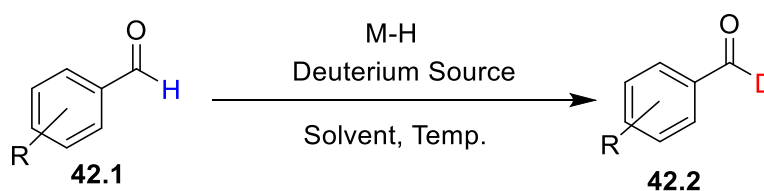
To test this hypothesis, we conducted deuterium labeling studies to track the transfer of the hydrogen. Therefore, we purposely doped the solution with common sources of deuterium such as d4-methanol and D₂O in hopes of forming a metal-deuterium (M-D) species from the metal-hydride (M-H) species (**Scheme 41**).



Scheme 41. Conversion of metal-hydride into metal-deuterium

⁷⁰ Work done in collaboration with undergraduates Eric Isbrandt, and Mohammad P. Jamshidi

Indeed, there was evidence of deuterated aldehyde as observed in the ^1H NMR, which suggests the validity of the competing π -bond insertion of the aldehyde. From this observation, we found it interesting to pursue this off-cycle catalytic system to synthesize deuterated aldehydes **42.2** (Scheme 42). In order to investigate the mechanism and scope of this reaction further, we performed optimization on this system and were able to achieve promising results.



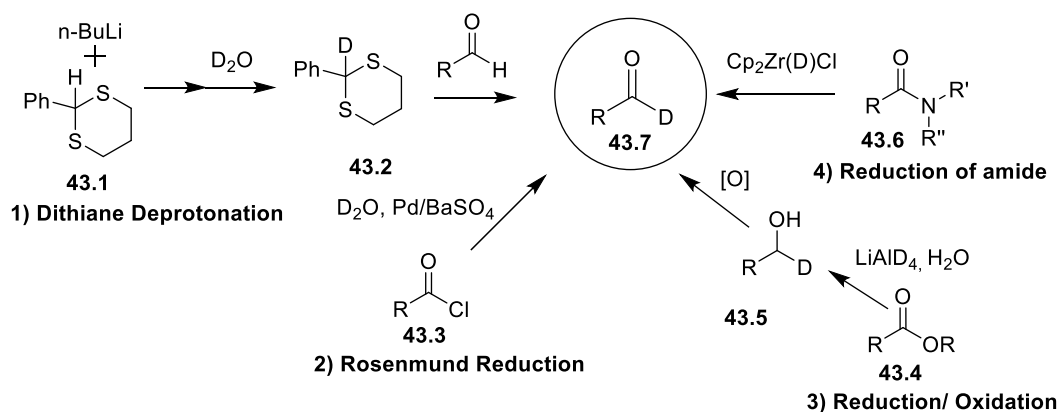
Scheme 42. General reaction scheme for catalytic deuteration of aldehydes

Deuterium-labeled compounds have many useful applications in organic and bioorganic studies, some of which can be used for solvents in NMR spectroscopy, probes for mechanistic studies, and labeling drugs or other useful compounds.⁷¹ There has been interest to develop efficient methods to access these species. In our system, we found a one-step method that allows synthesis of deuterated aldehydes via direct H/D exchange between organic compounds and D-source, which is novel and attractive. Previous methods often entail multi-step synthesis, harsh conditions such as the reduction of carbonyl with reagents such as NaBD_4 , LiAlD_4 , or pose limitations on the substrates.⁷² Some traditional pathways that require multi-step synthesis are shown below. The first requires a deprotonation of a dithiane species such that the deuterium source can be attached on the dithiane species **43.2**. The second example is the Rosenmund reduction of acid chlorides **43.2**, which give low deuterium incorporation. The third example

⁷¹ Krische, M. J.; Shibahara, F.; Bower, J. F., *J Am Chem Soc.* **2008**, *130*, 14120.

⁷² Bai, W.; Lee, K.-H.; Tse, S. K. S.; Chan, K. W.; Lin, Z.; Jia, G., *Organometallics.* **2015**, *34*, 3686.

demonstrates a lithium aluminum deuteride reduction followed by an oxidation. Finally, the fourth utilizes the zirconium catalyst to perform the reduction of an amide **43.6** to a carbonyl species and incorporating the deuterium (**Scheme 43**).⁷³



Scheme 43. Traditional methods of aldehyde deuteration

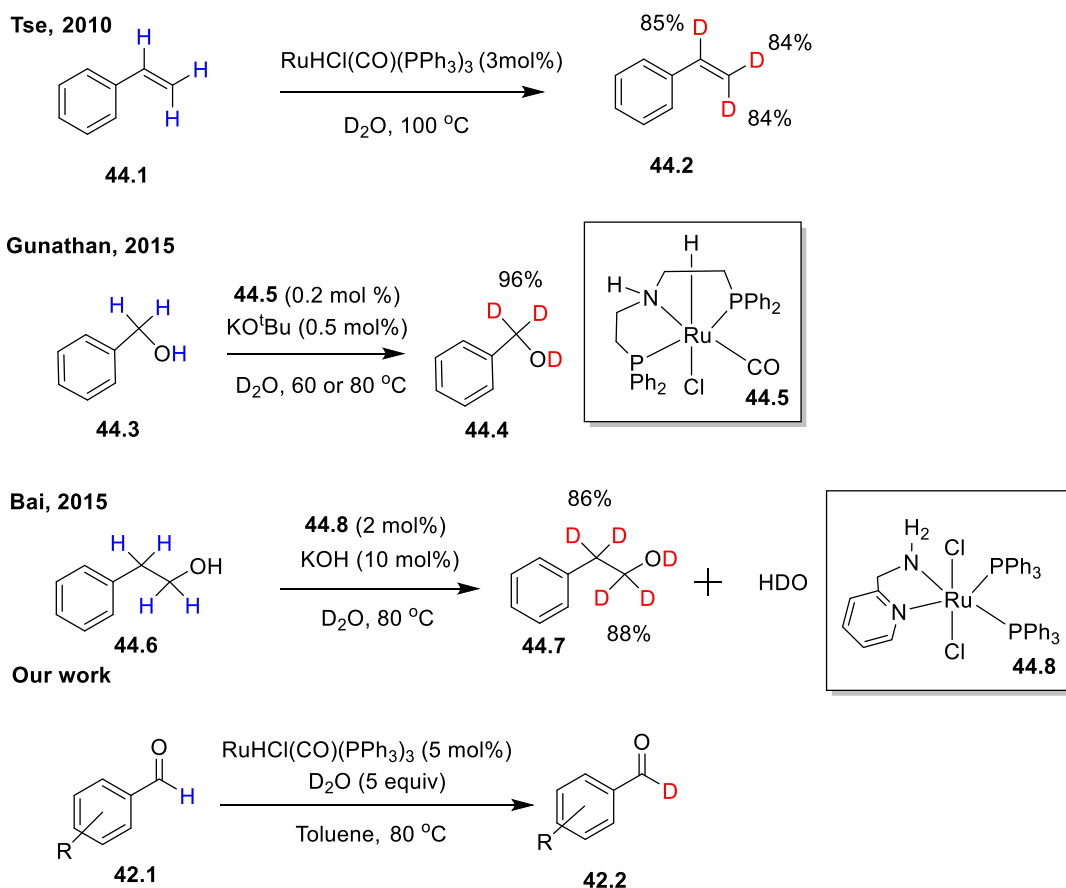
A few metal catalyzed methods have been investigated for deuterium incorporation. Not surprisingly, ruthenium catalysts have been investigated in this area. Tse's group successfully employed $RuHCl(CO)(PPh_3)_3$ to perform H/D exchange between olefins, using D_2O as their deuterium source.⁷⁴ Gunathan and co-workers also used a ruthenium catalyst with pincer ligands, also known as one of Milstein's catalysts **44.5** to perform deuteration of primary alcohols in the presence of D_2O .⁷⁵ Finally, Bai and co-workers also investigated a series of ruthenium catalysts that can perform the H/D exchange of alcohols with D_2O .⁷⁶ **Scheme 44** summarizes these previous studies of metal catalyzed deuteration. Our method shows to be a novel method to give access to the deuterated aldehyde in one-pot reaction and in one facile step.

⁷³ Spletstoser, J. T.; White, J. M.; Georg, G. I., *Tetrahedron Lett.* **2004**, 45, 2787.

⁷⁴ Tse, S. K. S.; Xue, P.; Lin, Z.; Jia, G., *Adv. Synth. Catal.* **2010**, 352, 1512.

⁷⁵ Chatterjee, B.; Gunanathan, C., *Org. Lett.* **2015**, 17, 4794.

⁷⁶ Bai, W.; Lee, K.-H.; Tse, S. K. S.; Chan, K. W.; Lin, Z.; Jia, G., *Organometallics.* **2015**, 34, 3686.

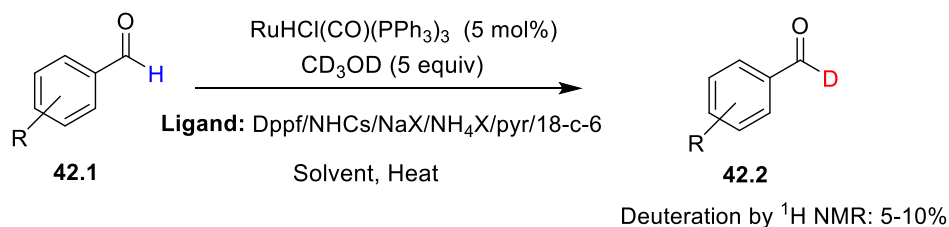


Scheme 44. Development in metal-catalyzed deuteration⁷⁴⁻⁷⁶

2.6.1.1. Optimization of ruthenium catalyzed deuteration of aldehydes⁷⁷

A catalyst and ligand screen was done to determine the most efficient catalyst for the deuteration of aldehydes (Table 3). Several different catalysts such as Pd(OAc)₂, PdCl₂, Ni(acac)₂, [Rh(COD)Cl]₂, [Ir(COD)Cl]₂ were explored in the reaction conditions and gave yields of less than 20% deuteration (entries 1-5). Returning to the parent catalyst RuHCl(CO)(PPh₃)₃, we also tried varying ligands to probe different reactivity; however, the addition of other phosphine ligands, NHCs or additives does not seem to influence reactivity (**Scheme 45**).

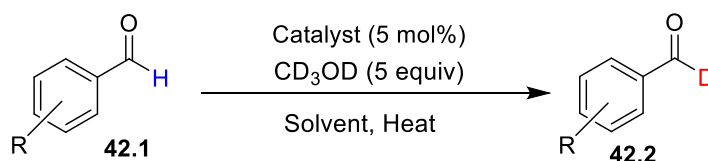
⁷⁷ Work done in collaboration with undergraduates, Eric Isbrandt, and Mohammad P. Jamshidi.



Scheme 45. Effect of ligands on ruthenium catalyzed deuteration of aldehydes

These results suggest that it is not facile to perform ligand exchange with the ligands already attached to the metal center. Using a slightly modified catalyst, $\text{RuHCl(CO)(PCy}_3)_2$, as discussed in Section 2.3, gave only 22% yield of the deuterated aldehyde (entry 6). The use of the parent catalyst $\text{RuHCl(CO)(PPh}_3)_3$ or $\text{RuH}_2(\text{CO})(\text{PPh}_3)_3$ with the presence of acids HX as an exchange ligand seem to give the best conversion above 70% (entry 7). After screening variables such as solvent, temperature and deuterium sources the optimal condition was found to be 5 mol% of the catalyst in Toluene at 80 °C over 17 hours. D_2O was used as the optimal deuterium source, but d-methanol could also be used.

Table 3. Catalyst and ligand screen for deuteration of aldehydes

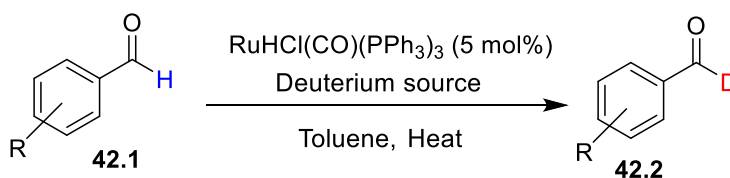


Entry	Catalyst	Ligand	% deuteration ^a
1	$[\text{Ir(COD)Cl}]_2$	---	0%
2	$[\text{Rh(COD)Cl}]_2$	PtBu ₃	<5%
3	Ni(acac)_2	dppf	20%
4	PdCl_2	dppf	<5%
5	Pd(OAc)_2	bpy	0%
6	$\text{RuHCl(CO)(PCy}_3)_2$	---	22%
7	$\text{RuH}_2(\text{CO})(\text{PPh}_3)_3$	HCl	70%

^a % deuteration determined by ¹H NMR

Table 4 shows the variation of deuterium source content on the effect on the yield. Conditions done with D₂O were screened on substrate p-methoxybenzaldehyde at 80 °C over 17h. It was found that using 7.5 equivalents of D₂O gave optimal yield of 82%. Increasing the deuterium source even more showed a slight decrease in yield to 69%. This decrease in yield is perhaps excessive water content in the reaction inhibit the reactivity of the catalyst. Conditions using CD₃OD were screened with the substrate 2-Naphthaldehyde at 100 °C. The use of CD₃OD required only a short time of 20 minutes to complete. However, it requires a higher temperature and deuterium loading. The deuterium source was increased up to 20 equivalents to reach optimal conditions of 93%. Iterative experiments were also done by doping the reaction vial with additional deuterium source after evaporation of solvent (See Experimental Section 4 for details).

Table 4. Optimization of deuterium source



Entry	D-Source	Equivalents	% deuteration ^a
1	D ₂ O	2	39%
2	D ₂ O	5	67%
3	D ₂ O	7.5	82%
4	D ₂ O	10	69%
5	CD ₃ OD	5	70%
6	CD ₃ OD	10	84%
7	CD ₃ OD	20	93%

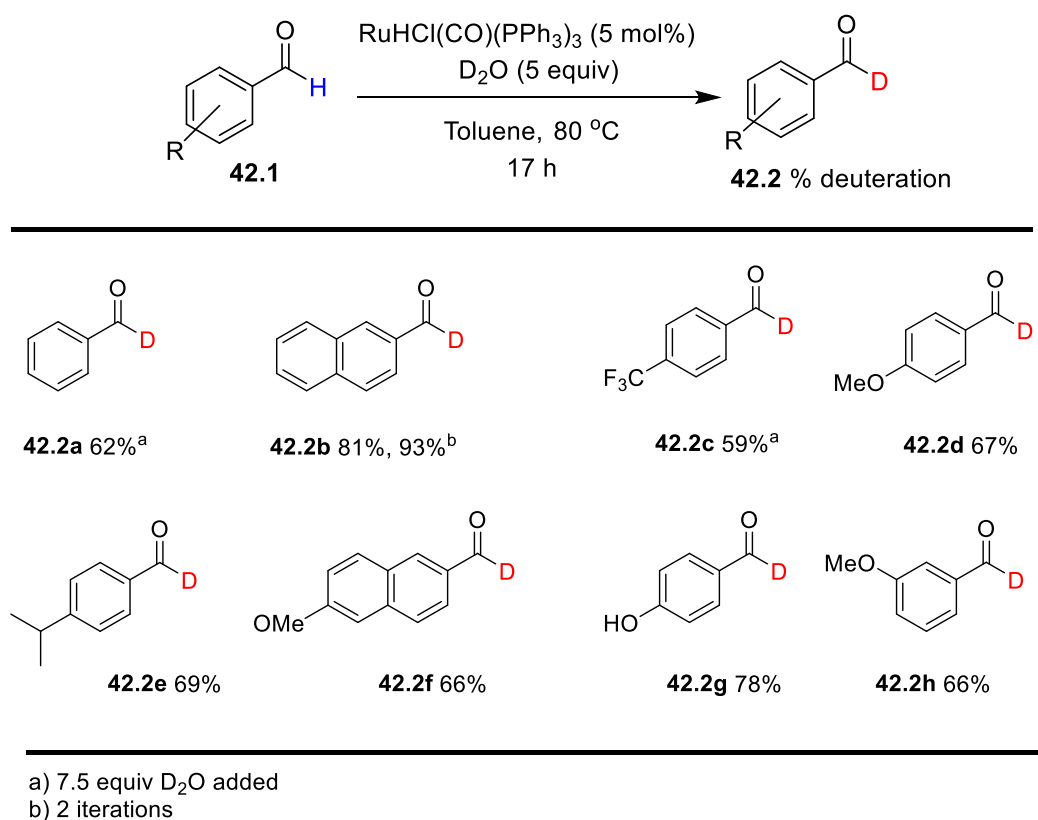
Note: Conditions with D₂O: p-methoxybenzaldehyde, 80 °C, 17 h. Conditions with CD₃OD: 2- Naphthaldehyde, 100 °C, 20min.

^a % deuteration determined by ¹H NMR.

2.6.1.2. Scope, proposed mechanism and limitations⁷⁸

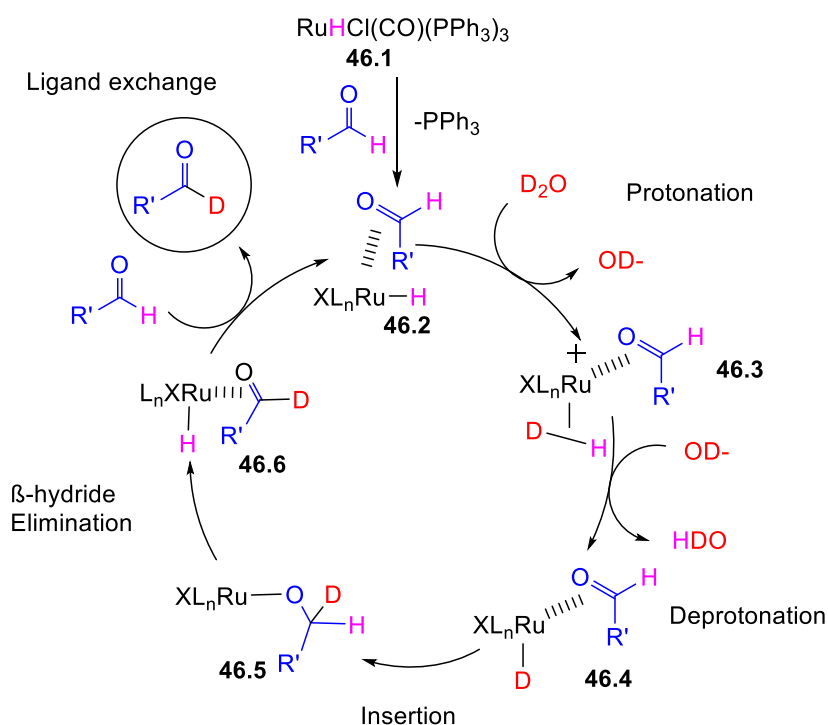
Satisfied with our optimal conditions, we explored the scope of the reaction by subjecting different aldehydes with varying functional group to test reactivity (**Table 5**). Electron withdrawing CF₃ and donating OMe groups were tried giving yields above 60%. The presence of a hydroxy group showed good selectivity for the site of deuteration. A few electron neutral species were also explored with good yields in the high 60%. Using 2- Naphthaldehyde (**42.2b**) gave the best yield thus far of 93% after two iterations. Current yields reported are NMR yields calculated with the ratio of an internal standard. Isolated yields have not yet been reported due to the difficulty of separation.

Table 5. Scope of deuterated aldehydes.



⁷⁸ Work done in collaboration with undergraduates, Eric Isbrandt, and Mohammad P. Jamshidi.

We proposed a possible mechanism for this transformation (Scheme 46). Starting with the ruthenium catalyst **46.1**, the aldehyde coordinates with the ruthenium center allowing the phosphine ligand to fall off. After coordination with the aldehyde, the Ru-H bond is protonated from the deuterium source such that the ruthenium center is a cationic species coordinating with a D-H ligand **46.3**. Then the OD⁻ species can deprotonate the hydrogen from the D-H ligand returning the ruthenium center back to its oxidation state of II. After the Ru-D species **46.4** is formed, the aldehyde would insert in the Ru-D bond giving complex **46.5**. Finally, after β -hydride elimination, it would yield the final deuterated aldehyde and the parent ruthenium hydride catalyst would be regenerated. Further mechanistic studies such as kinetic studies or trapping of intermediates remain to be done to elucidate the mechanism.



Scheme 46. Proposed mechanism for ruthenium catalyzed deuteration of aldehyde

In conclusion, efficient deuteration was achieved using facile and relatively cheap catalyst, $\text{RuHCl}(\text{CO})(\text{PPh}_3)_3$ and it was achieved using a one pot synthesis with mild conditions. Substrate scope demonstrated moderate success with most aromatic aldehydes. However, % deuteration was only reported from ^1H NMR and no isolated yield was reported which is a major limitation. In addition, aliphatic aldehydes would also need further investigation for its reactivity in this system. This is due to the fact of some inconsistencies with results and reproducibility. Nevertheless, this work has potential to be explored further with more challenging substrates.

3. Summary and future work

In summary, three methods of accessing a catalytic system for the intermolecular hydroacylation of aldehydes to alkenes were employed. First, reactivity between alkenes and aldehydes were attempted with different derivatives of styrene, unconjugated dienes, terminal aliphatic alkenes and benzaldehydes and aliphatic aldehydes. Upon applying Krische's optimized conditions for hydroacylation of conjugated dienes to our case of styrenes and benzaldehydes only gave trace amount of product detectable by GC. After several rounds of screening variables, 4% yield was obtained between a terminal aliphatic alkene, 1-octene and benzaldehyde. The highest yield is obtained from hydroacylation between the unconjugated diene 1, 5 hexadiene giving the corresponding product at 32%:12% (E:Z) yield. This result indicates that the formation of a π -allylmetal species is pertinent for the success of the reaction. Thus far, the choice of substrate poses limitations on substrate scope. $\text{RuHCl}(\text{CO})(\text{PPh}_3)_3$ remained to be the most effective catalyst out of the other ruthenium analogues. Exploration of synthetic methods of smaller ruthenium catalysts analogue remains to be done. The second method that was explored was the investigation of isomerization catalysts that can form metal-hydrides for

hydrometallation. Palladium catalysts that were used in catalytic systems that were developed by Skrydstrup, Gooßen, and Mazet were applied to our system in hopes of hydrometallating and then followed by the insertion step. However, none of the proposed catalysts exhibited reactivity in the system. Other catalysts that can perform these two steps remain to be explored as it is not covered in the extent of this research. Finally, selective olefin oxidation conditions were applied in hopes to perform the insertion step through oxidative allylation. However, the desired product was not observed. Extension of this work can be done by probing the difficulty of the oxidation and allylation step and isolating intermediates to better understand the mechanism.

Another project that stemmed from the high-throughput screening in attempts to find a system for oxidative allylation led to the formation of a self-aldol condensation product, which is postulated to be oxidized and then decarbonylate or decarboxylate. Catalytic oxidative conditions were applied to gain access to this synthetic pathway and prove this oxidative theory. The undehydrated aldol adduct intermediate was synthesized and oxidative conditions were applied to this substrate to test this theory. So far evidence supported this mechanistic pathway and the yield of the desired ketone product was improved up to 20%. However, due to the more favorable pathway of dehydration of the aldol adduct and possibly degradation, it remains a challenge to further improve the conditions. In addition, the scope of this reaction is quite limited to self-condensation. Therefore, further work of interest could be to explore cross-aldol adducts that can undergo a similar mechanistic pathway in a one-pot reaction. In addition, investigations towards the decarboxylative or decarbonylative step remain to be done.

Lastly, in attempts to study the potential competition between π -bond insertion of the olefin and aldehyde on metal hydride catalysts, deuterium labelling studies were done. From this study,

we conclude that the insertion of the aldehyde into the metal-hydride bond is indeed an off-cycle pathway that inhibits desired reactivity. Attempts have not been made to circumvent this competing pathway, but it was worthwhile to pursue a facile method for the synthesis of deuterated aldehydes via a ruthenium catalyst. However, yields remain modest, not isolated and scope is limited. More challenging substrates can be explored to probe its reactivity.

4. Experimental

General experimental details

Unless otherwise indicated, reactions were conducted under an atmosphere of argon in 5 mL screw-capped vials that were oven dried (120 °C). Column chromatography was either done manually using Silicycle F60 40-63 μm silica gel, or using a Combiflash Rf+ automated chromatography system with commercially available RediSep Rf normal-phase Silica Flash columns (35-70 μm). Analytical thin layer chromatography (TLC) was conducted with aluminum-backed EMD Millipore Silica Gel 60 F₂₅₄ pre-coated plates. Visualization of developed plates was performed under UV light (254 nm) and/or using KMnO₄ or ceric ammonium molybdate (CAM) stain.

Instrumentation

¹H, ¹³C, and ¹⁹F NMR spectra were recorded on a Bruker AVANCE 400 MHz spectrometer. ¹H NMR spectra were internally referenced to the residual solvent signal (e.g. CDCl₃ = 7.27 ppm). ¹³C NMR spectra were internally referenced to the residual solvent signal (e.g. CDCl₃ = 77.36 ppm). ¹⁹F spectra were unreferenced. Data for ¹H NMR are reported as follows: chemical shift (δ ppm), multiplicity (s = singlet, d = doublet, t = triplet, q = quartet, m = multiplet), coupling

constant (Hz), integration. NMR yields for optimization studies were obtained by ^1H NMR analysis of the crude reaction mixture using 1,3,5-trimethoxybenzene as an internal standard.

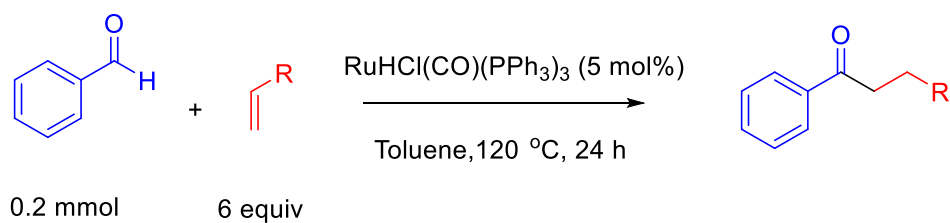
GC yields for optimization studies were obtained via a 5 point calibration curve using FID analysis on an Agilent Technologies 7890B GC with 30 m x 0.25 mm HP-5 column. Accurate mass data was obtained either via a Kratos Concept mass spectrometer at the uOttawa John L. Holmes Mass Spectrometry Facility, or via processing of data obtained from an Agilent 5977A GC/MSD using MassWorks 4.0 from CERNO bioscience.⁷⁹

Materials

Organic solvents were purified by rigorous degassing with nitrogen before passing through a PureSolv solvent purification system, and low water content was confirmed by Karl Fischer titration (<25 ppm for all solvents). Water was vigorously degassed for at least ten minutes prior to use. All reagents, metal catalysts, and ligands were purchased from Sigma-Aldrich, VWR International, or Strem Chemical Company and used as received unless otherwise noted. All N-heterocyclic carbene (NHC) ligands were prepared according to the literature.⁸⁰

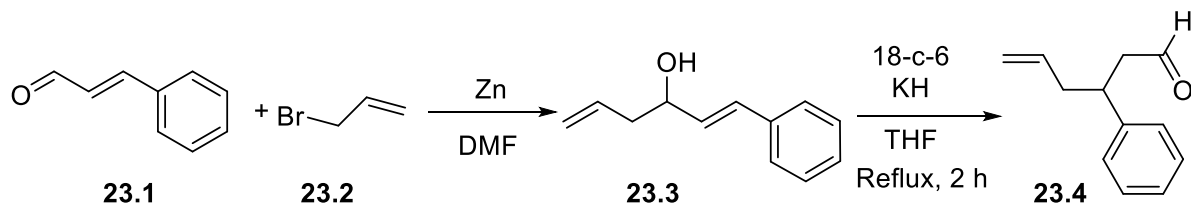
⁷⁹ Wang, Y.; Gu, M., *Anal. Chem.* **2010**, 82, 7055.

⁸⁰ Bantreil, X.; Nolan, S. P., *Nat. Protocols* **2011**, 6, 69.

Synthesis of Hydroacylation products

An oven dried screw-capped vial was charged with a magnetic stir bar, catalyst and solid substrates were added. The vial and contents were subjected to three cycles of vacuum and argon under a Schleck line. Fresh solvent (1 mL, 0.2 M) obtained from solvent purification system was then added under argon. Liquid substrates were subsequently added via micropipette under argon. The vial was sealed with a PTFE-lined screw cap and stirred vigorously (700 rpm) at the indicated temperature for 16 h. After cooling to room temperature, internal standard (1,3,5-trimethoxybenzene, 0.05 mmol in 1 mL THF) was added. Mixture was diluted with ethyl acetate and filtered through a plug of silica gel (10 mL of EtOAc eluent). Yields were determined by ^1H NMR.

Synthesis of 3-phenylhex-5-enal



To an oven-dried round-bottom flask charged with a magnetic stir bar, commercial zinc dust (25 mmol) in DMF (25 mL) was added under argon. Allyl bromide **23.2** (33 mmol) in DMF (1 mL) was added dropwise to the stirred suspension at room temperature. Mixture was stirred for 30 minutes, while the cinnamaldehyde **23.1** (1 mmol) in DMF (1 mL) was slowly added. Stirring was continued until completion of reaction as indicated by TLC. Reaction was quenched with water and extracted with ether. The organic layer was washed with brine and dried over Na₂SO₄. Resulting residue was concentrated *in vacuo* and purified by column chromatography (10:1 Hexanes: ethyl acetate) to afford **23.3** as a yellow oil (0.8g, 18.5% yield) before carrying on next step. Characterization data was in accordance with literature.⁸¹

Excess KH in mineral oil was washed with dry THF 3 times under argon. **23.3** (4.61 mmol) in 10 mL of THF and 18-crown-6 (0.5 equiv) in 1 mL of THF were added at room temperature. Mixture was heated under reflux for 2 hours and reaction was quenched with MeOH and water at -78°C. The organic layer was extracted with ether and washed with brine, water and dried over Na₂SO₄. Resulting residue was concentrated *in vacuo* and purified by column chromatography to afford 3-phenylhex-5-enal **23.4** as yellow oil (0.35 g, 43.7% yield). Characterization data was in accordance with literature.⁸² ¹H NMR (400 MHz, CDCl₃) δ 9.66 (t,

⁸¹ Garza, V. J.; Krische, M. J., *J. Am. Chem. Soc.* **2016**, *138*, 3655.

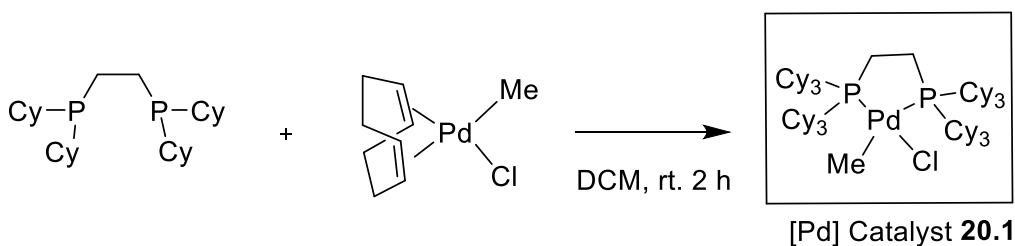
⁸² Allin, S. M.; Horro-Pita, C.; Essat, M.; Aspinall, I.; Shah, P., *Synth. Commun.* **2010**, *40*, 2696.

$J = 2.0$ Hz, 1H), 7.29 (t, $J = 7.3$ Hz, 2H), 7.19 (t, $J = 8.7$ Hz, 3H), 5.69 – 5.55 (m, 1H), 5.04 – 4.94 (m, 2H), 3.32 – 3.23 (m, 1H), 2.80 – 2.67 (m, 2H), 2.45 – 2.33 (m, 2H).

Synthesis of [PdCl(Me)(COD)Ln] catalysts

Complex **CODPd(CH₃)(Cl)** was prepared from **(COD)PdCl₂** according to literature procedure as precatalyst and characterization data was in accordance with literature.⁸³

Synthesis of (Cl)Pd(CH₃)(dcpe)



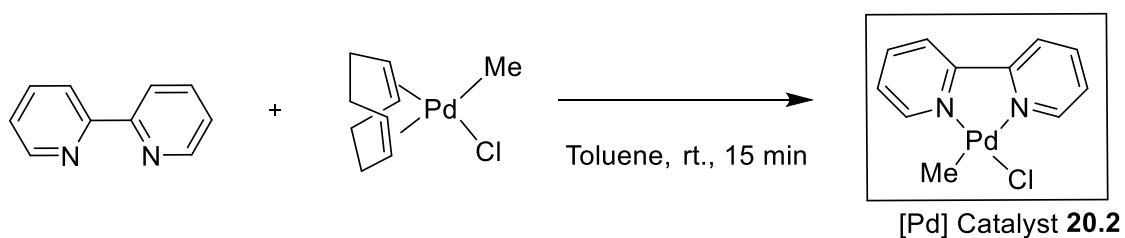
A solution of 1,2-bis(dicyclohexylphosphino)ethane (1 equiv) in dried DCM (5 mL) was added dropwise into a flask containing [PdCl(Me)(COD)] (0.29 mmol) in DCM (5 mL). Solution was allowed to be stirred for 2h before concentrating *in vacuo* to about 1mL. About 2mL of degassed hexanes were added to recrystallize. Gray precipitate was filtrated and washed with hexanes to give **20.1** (79 mg, 47% yield). Characterization data was in accordance with literature.

⁸⁴ **¹H NMR** (400 MHz, CDCl₃) δ 2.48 – 2.27 (m, 8H), 2.08 – 1.80 (m, 18H), 1.45 – 1.63 (d, $J = 11.6$ Hz, 4H), 1.15 – 1.40 (m, 18H), 0.53 (dd, $J = 7.7, 2.1$ Hz, 3H).

⁸³ Rulke, R. E.; Ernsting, J. M.; Spek, A. L.; Elsevier, C. J.; van Leeuwen, P. W. N. M.; Vrieze, K., *Inorg. Chem.* **1993**, *32*, 5769.

⁸⁴ Raebiger, J. W.; Miedaner, A.; Curtis, C. J.; Miller, S. M.; Anderson, O. P.; DuBois, D. L., *J. Am. Chem. Soc.* **2004**, *126*, 5502.

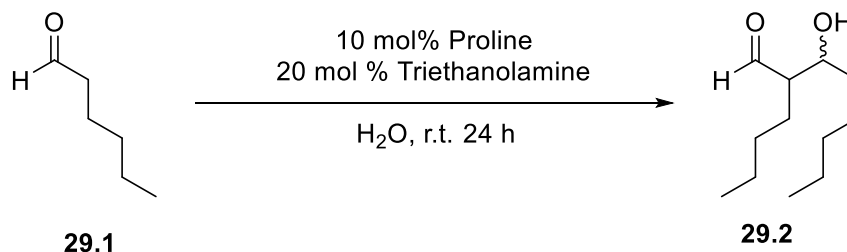
Synthesis of (Cl)Pd(CH₃)(bpy)



To a solution of [PdCl(Me)(COD)] (0.22 mmol) in dried toluene (6 mL) the diimine ligand (1.1 equiv) was added. After stirring for 15 minutes at r.t., the volume of the solution was reduced to 10mL and the precipitate product was filtrated. Yellow crystals were washed with ether and dried under vacuum to give **20.2** (44 mg, 64% yield). Characterization data was in accordance with literature.⁸⁵ ¹H NMR (400 MHz, CDCl₃) δ 9.27 (d, *J* = 4.6 Hz, 1H), 8.73 (d, *J* = 5.4 Hz, 1H), 8.13 – 7.98 (m, 4H), 7.61 – 7.52 (m, 2H), 1.07 (s, 3H).

⁸⁵ Klein, A.; Lepski, Z., *Anorg. Allg. Chem.* **2009**, 635, 878.

Synthesis of Aldol Adduct Intermediate (2-butyl-3-hydroxyoctanal)



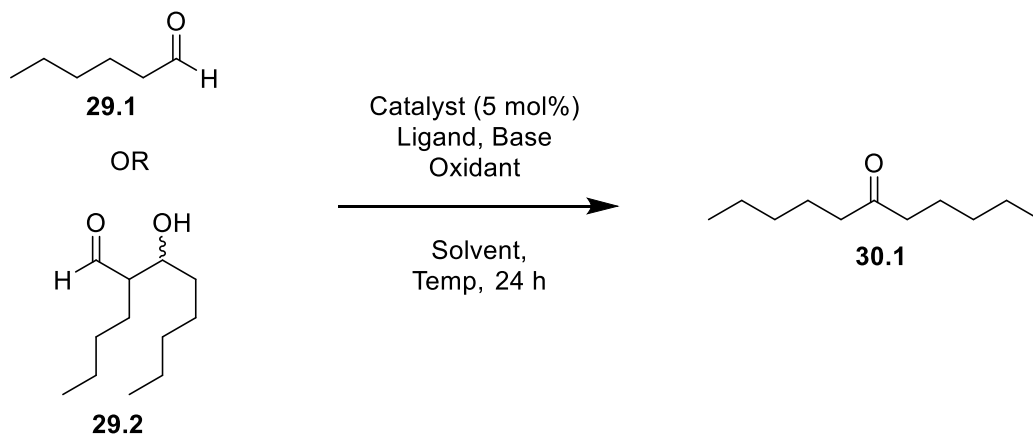
To a 50mL round bottom flask equipped with a magnetic stir bar, was added Proline (10 mol%) and Triethanolamine (20 mol%) dissolved in degassed H₂O (2.5 mL). Aldehyde (5 mmol) was added to the reaction mixture at room temperature. The mixture quickly turned milky upon stirring vigorously. The reaction mixture was stirred at room temperature for 24 hours. After completion of reaction, the mixture was extracted three times with CH₂Cl₂. Subsequent washes with NaOH_{aq} (1 M) were done as necessary to remove acid. The combined organic layers were dried over MgSO₄, and then filtered. The filtrate was concentrated *in vacuo*. Purification was done by column chromatography (hexanes : ethyl acetate, 10:1) to afford the corresponding racemic substrate. Characterization data was in accordance with literature.⁸⁶

Isomer 1: ¹H NMR (400 MHz, CDCl₃) δ 9.76 (d, *J* = 2.1 Hz, 1H), 3.98 – 3.91 (m, 1H), 2.42 – 2.28 (m, 2H), 1.79 – 1.14 (m, 6H), 0.99 – 0.84 (m, 3H).

Isomer 2: ¹H NMR (400 MHz, CDCl₃) δ 9.73 (d, *J* = 2.8 Hz, 1H), 3.85 – 3.78 (m, 1H), 1.79 – 1.14 (m, 6H), 0.99 – 0.84 (m, 3H).

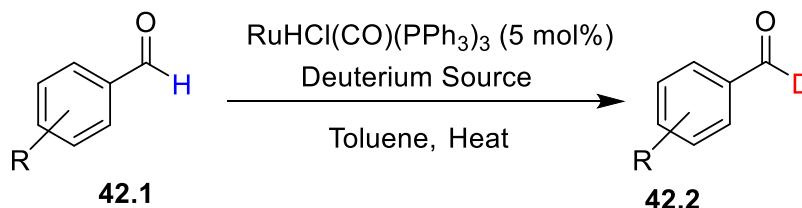
⁸⁶ Siedlecka, R.; Skarzewski, J.; Młochowski, J., *Tetrahedron Lett.* **1990**, *31*, 2177.

Synthesis of Ketone via Oxidative Decarbonylation of Aldol Adduct



A screw-capped vial was charged with a magnetic stir bar, catalyst (5mol %), base (1equiv), ligand (5 mol %), and oxidant (1-2.5 equiv). Reaction was done either under an oxygen balloon or under inert atmosphere. Fresh solvent (1 mL, 0.2 M) obtained from solvent purification system was then added. Liquid substrates were subsequently added via micropipette. The vial was sealed with a PTFE-lined screw cap and stirred vigorously (700 rpm) at the indicated temperature for 24 h. After cooling to room temperature, internal standard (1,3,5-trimethoxybenzene, 0.05 mmol in 1 mL THF) was added. Mixture was diluted with ethyl acetate and filtered through a plug of silica gel (10 mL of EtOAc eluent). Yields were determined by GC-MS Calibration Curve.

Synthesis of Deuterated Aldehydes



With an oven dried screw-capped vial equipped with magnetic stir bar, and loaded with catalyst, and sealed with a PTFE-lined screw cap. The vial and contents were subjected to three cycles of vacuum and argon under a Schleck line. Fresh solvent (1 mL, 0.2 M) obtained from solvent purification system was then added under argon. Liquid substrates and D-source were subsequently added via micropipette under argon. The reaction was stirred for indicated amount of time and temperature. After cooling to room temperature, internal standard (1,3,5-trimethoxybenzene, 0.05 mmol in 1 mL THF) was added. Mixture was diluted with ethyl acetate and filtered through a plug of silica gel (10 mL of EtOAc eluent) and concentrated in *vacuo*. Yields determined by H^1 NMR. Recovery determined from ratio of starting material and internal standard.

For more than one iterations, solvent and D-source were pumped off via Schlenk line. When dried, reaction vial doped with additional D-source and additional solvent. Work-up is same as above.

% deuteration formula:

$$\left(1 - \left[\frac{\int \text{characteristic peak of aldehyde}}{\int \text{Benzylic peak of aldehyde}}\right] * \left[\frac{\# \text{ protons of benzylic peak}}{1}\right]\right) * 100\%$$

Chapter 2: Palladium catalyzed cross-coupling reactions of esters

5. Transition metal catalysis for cross-coupling reactions

Cross-coupling reactions are among the most important carbon-carbon bond-forming reactions available. They traditionally occur between organohalide and organometallics reagents (**Scheme 47**). The nature of the metal is very important in determining the reactivity and selectivity of the organometallic catalyst.⁸⁷ Transition metals such as palladium or nickel among others are explored in cross-coupling reactions.⁸⁸



Scheme 47. General scheme for cross-coupling reactions

The first transition metal-catalyzed cross-coupling of C(sp²)-halides using organometallic compounds were independently developed by Kumada⁸⁹ and Corriu⁹⁰ in 1972. Since these discoveries, the development of metal-catalyzed cross-coupling reactions has grown dramatically.⁹¹ Among these include the palladium-catalyzed Stille reaction using organotin reagents⁹² and the Suzuki-Miyaura couplings involving boronic acids.⁹³ Other cross-coupling reactions have been developed giving different modes to access the C-C bond formation. For

⁸⁷ a) Boudier, A.; Bromm, L.O.; Lotz, M.; Knochel, P., *Angew. Chem. Int. Ed.* **2000**, *39*, 4414; b) Knochel, P., ed., *Handbook of Functionalized Organometallics*, Wiley-VCH, Weinheim, **2005**. c) Lipshutz, B.H in: *Organometallics in Synthesis. A Manual II*, M. Schlosser, ed., Wiley, Chichester, **1998**.

⁸⁸ a) Meijere, A. de; Diederich, F.; Eds., *Metal-Catalyzed Cross-Coupling Reactions* 2nd ed., Wiley-VCH, Weinheim, **2004**; b) J. Tsuji, *Transition Metal Reagents and Catalysts: Innovations in Organic Synthesis*, Wiley, Chichester, **1995**.

⁸⁹ Tamao, K.; Sumitani, K.; Kumada, M., *J. Am. Chem. Soc.* **1972**, *94*, 4374.

⁹⁰ Corriu, R. J. P.; Masse, J. P., *J. Chem. Soc., Chem. Commun.* **1972**, 144a.

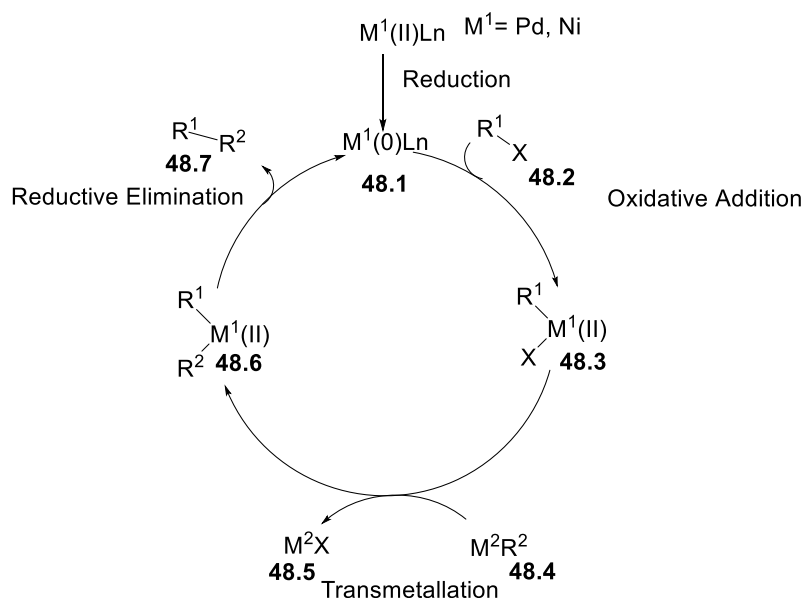
⁹¹ M. Beller, C. Bolm, eds., *Transition Metals for Organic Synthesis* 2nd ed., Wiley-VCH, Weinheim, **2008**.

⁹² Stille, J. K. *Angew. Chem. Int. Ed. Engl.* **1986**, *25*, 508.

⁹³ Miyaura, N.; Suzuki, A., *Chem. Rev.* **1995**, *95*, 2457.

example, palladium-catalyzed Hiyama- (organosilicon reagents),⁹⁴ Negishi- (organozinc reagents),⁹⁵ Sonogashira (alkynylcopper reagents)⁹⁶ coupling reactions among others, are valuable assets in organic synthesis.

A general metal-catalyzed cross-coupling reaction mechanism is represented in Scheme 48. If a $M^{II}Ln$ precatalyst is used, the species has to be reduced to the reactive species M^0Ln **48.1**, but if the metal precursor starts with an oxidation state of zero, then no reduction is required. The species then undergoes oxidative addition to the C-X bond, which acts as an electrophile giving the organometallic complex **48.3**. The next step involves a ligand exchange reaction, typically transmetallation with an organometallic reagent **48.4**, which gives complex **48.6**. Finally, the last step is reductive elimination which provides the desired cross-coupling product **48.7**, while regenerating the active catalyst. The reactivity, efficiency, and selectivity of the active catalyst can be tuned depending on the nature of the ligand.



Scheme 48. General catalytic cycle for transition metal-catalyzed cross-coupling reactions

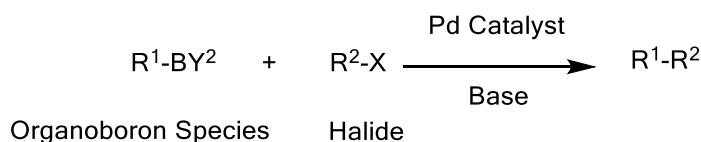
⁹⁴ Hatanaka, Y.; Hiyama, T., *J. Org. Chem.* **1988**, 53, 918.

⁹⁵ King, A. O.; Okukado, N.; Negishi, E.-i., *J. Chem. Soc., Chem. Commun.* **1977**, 683.

⁹⁶ Sonogashira, K., *J. Organomet. Chem.* **2002**, 653, 46.

5.1. Suzuki-Miyaura cross-coupling reaction

The Suzuki reaction is one of the most well-known and efficient cross-coupling reactions in organic chemistry. In 1979, Akira Suzuki and co-workers⁹⁷ first reported the successful coupling of a boronic acid with a halide via palladium (0) catalysis (Scheme 49). For this ground-breaking discovery and its high impact in organic chemistry, Suzuki shared the 2010 Nobel Prize in Chemistry with Richard F. Heck and Ei-ichi Negishi for their work in palladium-catalyzed cross-coupling reactions.



Scheme 49. General scheme for Suzuki-Miyaura cross-coupling reaction

This coupling reaction is used to synthesize poly-olefins⁹⁸, styrenes,⁹⁹ and substituted biphenyls¹⁰⁰ among other complex natural products such as Merck's CoazaarTM, (Figure 3) which is an important drug for treating hypertension.¹⁰¹

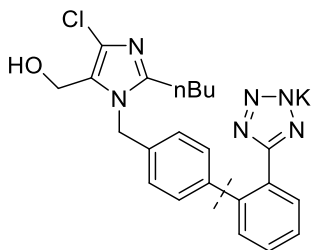


Figure 3. Structure of Coazaar

⁹⁷ Miyaura, N.; Suzuki, A., *Chem. Rev.* **1995**, 95, 2457.

⁹⁸ Baldwin, J. E.; James, D. A.; Lee, V., *Tetrahedron Lett.* **2000**, 41, 733.

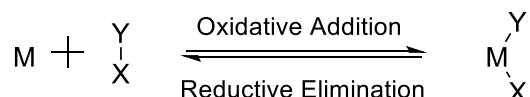
⁹⁹ Jiang, B.; Wang, Q.-F.; Yang, C.-G.; Xu, M., *Tetrahedron Lett.* **2001**, 42, 4083.

¹⁰⁰ Baudoin, O.; Guénard, D.; Guéritte, F., *J. Org. Chem.* **2000**, 65, 9268.

¹⁰¹ Yasuda, N., *J. Organomet. Chem.* **2002**, 253, 279.

5.1.1. Mechanism of reaction

The mechanism of this reaction follows the general catalytic cycle in Scheme 48, employing palladium or nickel as the catalyst. The first step in the cross-coupling reaction is oxidative addition, where the oxidation state and coordination number of a metal increases (**Scheme 50**).



Scheme 50. Oxidative addition and reductive elimination

In the context of the Suzuki reaction, the oxidative addition usually involves an aryl halide, with the order of reactivity being I > OTf > Br >> Cl.¹⁰² Besides halides, other functional groups such as diazonium salts and sulfonates can similarly undergo oxidative addition. These are typically referred to as “pseudohalides.” The activation of aryl halides is enhanced by the proximity of electron-withdrawing groups rather than those with donating groups.

The next step is transmetalation, which can be defined as the transfer of ligands from one metal to another. For example, in a cross-coupling reaction, it can be seen as the addition of an organometallic reagent to a palladium species. In the case of the Suzuki reaction, boronic acid acts as the nucleophilic coupling partner, which transmetalates with a palladium species. Previous studies showed that it could be the rate-determining step in many cross-coupling reactions.¹⁰³

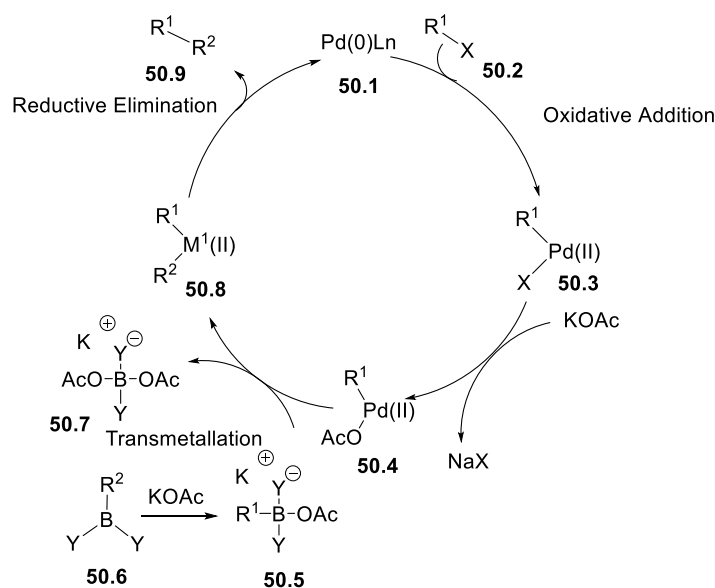
The last step is reductive elimination, which is essentially the reverse of oxidative addition where the oxidation and coordination number decreases. In contrast to oxidative

¹⁰² Fitton, P.; Rick, E. A., *J. Organomet. Chem.* **1971**, 28, 287.

¹⁰³ Nasielski, J.; Hadei, N.; Achonduh, G.; Kantchev, E. A. B.; O'Brien, C. J.; Lough, A.; Organ, M. G., *Eur. J. Org. Chem.* **2010**, 16, 10844.

addition, reductive elimination usually is favoured by electron poor metals and electron poor ligands.¹⁰⁴ The reaction takes place directly from cis-isomer of the metal-ligand complex and the trans-isomer will only react after isomerization to the corresponding cis product. It is often regarded as a facile process and relatively exothermic due to the formation of the new carbon-carbon bond.¹⁰⁵ The order of reactivity is diaryl- > (alkyl)aryl- > dipropyl- > diethyl-> dimethylpalladium.¹⁰⁶

The general mechanism of the Suzuki-Miyaura reaction is summarized in Scheme 51, using a palladium species as the representative catalyst. The first step is the oxidative addition into the carbon-halide bond to form the organopalladium species **50.3**. Then a base will displace the halogen ligand on the species to provide intermediate **50.4**. The next step involves transmetalation with the boronate complex **50.5** which is derived from a reaction with the base. Finally, reductive elimination gives the desired product **50.9** and restores the catalyst **50.1**.



Scheme 51. Representative catalytic cycle for Suzuki-Miyaura cross-coupling reaction¹⁰⁶

¹⁰⁴ Hartwig, J. F., *Inorg. Chem.* **2007**, *46*, 1936.

¹⁰⁵ Pérez-Rodríguez, M.; Braga, A. A. C.; García-Melchor, M.; Pérez-Temprano, M. H.; Casares, J. A.; Ujaque, G.; de Lera, A. R.; Álvarez, R.; Maseras, F.; Espinet, P., *J. Am. Chem. Soc.* **2009**, *131*, 3650.

¹⁰⁶ Miyaura, N.; Suzuki, A., *Chem. Rev.* **1995**, *95*, 2457.

5.1.1.1. Activation of the catalyst

Generally, there are three choices for catalyst precursors. The most common and inexpensive precursors fall into the category of Pd(II) salt such as Pd(OAc)₂, PdCl₂(PPh₃)₂ and PdCl₂ and these species must be reduced to active Pd(0) in order to perform the desired chemistry. Some pathways of reduction include using boronic acids¹⁰⁷ or basic amine additives¹⁰⁸ to reduce the Pd(II) species. Some common Pd(0) species that exist commercially include Pd₂(dba)₃ and Pd(PPh₃)₄. Although they are coordinatively saturated species, they can lose ligands upon heating in solution to make active catalysts. Therefore, palladium complexes with fewer than four phosphine ligands are in general more reactive for oxidative addition due to its availability to increase coordination number.¹⁰⁹

5.2. Suzuki-Miyaura cross-coupling reaction of carboxylate derivatives

As seen previously, traditional examples of Suzuki-Miyaura coupling uses organoboron nucleophiles with aryl halides as electrophilic coupling partners. This reactivity has led to the exploration of a broad range of starting materials including acid chlorides,¹¹⁰ thioesters¹¹¹ and anhydrides.¹¹² In general, aryl halides, pseudohalides and anhydrides are reactive towards any nucleophilic species and traditional Suzuki-Miyaura type couplings have been largely limited to those substrates. Therefore, other starting material alternatives were explored. In 2000,

¹⁰⁷ Huang, X.; Anderson, K. W.; Zim, D.; Jiang, L.; Klapars, A.; Buchwald, S. L., *J. Am. Chem. Soc.* **2003**, *125*, 6653.

¹⁰⁸ Yoshimura, N.; Moritani, I.; Shimamura, T.; Murahashi, S.-I., *J. Am. Chem. Soc.* **1973**, *95*, 3038.

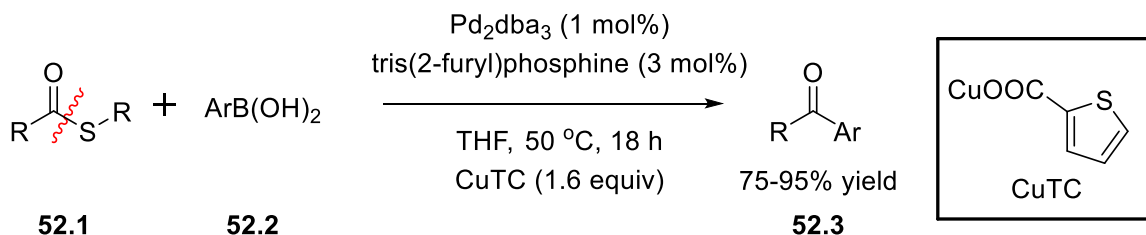
¹⁰⁹ Miyaura, N.; Suzuki, A., *Chem. Rev.* **1995**, *95*, 2457.

¹¹⁰ a) Cho, C. S.; Itotani, K.; Uemura, S., *J. Organomet. Chem.* **1993**, *443*, 253. For a review, see: b) Blangetti, M.; Rosso, H.; Prandi, C.; Deagostino, A.; Venturello, P. *Molecules*. **2013**, *18*, 1188.

¹¹¹ a) Liebeskind, L. S.; Srogl, J., *J. Am. Chem. Soc.* **2000**, *122*, 11260. b) Prokopcová, H.; Kappe, C. O., *Angew. Chem. Int. Ed.* **2009**, *48*, 2276.

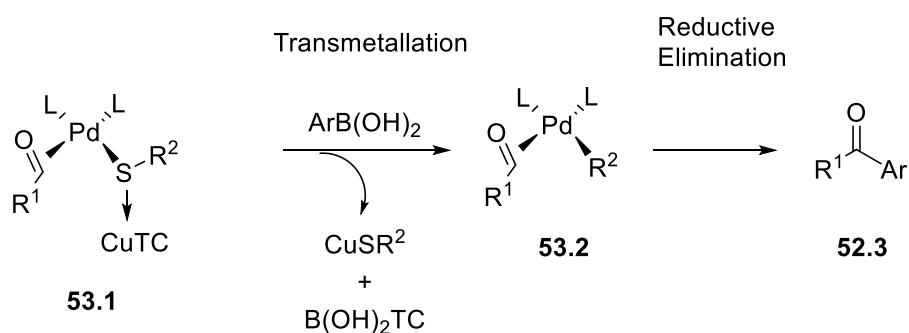
¹¹² Goößen, L. J.; Ghosh, K., *Angew. Chem. Int. Ed.* **2001**, *40*, 3458.

Liebeskind's group reported the use of thioester as a cross-coupling partner with boronic acid, using palladium catalysis in the presence of Cu^I thiophene-2-carboxylate (CuTC) (Scheme 52).



Scheme 52. Liebeskind's strategy for cross-coupling of thioesters¹¹³

Like normal esters, thioester possess a stable carbon-sulfur bond and would need the selective interaction of a transition metal to achieve selective cleavage of the carbon-sulfur bond to form the acylpalladium-thiolate **53.1**. In this case, CuTC mediates this intermediate through interaction with the sulfur atom and participates in boron to copper transmetalation (**Scheme 53**). This system performs efficiently with the absence of a base and strictly under neutral conditions, which is advantageous for synthesis of base-sensitive compounds.¹¹³ They also developed similar transformations using copper catalysis.¹¹⁴

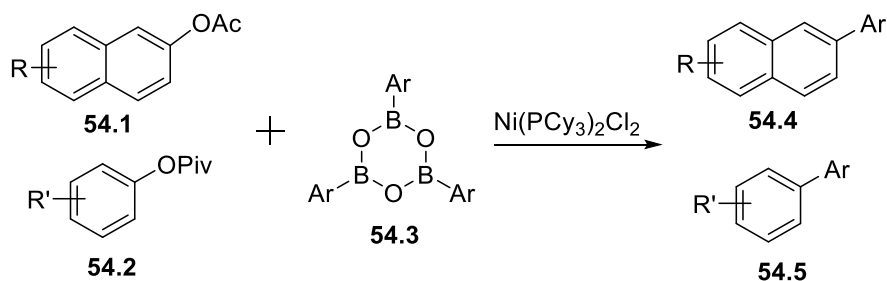


Scheme 53. Formation of ketone via acylpalladium-thiolate species mediated by CuTC¹¹³

¹¹³ Liebeskind, L. S.; Srogl, J., *J. Am. Chem. Soc.* **2000**, *122*, 11260.

¹¹⁴ Villalobos, J. M.; Srogl, J.; Liebeskind, L. S., *J. Am. Chem. Soc.* **2007**, *129*, 15734.

In contrast to Liebeskind's synthesis of ketones from thioesters, Garg¹¹⁵ and Shi¹¹⁶ were the first to independently report the use of a simple ester as starting material to give access to biaryl species. They successfully used nickel catalysis to couple boron derivatives with phenolic carboxylates. These mimic the reactivity of the aryl halides such that these esters react via a cleavage of the C(aryl)-O bond (Scheme 54).

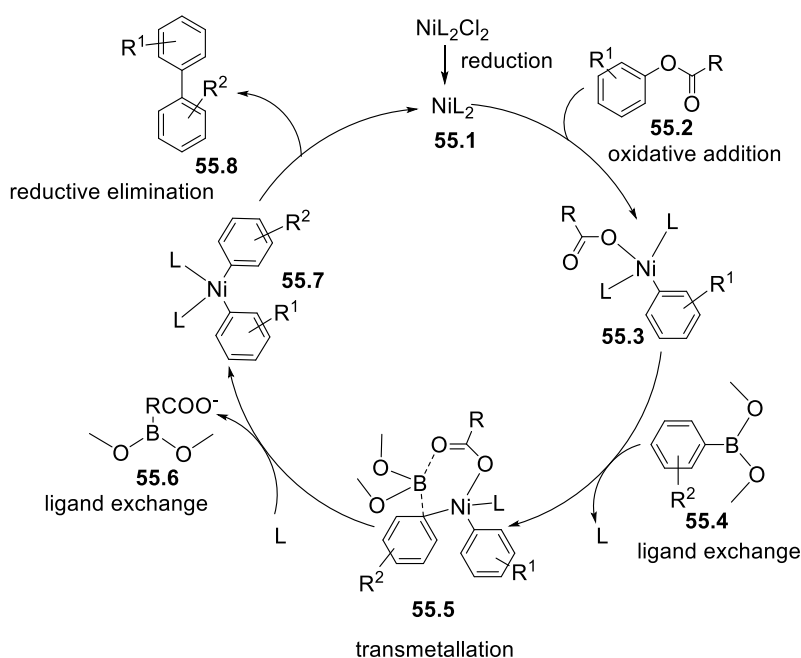


Scheme 54. Shi's strategy for coupling of boronic acid with phenolic carboxylates¹¹⁶

Their mechanism follows the typical pathway of metal catalyzed cross-coupling reaction, starting with the oxidative addition of nickel, followed by ligand exchange of the boron species to give a six-member ring transition state **55.5**. Then transmetalation of the carboxylic group occurs followed by reductive elimination to give the final bi-aryl species **55.8** (**Scheme 55**).

¹¹⁵ Quasdorf, K W.; Tian, X.; Garg, N. K., *J. Am. Chem. Soc.* **2008**, *130*, 14422.

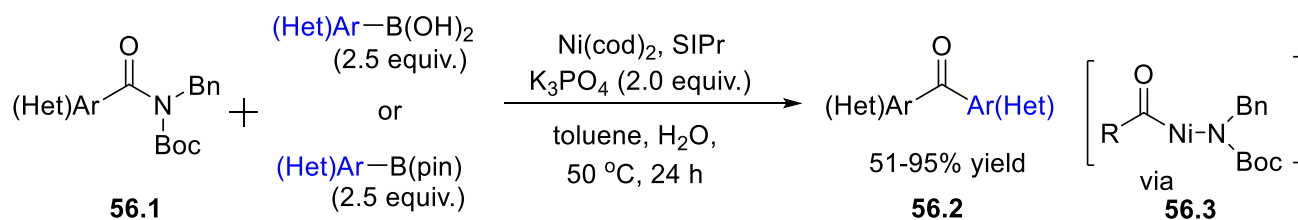
¹¹⁶ Guan, B.-T.; Wang, Y.; Li, B.-J.; Yu, D.-G.; Shi, Z.-J., *J. Am. Chem. Soc.* **2008**, *130*, 14468.



Scheme 55. Shi's catalytic cycle for biaryl synthesis¹¹⁶

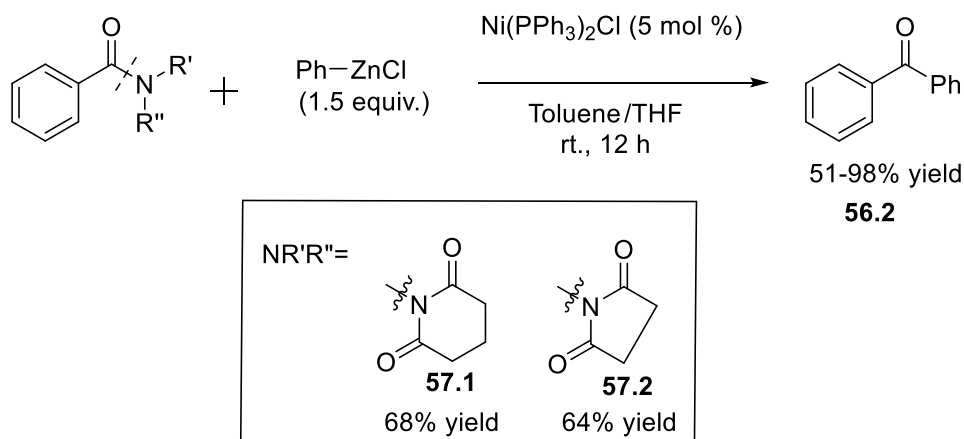
Garg demonstrated that amides, although typically inert, can be used to form C-C bonds through cleavage of the C-N bond using nickel catalysis (Scheme 56).¹¹⁷ They had first discovered the conversion of amides into esters using Ni/SIPr catalyst to activate the amide C-N bond, which is impressive because amides are poor electrophiles due to the resonance stability of the amide bond ($n_{\text{N}} \rightarrow \pi^*_{\text{CO}}$ conjugation). They extended this research to make carbon-carbon bond, using a carbon based nucleophile. In both methodologies, they postulate that this activation involves an oxidative addition intermediate **56.3**.

¹¹⁷ Hie, L.; Fine Nathel, N. F.; Shah, T. K.; Baker, E. L.; Hong, X.; Yang, Y.-F.; Liu, P.; Houk, K. N.; Garg, N. K., *Nature*. **2015**, 524, 79.



Scheme 56. Garg's scheme for cross-coupling of amides¹¹⁷

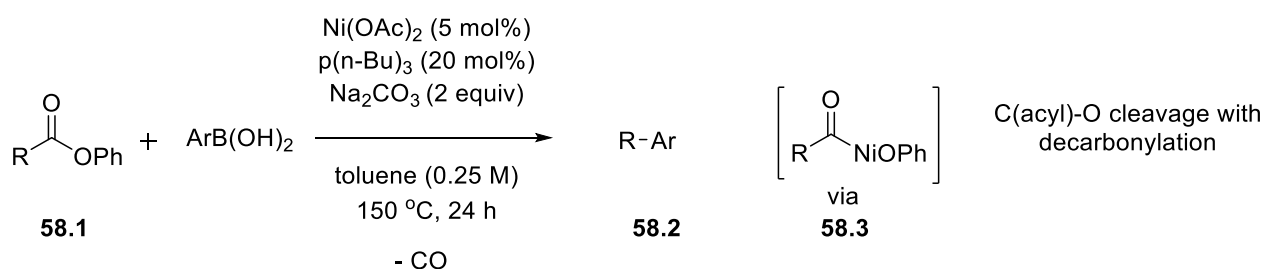
Similarly, Szostak and co-workers recently reported the synthesis of ketones via Negishi cross coupling of esters via C-N bond activation of amides using nickel catalysis (Scheme 57).¹¹⁸ Their activation of the C-N bond is analogous to Garg's method, except the use of an organozinc as the transmetallating agent. It is interesting to note the selectivity of the C-N bond activation. It is believed that metal insertion into the amide C-N bond occurs only if the amide bond has been distorted from planarity by steric and/or electronic means. This distortion subsequently weakens the N-C(O) bond, thus facilitating the oxidative addition step. In the case of Garg's group, they used a sterically bulky N-Bn-N-Boc-derivative to facilitate the oxidative addition step, while Szostak's group utilizes substrates such as **57.1**, **57.2** for their distortion properties.



Scheme 57. Szostak's strategy for cross-coupling of amides¹¹⁸

¹¹⁸ Shi, S.; Szostak, M., *Chemistry – A European Journal*. **2016**, 22, 10420.

Having access to reactivity of esters is potentially valuable in cross-coupling reactions as it gives way to numerous commercially and synthetically available ester containing molecules. In Garg's work, it is significant to note that there is no evidence of decarbonylation as their reaction gave rise to the ketone product. On the other hand, Itami and co-workers used nickel catalysis cross couple an ester with boronic acid to give access to biaryl products. The intermediate acyl-Ni species **58.3** would undergo transmetalation with the boronic acid and decarbonylation prior to C–C bond formation to give the desired product (Scheme 58).¹¹⁹

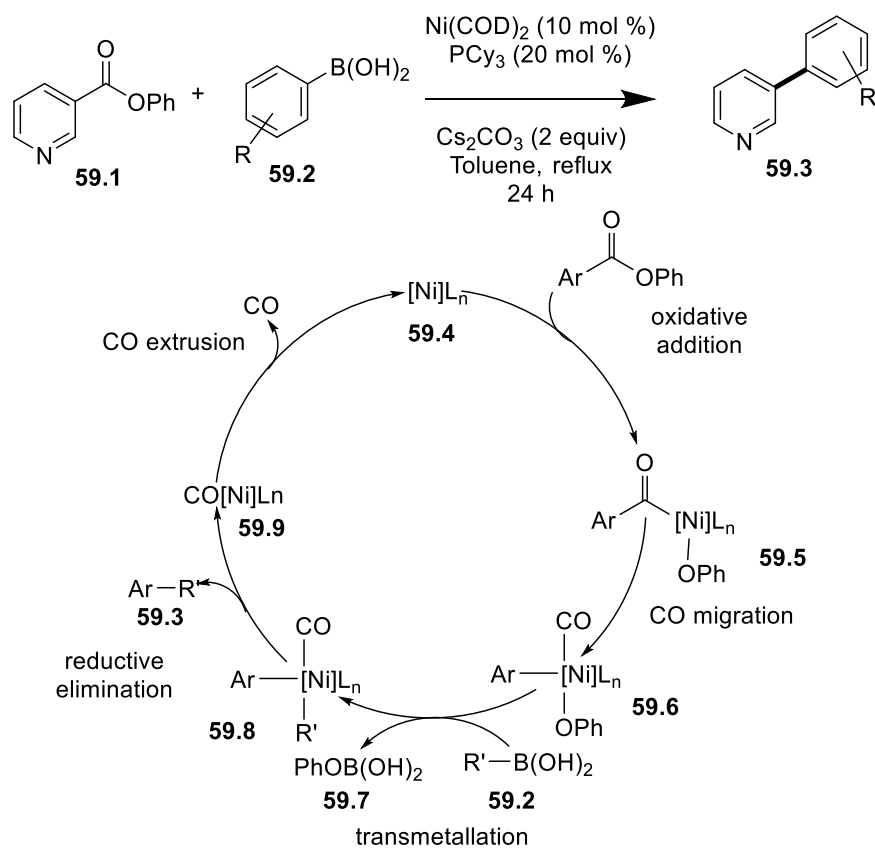


Scheme 58. Itami's scheme for decarbonylative cross-coupling using nickel catalysis¹¹⁹

Love's group independently reported yet another similar type of reaction mode for the Suzuki-Miyaura cross-coupling reaction with decarbonylation, thus giving access to the biaryl species.¹²⁰ The process undergoes the same mechanism as that of Itami's where the nickel catalyst oxidatively adds into the C-acyl bond to give **59.5**. Decarbonylation occurs via CO migration onto the nickel catalyst giving **59.6**. Transmetalation of the boronic acid, followed by reductive elimination then occurs to give the biaryl species **59.3**. The remaining CO is extruded to regenerate the nickel catalyst **59.4** (Scheme 59).

¹¹⁹ Muto, K.; Yamaguchi, J.; Musaev, D. G.; Itami, K., *Nat. Commun.* **2015**, *6*, 7508.

¹²⁰ LaBerge, N. A.; Love, J. A., *Eur. J. Org. Chem.* **2015**, *2015*, 5546.



Scheme 59. Love's proposed mechanism for decarbonylative cross-coupling of esters and boronic acids¹²⁰

5.3. Using surfactants with Suzuki-Miyaura cross-coupling reactions

In most Suzuki-Miyaura reactions, an organic solvent such as toluene or dioxane are usually used.¹²¹ Recently, there have been precedents of using water as a co-solvent¹²² or purely as the solvent itself for cross-coupling reactions. Using aqueous media has obvious advantages from a green chemistry point of view as it is economical, naturally abundant and environmentally friendly. It is also notable that Suzuki-Miyaura reactions in organic solvents

¹²¹ Miyaura, N.; Suzuki, A., *Chem. Rev.* **1995**, 95, 2457.

¹²² Li, S.; Lin, Y.; Cao, J.; Zhang, S., *J. Org. Chem.* **2007**, 72, 4067.

take place at elevated temperatures,¹²³ while the in the water/surfactant system the reaction can take place at room temperature.¹²⁴

The introduction of surfactants to enhance reactivity in the system is inherently unique. There has been an increasing use of surfactants in industry such as paint, cosmetics, cleaning, pulp and paper etc.¹²⁵ A surfactant generally is an amphiphile, consisting of hydrophilic and hydrophobic portion. This feature enables the dissolution of water-insoluble moieties in aqueous media. As organic reactions are sensitive to solvent effects, surfactants with varying degrees of lipophilicity have a profound impact on metal catalyzed reactions. These surfactants have the ability to self-aggregate to form micelles or nanoreactors.¹²⁶ These nanoreactors can take form in the shape of worm-, rod- or spherical-like particles. Fujita and co-workers refer to these as “functional molecular flasks.”¹²⁷ These reactions are technically under homogenous conditions taking place within the lipophilic inner core of the micelle. Hydrophobic effects may play an important role in reactions that involve lipophilic substrates. The effect may influence how molecules cluster together to reduce the amount of non-polar surface that is exposed to water or influence the ability for the molecules to enter a separate phase.¹²⁸

There are three main classes of surfactants, namely neutral, anionic and cationic. They all feature a hydrophilic head and hydrophobic tail. Some examples are illustrated below in **Figure 4**. The first example TX-100 (**F4.1**) illustrates a neutral surfactant, where there is no net charge on the molecule. The second and third example, **F4.2**, **F4.3** illustrates sodium dodecyl

¹²³ a) Hoshi, T.; Honma, T.; Mori, A.; Konishi, M.; Sato T.; Hagiwara H.; Suzuki, T., *J. Org. Chem.* **2013**, *78*, 11513. b) So, C. M.; Yeung, C. C.; Lau, C. P.; Kwong, F. Y., *J. Org. Chem.* **2008**, *73*, 7803.

¹²⁴ Lipshutz, B. H.; Ghorai, S., *Aldrichimica acta.* **2012**, *45*, 3.

¹²⁵ a) Banat, I. M.; Makkar, R. S.; Cameotra, S. S., *Appl. Microbiol. Biotechnol.* **2000**, *53*, 495. b) Rahman, K. S. M.; Thahira-Rahman, J., McClean, S.; Marchant, R., Banat, *I.M Biotechnol Prog.* **2002**, *18*, 1277.

¹²⁶ Vriezema, D.M.; Aragonés, M.C; Elemans, J.A.A. W.; Cornelissen, J.J.L. M; Rowan, A. E; Nolte, R. J.M., *Chem. Rev.* **2005**, *105*, 1445.

¹²⁷ Yoshizawa, M.; Klosterman, J.K; Fujita, M., *Angew. Chem., Int. Ed.* **2009**, *48*, 3418.

¹²⁸ Soomro, S. S.; Röhlich, C.; Köhler, K., *Adv. Synth. Catal.* **2011**, *353*, 767.

sulfate (SDS) and Cetyl trimethylammonium bromide (CTAB) respectively. SDS bears a negative charge on the hydrophilic head and CTAB bears a positive charge. These variations potentially can aid in the degree of solubility of organic molecules.

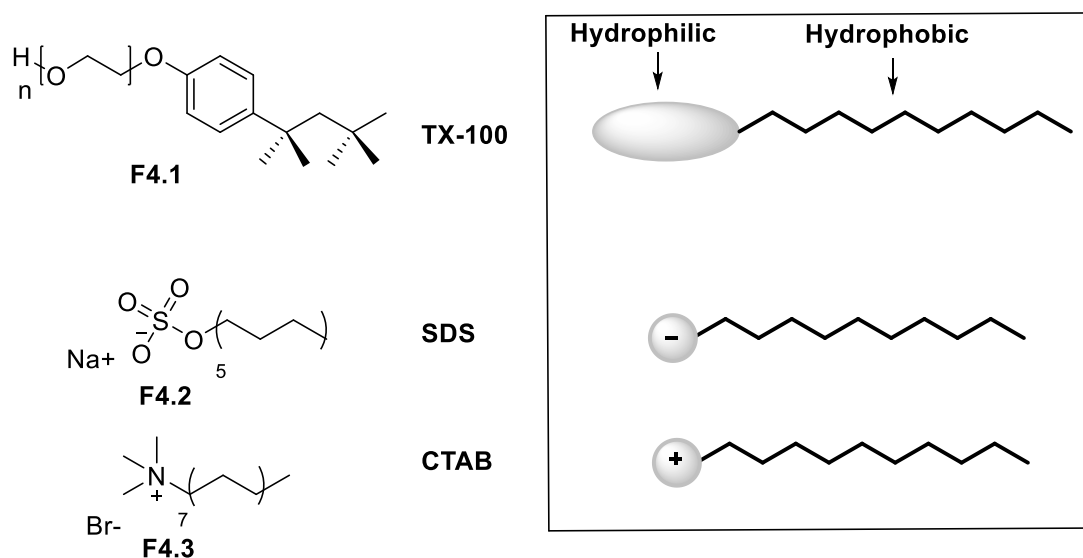


Figure 4. Classes of surfactants used in aqueous media

In an aqueous medium, they exhibit the “hydrophobic effect”, which is the tendency for non-polar groups to cluster together. This cluster aids to shield dissolved organic molecules from contact with the aqueous environment, should they be relatively sensitive to water. This is especially useful in organometallic processes such as oxidation and reduction reactions, as they are quite water sensitive.¹²⁹

To extend this idea further, Lipshutz¹³⁰ and co-workers set to develop “designer” surfactants to be specially tuned for use in transition-metal-catalyzed cross-coupling reactions. The use of surfactants in metal-catalyzed reactions were first explored on a series of known Pd-

¹²⁹ Lindstrom, Marcus. *Organic Reactions in Water: Principles, Strategies and Applications*. Wiley-Blackwell. 2007.

¹³⁰ Lipshutz, B. H.; Ghorai, S., *Aldrichimica acta*. **2012**, *45*, 3.

catalyzed cross-couplings such as Heck,¹³¹ Suzuki-Miyaura,¹³² Sonogashira¹³³ as well as olefin cross- and ring closing metathesis. These reactions have been carried out in water at room temperature. The first generation amphiphile that was developed was PTS, a non-ionic surfactant (PEG-600/ α -Tocopherol-based diester of Sebacic acid) (**Figure 5**). 2nd generation surfactants were also developed based on the same micellar lipophilic interior, which in this case is α -tocopherol.

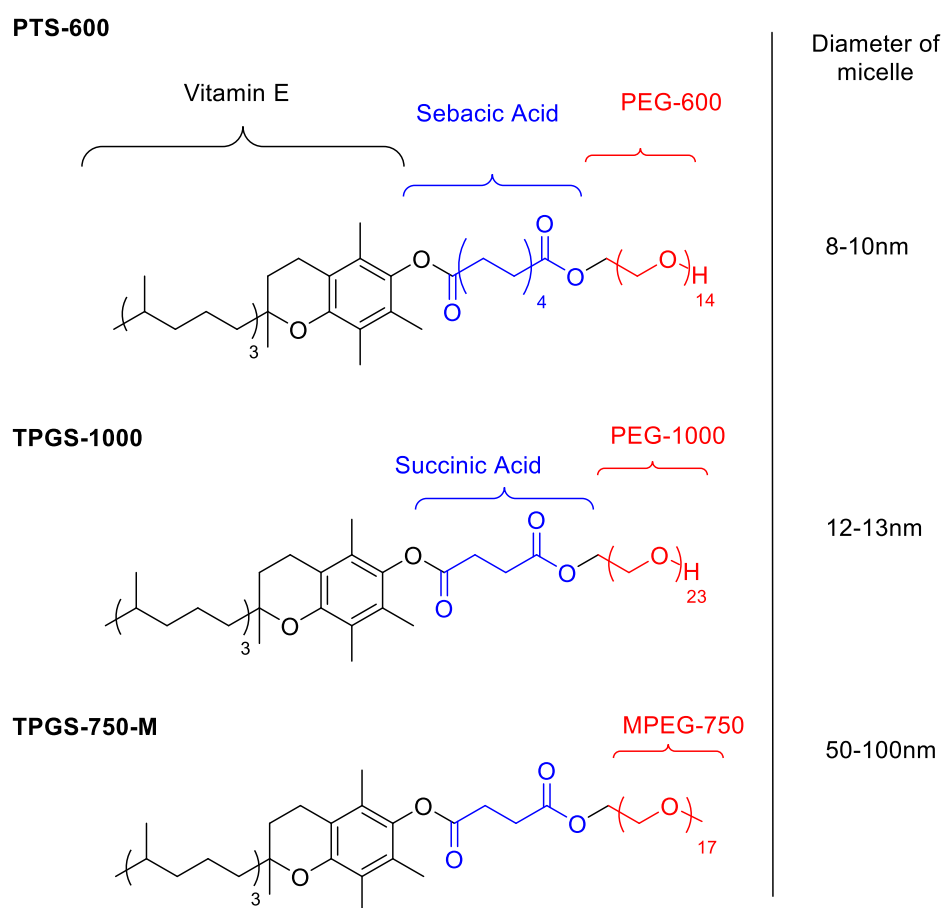


Figure 5. Lipshutz's 1st and 2nd generation designer surfactants used in cross-coupling reactions in aqueous media¹³⁰

¹³¹ Lipshutz, B. H.; Taft, B. R., *Org. Lett.* **2008**, *10*, 1329.

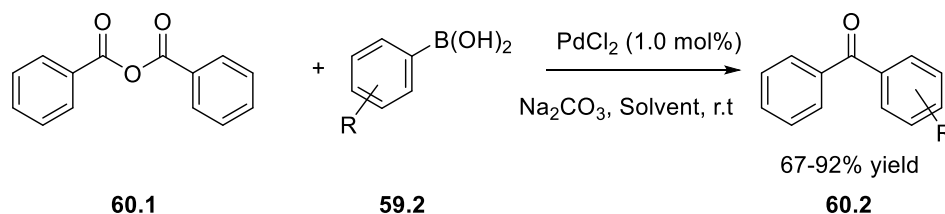
¹³² Lipshutz, B. H.; Petersen, T. B.; Abela, A. R., *Org. Lett.* **2008**, *10*, 1333.

¹³³ Lipshutz, B. H.; Chung, D. W.; Rich, B., *Org. Lett.* **2008**, *10*, 3793.

As the success rates in various cross-coupling reactions differ in the type of surfactants used, it shows that both the size and shape of the nanoparticles are significant. Coupling reactions likely occur within the lipophilic portions of the micelles. However, there is a constant exchange of monomeric units of the surfactant between micellar arrays which gives the micelle a dynamic property. Thus, the micelle's occupants may at any time be in contact with the surrounding water.¹³⁴

Xin and co-workers reported the Suzuki-Miyaura cross-coupling between carboxylic anhydrides and boronic acids in aqueous media using a simple PdCl₂ catalyst to achieve the transformation at room temperature (

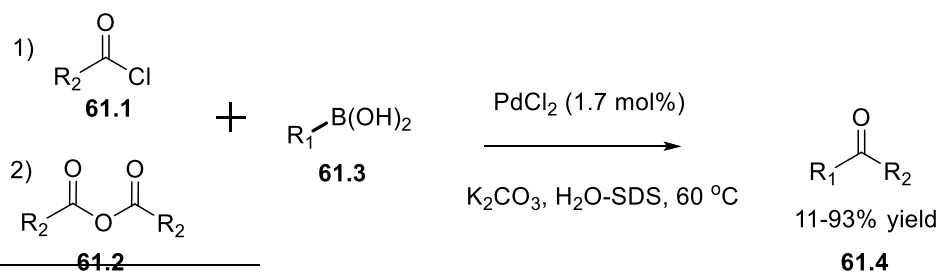
Scheme 60).¹³⁵



Scheme 60. Xin's strategy for Suzuki-Miyaura cross-coupling in aqueous media¹³⁵

Their group also reported a similar transformation with the aid of surfactant in aqueous media (

media (



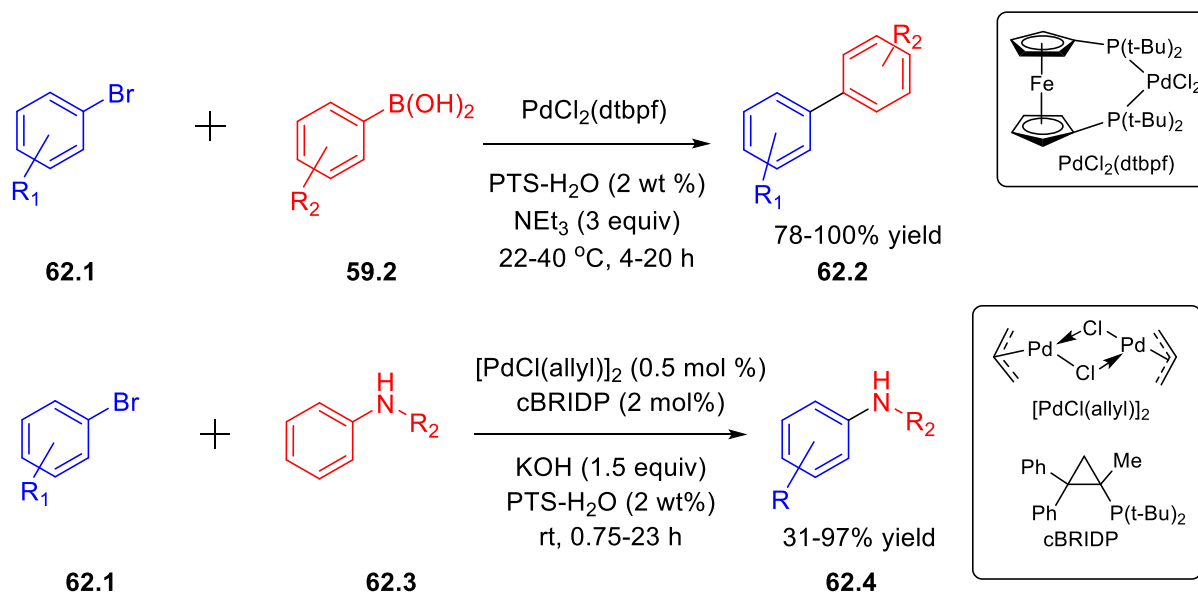
¹³⁴ Lipshutz, B. H.; Ghorai, S., *Aldrichimica acta*. **2012**, *45*, 3.

¹³⁵ Xin, B.-W., *Synth. Commun.* **2008**, *38*, 2826.

Scheme 61). ¹³⁶ However, their work was strictly limited to anhydrides and acyl chlorides.

Scheme 61. Xin's strategy for Suzuki-Miyaura cross-coupling in aqueous media with surfactant¹³⁶

While many applications of the surfactant system in aqueous media have been explored, the Suzuki-Miyaura coupling and amidation of esters under this media is unprecedented, likely due to the difficulty of reactivity of the starting material. The C(acyl)-O of the ester is significantly more challenging to cleave than anhydrides, acyl chlorides or thioesters as will be discussed further in Section 7.



Scheme 62. Lipshutz' development of Pd-catalyzed cross-coupling reactions in aqueous media with the aid of surfactants¹³⁷

¹³⁶ Xin, B.; Zhang, Y.; Cheng K., *Synthesis*. 2007, 1970.

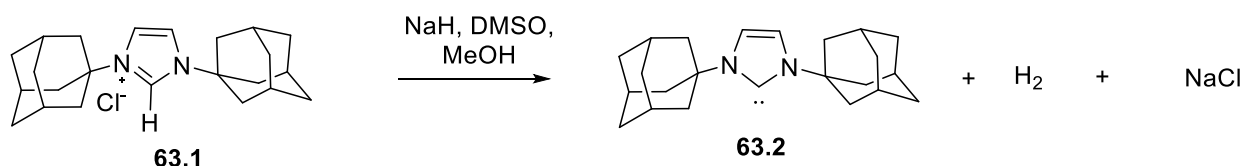
Additionally, Lipshutz and co-workers enabled the traditional Suzuki cross-coupling reaction with palladium catalysis under aqueous media with the aid of the surfactant PTS (**Scheme 62**).¹³⁷ His conditions for the transformations are not only unique in terms of the avoidance of the use of organic solvent, but they also can be run at room temperature with excellent yields.

5.4. Pd catalysis with NHC ligands

Palladium-catalyzed cross-coupling reactions have been widely used in the last 20 years not only in the laboratory setting, but also in industry. Palladium remains one of the most popular metals for cross-coupling reactions, especially to the Suzuki-Miyaura coupling reaction. Due to its popularity, there have been studies done to develop new ligands to accompany the metal in order to control catalytic performance and perhaps even selectivity. The traditional ligands such as phosphines are good σ -donor ligands, which are compatible with the metal's electronic properties and minimize palladium precipitation. However, these ligands are generally used as free ligands to form the active monoligated [PdL] species]. A more efficient catalytic system would be to synthesize the air-stable and moisture stable NHC-bearing palladium (II) complexes (NHC=N-heterocyclic carbene).

¹³⁷ a) Lipshutz, B. H.; Petersen, T. B.; Abela, A. R., *Org. Lett.* **2008**, *10*, 1333. b) Lipshutz, B. H.; Chung, D. W.; Rich, B., *Adv. Synth. Catal.* **2009**, *351*, 1717.

N-heterocyclic carbenes are a special class of carbenes that proves to be a useful moiety for good reactivity. In 1991, Arduengo¹³⁸ and co-workers reported the isolation of a crystalline NHC (**Scheme 63**).



Scheme 63. Arguengo's scheme for synthesis and isolation of NHC ligands¹³⁸

These N-heterocyclic carbenes are not only electronically stabilized due to good orbital overlap with the corresponding nitrogen atoms, but also sterically and kinetically stabilized given their bulky nature. This nature works against dimerization of the corresponding olefin, which is known as the Wanzlick equilibrium. As suggested by Figure 6, the lone pair of the nitrogen donates electron density to the p-orbital at the C2 carbon. The adjacent σ -electron-withdrawing and π -electron donating nitrogen atoms helps to stabilize the structure and lowers the energy of the occupied σ -orbital.¹³⁹

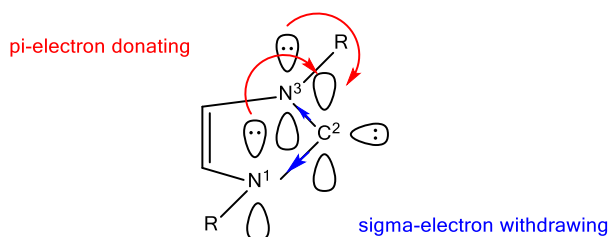


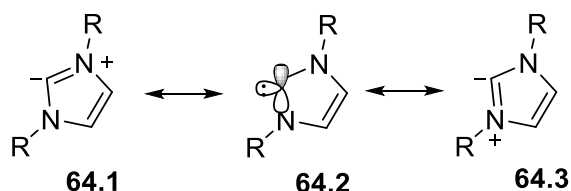
Figure 6. Electron donation of a typical NHC ligand¹³⁹

As suggested by the free electrons on the carbon and as illustrated by the various resonance forms of the carbenes, they are very electron rich (**Scheme 64**). NHCs derived from

¹³⁸ Arduengo, A. J.; Harlow, R. L.; Kline, M., *J. Am. Chem. Soc.* **1991**, *113*, 361.

¹³⁹ Ling, K. B.; Smith, A. D., *Chem. Commun.* **2011**, *47*, 373.

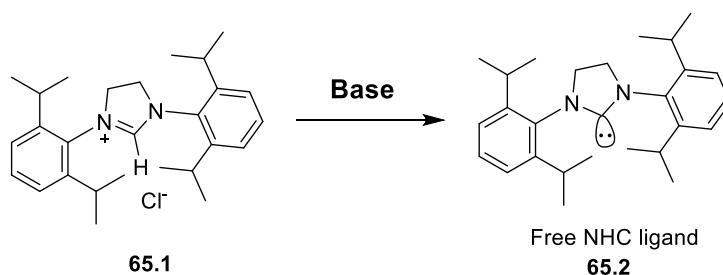
heteroaromatic compounds have greater stability due to their aromatization. These electronics can be tuned by changing the nature of the azole ring. Theoretically, the order of electron donating power would be as follows: benzimidazole < imidazole < imidazoline.



Scheme 64. Resonance structures of aromatic carbenes

Most applications of NHCs involve coordinating to transition metals. Due to its strong σ -donor properties into a σ -accepting orbital of the transition metal, NHCs form very strong bonds with most metals compared with phosphines. More details of the nature of the bonding of these complexes have been studied by several groups such as Nolan¹⁴⁰ and Cavallo¹⁴¹ and co-workers.

Usually, the protonated version of the NHC ligand is isolated rather than the free ligand due to the carbene's sensitivity to moisture. In a catalytic system, they are subsequently activated by a base via deprotonation of the corresponding cationic heterocyclic azolium salt (**Scheme 65**).



Scheme 65. Deprotonation of NHC ligand by base

¹⁴⁰ Díez-González, S. & Nolan, S. P., *Coord. Chem. Rev.* **2007** 251, 874.

¹⁴¹ Jacobsen, H.; Correa, A.; Poater, A.; Costabile, C.; Cavallo, L., *Coord. Chem. Rev.* **2009**, 253, 687.

In the context of a transition-metal catalytic cycle, an electron rich ligand on the catalyst can facilitate oxidative addition step where sterically hindered ligands enhance reductive elimination step. Attaching the ligand directly on the palladium metal allows a good control of the ligand/palladium ratio, which ultimately enhances catalytic activity. Synthesis of these complexes are adapted from Nolan's group procedures,¹⁴² starting with the corresponding $[\text{Pd}(\text{R-allyl})\text{Cl}]_2$ dimer and appropriate NHC ligand. **Figure 7** illustrates the Pd-NHC catalysts that were synthesized for this project.¹⁴³

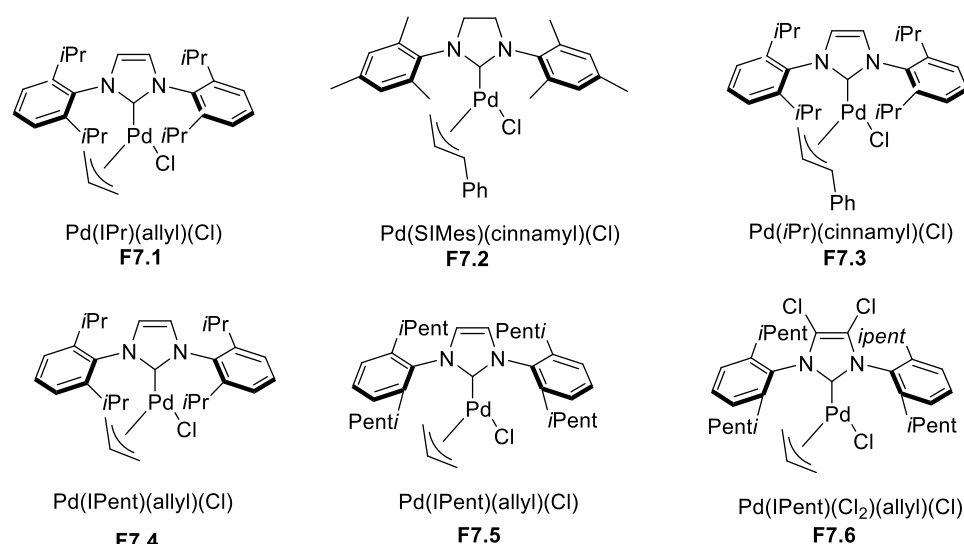


Figure 7. Structures of Pd-NHC catalysts

5.5. Research goals

As outlined above, several groups presented different modes of reactivity for the cross-coupling of esters. Liebeskind demonstrated cleavage of a thioester followed by coupling with

¹⁴² Marion, N.; Navarro, O.; Mei, J.; Stevens, E. D.; Scott, N. M.; Nolan, S. P., *J. Am. Chem. Soc.* **2006**, *128*, 4101.

¹⁴³ Catalysts synthesized by Ph.D student Taoufik Ben Halima. I synthesized NHC ligand precursors.

boronic acid to give access to ketones. Garg and Shi reported cross-coupling of esters via C(aryl)-O cleavage, forming a biaryl species as the carboxylate moiety is transmetallated on the boronic acid. Finally, the Itami and Love groups reported transformation with observed decarbonylation, giving access to biaryl species. The unusual diverging reaction pathway for the coupling of phenyl esters gives an interesting contrast to Pd-catalyzed couplings of activated esters, which gives access to carbonyl containing products. Our goal was to determine if acylative couplings could be achieved on simple phenyl esters and to investigate the underlying rules that dictate selectivity. Thus, we would present another mode of reactivity without decarbonylation to provide a broader range of starting materials to give rise to more diverse ketone products.

Using high-throughput screening to maximize discovery, we explored a broad range of catalysts, ligands and bases to enable this transformation. When results from the high-throughput screening gave satisfactory results, we intended to do a more focused screening to optimize the conditions. Exploration of various catalysts was also of particular interest, especially the use of NHC on metals, which was discussed in Section 5.4. Careful choice of the metal allows selective cleavage of the C(acyl)-O bond to give the desired ketone product.

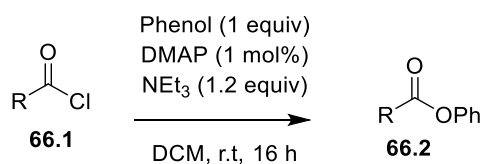
Inspired by Lipshutz' conditions, we decided to explore the reactivity of the Suzuki-Miyaura coupling and amidation of esters in aqueous media and sought to further explore catalysts and vary conditions to enable our transformation under milder conditions. The use of aqueous conditions in cross-coupling reactions will be elaborated in Section 6.3.1.

6. Results and discussion

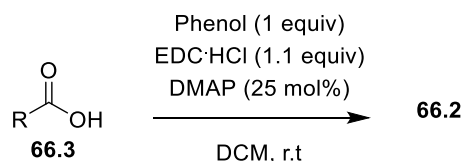
6.1. Starting material preparation

The starting materials that required synthesis in this project were predominately esters. Several substrates were designed to explore the scope of the reaction. Various esters including electron-withdrawing, electron donating, sterically hindered and various heteroatoms were synthesized to fully test the electronics and push the scope. Most esters have been previously synthesized in literature and are made starting from the commercially available acyl chloride or carboxylic acid (**Scheme 66**). Phenol was used as the coupling partner and the substituents on the starting acyl chloride, carboxylic acid or phenol can be modified to synthesize the desired ester.

Esterification of Acyl Chloride



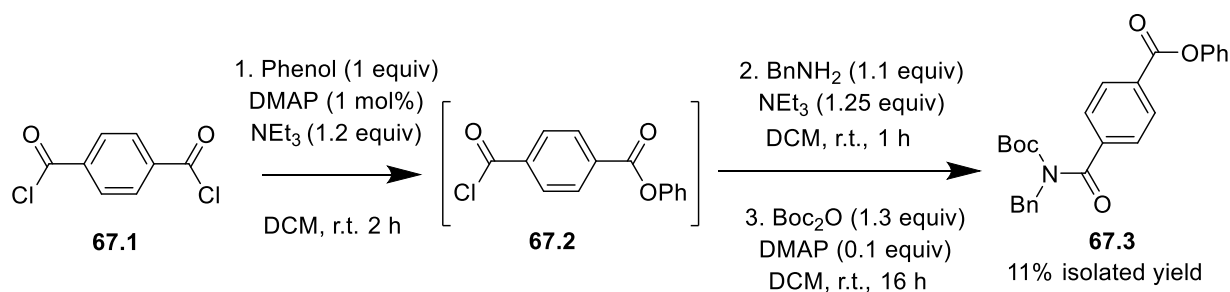
EDC Coupling



Scheme 66. Methods of synthesis of esters

One of the substrates that differ from the previous methods is forming the ester and an amide on the same aromatic ring giving **67.3**. The substrate was synthesized to test selectivity between cleavage of the acyl oxygen bond or the amide oxygen bond. The method for this molecule was

inspired from the typical esterification reaction starting from the acyl chloride and then followed by Garg's procedure for amidation¹⁴⁴ (**Scheme 67**).



Scheme 67. Synthesis of phenyl 4-(benzyl(tert-butoxycarbonyl)carbamoyl)benzoate

6.2. Reaction optimization

This project initiated with a high-throughput screening mindset to screen as many variables as possible that are pertinent to the transformation. With the university's high-throughput facility, we were able to screen up to 96 reactions at a time. This screening led us to our initial discovery of the possibility of the transformation.¹⁴⁵ The goal of this initial screening was to probe new reactivity between substrates that can lead to cross-coupling reactions. A various number of esters were used as the electrophilic species, whereas boronic acid, among a few other substrates was used as the nucleophilic species. Typical catalysts and ligands used in cross-coupling reactions were used in the screening, Pd₂(dba)₂, Ni(COD)₂, Pd(OAc)₂, Ru₃(Co)₁₂, [Ru(cod)Cl], RhCl(PPh₃)₃. Various phosphine and NHC ligands were used, such as dppf, dppb, SPhos, PPh₃,

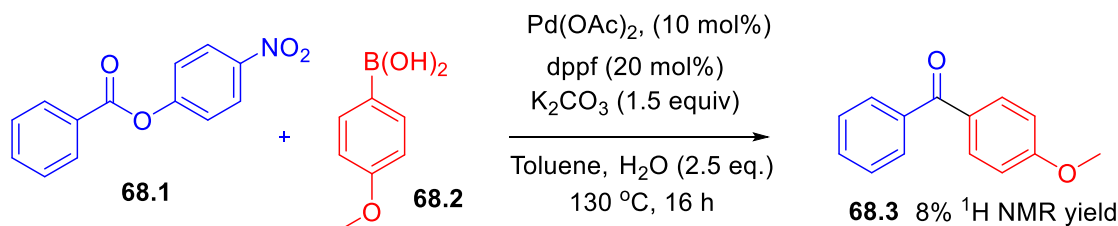
¹⁴⁴ Weires, N. A.; Baker, E. L.; Garg, N. K., *Nat Chem.* **2016**, 8, 75.

¹⁴⁵ Initial high-throughput screening was done by M.Sc. exchange student Imane Yalaoui in collaboration with Ph.D student Taoufik Ben Halima.

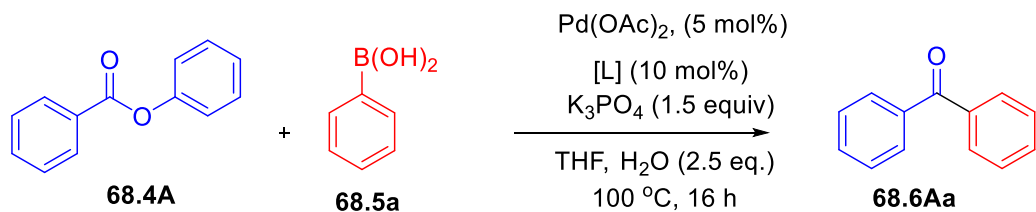
IPr•HCl, P(*o*-tol)₃, dppp, BINAP and tBuxphos. Typical bases used in cross coupling reactions were also used, namely, KO^tBu, K₂CO₃, NEt₃, Cs₂CO₃ and K₃PO₄.

From this screening, it was discovered that 4-nitrophenyl benzoate can couple with 4-methoxy-phenylboronic acid to give the corresponding ketone product **68.3** with the presence of Pd(OAc)₂ as the catalyst at 130 °C (Scheme 68). It is interesting to note that the para-nitro group on the phenolic moiety provided some reactivity as the electron withdrawing properties of the functional group weakens the C(acyl)-O bond of the ester, which enhances the oxidative addition step. Many bench experiments were done to optimize the conditions further by change of temperature, solvent, ligand and base. The product yield increased slightly to 11% using an NHC ligand starting from phenyl benzoate (Scheme 68).¹⁴⁶

Initial hit from high-throughput screening



After some optimization



When L= dppf, dppb, SPhos, PPh₃, P(*o*-tol)₃, dppp, BINAP, tBuxphos, GC yield= <5%

When L= IPr•HCl, GC yield= 11%

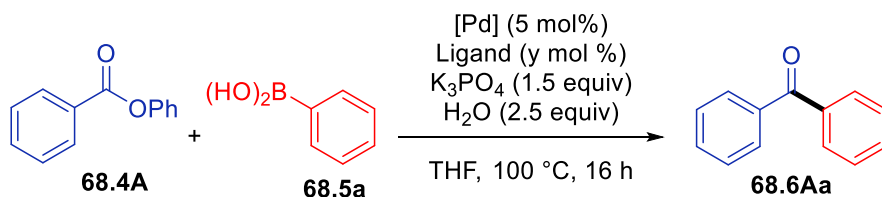
¹⁴⁶ Work done in collaboration with Ph.D student Taoufik Ben Halima. Visiting Masters student Imane Yalaoui left and I continued optimization from her work by varying ligands on Pd(OAc)₂ on phenyl benzoate as opposed to a nitro-group containing ester. Then, I continued to optimize solvent, temperature, base etc.

Scheme 68. Results from initial high throughput screening and optimization

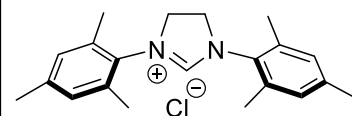
After hundreds of reactions of varying temperature, solvent, base and ligands, reactivity of the cross-coupling seems limited with Pd(OAc)₂. For example, using a broad range of phosphine ligands as used in the initial screening had little effect on the catalyst system, giving yields of <5% for electronically neutral starting materials. However, by switching the phosphine ligand to an NHC ligand under the same conditions, IPr•HCl pushed the yield up to 11%. This was likely due to the good electron donating properties of the NHC ligands. Therefore, research was done to synthesize a more active catalyst as outlined in Section 5.4.

After many more reactions with Pd-NHC ligand combinations, the desired transformation was optimized to high yields. Key results are highlighted in Table 6. Other palladium catalysts such as Pd(dba)₂, PdCl₂, and PdCl₂(COD) were tried with limited success with yields remaining less than 20% (entries 1-6). [Pd(allyl)Cl₂]₂ and [Pd(cinnamyl)Cl₂]₂ are common precursors to many Pd-NHC ligands and are effective in traditional Suzuki-Miyaura coupling reactions.¹⁴⁷ From these precursors, exploration of NHC ligand and catalysts was done. A control experiment using [Pd(cinnamyl)Cl₂]₂ without ligand was done with significantly low yield of 6% (entry 7). Using various NHC in combination with [Pd(cinnamyl)Cl₂]₂, we found that IPr•HCl and SIMes•HCl NHC ligands worked the best improving yields over 20% (entries 8-11).

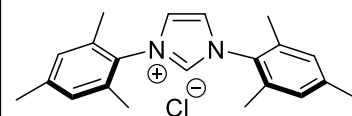
¹⁴⁷ Marion, N.; Navarro, O.; Mei, J.; Stevens, E. D.; Scott, N. M.; Nolan, S. P., *J. Am. Chem. Soc.* **2006**, *128*, 4101.

Table 6. Ligand screening for Suzuki-Miyaura coupling of esters

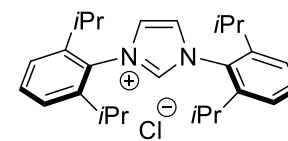
Entry	Pd source	Ligand	y	Yield
1	Pd(OAc) ₂	IMes•HCl	10	13%
2	Pd(OAc) ₂	IPr•HCl	10	11%
3	Pd ₂ (dba) ₃	IPr•HCl	10	16%
4	[Pd(allyl)Cl] ₂	IMes•HCl	10	<5%
5	PdCl ₂	IPr•HCl	10	18%
6	PdCl ₂ (COD)	IPr•HCl	10	10%
7	[Pd(cinammyl)Cl] ₂	N/A	N/A	6%
8	[Pd(cinammyl)Cl] ₂	IPr•HCl	10	21%
9	[Pd(cinammyl)Cl] ₂	SIMes•HCl	10	25%
10	[Pd(cinammyl)Cl] ₂	IPr•HCl	5	59%
11	[Pd(cinammyl)Cl] ₂	IMes•HCl	10	10%
12	Pd(IPr)(cinammyl)Cl	n/a	n/a	95%

Structures of NHC ligands:

SIMes•HCl



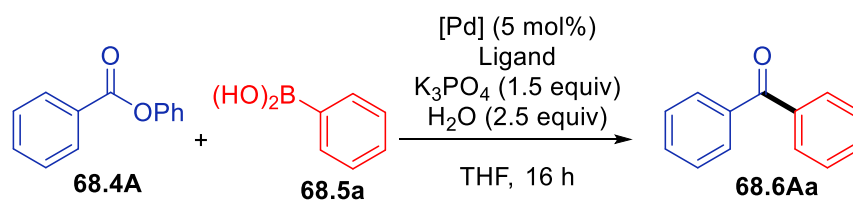
IMes•HCl



IPr•HCl

After identifying the best NHC ligands, we proceeded to use Nolan's procedure as discussed in Section 5.4 to synthesize Pd-NHC catalysts. Synthesized catalysts include, Pd(IPr)(Cinnammyl)Cl, Pd(SIMes)(Cinnammyl)Cl, Pd(IPr)(allyl)Cl, Pd(IPent)(Cinnammyl)Cl, Pd(IPent)(Cl₂)(Cinnammyl)Cl (Figure 7). Using cinnammyl as the coordinating allyl moiety, seems perform better than just an allyl species, which gave an yield of only 47% (entry 3). Further modifications of the NHC ligand on the palladium species bearing the cinnammyl moiety gave more promising results. Pd(SIMes)(Cinnammyl)Cl and Pd(IPr)(Cinnammyl)Cl show promising and similar results giving 93% (entry 6) and 94% (entry 9) yields respectively at 100 °C, at which the temperature most of the initial screening was done. It was found that lowering the temperature to 90 °C did not have an impact on the yield (Table 7). Interestingly, modifying the NHC to IPent derivatives exhibited low reactivity giving yield less than 25% (Entry 8-9). We conclude that Pd(IPr)(Cinnammyl)Cl was the best catalyst for this transformation.

Table 7. Catalyst and temperature screening for Suzuki-Miyaura coupling of esters



Entry	Pd source	Temperature (C °)	Yield
1	Pd(IPr)(cinammyl)Cl	80	76%
2	Pd(SIMes)(cinammyl)Cl	80	74%
3	Pd(IPr)(allyl)Cl	90	47%
4	Pd(IPr)(cinammyl)Cl	90	95%
5	Pd(IPr)(cinammyl)Cl	100	95%
6	Pd(SIMes)(cinammyl)Cl	100	93%
7	Pd(IPent)(cinammyl)Cl	100	24% ^a
8	Pd(IPent)(Cl ₂)(cinammyl)Cl	100	2% ^a
9	Pd(IPr)(cinammyl)Cl	100	94% ^b
10	Pd(IPr)(cinammyl)Cl	90	91% ^c

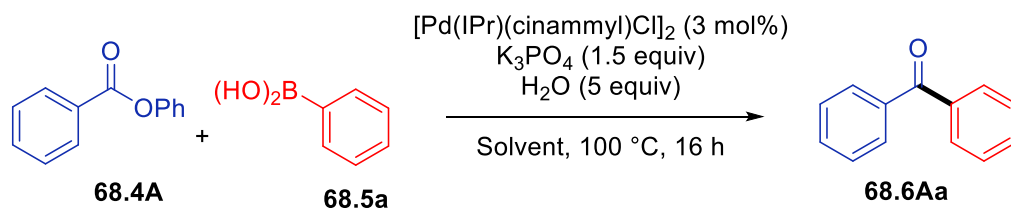
^aReaction run for 2 hours.

^bReaction with 3 mol% catalyst loading.

^cReaction run for 2 hours with 3 mol% catalyst loading. Isolated yield.

A variety of solvents were screened including polar, non-polar solvents and organic and aqueous (Table 8). There does not seem to be a trend in the type of solvent used. Solvents such as MeCN and DCE are not compatible with this system, giving yields <5% (entries 3, 5). Toluene, dioxane and notably water are more compatible solvents giving yields of 70%, 67% and 57% respectively (entries 2, 4, 6). THF remains the optimal solvent of choice giving up to 94% yield (entry 1).

Table 8. Solvent screen for Suzuki-Miyaura coupling of esters

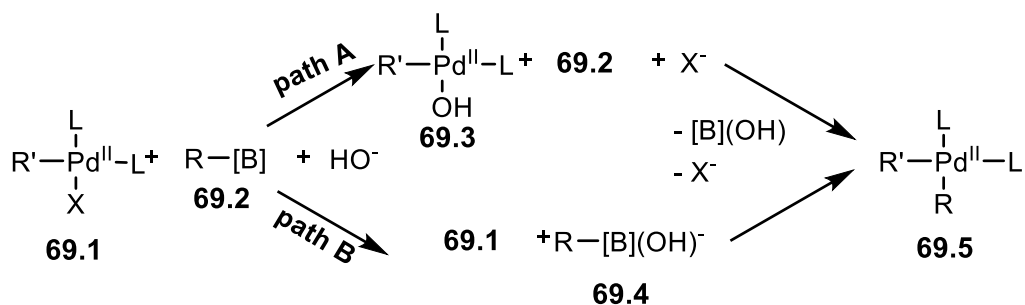


Entry	Solvent	Yield
1	THF	94%
2	toluene	70%
3	MeCN	<5%
4	dioxane	67%
5	DCE	<5%
6	water	57%

Base seems to have a profound impact on the catalytic system, especially in the transmetalation step. In the traditional Suzuki reaction, the role of the base is considered to act like an anionic species such as HO^- , but other bases are possible. There are two possible pathways (Scheme 69) that can explain the role of the base. Path A suggests that the anionic base participates in an exchange of a halogen or triflate in the Pd complex **69.3** formed after oxidative addition. In this case, the base must have significant nucleophilicity to displace the X group acting as the leaving group. This intermediate then proceeds to react with the boronic acid through transmetalation to give **69.5**. Path B suggests the formation of a quaternary boron species **69.4** with the base, which can be associated with faster ligand exchanges during transmetalation.¹⁴⁸ Keeping this in mind several bases typically used in these cross-coupling reactions were screened (Table 9). Use of NEt_3 , CsCO_3 , and tBuOK gave poor yields from the 10-20% range (entries 2, 4, 5). KHPO_4 and

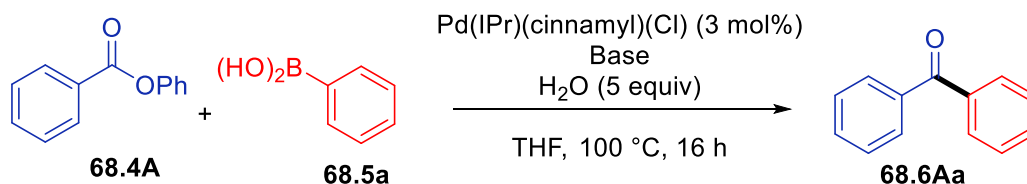
¹⁴⁸ Lima, C. F. R. A. C.; Rodrigues, A. S. M. C.; Silva, V. L. M.; Silva, A. M. S.; Santos, L. M. N. B. F., *ChemCatChem*, **2014**, 6, 1291.

K_2CO_3 gave moderately high yields of 60% and 88% respectively (entries 1, 2). K_3PO_4 was the optimal base in this reaction (entries 6-8). Its superiority of this base over the other bases could be due differences such as solubility, pkb and particle size. Performing a bit further optimization, we concluded that the amount of base was relevant to the experimental conditions.



Scheme 69. Role of the base in possible pathways during transmetallation¹⁴⁸

Table 9. Base screen for Suzuki-Miyaura coupling of esters



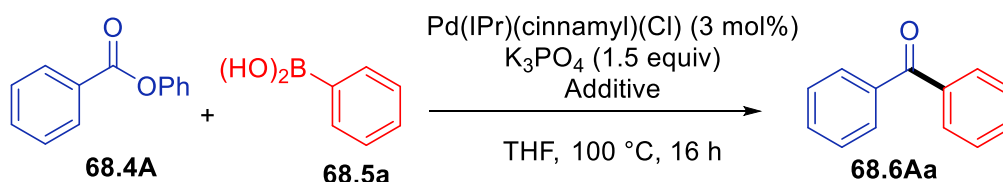
Entry	Base	equiv	Yield
1	K ₂ HPO ₄	1.5	60%
2	K ₂ CO ₃	1.5	88%
3	^t BuOK	1.5	10%
4	Cs ₂ CO ₃	1.5	26%
5	Et ₃ N	1.5	7%
6	K ₃ PO ₄	1	75%
7	K ₃ PO ₄	1.5	94%
8	K ₃ PO ₄	2	77%
9	No base	N/A	<5%

The presence of water in this reaction potentially could have several different roles. Therefore, the amount of water as an additive was screened (Table 10, entries 1-3). One potential role of the water is to aid in the dissolution of the base, and thus aiding in the formation of the boronate from boronic acid or to form the active palladium hydroxide after oxidative addition. Water can also dissolve any potential by-products (salts) in the reactions, which can help push the reaction equilibrium forward.¹⁴⁹ A control experiment was done to verify the necessity of water and the yield was only 60% in the absence of water as an additive (entry 4). In our reaction, we found that 2.5 equivalents of water were enough to increase yield to 94% (entry 1). Various other additives were added in attempt to improve reaction yields. DMAP, a common activator of

¹⁴⁹ Soomro, S. S.; Röhlich, C.; Köhler, K., *Adv. Synth. Catal.* **2011**, 353, 767.

esters,¹⁵⁰ and salt additives such as LiCl,¹⁵¹ and KF¹⁵² that are commonly used as additives in Suzuki-Miyaura cross coupling reactions seemed to have a negative impact on the catalytic system (entries 5-7).

Table 10. Additive screen for Suzuki-Miyaura coupling of esters



Entry	Additive	Amount	Yield
1	Water	2.5 equiv	94%
2	Water	5 equiv	93%
3	Water	20 equiv	64%
4	No additive	N/A	60%
5	LiCl ^a	30 mol%	76%
6	DMAP ^a	30 mol%	28%
7	KF ^a	30 mol%	71%

^aReaction with 5 equiv of water.

6.3. Scope¹⁵³

¹⁵⁰ B. Neises, W. Steglich, *Angew. Chem. Int. Ed.*, **1978**, *17*, 522.

¹⁵¹ Boruah, P. R.; Koiri, M. J.; Bora, U.; Sarma, D., *Tetrahedron Lett.* **2014**, *55*, 2423.

¹⁵² Bernhardt, F.; Trotzki, R.; Szuppa, T.; Stolle, A.; Ondruschka, B., *Beilstein Journal of Organic Chemistry* **2010**, *6*, 7.

¹⁵³ Work done in collaboration with Ph.D student Taoufik Ben Halima. I was responsible for synthesizing and isolating starting material esters, while Taoufik isolated the ketones product from the cross-coupling reaction.

To determine the scope of the reaction, a variety of boronic esters were subjected to the reaction conditions with the parent ester, phenyl benzoate (**68.4A**) (Table 11). The use of electron neutral (**68.6Ab**) and electron rich (**68.6Ac-68.6Ae**) boronic acids showed success in the reaction in more than 80% yield. The use of an unprotected phenol-containing boronic acid (**68.6Af**) was tolerated, giving 58% yield. Products derived from electron-deficient (**68.6Ag-3Aj**) and sterically hindered (**68.6Ak** and **68.6Al**) boronic acids gave slightly lower yields, but in the 70% range. The use of a methyl ester-containing boronic acid is interesting, as it shows selective cleavage of the phenyl benzoate ester bond to provide **68.6Ag** in 79% yield. Electron-rich **68.6Fa** and, electron-poor **68.6Ga**, and furanyl-containing **68.6Ha** could all be prepared in similarly good yields. These products are structurally identical to **68.6Ac**, **68.6Ai**, and **68.6Ad**, respectively, as are **68.6Ab** and **68.6Ba**, but with the functionality placed on the ester starting material rather than the boronic acid.

Satisfied with the scope of the boronic acid, we sought to explore the scope of the ester starting material. Therefore, a variety of esters with different functional groups, aliphatic, sterically hindered and heteroatoms containing esters were also prepared. Several electron neutral esters were prepared: phenyl 2-naphthoate (**68.4B**), *p*-Methyl benzoic acid phenyl ester and (**68.4C**), phenyl 3,5-dimethylbenzoate (**68.4D**). Only the fluorine halogen group is tolerant in this reaction (**68.6Ea**) giving 94% yield. Functional groups of methoxy- (**68.6Fa**), trifluoromethyl- (**68.6Ga**), dimethylamino- (**68.6Ia**) on the ester starting material is tolerated. Heterocycles such as furans (**68.6Ha**) and pyridine (**68.6Ka**) containing esters demonstrated good reactivity with good yields. Various different types of boronic esters were also subjected to our reaction conditions. As the reaction is sensitive to electronics, sterically hindered substrate (**68.6Ma**) worked only with relatively low yields. Various aliphatic esters **68.6Na**, **68.6Oa** and

68.6Pa also showed good reactivity with 66%, 74% and 42% respectively, which is rare in this chemistry.¹⁵⁴ Finally, having both components contain an electron-donating group (**68.6Fe**), an electron-rich and electron-withdrawing group (**68.6Fi**, **68.6Ge**), or electron-withdrawing groups (**68.6Gi**) were all tolerated, with the best yields from the CF₃-containing ester and OMe-containing boronic acid.

Comparing yields of these identical products prepared using different starting material shows that the efficiency of the reaction is more sensitive to the electronics of the boronic acid than the starting ester. Electronic influence of substrate is further discussed in Section 8. It is interesting to observe that while efficient reactions can be obtained at comparable yields whether the starting ester has an electron donating or withdrawing group (**68.6Fa**, 85% and **68.6Ga**, 87%), changing the electronics on the boronic acid accentuates the difference in the outcome of the yield. Using an electron donating group, methoxy on the boronic acid give 87% (**68.6Ac**) yield while replacing the functional group on the boronic acid with an electron-withdrawing CF₃ group, only gives a 71% (**68.6Ai**) yield even with higher catalyst loading and longer reaction time.

¹⁵⁴ a) Shimizu, R.; Fuchikami T., *Tetrahedron Lett.* **1996**, 37, 8405. b) Shimizu, R.; Fuchikami T., *Tetrahedron Lett.* **2001**, 42, 6891. c) Medio-Simón, M.; Mollar C., Rodriguez, N.; Asensio G., *Org. Lett.* **2005**, 7, 4669. d) Wu, X.-F.; Neumann H.; Beller M.; *Adv. Synth. Catal.* **2011**, 353, 788. e) Ishiyama T.; Miyaura N.; Suzuki A., *Tetrahedron Lett.* **1991**, 32, 6923.

6.3.1. Aqueous conditions for Suzuki-Miyaura coupling reaction

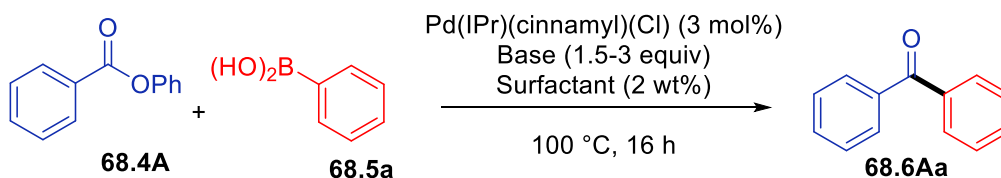
It is interesting to note that during the solvent screen for the Suzuki-Miyaura coupling of esters, the transformation was able to take place in pure water at a moderate yield of 57% (Table 8, entry 6). Taking this result, we decided to apply Lipshutz-like conditions on our system by utilizing the surfactant-water combination as discussed in Section 5.3.¹⁵⁵ Starting from the optimized conditions under organic solvent, we re-optimized the reaction under aqueous media (Table 12). The addition of surfactants dramatically increased the yield from 57% to high 80% yields (entries 1-10). Increasing the temperature from 100 °C to 120 °C with the presence of surfactants seems to be detrimental to the outcome of the reaction (entry 4, 5). This decrease in yield is likely due to the inability to form micelles as efficiently at higher temperatures. Different designer surfactants such as Brij30, Triton-X-M, SPGS-550-M and TPGS-750-M were screened and all gave good yields (entries 2, 8-10). As discussed in Section 5.3, the size of the monomeric unit of surfactant will influence the diameter of the subsequent micelle formation, which would influence the rate of reaction. Different surfactants will give different diameters of micelles upon its formation in water. The optimal concentration of the surfactant was found to be 2 wt%, which is in accordance with literature.¹⁵⁶ This is the critical micelle concentration, in which is the concentration required to form micelles. With this concentration of the surfactant present, it renders concentrations of reactants higher than in organic solvent as it brings molecules closer together due to the hydrophobic effect.

¹⁵⁵ Lipshutz, B. H.; Ghorai, S., *Aldrichimica acta* **2012**, *45*, 3.

¹⁵⁶ Lipshutz, B. H.; Ghorai, S.; Abela, A. R.; Moser, R.; Nishikata, T.; Duplais, C.; Krasovskiy, A.; Gaston, R. D.; Gadwood, R. C., *J. Org. Chem.* **2011**, *76*, 4379.

Overall, reaction outcomes at lower temperatures are competitive with those at higher temperatures. This theory is proven correct in this transformation as optimized conditions in organic solvent require up to 90 °C whereas only 60 °C under aqueous media in the presence of surfactants. As designer surfactants are quite costly, we tried cheaper variations such as Polyethylene glycol derivatives as they have been shown to enable the traditional Suzuki-Miyaura Coupling in water (entries 3-7).¹⁵⁷ To our delight, PEG1000 gave promising yield of 75% yield (entry 4).

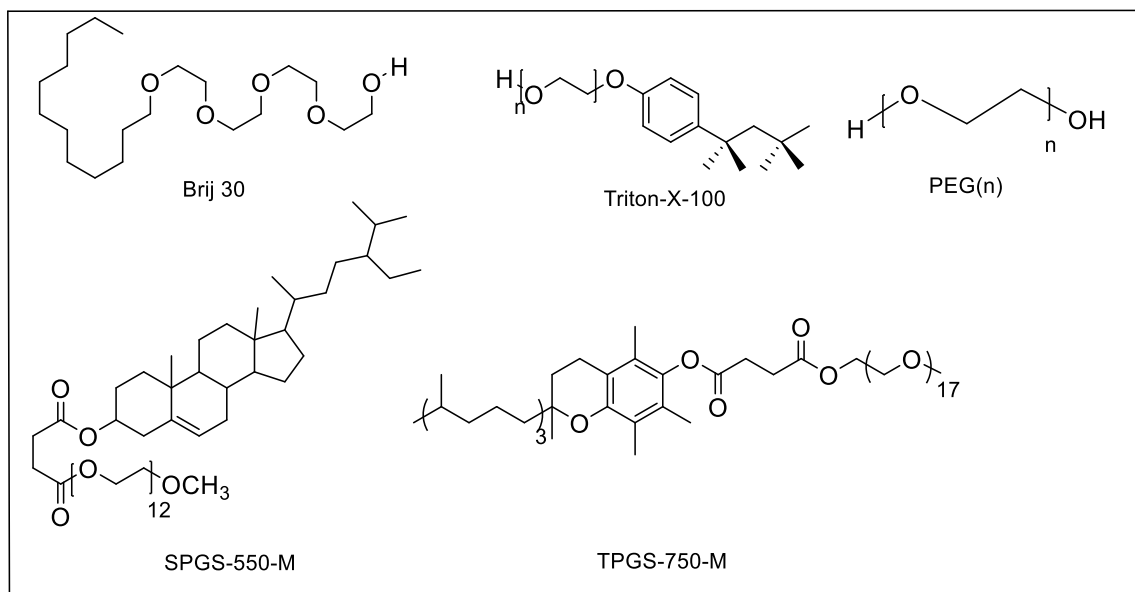
¹⁵⁷ Xiang, L.; Xiaohua, Z.; Ming, L., *Appl. Organomet. Chem.* **2013**, *27*, 615.

Table 12. Surfactant screen for Suzuki-Miyaura coupling of esters

Entry	Surfactant	Base	Yield
1	None	K_3PO_4 (1.5 equiv)	57%
2	Brij ₃₀	K_3PO_4 (1.5 equiv)	96% ^a
3	PEG ₄₀₀	NEt_3 (3 equiv)	85% ^a
4	PEG ₁₀₀₀	K_3PO_4 (1.5 equiv)	75%
5	PEG ₁₀₀₀	K_3PO_4 (1.5 equiv)	69% ^b
6	PEG ₁₀₀₀	NEt_3 (3 equiv)	96% ^a
7	PEG ₄₀₀₀	K_3PO_4 (1.5 equiv)	80%
8	Triton-X-M	K_3PO_4 (1.5 equiv)	74%
9	SPGS-550-M	K_3PO_4 (1.5 equiv)	22%
10	TPGS-750-M	NEt_3 (3 equiv)	93% ^a

^a Reaction done at 80 °C. ^b Reaction done at 120 °C.

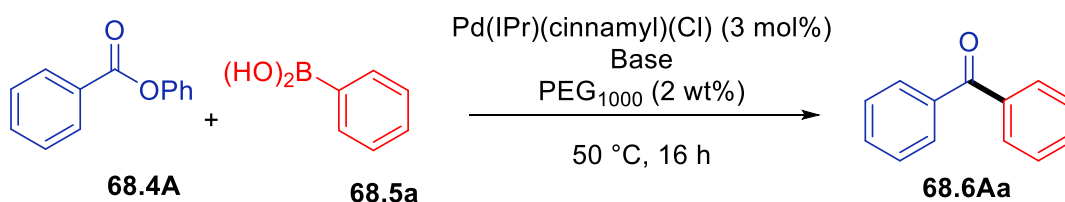
Structures of Surfactants:



Typical bases used in the Suzuki-Miyaura coupling reaction under aqueous conditions were screened with the presence of PEG₁₀₀₀ (**Table 13**).¹⁵⁸ The role of the base plays the same role as it does under organic conditions. Most bases such as K₃PO₄ (entry 1), KOSiMe₃ (entry 3), and K₂CO₃ (entry 4) gave poor yields of less than 10% at lower temperature at 50 °C, with the exception of NEt₃, giving a yield of 91% (entry 8). Increasing the temperature from 50 °C to 80 °C, yields increased significantly from 4% to 87% in the case of K₂CO₃ (entry 5). Only NEt₃ gave good yields at a lower temperature and thus it was found to be the optimal base at 60 °C, giving yield of 96% (entry 7). The use of NEt₃ in Lipshutz' cross-coupling reactions in aqueous media is precedented. NEt₃ was found to be the optimal base in this reaction perhaps due to its compatibility with water and minimizes competing hydrolysis of the ester.¹⁵⁹

¹⁵⁸ Lipshutz, B. H.; Petersen, T. B.; Abela, A. R., *Org. Lett.* **2008**, *10*, 1333.

¹⁵⁹ Lipshutz, B. H.; Chung, D. W.; Rich, B., *Adv. Synth. Catal.* **2009**, *351*, 1717.

Table 13. Base screen under aqueous conditions for Suzuki-Miyaura coupling of esters

Entry	Base	equiv	Yield
1	K ₃ PO ₄	1.5	11%
2	KOH	1.5	52% ^a
3	KOSiMe ₃	1.5	6%
4	K ₂ CO ₃	1.5	4%
5	K ₂ CO ₃	1.5	87% ^a
6	Et ₃ N	1.5	93% ^b
7	Et ₃ N	3	96% ^b
8	Et ₃ N	3	91%
9	No base	N/A	xx%

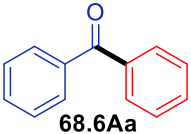
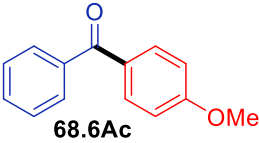
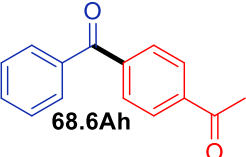
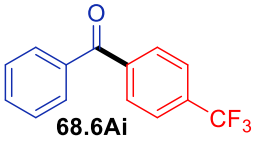
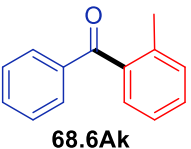
^a Reaction done at 80 °C. ^b Reaction done at 60 °C.

Once the reaction conditions are optimized, we looked at a brief scope of this transformation to investigate the tolerance of functional groups under aqueous conditions and to compare results to those under organic conditions. Varying the groups of the boronic acid side gave comparable yields as shown in Table 14. The yields obtained thus far under aqueous conditions are ¹H NMR yields as we are in the progress of exploring different substrates under this condition. More studies under organic conditions also remain to be done in order to better understand the mechanism of this transformation. However, these results open up a promising possibility to pursue transformations that perhaps cannot be done under organic conditions. It is

also notable that the yields are still comparable to that of organic conditions despite the lower temperature, showing the effectiveness of the surfactant-water system.

Table 14. Boronic acid scope of Suzuki-Miyaura cross-coupling of esters under aqueous conditions

$\text{Pd(IPr)(cinnamyl)(Cl)} \text{ (3 mol\%)}$
 $\text{NEt}_3 \text{ (3 equiv)}$
 $\text{PEG}_{1000} \text{ (2 wt\%)}$
 $60\text{ }^\circ\text{C, 16 h}$

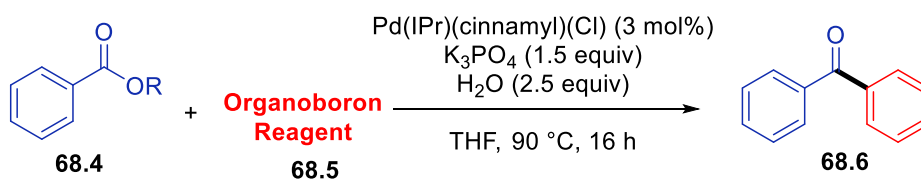
Entry	Final Product	(Aqueous Conditions) ¹ H NMR yields	(Organic Conditions) Isolated Yields
1	 68.6Aa	95%	95%
2	 68.6Ac	95%	87%
3	 68.6Ah	73%	77%
4	 68.6Ai	63%	71%
5	 68.6Ak	87%	76%

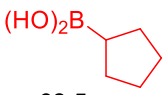

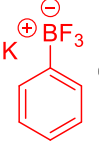
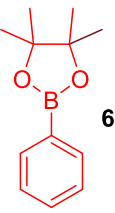
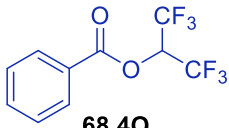
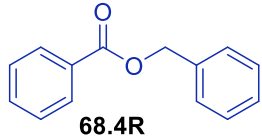
6.3.2. Limitations

There were several esters starting material and boronic acids that were not compatible in our Suzuki-Miyaura coupling of esters, which are summarized in **Table 15**. While exploring the scope of the reaction, it was observed that alkylboronic acids were not compatible as they are less reactive than arylboron derivatives likely due to its difference in their rates of transmetallation (entry 1-2).¹⁶⁰ It attempts to broaden the scope of boronic species that could potentially exhibit reactivity in our reaction system; trifluoroborate **68.5o** and pinacol boronic ester **68.5p** were used with limited success. These boron species have been used successfully during the transmetallation step in cross-coupling reactions.¹⁶¹ For example, Garg's group cross-coupling strategy involves cross coupling of amides and pinacol boronic ester or boronic acid as discussed in Section 5.2. However, upon applying our reaction conditions, it was found that **68.5o** and **68.5p** also exhibit low reactivity in this coupling of esters giving yields of only 25% and 13% of respectively under optimized conditions (Table 15, Entry 3, 4).

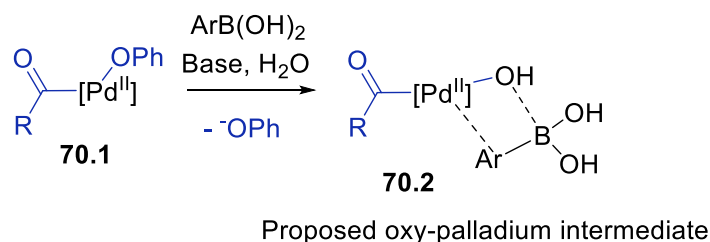
¹⁶⁰ Doucet, H., *Eur. J. Org. Chem.* **2008**, 2008, 2013.

¹⁶¹ Lennox, A.; Lloyd-Jones, G C., *Chem. Soc. Rev.* **2014**, 43, 412.

Table 15. Substrate and boronic acid screen for Suzuki-Miyaura coupling of esters

Entry	Ester	Organoboron	¹ H NMR Yield
1	68.4A	 68.5m	68.6Am 0%
2	68.4A	 68.5n	68.6An 0%
3	68.4A	 68.5o	68.6Aa 25%
4	68.4A	 68.5p	68.6Aa 13%
5	 68.4Q	68.5a, PhB(OH) ₂	68.6Aa 47%
6	 68.4R	68.5a, PhB(OH) ₂	68.6Aa 0%

The outer shell of neutral boron can engage in three sp^2 hybridized bonds, giving the expected trigonal planar geometry. The resulting vacant p-orbital on the orthogonal plane dominates the reactivity patterns of the boronic reagents and accepts electrons from Lewis bases.¹⁶² During the transmetalation step of the Suzuki Miyaura coupling of esters, it is thought that it proceeds through an oxy-palladium intermediate **70.2** (Scheme 70).¹⁶³ For a boronic acid, the geometry is the expected trigonal planar geometry and is a good Lewis acid especially in the presence of water, which in turn favors the transmetalation step.



Scheme 70. Intermediate of transmetalation step in Suzuki-Miyaura cross coupling

On the other hand, organotrifluoroborates are tetrahedral in geometry. However, upon the presence of water, they can easily form the corresponding boronic acid, which can undergo transmetalation.¹⁶⁴ According to Mayr's nucleophilicity scale,¹⁶⁵ organotrifluoroborates are about three to four orders of magnitude faster than boronic ester in terms of reactivity, which is somewhat consistent with the observation. Nevertheless, boronic acid shows to be superior under our reaction conditions and further investigation remains to be done to understand the different reactivity of boron species in our chemistry.

¹⁶² Lennox, A.; Lloyd-Jones, G C. *Chem. Soc. Rev.*, **2014**, *43*, 412.

¹⁶³ Braga, A. A. C.; Morgon, N. H.; Ujaque, G., Maseras, F., *J. Am. Chem. Soc.* **2005**, *127*, 9298.

¹⁶⁴ Lennox, A. J. J.; Lloyd-Jones, G. C., *J. Am. Chem. Soc.* **2012**, *134*, 7431.

¹⁶⁵ a) Berionni, G.; Maji, B.; Knochel, P.; Mayr, H., *Chem. Sci.* **2012**, *3*, 878 b) Lennox, A.; Lloyd-Jones, G C. *Chem. Soc. Rev.*, **2014**, *43*, 412.

Several esters of varying functional group were synthesized and applied in our system to investigate their reactivity. There were a few limitations on the type of esters that were used (**Figure 8**). Halogen functional groups on the ester starting material that are further down the periodic table than fluoride such as bromides **68.4S** and chlorides are not tolerated likely due to the competing oxidative addition reactions with the Pd center. Thiozole containing ester **68.4T** was not tolerant, perhaps due to competing C-H activation on the thiozole ring. More hindered substrates such as phenyl 2,4,6-trimethylbenzoate **68.4U** did not work in this reaction possibly due to steric hindrance. Conjugated carbonyl **68.4V** was not successful possibly due to other competing pathways. A non-phenolic leaving group, hexafluoropropan-2-yl **68.4Q**, was employed, showing lower reactivity, giving yield of 47% (Table 15, Entry 3). Employing a benzyl group on the phenolic leaving group of the ester (**68.4 R**) hindered reactivity as the bond is much more challenging to cleave (Table 15, Entry 4).

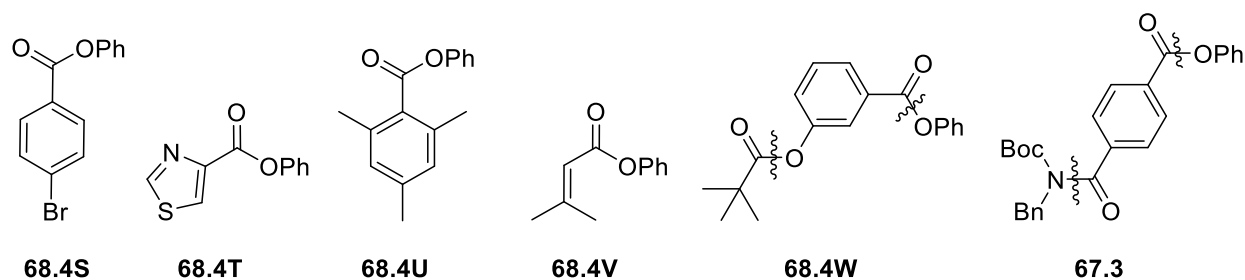


Figure 8. Esters that exhibit low reactivity in the Pd-catalyzed cross-coupling of esters

Inspired by Itami¹⁶⁶ and Garg,¹⁶⁷ a few unique molecules were synthesized to test chemoselectivity in oxidative addition step of the reaction. Itami's ester possesses a pivalate functional group on the phenyl ester **68.4W**. Their group showed that their nickel catalyzed decarbonylative cross-coupling demonstrated selectivity in the activation of phenyl ester moiety,

¹⁶⁶ Muto, K.; Yamaguchi, J.; Musaev, D. G.; Itami, K., *Nat Commun* **2015**, 6.

¹⁶⁷ Weires, N. A.; Baker, E. L.; Garg, N. K., *Nat Chem* **2016**, 8, 75.

forming the desired product in good yield. Upon applying our system, we observed a mixture of products. Not only was there reactivity for the desired bond cleavage of the C(acyl)–O, but there was also cleavage of the C(acyl)–O of the pivalate. Therefore, our system however failed to show selectivity for our desired cleavage position.

Another ester **67.3** that possesses a benzyl N-boc group was synthesized due to the inspiration from Garg's Suzuki coupling of amides. Starting from a terephthaloyl dichloride we were able to successfully functionalize one side with the phenyl ester and the other side with the N-Boc benzyl group. However, subjecting this molecule under our optimized conditions again failed to show selectivity as a mixture of substrates was observed from the cleavage of the C(acyl)–O, and also cleavage of C(acyl)–N bond. From these two experiments, it shows that our catalyst is unselective towards the desired bond cleavage and may be too reactive toward these substrates.

7. Robustness studies

Synthesis of ketones with carboxylic acid derivatives are well established with a wide variety of substrate, catalyst and nucleophile combination as discussed in Section 5.2. Therefore it is worthwhile to consider the merits of our new method of accessing ketones. A key advantage of the method is the ability to cleave relatively strong bonds selectively, which is desirable in multi-step synthesis. To compare the robustness of many acid derivatives that undergo acylative coupling, competitive methanolysis experiment was done. We were particularly interested in the robustness of our phenyl ester starting material compared with other bonds of similar nature. Conditions for this experiment were adapted from Buchwald's procedure for methanolysis of

phenyl esters.¹⁶⁸ The following substrates were subjected to these conditions in the same pot, benzoic anhydride **F9.1**, pyridin-2-yl benzoate **F9.2**, 2,6-dioxopiperidin-1-yl benzoate **F9.3**, *s*-phenyl benzothioate **F9.4** and phenyl benzoate **68.4A**. The disappearance of the starting material was monitored over 96 hours. Quantitative disappearance was measured by integration ratios on the GC-MS relative to an internal standard. The ratios were then normalized to track the relative percentage of substrate over time as it is being consumed (See **Table 20** in Experimental Section 11.4).

Figure 9 shows the resulting order of degradation. By taking the log values of the experimental data, the rate of 1st order degradation can be better visualized in Figure 10. Applying linear regression, this rate could be approximated from the slope of the curve.¹⁶⁹ This is with the assumption that the reaction follows first order kinetics with respect to the starting ester and product and that the degradation of each substrate is independent of one another.

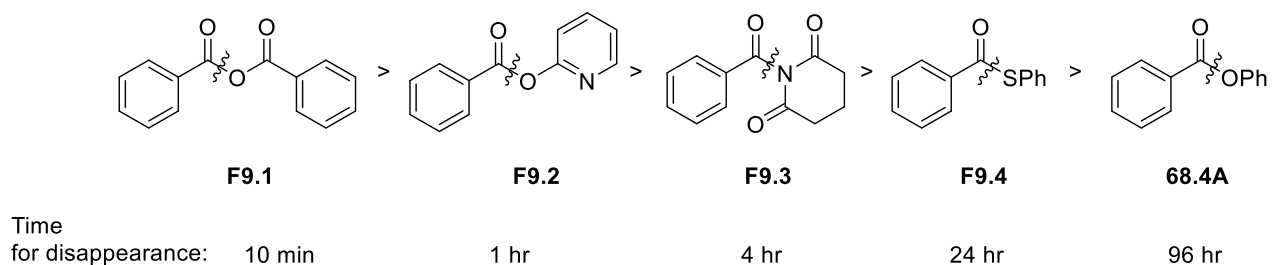


Figure 9. Scale of relative rate of degradation

¹⁶⁸ Watson, D. A.; Fan, X.; Buchwald, S. L., *J. Org. Chem.* **2008**, 73, 7096.

¹⁶⁹ Graph is a representation of relative order of degradation of substrates, so rates are only approximations. Where linear curve $y=mx+b$, $m= k$ (rate constant)

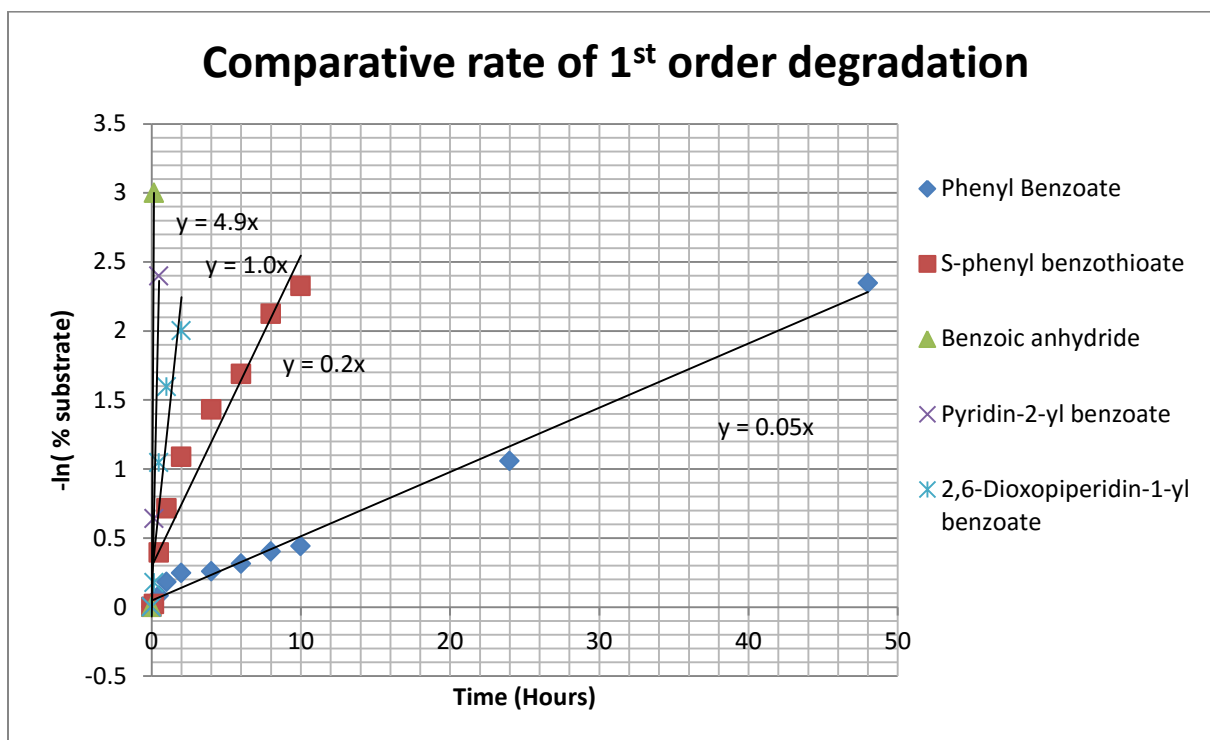


Figure 10. Comparative rate of 1st order degradation

F9.1 was unsurprisingly the first to convert into the methyl ester within the first 10 minutes of the reaction, as it possesses the weakest C(acyl)–X out of the substrates in this reaction and the carboxylic acid moiety is an excellent leaving group compared to the others. The rate of this disappearance is not reported due to the speed in which it disappeared as it only provided two points. The second weakest C(acyl)–O out of these substrates was that of **F9.2**, which degraded with a rate constant of 4.8 hr^{-1} , disappearing within 1 hour. The nitrogen on the pyridine of the aromatic ring is electronegative, which renders the leaving group more electrons deficient. The third substrate **F9.3** disappeared at a rate constant of 1 hr^{-1} , which took 4 hours to completely disappear. In general, the N-CO bond of an amide is relatively hard to cleave as the nitrogen on the cyclohexane ring donates some electron density to the carbonyl through the π^*_{CO} bond. However, the steric distortion of the amide also contributes to the weakening of the bond

compared to typical amides. The cleavage of this substrate was explored by Szostak¹⁷⁰ and co-workers as discussed earlier in Section 5.2.

The second slowest conversion is **F9.4** with a rate constant of 0.23 hr⁻¹, disappearing after 24 hours. The cleavage of the C(acyl)-S bond has been explored in the Liebeskind–Srogl coupling as discussed in Section 5.2. The nature of the bond between a thioester and phenyl-ester is the most similar as the π -donating ability of both attached substituent aids in the stabilization of the carbonyl group,¹⁷¹ but **F9.4** may have poorer orbital overlap and weaker bonding than **68.4A**. Therefore, compared to phenyl ester, **F9.4** is more prone to degradation than phenyl ester **68.4A**. The phenyl ester had a rate constant of 0.05 hr⁻¹, which is about four times slower than **F9.4**.

This experimental evidence gives insight to the differing electrophilicity and stability of these cross-coupling precursors. It is impressive that the phenyl benzoate shows to be the most robust and resistant to degradation at such a magnitude compared to the other substrates, as it proves that cleavage of the C(acyl)-O bond is not trivial. Therefore, the development of our catalytic system is gives a unique transformation that is selective to the cleavage of this particular bond.

8. Electronic influence and proposed mechanism¹⁷²

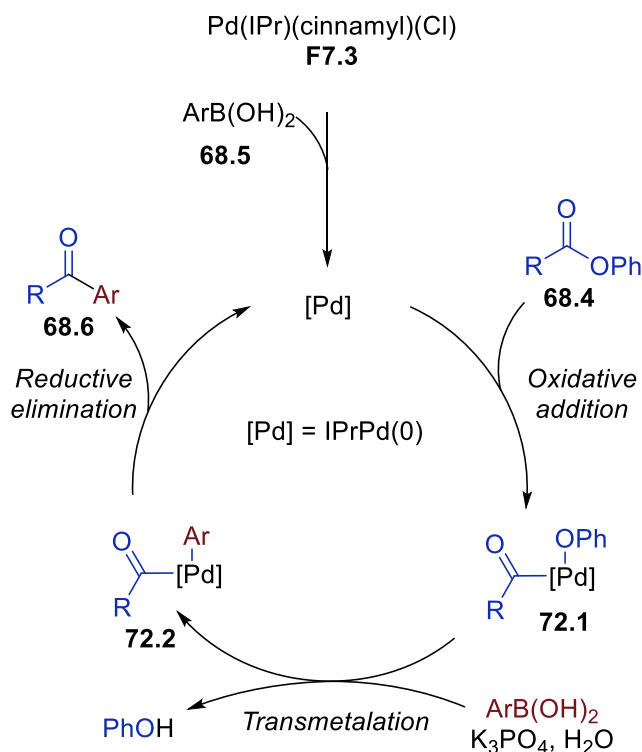
A rigorous mechanistic investigation has not been studied yet, but a reasonable reaction mechanism can be proposed by the observed trends. We propose a catalytic cycle that is analogous to Pd-catalyzed cross-couplings. The Pd(II) precatalyst **F7.3** is reduced by the phenylboronic acid to provide monoligated IPrPd(0) which may oxidatively add to the C(acyl)-

¹⁷⁰ Meng, G.; Szostak, M., *Org. Lett.* **2016**, *18*, 796.

¹⁷¹ Hadad, C. M.; Rablen, P. R.; Wiberg, K. B., *J. Org. Chem.* **1998**, *63*, 8668.

¹⁷² Studies on electronic influence were predominately done by Taoufik Ben Halima. I synthesized the starting materials for the study.

O bond of the starting ester to form **72.1**. Transmetalation of **72.1** to provide **72.2** likely occurs with the presence of the base and water as their roles are described in the prior section.¹⁷³ Finally, reductive elimination of the C–C bond would be expected to form the final ketone product and regenerate the active Pd(0) catalyst (Scheme 71).¹⁷⁴



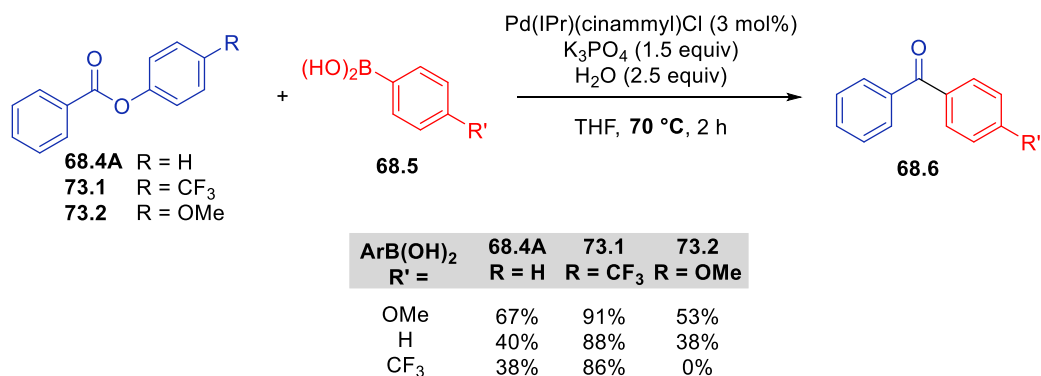
Scheme 71. Proposed mechanism for palladium catalyzed cross-coupling of esters

Trends were studied in the attempt to better understand the electronic influence of substituents on the outcome of the reaction. Thus we varied the functional group on the phenolic leaving group component of the ester with an electron donating and withdrawing group. The temperature was reduced to 70 °C to accentuate differences in reactivity (Scheme 72) (See experimental Section 11.3 for details). Under these conditions, phenyl benzoate **68.4A** provided

¹⁷³ Lima, C. F. R. A. C.; Rodrigues, A. S. M. C.; Silva, V. L. M.; Silva, A. M. S.; Santos, L. M. N. B. F., *ChemCatChem*. **2014**, *6*, 1291.

¹⁷⁴ Ishiyama, T.; Kizaki, H.; Hayashi, T.; Suzuki, A.; Miyaura, N., *J. Org. Chem.* **1998**, *63*, 4726.

the same trend observed at 90 °C, with electron-rich boronic acids providing higher yields than electron-poor. Interestingly, when CF₃-containing benzoate **73.1** was used as a starting material, the same products were obtained in significantly higher yields. In contrast, the use of OMe-containing benzoate **73.2** was used, very low yields were obtained. Since the electronics of the boronic acid seems to have a large influence, it seems when an electron donating boronic acids are used it may facilitate the transmetallation step. However, when electron poor boronic acid is used the transmetallation step is more challenging due to the less nucleophilic species. On the other hand, while an electron donating group on the leaving phenolic group is used the yield is also affected, demonstrating the possible difficulty of the oxidative addition step here. Similarly, using an electron poor group on the leaving phenolic group renders the C-acyl-O bond weaker and facilitates the oxidative addition step. A combination of an electron withdrawing group on the ester and an electron donating group on the boronic acid gives a high yield of 91% under these conditions. When electronics are reversed on these two substrates, reactivity dramatically drops to zero. These trends suggest that the rate determining step of the reaction may change depending on the choice of the substrate.



Scheme 72. Electronic influence of substituents in the Pd-catalyzed cross-coupling of esters

So far our studies support that our reaction pathway is unique in comparison to the established C(aryl)–O cleavage¹⁷⁵ and C(acyl)–O decarbonylative cleavage using Ni-phosphine systems.¹⁷⁶ Further studies are underway to elucidate the mechanism.

9. Aqueous conditions for cross-coupling of esters for amidation

After the optimization of the Suzuki-Miyaura coupling reaction of esters in organic and aqueous media, we sought to apply similar conditions to cross-coupling of esters and amines to make amides. There has been some precedents that cross-coupling reactions involving C–N bond formation can be conducted under aqueous conditions.¹⁷⁷ A broad range of these reactions from traditional methods to catalytic methods are available, but limitations are often the choice of substrates and harshness of conditions. The most well-known is the Buchwald–Hartwig amination where the synthesis of the C–N bond is formed via a palladium cross-coupling between aryl halides or pseudohalides and amines.¹⁷⁸ Traditional methods of amidation reaction involve the use of stoichiometric amount of AlMe_3 ¹⁷⁹ or other coupling reagents and require activation of starting material. More recently, Buchwald and co-workers reported amidation from

¹⁷⁵ A) Quasdorf, K. W.; Tian, X.; Garg, N. K., *J. Am. Chem. Soc.* **2008**, *130*, 14422. B) Guan, B.-T.; Wang, Y.; Li, B.-J.; Yu, D.-G.; Shi, Z.-J., *J. Am. Chem. Soc.* **2008**, *130*, 14468.

¹⁷⁶ a) Muto, K.; Yamaguchi, J.; Musaev, D. G.; Itami, K., *Nat. Commun.* **2015**, *6*, 7508. B) LaBerge, N. A.; Love, J. A., *Eur. J. Org. Chem.* **2015**, *2015*, 5546.

¹⁷⁷ a) Lipshutz, B. H.; Chung, D. W.; Rich, B., *Adv. Synth. Catal.* **2009**, *351* (11-12), 1717-1721. b) Shimasaki, T.; Tobisu, M.; Chatani, N., *Angew. Chem. Int. Ed.* **2010**, *49* (16), 2929-2932 c) Sasaki, K.; Crich, D., *Org. Lett.* **2011**, *13*, 2256.

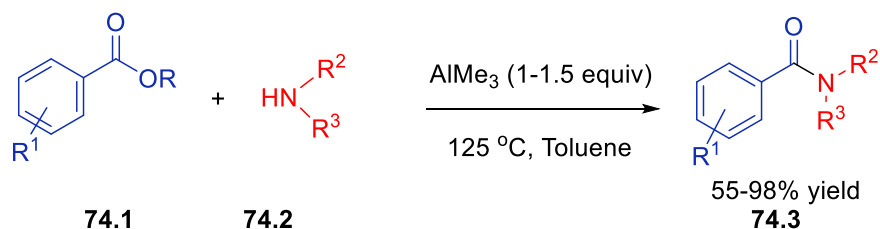
¹⁷⁸ Muci, A. R.; Buchwald, S. L., Practical Palladium Catalysts for C–N and C–O Bond Formation. In *Cross-Coupling Reactions: A Practical Guide*, Miyaura, N., Ed. Springer Berlin Heidelberg: Berlin, Heidelberg, **2002**, 131-209

¹⁷⁹ a) Gustafsson, T.; Ponten, F.; Seeberger, P. H., *Chem. Commun.* **2008**, 1100. b) Basha A. Lipton M. Weinreb SM. *Tetrahedron Lett.* **1977**, *48*, 4171.

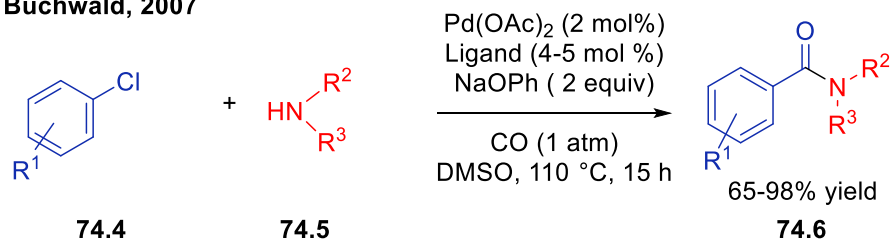
palladium cross coupling between aryl halides.¹⁸⁰ However, the major limitation is the use of CO pressure to access the amide substrate.

Most previous studies rely on the use of halides, pseudohalides or carboxylic acids as a coupling partner to amines to form amides. The type of coupling partners poses a limitation on the types of substrates used (Scheme 73). We sought to extend the scope of reactivity to esters starting material giving access to more diverse products. We present a novel reactivity analogous to the Suzuki-Miyaura coupling of esters using NHC-palladium catalysis to selectively cleave the C-(acyl)-O bond to give access to amides.

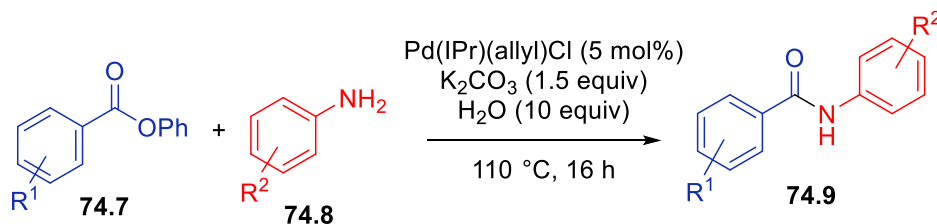
Weinreb, 1977



Buchwald, 2007



Our work



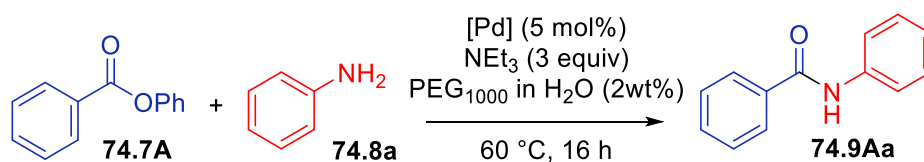
Scheme 73. Development of C-N bond forming reactions^{179,180}

¹⁸⁰ Martinelli, J. R.; Clark, T. P.; Watson, D. A.; Munday, R. H.; Buchwald, S. L., *Angew. Chem. Int. Ed.* **2007**, *46*, 8460.

9.1. Optimization

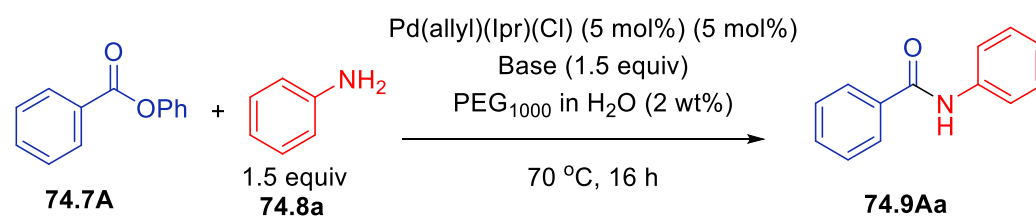
This project was similarly also derived from the same high-throughput screening that led us to the discovery of the Suzuki-Miyaura coupling of esters as discussed in Section 6.2. Optimization of this transformation was done for organic conditions¹⁸¹ and gave high yields at a high temperature of 110 °C (Scheme 73). A control experiment was also done under organic conditions with no catalyst, which did not give desired product, showing the necessity of the catalyst for this transformation to take place. Using the optimized water-surfactant conditions for the Suzuki-Miyaura coupling of esters from Section 6.3.1 as a starting point, various palladium catalysts that were also used for the preceding project was also screened for this transformation (**Table 16**). Surprisingly, we found that the Pd(IPr)(Cinnamyl)Cl and Pd(SIMes)(Cinnamyl)Cl catalyst gave yields of less and 10%, despite being the best catalysts for the Suzuki-Miyaura coupling. Varying the NHC on the Pd catalyst to IPent with the cinnamyl moiety slightly improved yields, but were still low in the 30-40% range (entries 3-4). In this case, using allyl as the coordinating allyl moiety seems to perform better than the cinnamyl species, which was opposite of the trend observed in the Suzuki-Miyaura coupling of esters. Pd(IPr)(allyl)Cl and Pd(IPent)(allyl)Cl seems to perform equivalently at higher temperature at 80 °C (entry 7-8) giving yields of 86% and 85% respectively as opposed to at 60 °C where yields are 44% and 64% respectively.

¹⁸¹ Initial high-throughput screening was done by M.Sc. exchange student, Imane Yalaoui and optimization of organic conditions was done by Ph.D student Taoufik Ben Halima.

Table 16. Catalyst optimization for amidation of esters under aqueous conditions

Entry	Pd source (5 mol%)	Temperature (°C)	Yield
1	Pd(IPr)(cinammyl)Cl	60	<5%
2	Pd(SIMes)(cinammyl)Cl	60	<10%
3	Pd(IPent)(cinammyl)Cl	60	43%
4	Pd(IPentCl ₂)(cinammyl)Cl	60	34%
5	Pd(IPr)(allyl)Cl	60	44%
6	Pd(IPent)(allyl)Cl	60	64%
7	Pd(IPr)(allyl)Cl	80	86%
8	Pd(IPent)(allyl)Cl	80	85%

With the optimal catalyst identified, typical bases used in the coupling of amides were screened. Other bases of anionic properties (K₂CO₃, tBuOK, KOSiMe₃) and amine bases (DBU, DIEA, dicyclohexyl methyl) that were thought to be lipophilic in water were also screened (Table 17, entries 2-6) The role of the base in this reaction enables deprotonation of the nucleophilic aniline. A control experiment was done to test the necessity of base and the results showed no reactivity (entry 1). Again, the use of NEt₃ seems to find precedents in literature, especially in Lipshutz' cross-coupling reactions in aqueous media and proved to be the optimal base (entries 8-10).

Table 17. Base optimization for amidation of esters under aqueous conditions

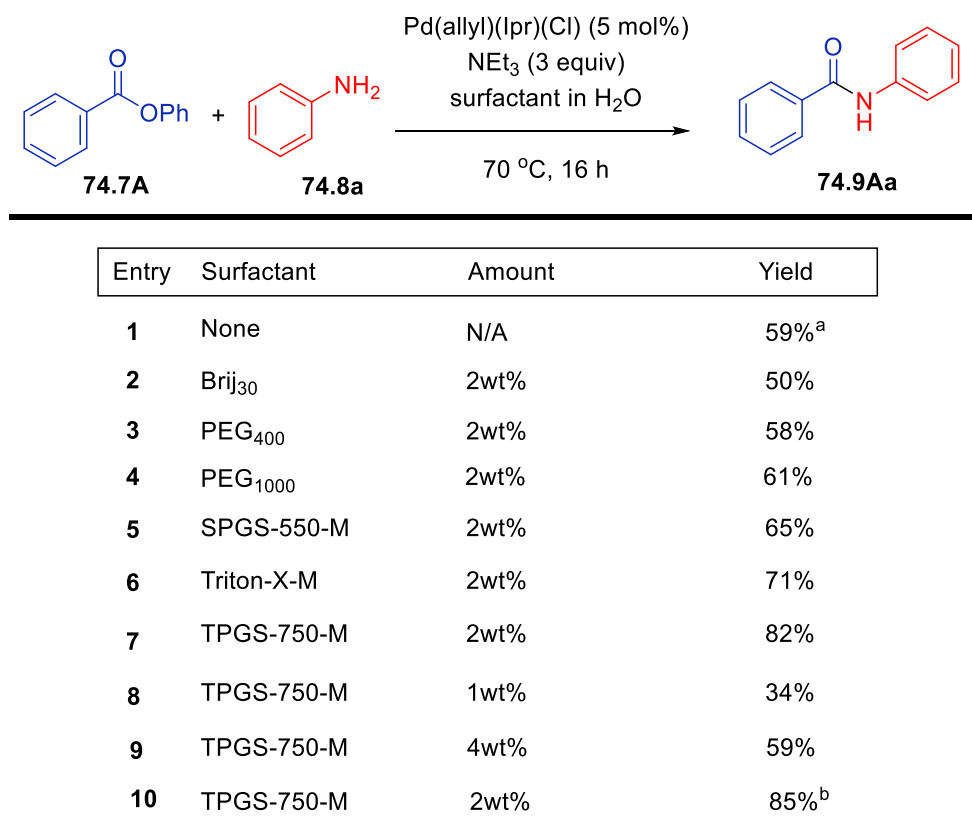
Entry	Base	equiv	Yield
1	No base	N/A	0%
2	K ₂ CO ₃	1.5	39%
3	^t BuOK	1.5	<5%
4	KOSiMe ₃	1.5	26%
5	DBU	1.5	0%
6	DIEA	1.5	32%
7	Dicyclohexylmethyl amine	1.5	<10%
8	Et ₃ N	1.5	51%
9	Et ₃ N	3	61%

A broad range of surfactants typically used for cross-coupling reactions were screened (Table 18).¹⁸² Refer to section 5.3 and 6.3.1 for discussion on influence of surfactants in cross-coupling reactions. There is a significant increase in yield with the presence of surfactant versus without (entry 1) from 59% to mid-80% yields. PEG derivatives, Brij30, Triton-X-M, SPGS-550-M, and TPGS-750-M were the surfactants screened in this reaction (entries 2-5). TPGS-750-M was found to be the optimal surfactant, giving yield up to 85% (entry 9). This finding is not surprising as it the second generation of surfactant developed by Lipshutz and co-workers. The first generation surfactant PTS showed its effectiveness in the amination of aryl halides as discussed in Section 5.3. **Figure 5** shows their similarity in the backbone of the structure,

¹⁸² Lipshutz, B. H.; Ghorai, S., *Aldrichimica acta*. **2012**, *45*, 3.

composing of a racemic alpha-tocopherol diester. Other surfactants either only slightly enhanced the reaction or have no effect on the reaction conditions in aqueous media.

Table 18. Surfactant optimization for amidation of esters under aqueous conditions



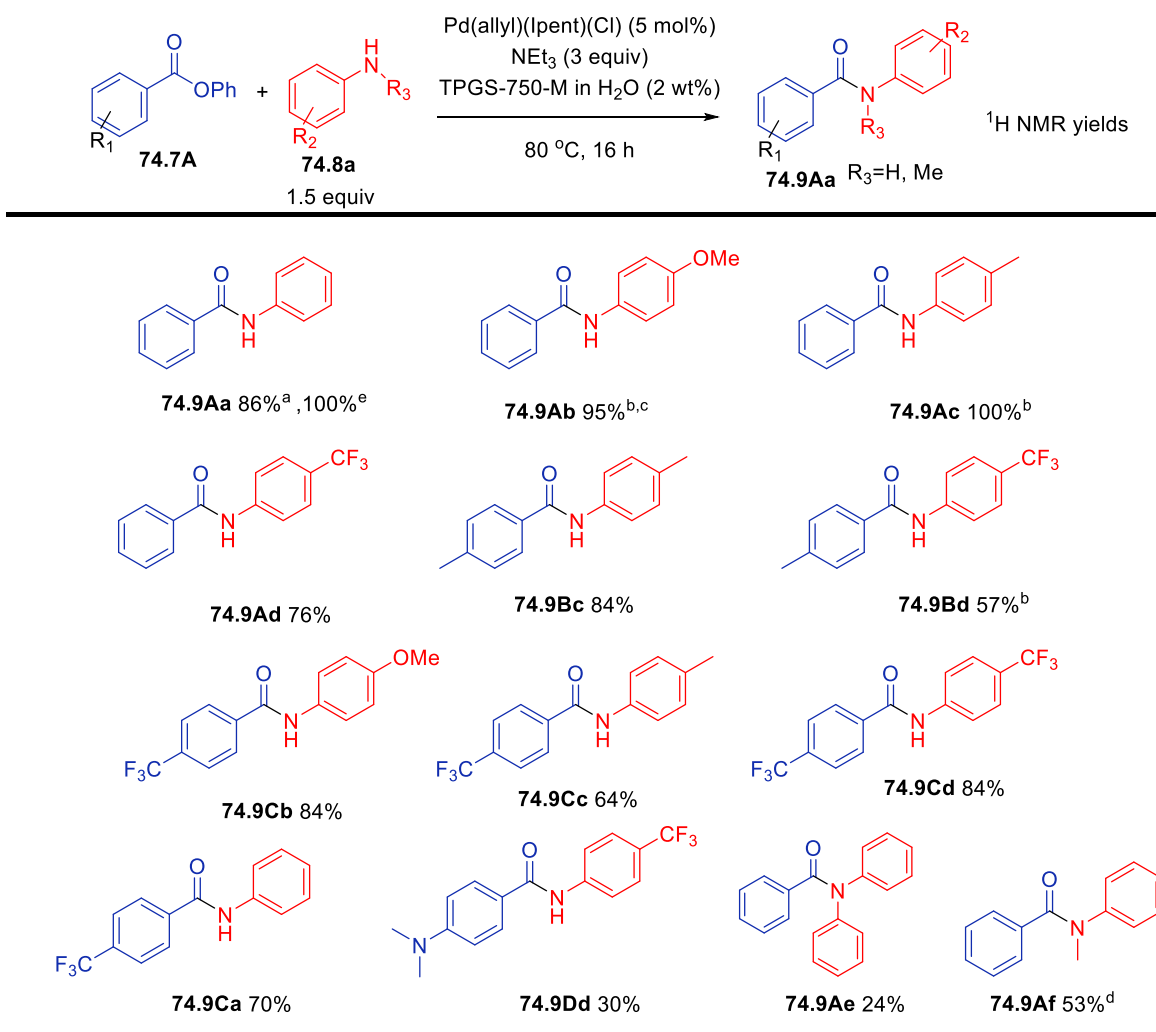
^aReaction at 90 °C. ^bReaction at 80 °C, 2 equiv aniline used.

9.2. Scope and limitations

To determine the scope of the reaction, several electron donating and withdrawing groups on the starting ester and the aniline substrate were varied (Table 19). Electronics of the substrates seem to have no consistent trend in the outcome of the reaction. The possible effect of electronics on the ester is perhaps the competing hydrolysis pathway. Using electron donating or electron neutral anilines tend to be a bit better than electron withdrawing groups. Interestingly,

this system also works moderately with secondary amines. This study is not comprehensive scope as we are still in the progress of exploring different aspects of the reaction and reactivity with different substrates, thus only ^1H NMR yields are reported thus far. Nevertheless, the scope of the reaction show promising possibilities of functional group tolerance under aqueous conditions and under relatively mild conditions. More investigation remains to be done to compare reactivity of substrates under organic and aqueous conditions, but access to this new reactivity under different conditions opens up possibilities of broader substrate scope.

Table 19. Synthesis of amides under aqueous conditions



^a2 equiv aniline, same yield using Pd(allyl)(Ipr)Cl. ^b1.7 equiv aniline. ^c3 hours, 3 mol% catalyst. ^d5 mol% Pd(allyl)(Ipr)Cl, 4 equiv NEt₃. ^e1.2 equiv aniline, K₂CO₃, 10 equiv water, 110 °C, Toluene.

10. Summary and future work

Through this project, we have shown that catalytically cleaving a strong C(acyl)-O bond is possible to allow the synthesis of ketones via the Suzuki-Miyaura cross-coupling reaction. We also demonstrated that cleaving the same C(acyl)-O bond is possible to allow the synthesis of amides via cross-coupling of anilines and esters. Through the exploration of several different palladium catalysts, we conclude that the use of Pd-NHC system proves to be most effective in this transformation. This catalyst is efficient in the cleavage of simple phenyl esters via oxidative addition allowing excellent yields with broad range of substrates. This work represents a rare entry of Pd into the field of C-O activation, giving a unique reaction pathway compared to previous studies done in this field, especially compared to the decarbonylative cross-coupling using nickel catalysis.

It is notable that these cross-coupling reactions are can be conducted successfully under aqueous environment with the presence of surfactant. Conducting these experiments under lower temperatures proved to be comparable in yields and scope so far. These conditions can have significant positive environmental impact and make a step towards greener chemistry. This project opens up a new field of cross-coupling reactions that could be explored under aqueous conditions. Further work on the scope to probe reactivity remains to be done.

Our future work encompasses extending this reaction scope to more challenging substrates such as esters possessing a leaving group other than a phenolic moiety. Re-optimization of more challenging substrates such as more hindered substrates and 1,1,1,3,3,3-hexafluoropropan-2-yl benzoate and methyl benzoate are currently being done. Mechanistic studies to further elucidate

the mechanism are also currently being conducted with preliminary support for the proposed mechanism using DFT calculations.

This project opens up different possibilities to enable different routes of reactivity in cross-coupling reactions. Although there remains to be limitations in the nature of the substrate being used, further catalyst development can perhaps overcome these challenges.

11. Experimental

General experimental details

Unless otherwise indicated, reactions were conducted under an atmosphere of argon in 5 mL screw-capped vials that were oven dried (120 °C). Column chromatography was either done manually using Silicycle F60 40-63 μm silica gel, or using a Combiflash Rf+ automated chromatography system with commercially available RediSep Rf normal-phase Silica Flash columns (35-70 μm). Analytical thin layer chromatography (TLC) was conducted with aluminum-backed EMD Millipore Silica Gel 60 F₂₅₄ pre-coated plates. Visualization of developed plates was performed under UV light (254 nm) and/or using KMnO₄ or ceric ammonium molybdate (CAM) stain.

Instrumentation

¹H, ¹³C, and ¹⁹F NMR spectra were recorded on a Bruker AVANCE 400 MHz spectrometer. ¹H NMR spectra were internally referenced to the residual solvent signal (e.g. CDCl₃ = 7.27 ppm). ¹³C NMR spectra were internally referenced to the residual solvent signal (e.g. CDCl₃ = 77.36 ppm). ¹⁹F spectra were unreferenced. Data for ¹H NMR are reported as follows: chemical shift (δ ppm), multiplicity (s = singlet, d = doublet, t = triplet, q = quartet, m = multiplet), coupling constant (Hz), integration. NMR yields for optimization studies were obtained by ¹H NMR analysis of the crude reaction mixture using 1,3,5-trimethoxybenzene as an internal standard.

GC yields for optimization studies were obtained via a 5 point calibration curve using FID analysis on an Agilent Technologies 7890B GC with 30 m x 0.25 mm HP-5 column. Accurate mass data was obtained either via a Kratos Concept mass spectrometer at the uOttawa John L.

Holmes Mass Spectrometry Facility, or via processing of data obtained from an Agilent 5977A GC/MSD using MassWorks 4.0 from CERNO bioscience.¹⁸³

Materials

Organic solvents were purified by rigorous degassing with nitrogen before passing through a PureSolv solvent purification system, and low water content was confirmed by Karl Fischer titration (<25 ppm for all solvents). Water was vigorously degassed for at least ten minutes prior to use. The following reagents are commercially obtained and were used as received. K₃PO₄ was obtained from Strem Chemicals. K₂CO₃ was obtained from Alfa Aesar. Cs₂CO₃, tBuOK, K₂HPO₄, NEt₃, PPh₃, PtBu₃, P(*o*-tol)₃, and Phenol were obtained from Sigma Aldrich. Dppf, SPhos, and BINAP were obtained commercially from Combi-Blocks. Pd(OAc)₂, Pd₂(dba)₃, PdCl₂, PdCl₂(COD) were obtained from Strem Chemicals. All boronic acids, **2a-2l**, were obtained from Combi-Blocks. *N,N*-dimethyl-4-aminopyridine (DMAP) was obtained from Matrix Scientific. 1-(3-dimethylaminopropyl)-3-ethylcarbodiimide hydrochloride (EDC·HCl) was obtained from Combi-Blocks. *N*-heterocyclic carbene (NHC) ligands were prepared according to the literature.¹⁸⁴ Pd catalysts Pd(IPr)(cinammyl)Cl, Pd(IMes)(cinammyl)Cl, and Pd(IPr)(allyl)Cl were prepared according to the literature.¹⁸⁵ Phenyl benzoate **68.4A** was obtained from Alfa Aesar. Benzyl benzoate **68.4R** was obtained from Sigma Aldrich. The following esters were prepared according to literature: Phenyl 4-(dimethylamino)benzoate (**68.4I**),¹⁸⁶ Phenyl Isonicotinate (**68.4J**),¹⁸⁷ Phenyl furan-2-carboxylate (**68.4K**),¹⁸⁸ phenyl 2-

¹⁸³ Wang, Y.; Gu, M., *Anal. Chem.* **2010**, *82*, 7055.

¹⁸⁴ Bantreil, X.; Nolan, S. P., *Nat. Protocols* **2011**, *6*, 69.

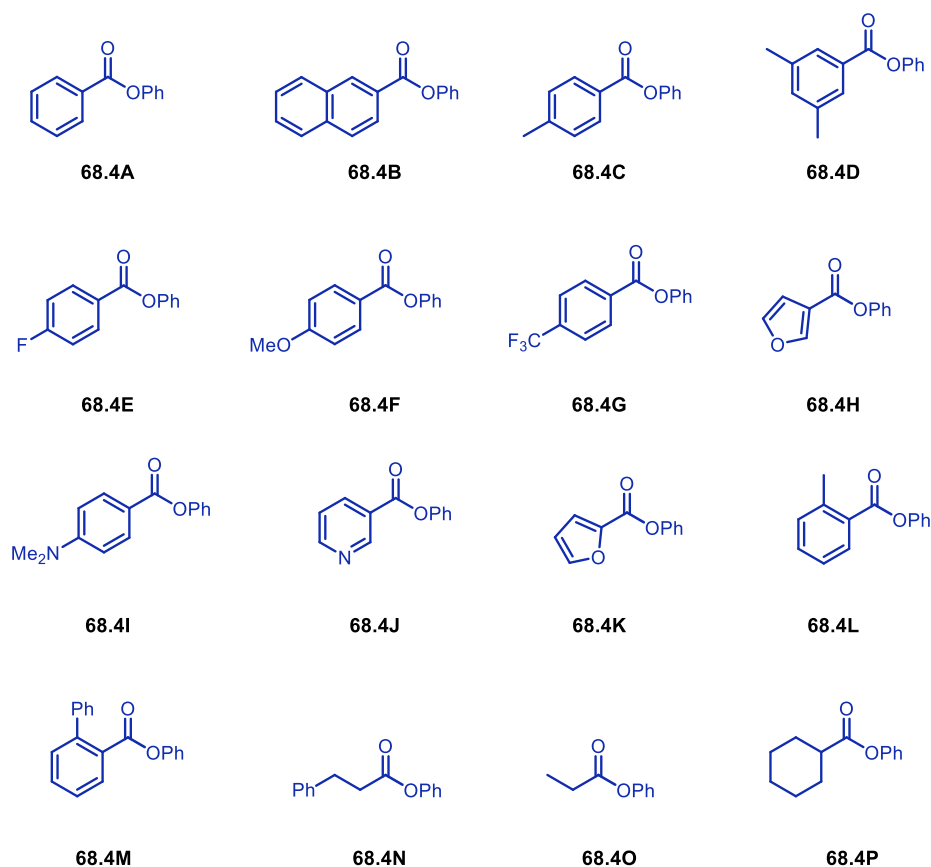
¹⁸⁵ Nareddy, P.; Mazet, C., *Chemistry – An Asian Journal* **2013**, *8*, 2579.

¹⁸⁶ Neuvonen, H.; Neuvonen, K.; Pasanen, P., *J. Org. Chem.* **2004**, *69*, 3794.

¹⁸⁷ LaBerge, N. A.; Love, J. A., *Eur. J. Org. Chem.* **2015**, *2015*, 5546.

methylbenzoate (**68.4L**),¹⁸⁹ Phenyl [1,1'-biphenyl]-2-carboxylate (**68.4M**),¹⁹⁰ Phenyl 3-phenylpropanoate (**68.4N**),¹⁹¹ Phenyl cyclohexanecarboxylate (**68.4P**)¹⁹² 4-methoxyphenyl benzoate (**73.1**),¹⁹³ hexafluoropropan-2-yl (**68.4Q**),¹⁹⁴ Phenyl 4-bromobenzoate (**68.4S**)¹⁹⁵ pyridin-2-yl benzoate (**F9.2**),¹⁹⁶ s-phenyl benzothioate (**F9.4**).¹⁹⁷

Figure 11. Number of esters



¹⁸⁸ Lee, C. K.; Yu, J. S.; Lee, H.-J., *J. Heterocycl. Chem.* **2002**, *39*, 1207.

¹⁸⁹ Engbersen, J. F. J.; Geurtsen, G.; De Bie, D. A.; Van Der Plas, H. C., *Tetrahedron.* **1988**, *44*, 1795.

¹⁹⁰ Ueda, T.; Konishi, H.; Manabe, K., *Org. Lett.* **2012**, *14*, 3100.

¹⁹¹ Yamazaki, J.; Watanabe, T.; Tanaka, K., *Tetrahedron: Asymmetry* **2001**, *12*, 669.

¹⁹² Sasse, A.; Ligneau, X.; Sadek, B.; Elz, S.; Pertz, H. H.; Ganellin, C. R.; Arrang, J.-M.; Schwartz, J.-C.; Schunack, W.; Stark, H., *Arch. Pharm.* **2001**, *334*, 45.

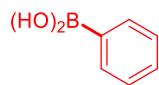
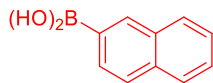
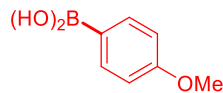
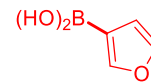
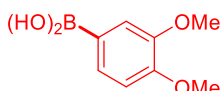
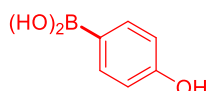
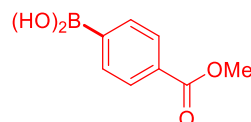
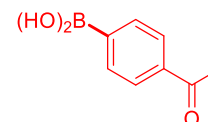
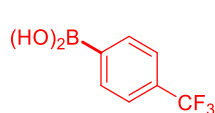
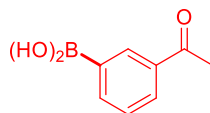
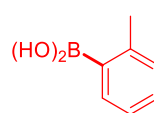
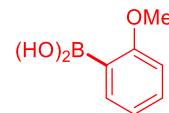
¹⁹³ Lee, C. K.; Yu, J. S.; Lee, H.-J., *J. Heterocycl. Chem.* **2002**, *39*, 1207.

¹⁹⁴ Zell, T.; Ben-David, Y.; Milstein, D., *Angew. Chem. Int. Ed.* **2014**, *53*, 4685.

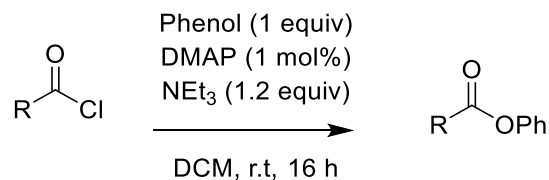
¹⁹⁵ Tao, Z.-F.; Li, G.; Tong, Y.; Chen, Z.; Merta, P.; Kovar, P.; Zhang, H.; Rosenberg, S. H.; Sham, H. L.; Sowin, T. J.; Lin, N.-H., *Bioorg. Med. Chem. Lett.* **2007**, *17*, 4308.

¹⁹⁶ Yamada, S.; Abe, M., *Tetrahedron.* **2010**, *66*, 8667.

¹⁹⁷ Chowdhury, S.; Roy, S., *Tetrahedron Lett.* **1997**, *38*, 2149.

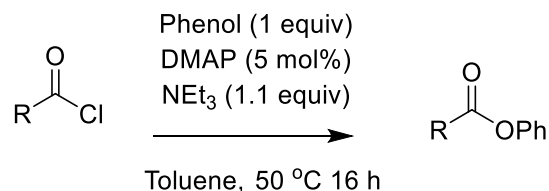
Figure 12. Numbering of boronic acids**68.5a****68.5b****68.5c****68.5d****68.5e****68.5f****68.5g****68.5h****68.5i****68.5j****68.5k****68.5l**

11.1. Synthesis of starting materials



Method A

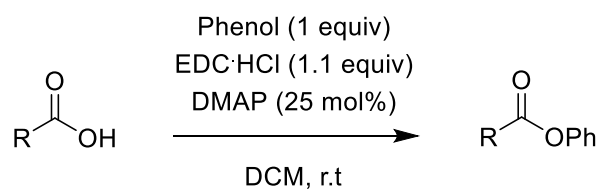
Acyl chloride was added to DCM (0.5 M), phenol (1.0 equiv), and *N,N*-dimethyl-4-aminopyridine (DMAP: 1 mol%) in a round bottom flask. Flask was purged with argon. After cooling the mixture to 0 °C, triethylamine (1.2 equiv) was added dropwise. Reaction mixture was warmed to room temperature and stirred overnight. Completion of reaction monitored by TLC. After completion of reaction, reaction was quenched with saturated $\text{NaHCO}_3(\text{aq})$. The mixture was extracted three times with CH_2Cl_2 . Subsequent washes with NaOH_{aq} (1 M) were done as necessary to remove phenol. The combined organic layers were dried over Na_2SO_4 , and then filtered. The filtrate was concentrated *in vacuo*. Purification was done by flash chromatography (hexanes : ethyl acetate) to afford the corresponding ester substrate.



Method B

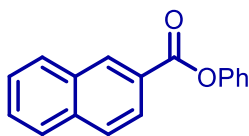
Acyl chloride was added to phenol (1.0 equiv), and *N,N*-dimethyl-4-aminopyridine (DMAP: 5 mol%) in a round bottom flask in toluene (0.3 M). Flask was purged with argon. Triethylamine

(1.1 equiv) was added dropwise. Reaction mixture was warmed to 55°C and stirred overnight. Reaction was monitored by TLC. After completion, reaction was quenched with saturated $\text{NaHCO}_{3(\text{aq})}$. The mixture was extracted three times with EtOAc. Subsequent washes with NaOH_{aq} (1 M) were done as necessary to remove phenol. The combined organic layers were dried over Na_2SO_4 , and then filtered. The filtrate was concentrated *in vacuo*. Purification was done by manual column chromatography to afford the corresponding ester substrate.

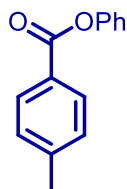


Method C

Carboxylic acid, phenol (1.0 equiv), 1-(3-dimethylaminopropyl)-3-ethylcarbodiimide hydrochloride (EDC·HCl: 1.1 equiv), and *N,N*-dimethyl-4-aminopyridine (DMAP: 25 mol%) were added to a round-bottom flask. Flask was purged with argon. DCM was added (0.5 M) to the mixture. Completion of reaction monitored by TLC. After stirring the mixture overnight, reaction was quenched with saturated $\text{NaHCO}_{3(\text{aq})}$. The mixture was extracted three times with CH_2Cl_2 . Subsequent washes with NaOH_{aq} (1 M) were done as necessary to remove phenol. The combined organic layers were dried over Na_2SO_4 , and then filtered. The filtrate was concentrated *in vacuo*. Purification was done by flash chromatography to afford the corresponding ester substrate.



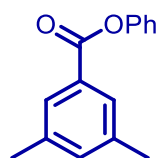
phenyl 2-naphthoate (68.4B) was synthesized following method A using 2-naphthoyl chloride (760 mg, 4 mmol), phenol (376 mg, 1.0 equiv), *N,N*-dimethyl-4-aminopyridine (DMAP: 1 mol %) and triethylamine (1.2 equiv). Purification by flash chromatography (0% → 25% EtOAc in hexane) afforded **68.4B** as white solid (208mg, 21% Yield). Characterization data was in accordance with literature.¹⁹⁸ **¹H NMR** (CDCl₃, 400MHz) δ 8.81 (s, 1H), 8.20 (dd, J=8.61, 1.7 Hz, 1H), 8.00 (d, J=8.0 Hz, 1H), 7.94 (dd, J=11.4 Hz, 2H), 7.55-7.65 (m, 2H), 7.4-7.45 (m, 2H), 7.25-7.39 (m, 3H). **¹³C NMR** (CDCl₃, 100MHz) 165.66, 151.40, 136.14, 132.83, 132.24, 129.85, 129.81, 128.71, 128.16, 127.11, 126.23, 125.79, 122.10.



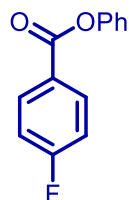
***p*-Methyl benzoic acid phenyl ester (68.4C)** was synthesized following method B using 4-methylbenzoyl chloride (0.29 ml, 2.2 mmol), phenol (187 mg, 1.0 equiv), *N,N*-dimethyl-4-aminopyridine (DMAP: 1 mol %) and triethylamine (1.1 equiv). Purification by column chromatography (0% → 20% EtOAc in hexane) afforded **68.4C** as a white solid (239.9 mg, 75% yield). Characterization data was in accordance with literature.¹⁹⁹ **¹H NMR** (CDCl₃, 400MHz) δ 8.08 (d, J=8.2 Hz, 2H), 7.41 (t, J=9.1 Hz, 2H), 7.29 (d, J=8.5 Hz, 2H), 7.25 (tt, J=8.3, 1.0 Hz, 1H), 7.19 (ddd, J=7.3, 2.0, 1.0 Hz, 2H), 2.49 (s, 3H). **¹³C NMR** (CDCl₃, 100MHz) 165.56, 151.38, 144.72, 130.54, 129.78, 129.61, 127.18, 126.10, 122.09, 22.08.

¹⁹⁸ Zhang, L.; Zhang, G.; Zhang, M.; Cheng, J., *J. Org. Chem.* **2010**, *75*, 7472.

¹⁹⁹ Ueda, T.; Konishi, H.; Manabe, K., *Org. Lett.* **2012**, *14*, 3100.



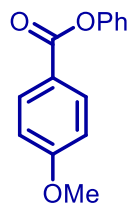
phenyl 3,5-dimethylbenzoate (68.4D) was synthesized following method A using 3,5-dimethylbenzoyl chloride (592 mg, 3.5 mmol), phenol (320 mg, 1.0 equiv), *N,N*-dimethyl-4-aminopyridine (DMAP: 1 mol %) and triethylamine (1.2 equiv). Purification by flash chromatography (0% → 20% EtOAc in hexane) afforded **68.4D** as a clear oil (347mg, 44% yield). Characterization data was in accordance with literature.²⁰⁰ ¹H NMR (CDCl₃, 400MHz) δ 7.85 (s, 2H), 7.45 (t, J=9.0 Hz, 2H), 7.32-7.26 (m, 2H), 7.23 (d, J=7.5 Hz, 2H), 2.43 (s, 6H). ¹³C NMR (CDCl₃, 100MHz) 165.69, 151.33, 138.49, 135.48, 129.70, 126.02, 122.00, 21.40.



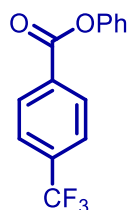
4-Fluoro-benzoic acid phenyl ester (68.4E) was synthesized following method B using 4-fluorobenzoyl chloride (0.26 mg, 2.2 mmol), phenol (188 mg, 1.0 equiv), *N,N*-dimethyl-4-aminopyridine (DMAP: 1 mol %) and triethylamine (1.1 equiv). Purification by column chromatography (0% → 20% EtOAc in hexane) afforded **68.4E** as a white solid (367.5 mg, 85% yield). Characterization data was in accordance with literature.²⁰¹ ¹H NMR (CDCl₃, 400MHz) δ 8.24 (m, J=9.0, 5.4 Hz, 2H), 7.41 (t, J=7.0 Hz, 2H), 7.27 (d, J=7.2 Hz, 1H), 7.18 (m, 4H). ¹³C NMR (CDCl₃, 100 MHz) δ 166.43 (d, J=255.0 Hz), 164.46, 151.15, 133.07 (d, J=9.4 Hz) 129.81, 126.27, 126.14 (d, J= 3.0 Hz), 121.95, 116.06 (d, J=22.1 Hz).

²⁰⁰ Masamichi, M.; Takuo, O.; Hiroaki, O.; Hidefumi H. Method for preparing aromatic carbonate US Patent 5714627 A1, 1998.

²⁰¹ LaBerge, N. A.; Love, J. A., *Eur. J. Org. Chem.* **2015**, 2015, 5546.



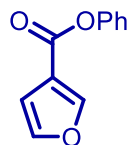
4-Methoxybenzoic acid phenyl ester (68.4F) was synthesized following method B using 4-methoxybenzoyl chloride (375 mg, 2.2 mmol), phenol (188 mg, 1.0 equiv), *N,N*-dimethyl-4-aminopyridine (DMAP: 1 mol %) and triethylamine (1.1 equiv). Purification by column chromatography (0% → 40% EtOAc in hexane) afforded **68.4F** as a white solid (400.3 mg, 88% yield). Characterization data was in accordance with literature.²⁰² $^1\text{H NMR}$ (400 MHz, CDCl_3) δ 8.17 (d, $J = 9.0$ Hz, 2H), 7.44 (t, $J = 9.0$ Hz, 2H), 7.27 (d, $J = 14.9$ Hz, 1H), 7.22 (d, $J = 7.5$ Hz, 2H), 6.83 (t, $J = 106.1$ Hz, 2H), 3.91 (s, 3H). $^{13}\text{C NMR}$ (CDCl_3 , 100 MHz) δ 132.56, 129.96, 126.19, 122.25, 114.27.



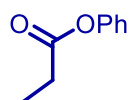
phenyl 4-(trifluoromethyl)benzoate (68.4G), was synthesized following method A using 4-(trifluoromethyl)benzoyl chloride (834 mg, 4 mmol), phenol (376 mg, 1.0 equiv), *N,N*-dimethyl-4-aminopyridine (DMAP: 1 mol %) and triethylamine (1.2 equiv). Purification by flash chromatography (0% → 30% EtOAc in hexane) afforded **68.4G** as white solid (579mg, 54% yield). Characterization data was in accordance with literature.²⁰³ $^1\text{H NMR}$ (CDCl_3 , 400MHz) δ 8.33 (d, $J = 8.1$ Hz, 2H), 7.79 (d, $J = 8.3$ Hz, 2H), 7.45 (t, $J = 9.1$ Hz, 2H), 7.31 (t, $J = 7.4$ Hz, 1H), 7.23 (d, $J = 7.5$ Hz, 2H). $^{13}\text{C NMR}$ (CDCl_3 , 100MHz) 164.30, 151.03, 135.55 (q, $J = 32.7$ Hz), 133.20, 130.89, 129.94, 126.55, 125.94 (q, $J = 3.7$ Hz), 124.03 (q, $J = 272.8$ Hz), 121.87.

²⁰² Zhang, L.; Zhang, G.; Zhang, M.; Cheng, J., *J. Org. Chem.* **2010**, *75*, 7472.

²⁰³ Ueda, T.; Konishi, H.; Manabe, K., *Org. Lett.* **2012**, *14*, 3100.



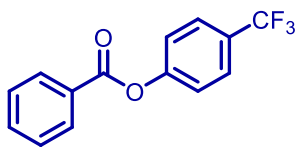
phenyl furan-3-carboxylate (68.4H), was synthesized following method C using furan-3-carboxylic acid (448 mg, 4 mmol), phenol (376 mg, 1.0 equiv), 1-(3-dimethylaminopropyl)-3-ethylcarbodiimide hydrochloride (EDC·HCl: 568 mg, 1.1 equiv), and *N,N*-dimethyl-4-aminopyridine (DMAP: 25 mol %). Purification by flash chromatography (0% → 30% EtOAc in hexane) afforded **68.4H** as clear oil (426mg, 57% yield). Characterization data was in accordance with literature.²⁰⁴ **¹H NMR** (400 MHz, CDCl₃) δ 8.22 (d, *J* = 0.7 Hz, 1H), 7.52 (t, *J* = 1.7 Hz, 1H), 7.44 (t, *J* = 7.9 Hz, 2H), 7.28 (t, *J* = 7.4 Hz, 1H), 7.21 (d, *J* = 7.6 Hz, 2H), 6.90 (d, *J* = 1.9 Hz, 1H). **¹³C NMR** (CDCl₃, 100MHz) 161.41, 150.47, 148.69, 144.08, 129.50, 125.95, 121.72, 118.93, 110.10.



phenyl propionate (68.4M) was synthesized following method B using propionyl chloride (0.2 ml, 2.2 mmol), phenol (188 mg, 1.0 equiv), *N,N*-dimethyl-4-aminopyridine (DMAP: 1 mol %) and triethylamine (1.1 equiv). Purification by column chromatography (0% → 20% EtOAc in hexane) afforded **68.4M** as yellowish oil. (231.3 mg, 70% yield). Characterization data was in accordance with literature.²⁰⁵ **¹H NMR** (CDCl₃, 400MHz) δ 7.39 (t, *J*=7.1 Hz, 1H), 7.23 (t, *J*=7.4 Hz, 1H), 7.09 (d, *J*= 8.4 Hz, 2H), 2.61 (q, *J*=7.6 Hz, 2H), 1.28 (t, *J*=7.6 Hz, 3H). **¹³C NMR** (CDCl₃, 100MHz) 173.01, 151.02, 129.54, 125.84, 121.74, 27.87.

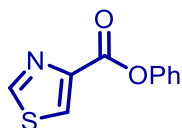
²⁰⁴ Ueda, T.; Konishi, H.; Manabe, K., *Org. Lett.* **2012**, *14*, 3100.

²⁰⁵ Ling, K. B.; Smith, A. D., *Chem. Commun.* **2011**, *47*, 373.



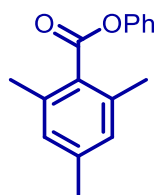
4-(trifluoromethyl)phenyl benzoate (73.2), was synthesized following method A using benzoyl chloride (464 mg, 4 mmol), 4-(trifluoromethyl)phenol (648 mg, 1.0 equiv), *N,N*-dimethyl-4-aminopyridine (DMAP: 1 mol %) and triethylamine (1.2 equiv). Purification by flash chromatography (0% → 20% EtOAc in hexane) afforded **73.2** as a white solid (404mg, 48% yield). Characterization data was in accordance with literature.²⁰⁶ **¹H NMR** (400 MHz, CDCl₃) δ 8.22 (d, *J* = 7.1 Hz, 2H), 7.70-7.64 (m, 2H), 7.69 – 7.65 (m, 1H), 7.55 (t, *J* = 7.7 Hz, 2H), 7.37 (d, *J* = 8.4 Hz, 2H). **¹³C NMR** (100 MHz, CDCl₃) δ 165.01, 153.84, 134.32, 130.62, 129.32, 129.05, 128.54 (q, *J*=32.8 Hz), 127.21 (q, *J*=3.7 Hz), 123.0 (q, *J*=270.3 Hz), 122.61.

Miscellaneous Esters

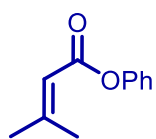


Phenyl thiazole-4-carboxylate 68.4T was synthesized following method C, using thiazole-4-carboxylic acid (258.3mg, 2mmol), phenol (188 mg, 1.0 equiv), 1-(3-dimethylaminopropyl)-3-ethylcarbodiimide hydrochloride (EDC·HCl: 284 mg, 1.1 equiv), and *N,N*-dimethyl-4-aminopyridine (DMAP: 25 mol %). Purification by flash chromatography (0% → 25% EtOAc in hexane) afforded **68.4T** as a white solid (182mg, 44% yield). **¹H NMR** (400 MHz, CDCl₃) δ 8.94 (d, *J* = 2.1 Hz, 1H), 8.45 (d, *J* = 2.1 Hz, 1H), 7.44 (t, *J* = 7.0 Hz, 2H), 7.32 – 7.23 (m, 3H). **¹³C NMR** (100 MHz, CDCl₃) δ 154.09, 150.87, 129.89, 129.06, 126.51, 121.95

²⁰⁶ Zhang, L.; Zhang, G.; Zhang, M.; Cheng, J., *J. Org. Chem.* **2010**, *75*, 7472.



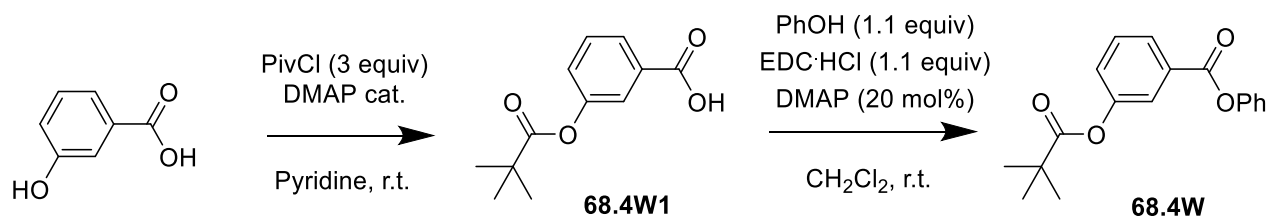
Phenyl 2,4,6-trimethylbenzoate (68.4U) was synthesized following method C, using 2,4,6-trimethylbenzoic acid (1150mg, 7mmol), phenol (659 mg, 1.0 equiv), 1-(3-dimethylaminopropyl)-3-ethylcarbodiimide hydrochloride (EDC·HCl: 1476 mg, 1.1 equiv), and *N,N*-dimethyl-4-aminopyridine (DMAP: 25 mol %). Product was isolated via described extraction and an additional 1 equiv of phenol was added in toluene followed by DMAP (5 mol%) in order to convert anhydride side product to desired ester. Mixture was heated to 60°C. Completion of reaction monitored by GC-MS. Product was extracted with ethyl acetate and dried over Na₂SO₄, and then filtered. Purification by flash chromatography (0% → 25% EtOAc in hexane) afforded **68.4U** as a colorless oil (371mg, 22% yield). Characterization data was in accordance with literature.²⁰⁷ **¹H NMR** (400 MHz, CDCl₃) δ 7.43 (t, *J* = 7.0 Hz, 2H), 7.29 – 7.20 (m, 3H), 6.91 (s, 2H), 2.45 (s, 6H), 2.31 (s, 3H). **¹³C NMR** (101 MHz, CDCl₃) δ 168.73, 151.09, 140.28, 136.64, 130.31, 129.19, 128.97, 126.30, 121.93, 21.51, 20.32.



Phenyl 3-methylbut-2-enoate 68.4V was synthesized following method A using 3-methylbut-2-enoyl chloride (450 mg, 4 mmol), phenol (376 mg, 1.0 equiv), *N,N*-dimethyl-4-aminopyridine (DMAP: 1 mol %) and triethylamine (1.2 equiv). Purification by flash chromatography (0% → 25% EtOAc in hexane) afforded **68.4V** as a yellow oil (170mg, 25% Yield). Characterization

²⁰⁷ Petersen, T. B.; Khan, R.; Olofsson, B., *Org. Lett.* **2011**, *13*, 3462.

data was in accordance with literature.²⁰⁸ ¹H NMR (400 MHz, CDCl₃) δ 7.39 (t, *J* = 7.0 Hz, 2H), 7.23 (t, *J* = 7.4 Hz, 1H), 7.11 (d, *J* = 7.5 Hz, 2H), 5.94 (dt, *J* = 2.6, 1.3 Hz, 1H), 2.25 (d, *J* = 1.2 Hz, 3H), 2.00 (d, *J* = 1.3 Hz, 3H).

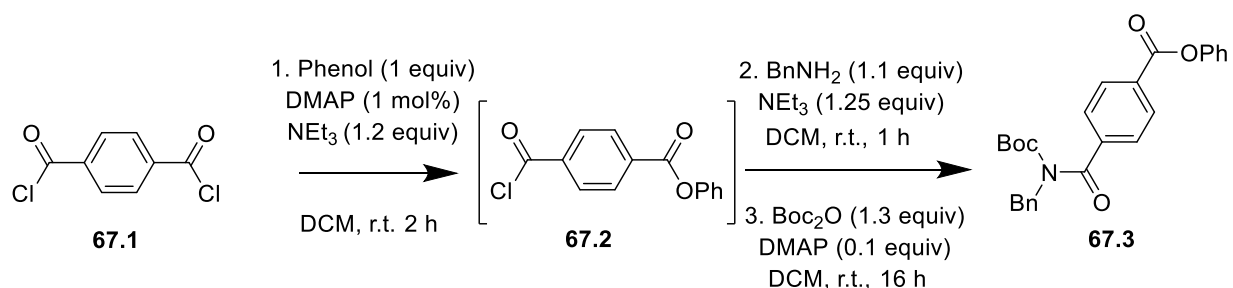


Phenyl 3-(pivaloyloxy)benzoate 68.4W. To a solution of 3-hydroxybenzoic acid (2.76g, 20 mmol) and DMAP (24.0 mg, 0.2 mmol, 1 mol%) in pyridine was added pivaloyl chloride (7.24g, 60 mmol, 6.0 equiv) at 0°C. The solution was warmed to room temperature and stirred for 1h before 30 mL of water was carefully added. Reaction mixture was allowed to stir overnight at room temperature. Solution was extracted three times with DCM. The combined organic layer was washed in 1 M H₂SO₄ several times as necessary to remove pyridine. The organic layer was dried over Na₂SO₄ and filtrated. Filtrate was concentrated *in vacuo* then diluted with toluene and concentrated *in vacuo* several times to remove excess pyridine and to afford 3-(pivaloyloxy)benzoic acid **68.4W1** (4.0g, 90% yield) as a white solid. **68.4W1** was used in the next step without further purification.

Phenyl 3-(pivaloyloxy)benzoate 68.4W was synthesized following method C using . **3-(pivaloyloxy)benzoic acid** (2.22 g, 10 mmol), phenol (1.03 g, 1.0 equiv), 1-(3-

²⁰⁸ López, C. S.; Erra-Balsells, R.; Bonesi, S. M., *Tetrahedron Lett.* **2010**, *51*, 4387.

dimethylaminopropyl)-3-ethylcarbodiimide hydrochloride (EDC·HCl: 1.42g, 1.1 equiv), and *N,N*-dimethyl-4-aminopyridine (DMAP: 25 mol %). Purification by flash chromatography (ethyl acetate: hexanes) afforded **68.4W** as white solid. (26% yield). Characterization data was in accordance with literature.²⁰⁹ **¹H NMR** (400 MHz, CDCl₃) δ 8.08 (d, *J* = 9.3 Hz, 1H), 7.89 – 7.88 (m, 1H), 7.53 (t, *J* = 8.0 Hz, 1H), 7.47 – 7.41 (m, 2H), 7.35 (dd, *J* = 7.6, 2.9 Hz, 1H), 7.30 (dd, *J* = 7.5, 2.7 Hz, 1H), 7.21 (d, *J* = 8.5 Hz, 2H), 1.39 (s, 9H). **¹³C NMR** (100 MHz, CDCl₃) δ 176.9, 164.69, 151.56, 151.17, 131.41, 129.92, 129.88, 127.79, 127.34, 126.37, 123.67, 122.01, 39.50, 27.47



Phenyl 3-(benzyl(tert-butoxycarbonyl)carbamoyl)benzoate (67.3). Intermediate **67.2** was synthesized following method A using terephthaloyl dichloride **67.1** (1.06g, 5.25 mmol), phenol (490 mg, 1.0 equiv), *N,N*-dimethyl-4-aminopyridine (DMAP: 1 mol %) and triethylamine (1.2 equiv). Reaction was monitored using TLC. Reaction mixture was used in next step without further purification.

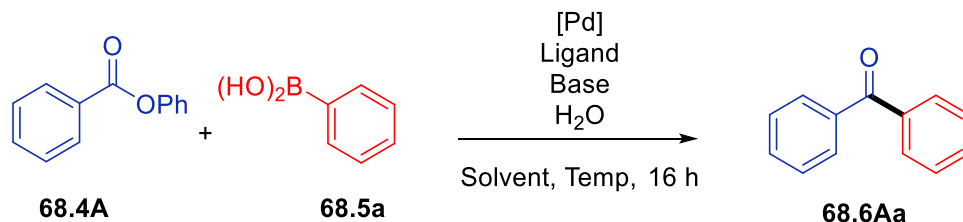
²⁰⁹ Muto, K.; Yamaguchi, J.; Musaev, D. G.; Itami, K., *Nat Commun.* **2015**, *6*.

To the milky white reaction mixture was added additional triethylamine (1.25 equiv) and followed by a dropwise addition of a solution of benzylamine (0.629 mL, 5.77 mmol, 1.1 equiv) in DCM (4.5mL). The reaction mixture was stirred at room temperature for 1 h, then diluted with EtOAc (50 mL) and washed successively with 1M HCl (50mL) and brine (50 mL). The organic layer was dried over Na₂SO₄ and concentrated *in vacuo*. Crude white solid was dried under vacuum and used in the next step without further purification.

To a flask containing the crude material from the previous step, was added DMAP (64.1 mg, 0.525 mmol, 0.1 equiv) followed by MeCN (26.2 mL, 0.2 M) and Boc₂O (1.42 g, 6.83 mmol, 1.3 equiv) under argon. The reaction mixture was allowed to stir at room temperature for 16 h. The reaction was quenched with saturated NaHCO_{3(aq)}. The reaction mixture was diluted with EtOAc (30mL) and H₂O (30 mL) and extracted with EtOAc (3 x 20 mL). The organic layers were combined and dried over Na₂SO₄ and concentrated *in vacuo*. The resulting crude mixture purified by flash chromatography (Ethyl acetate: Hexanes) to isolate product. (0.259g, 11% yield). Product was characterized by ¹H NMR and ¹³C NMR. **¹H NMR** (400 MHz, CDCl₃) δ 8.25 (d, *J* = 8.1 Hz, 2H), 7.64 (d, *J* = 8.2 Hz, 2H), 7.46 (t, *J* = 7.7 Hz, 4H), 7.37 (t, *J* = 7.5 Hz, 2H), 7.30 (t, *J* = 7.5 Hz, 2H), 7.24 (d, *J* = 8.4 Hz, 2H), 5.04 (s, 2H), 1.20 (s, 9H). **¹³C NMR** (101 MHz, CDCl₃) δ 172.38, 164.74, 153.37, 151.14, 142.72, 137.88, 131.72, 130.31, 129.90, 128.89, 128.48, 127.93, 127.65, 126.43, 121.95, 84.22, 49.14, 27.82.

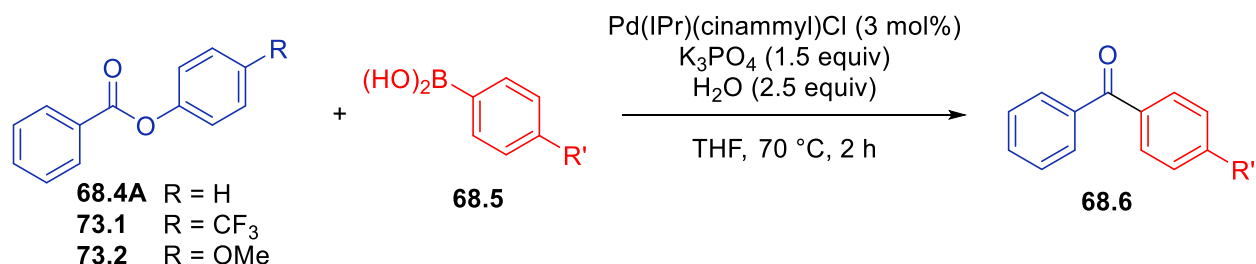
11.2. Reaction development

Optimization and control experiments



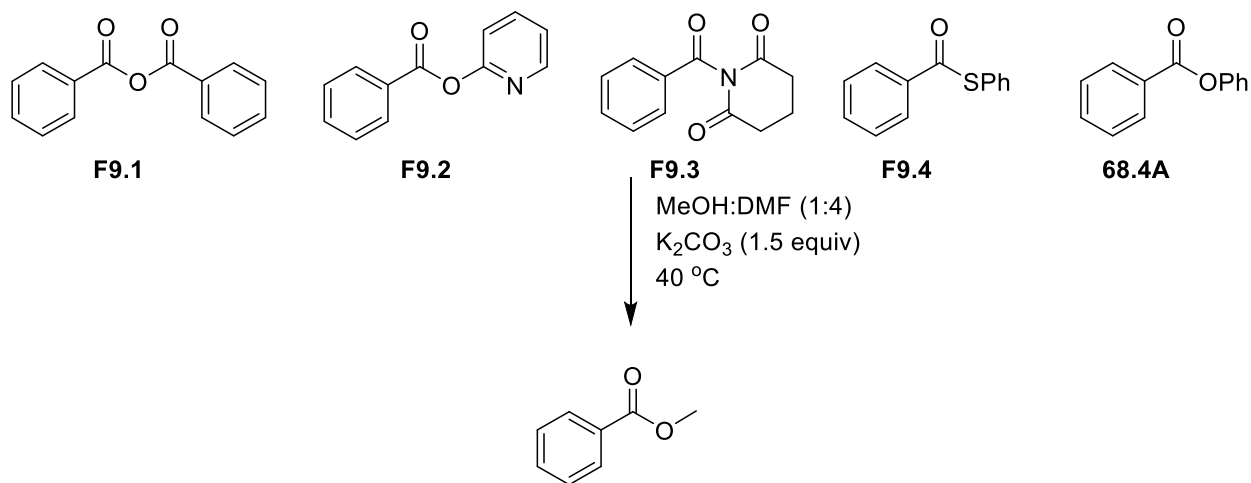
An oven dried screw-capped vial was charged with a magnetic stir bar, base, catalyst/ligand and solid substrates **68.4A** (0.1 mmol) and **68.5a** (1.7 equiv). The vial and contents were subjected to three cycles of vacuum and argon under a Schleck line. Fresh solvent (0.5 mL, 0.2 M) obtained from solvent purification system was then added under argon. Degassed water was subsequently added via micropipette under argon. The vial was sealed with a PTFE-lined screw cap and stirred vigorously (700 rpm) at the indicated temperature for 16 h. After cooling to room temperature, internal standard (1,3,5-trimethoxybenzene, 0.025 mmol in 0.5 mL THF) was added. Mixture was diluted with ethyl acetate and filtered through a plug of silica gel (10 mL of EtOAc eluent). Yields were determined by GC using a 5 point calibration curve.

11.3. Study of substrate and boronic acid electronics



An oven dried screw-capped vial was charged with a magnetic stir bar, powdered K_3PO_4 (1.5 equiv), $\text{Pd(IPr)(cinammyl)Cl}$ (3 mol%), corresponding ester **68.4A**, **73.1** or **73.2** (0.2 mmol), and boronic acid **68.5a** (1.2 equiv). The vial and contents were placed under vacuum and back-filled with Argon under a Schleck line three times. Fresh solvent (1 mL, 0.2 M) obtained from a solvent purification system was then added under argon. Degassed water (2.5 equiv) was subsequently added via micropipette. The vial was sealed with a PTFE-lined screw cap and stirred vigorously (700 rpm) at 70 °C for 2 h. After cooling to room temperature, internal standard, 1,3,5-trimethoxybenzene (0.025 mmol) in 0.5 mL THF was added. Reaction mixture was filtered through a plug of silica gel (10 mL of EtOAc eluent). The crude mixture was concentrated *in vacuo* and characterized by ^1H NMR. Yield determined by ^1H NMR.

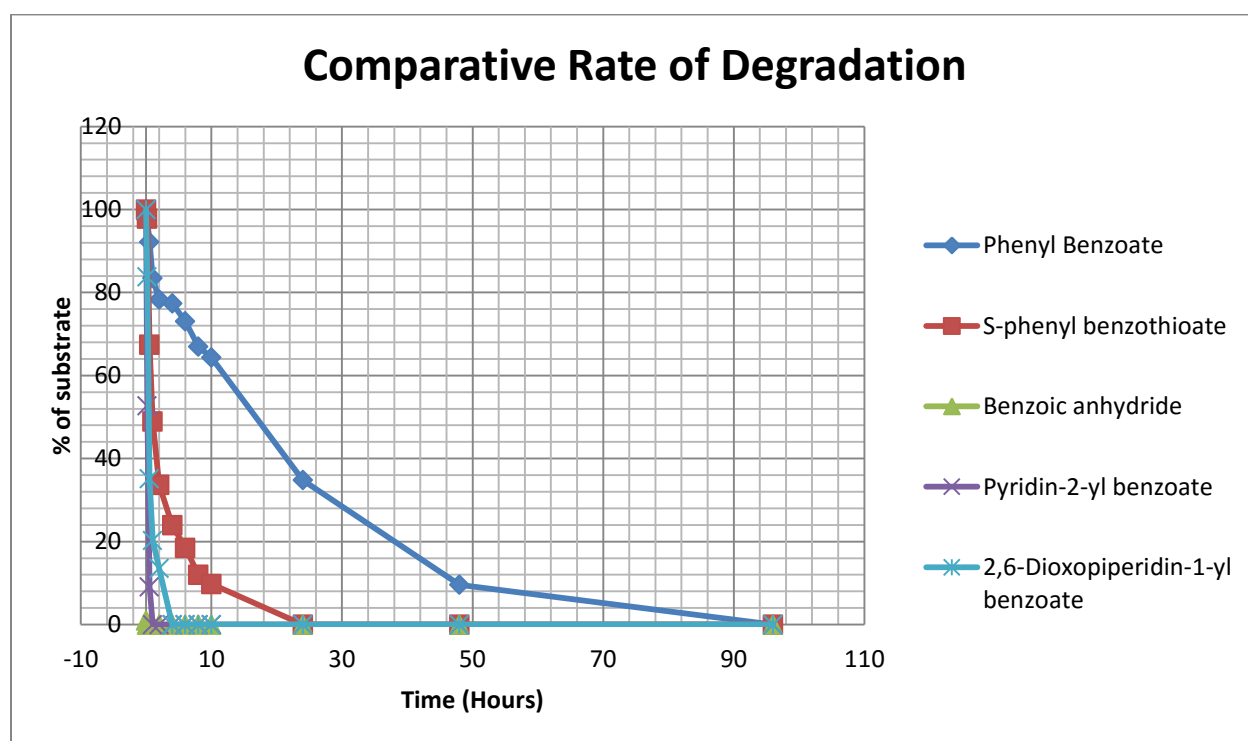
11.4. Study of relative rates of degradation



A screw-capped vial was charged with a magnetic stir bar and substrates **68A**, **F9.1-F9.4** (0.05mmol each), K₂CO₃ (1.5 equiv), and internal standard (1,3,5-trimethoxybenzene, 0.05 mmol) were dissolved in a 1:4 mixture of MeOH:DMF (0.02M). Solution was let stir at 40°C for appropriate amount of time until full conversion of methyl benzoate is observed and no starting material is left. GC-MS samples were taken at regular intervals to track rate of degradation. Data was calculated based on the change in ratio between the internal standard and respective substrate and normalized to 100% at time zero (**Table 20, Figure 13**).

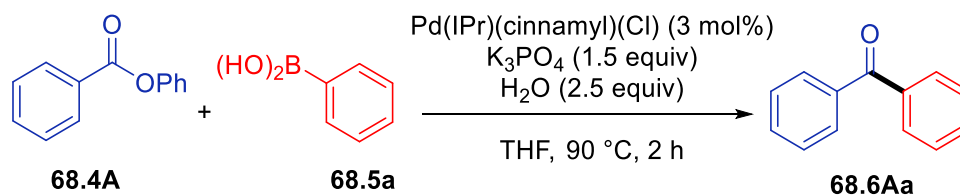
Table 20. Percentage of substrate degradation over time

Time (hours)	Substrate F9.1	Substrate F9.2	Substrate F9.3	Substrate 9.4	Substrate 68.4A
0	100%	100%	100%	100%	100%
0.17	0%	53%	84%	98%	97%
0.5	0%	9%	35%	67%	92%
1	0%	0%	20%	49%	83%
2	0%	0%	14%	34%	78%
4	0%	0%	0%	24%	77%
6	0%	0%	0%	19%	73%
8	0%	0%	0%	12%	67%
10	0%	0%	0%	10%	64%
24	0%	0%	0%	0%	35%
48	0%	0%	0%	0%	10%
96	0%	0%	0%	0%	0%

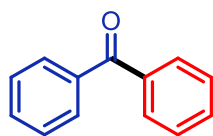
**Figure 13.** Comparative rate of degradation

11.5. Synthesis of final products

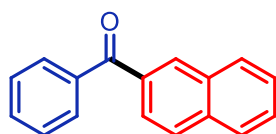
Representative procedure for Suzuki-Miyaura coupling of esters



An oven dried screw-capped vial was charged with a magnetic stir bar, powdered K₃PO₄ (1.5 equiv), Pd(IPr)(cinnamyl)(Cl) (3 mol%), ester **68.4A** (0.2 mmol), and boronic acid **68.5a** (1.7 equiv). The vial and contents were placed under vacuum and back-filled with Argon under a Schleck line three times. Fresh solvent (1 mL, 0.2 M) obtained from a solvent purification system was then added under argon. Degassed water (2.5 equiv) was subsequently added via micropipette. The vial was sealed with a PTFE-lined screw cap and stirred vigorously (700 rpm) at 90 °C for 2 h. After cooling to room temperature, the reaction mixture was diluted with ethyl acetate and filtered through a plug of silica gel (10 mL of EtOAc eluent). The crude mixture was concentrated *in vacuo* and subjected to manual column chromatography. If ester starting material is present and inseparable, the reaction mixture was heated to 60 °C in 1:1 THF : KOH_(aq) (0.1 M). Products are numbered according to corresponding starting materials. For example, ester **68.4A** and boronic acid **68.5a** give ketone **68.6Aa**. Ester **68.4F** and boronic acid **68.5i** give ketone **68.6Fi**.



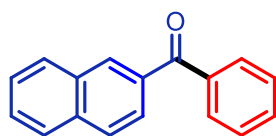
benzophenone (68.6Aa) was prepared according to the general procedure. Purification was done by column chromatography. The first 5 fractions were collected using 20% DCM in hexane, followed by a gradient of 5% \rightarrow 10% EtOAc in hexane to afford **68.6Aa** as a white solid (34.2 mg, 91%). Characterization data matched those previously reported.²¹⁰ $^1\text{H NMR}$ (CDCl_3 , 400 MHz) δ 7.82 (d, $J = 7.1$ Hz, 4H), 7.60 (t, $J = 7.4$ Hz, 2H), 7.50 (t, $J = 7.5$ Hz, 4H); $^{13}\text{C NMR}$ (CDCl_3 , 100 MHz) δ 197.09, 137.97, 132.75, 130.40, 128.62.



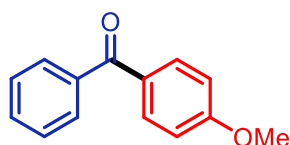
naphthalen-2-yl(phenyl)methanone (68.6Ab) was prepared according to the general procedure. Purification was done by column chromatography. The first 5 fractions were collected using 20% DCM in hexane, followed by a gradient of 5% \rightarrow 10% EtOAc in hexane to afford **68.6Ab** as white solid, (37.8 mg, 84%). Characterization data matched those previously reported.²¹¹ $^1\text{H NMR}$ (400 MHz, CDCl_3) δ 8.29 (s, 1H), 7.97 (d, $J = 1.2$ Hz, 2H), 7.93 (d, $J = 8.1$ Hz, 2H), 7.88 (dd, $J = 8.3, 1.3$ Hz, 2H), 7.67 – 7.60 (m, 2H), 7.59 – 7.51 (m, 3H). $^{13}\text{C NMR}$ (CDCl_3 , 100 MHz) δ 197.07, 138.25, 135.61, 135.17, 132.70, 132.60, 132.19, 130.43, 129.75, 128.67, 128.65, 128.63, 128.15, 127.13, 126.12.

²¹⁰ Kuang, Y.; Wang, Y., *Eur. J. Org. Chem.* **2014**, 2014, 1163.

²¹¹ Kuang, Y.; Wang, Y., *Eur. J. Org. Chem.* **2014**, 2014, 1163.

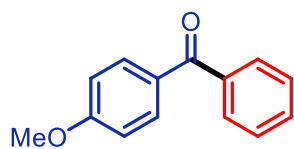


naphthalen-2-yl(phenyl)methanone (68.6Ba) was prepared according to the general procedure. Purification was done by column chromatography. The first 5 fractions were collected using 20% DCM in hexane, followed by a gradient of 5% \rightarrow 10% EtOAc in hexane to afford **68.6Ba** as white solid, (35.8 mg, 81%). Characterization data matched that of **68.6Ab**.

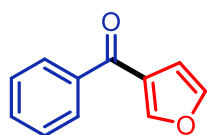


(4-methoxyphenyl)(phenyl)methanone (68.6Ac) was prepared according to the general procedure. Purification was done by column chromatography. The first 5 fractions were collected using 20% DCM in hexane, followed by a gradient of 5% \rightarrow 10% EtOAc in hexane to afford **68.6Ac** as a white solid, (36.9 mg, 87%). Characterization data matched those previously reported.²¹² $^1\text{H NMR}$ (400 MHz, CDCl_3) δ 7.83 (d, $J = 8.8$ Hz, 2H), 7.76 (d, $J = 6.9$ Hz, 2H), 7.56 (t, $J = 6.8$ Hz, 1H), 7.47 (t, $J = 7.4$ Hz, 2H), 6.96 (d, $J = 8.9$ Hz, 2H), 3.89 (s, 3H). $^{13}\text{C NMR}$ (CDCl_3 , 100 MHz) δ 195.89, 163.56, 138.63, 132.89, 130.51, 130.51, 130.06, 128.52, 113.89, 55.82

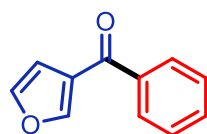
²¹² Kuang, Y.; Wang, Y., *Eur. J. Org. Chem.* **2014**, 2014, 1163.



(4-methoxyphenyl)(phenyl)methanone (68.6Fa) was prepared according to the general procedure. Purification was done by column chromatography. The first 5 fractions were collected using 20% DCM in hexane, followed by a gradient of 5% \rightarrow 10% EtOAc in hexane to afford **68.6Ac** as a white solid, (36.1 mg, 85%) Characterization data matched that of **68.6Ac**.

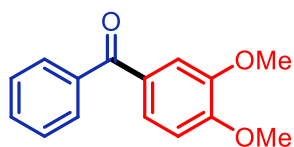


furan-3-yl(phenyl)methanone (68.6Ad) was prepared according to the general procedure. Purification by column chromatography (gradient of 5% \rightarrow 15% EtOAc in hexane) afforded **68.6Ad** as a white solid, (31.5 mg, 95%). Characterization data matched those previously reported.²¹³ **¹H NMR** (400 MHz, CDCl₃) δ 7.93 (s, 1H), 7.87 (d, J = 7.0 Hz, 2H), 7.60 (t, J = 7.4 Hz, 1H), 7.50 (t, J = 7.0 Hz, 3H), 6.92 (d, J = 1.2 Hz, 1H). **¹³C NMR** (CDCl₃, 100 Hz) δ 189.75, 148.89, 144.29, 139.17, 132.80, 129.16, 128.88, 126.86, 110.55.

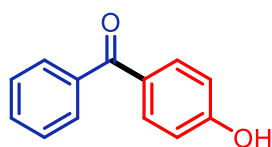


furan-2-yl(phenyl)methanone (68.6Ha) was prepared according to the general procedure. Purification by column chromatography (gradient of 5% \rightarrow 15% EtOAc in hexane) afforded **68.6Ha** as a white solid, (26.1 mg, 81%). Characterization data matched that of **68.6Ad**.

²¹³ Rieke, R. D.; Suh, Y.; Kim, S.-H., *Tetrahedron Lett.* **2005**, *46*, 5961.



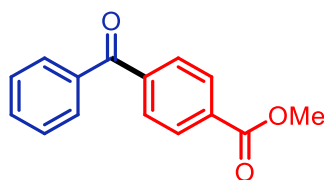
(3,4-dimethoxyphenyl)(phenyl)methanone (68.6Ae) was prepared according to the general procedure. Purification by column chromatography (gradient of 5% → 20% EtOAc in hexane) afforded **68.6Ae** as a white solid, (46.8 mg, 93%). Characterization data matched those previously reported.²¹⁴ **¹H NMR** (400 MHz, CDCl₃) δ 7.78 (d, *J* = 7.0 Hz, 2H), 7.58 (t, *J* = 7.4 Hz, 1H), 7.53 – 7.42 (m, 3H), 7.39 (dd, *J* = 8.3, 2.0 Hz, 1H), 6.91 (d, *J* = 8.4 Hz, 1H), 3.96 (s, 3H), 3.94 (s, 3H). **¹³C NMR** (CDCl₃, 100 MHz) δ 189.75, 148.89, 144.29, 139.17, 132.80, 129.16, 128.88, 126.86, 110.55.



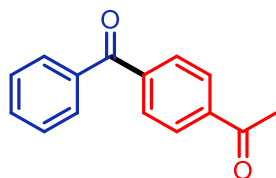
(4-hydroxyphenyl)(phenyl)methanone (68.6Af) was prepared according to the general procedure. Purification by column chromatography (gradient of 5% → 50% EtOAc in hexane) afforded **68.6Af** as an off-white solid, (22.3 mg, 58%). Characterization data matched those previously reported.²¹⁵ **¹H NMR** (400 MHz, CDCl₃) δ 7.78 (t, *J* = 8.7 Hz, 4H), 7.59 (t, *J* = 7.4 Hz, 1H), 7.49 (t, *J* = 7.5 Hz, 2H), 7.06 (s, 1H), 6.95 (d, *J* = 8.8 Hz, 2H). **¹³C NMR** (CDCl₃, 100 MHz) δ 197.01, 160.95, 138.39, 133.43, 132.52, 130.19, 130.03, 128.61, 115.69.

²¹⁴ Tripathi, S.; Singh, S. N.; Yadav, L. D. S., *Tetrahedron Lett.* **2015**, 56, 4211.

²¹⁵ Wang, G.-Z.; Li, X.-L.; Dai, J.-J.; Xu, H.-J., *J. Org. Chem.* **2014**, 79, 7220.



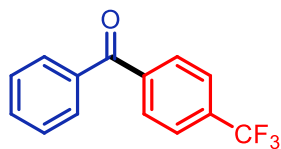
methyl 4-benzoylbenzoate (68.6Ag) was prepared according to the general procedure. Purification by column chromatography (gradient of 5% → 20% EtOAc in hexane) afforded **68.6Ag** as a white solid, (37.2 mg, 79%). Characterization data matched those previously reported.²¹⁶ ¹H NMR (400 MHz, CDCl₃) δ 8.16 (d, *J* = 8.6 Hz, 2H), 7.85 (d, *J* = 8.6 Hz, 2H), 7.81 (d, *J* = 7.0 Hz, 2H), 7.63 (t, *J* = 7.4 Hz, 1H), 7.51 (t, *J* = 7.6 Hz, 2H), 3.97 (s, *J* = 6.9 Hz, 3H). ¹³C NMR (CDCl₃, 100 MHz) δ 196.35, 166.64, 141.66, 137.29, 133.55, 133.27, 130.43, 130.10, 129.83, 128.79, 52.79.



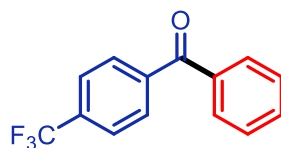
1-(4-benzoylphenyl)ethan-1-one (68.6Ah) was prepared according to the general procedure. Purification by column chromatography (gradient of 5% → 10% EtOAc in hexane) afforded **68.6Ah** as a white solid, (33.6 mg, 77%). Characterization data matched those previously reported.²¹⁷ ¹H NMR (400 MHz, CDCl₃) δ 8.07 (d, *J* = 8.6 Hz, 2H), 7.87 (d, *J* = 8.6 Hz, 2H), 7.81 (dd, *J* = 8.3, 1.3 Hz, 2H), 7.63 (t, *J* = 7.4 Hz, 1H), 7.51 (t, *J* = 7.6 Hz, 2H), 2.68 (s, 3H). ¹³C NMR (CDCl₃, 100 MHz) δ 197.84, 196.28, 141.68, 139.91, 137.27, 133.32, 130.43, 130.38, 128.82, 128.50, 27.22.

²¹⁶ Li, X.; Zou, G., *Chem. Commun.* **2015**, 51, 5089.

²¹⁷ Wang, G.-Z.; Li, X.-L.; Dai, J.-J.; Xu, H.-J., *J. Org. Chem.* **2014**, 79, 7220.

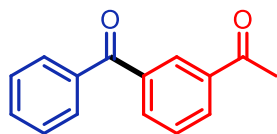


phenyl(4-(trifluoromethyl)phenyl)methanone (68.6Ai) was prepared according to a modified general procedure. Pd(IPr)(cinnamyl)(Cl) (5 mol%) was used as the catalyst, and the reaction was stirred for 16 hours. Purification was done by column chromatography. The first 5 fractions were collected using 20% DCM in hexane, followed by a gradient of 5% → 10% EtOAc in hexane to afford **68.6Ai** as a white solid, (32.1 mg, 71%). Characterization data matched those previously reported.²¹⁸ ¹H NMR (400 MHz, CDCl₃) δ 7.91 (d, *J* = 8.0 Hz, 2H), 7.82 (dd, *J* = 8.3, 1.3 Hz, 2H), 7.77 (d, *J* = 8.1 Hz, 2H), 7.64 (t, *J* = 7.4 Hz, 1H), 7.52 (t, *J* = 7.6 Hz, 2H). ¹³C NMR (CDCl₃, 100 MHz) δ 195.85, 141.09, 137.09, 133.42 (q, *J* = 32.6 Hz), 130.44, 128.87, 125.74, 125.71, 125.69 (q, *J* = 3.7 Hz), 123.73 (q, *J* = 272.5).

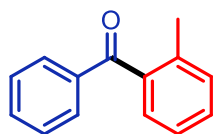


phenyl(4-(trifluoromethyl)phenyl)methanone (68.6Ga) was prepared according to the general procedure. Purification was done by column chromatography. The first 5 fractions were collected using 20% DCM in hexane, followed by a gradient of 5% → 10% EtOAc in hexane to afford **68.6Ga** as a white solid, (42.6 mg, 87%). Characterization data matched that of **3Ai**.

²¹⁸ Wang, G.-Z.; Li, X.-L.; Dai, J.-J.; Xu, H.-J., *J. Org. Chem.* **2014**, *79*, 7220



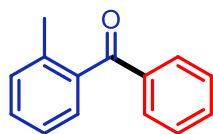
1-(3-benzoylphenyl)ethan-1-one (68.6Aj) was prepared according to the general procedure. Purification by column chromatography (gradient of 5% \rightarrow 20% EtOAc in hexane) afforded **68.6Aj** as a white solid, (40.3 mg, 91%). Characterization data matched those previously reported.²¹⁹ $^1\text{H NMR}$ (400 MHz, CDCl_3) δ 8.37 (s, $J = 1.6$ Hz, 1H), 8.19 (d, $J = 7.8$ Hz, 1H), 7.99 (d, $J = 7.7$ Hz, 1H), 7.80 (d, $J = 7.0$ Hz, 2H), 7.61 (q, $J = 7.7$ Hz, 2H), 7.51 (t, $J = 7.6$ Hz, 2H), 2.65 (s, 3H). $^{13}\text{C NMR}$ (CDCl_3 , 100 MHz) δ 197.61, 196.17, 138.41, 137.53, 137.34, 134.56, 133.21, 132.08, 130.36, 130.02, 129.07, 128.84, 27.07.



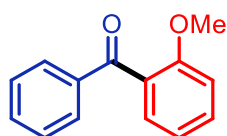
phenyl(o-tolyl)methanone (68.6Ak) was prepared according to the general procedure. Purification was done by column chromatography. The first 5 fractions were collected using 20% DCM in hexane, followed by a gradient of 5% \rightarrow 10% EtOAc in hexane to afford **68.6Ak** as a colorless oil, (29.8 mg, 76%). Characterization data matched those previously reported.²²⁰ $^1\text{H NMR}$ (400 MHz, CDCl_3) δ 7.82 (dd, $J = 8.4, 1.3$ Hz, 2H), 7.59 (t, $J = 7.4$ Hz, 1H), 7.47 (t, $J = 7.6$ Hz, 2H), 7.41 (t, $J = 8.2$ Hz, 1H), 7.32 (t, $J = 8.9$ Hz, 2H), 7.26 (t, $J = 7.4$ Hz, 1H), 2.35 (s, 3H). $^{13}\text{C NMR}$ (CDCl_3 , 100 MHz) δ 198.96, 138.96, 138.08, 137.07, 133.45, 131.32, 130.56, 130.45, 128.84, 128.78, 125.52, 20.30.

²¹⁹ Tripathi, S.; Singh, S. N.; Yadav, L. D. S., *Tetrahedron Lett.* **2015**, 56, 4211.

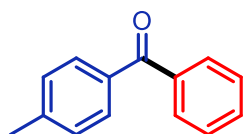
²²⁰ Tripathi, S.; Singh, S. N.; Yadav, L. D. S., *Tetrahedron Lett.* **2015**, 56, 4211.



phenyl(o-tolyl)methanone (68.6La) was prepared according to the general procedure. Purification was done by column chromatography. The first 5 fractions were collected using 20% DCM in hexane, followed by a gradient of 5% \rightarrow 10% EtOAc in hexane to afford **68.6La** as a colorless oil, (29.1 mg, 75%). Characterization data matched that of **68.6Ak**.



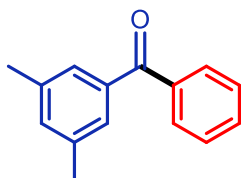
(2-methoxyphenyl)(phenyl)methanone (68.6AI) was prepared according to the general procedure. Purification by column chromatography (gradient of 5% \rightarrow 20% EtOAc in hexane) afforded **68.6AI** as a white solid, (32.5 mg, 80%). Characterization data matched those previously reported.²²¹ **¹H NMR** (400 MHz, CDCl₃) δ 7.83 (d, J = 7.0 Hz, 2H), 7.56 (t, J = 7.4 Hz, 1H), 7.50 – 7.43 (m, 3H), 7.37 (dd, J = 7.5, 1.7 Hz, 1H), 7.05 (t, J = 7.5 Hz, 1H), 7.01 (d, J = 8.4 Hz, 1H), 3.73 (s, 3H). **¹³C NMR** (CDCl₃, 100 MHz) δ 196.78, 157.69, 138.16, 132.23, 132.19, 130.15, 129.91, 129.21, 128.54, 120.82, 111.80, 55.93.



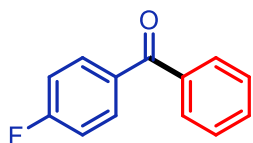
phenyl(p-tolyl)methanone (68.6Ca) was prepared according to the general procedure. Purification was done by column chromatography. The first 5 fractions were collected using 20% DCM in hexane, followed by a gradient of 5% \rightarrow 10% EtOAc in hexane to afford **68.6Ca** as a

²²¹ Kuang, Y.; Wang, Y., *Eur. J. Org. Chem.* **2014**, 2014, 1163.

white solid, (36.6 mg, 93%). Characterization data matched those previously reported.²²² ^1H NMR (400 MHz, CDCl_3) δ 7.80 (d, $J = 7.0$ Hz, 2H), 7.74 (d, $J = 8.2$ Hz, 2H), 7.59 (t, $J = 7.4$ Hz, 1H), 7.48 (t, $J = 7.5$ Hz, 2H), 7.29 (d, $J = 7.9$ Hz, 2H), 2.45 (s, 3H). ^{13}C NMR (CDCl_3 , 100 MHz) δ 196.83, 143.56, 138.31, 135.24, 132.48, 130.64, 130.26, 129.31, 128.54, 21.99.



(3,5-dimethylphenyl)(phenyl)methanone (68.6Da) was prepared according to the general procedure. Purification was done by column chromatography. The first 5 fractions were collected using 20% DCM in hexane, followed by a gradient of 5% \rightarrow 10% EtOAc in hexane to afford **68.6Da** as a pale yellow solid, (32.7 mg, 78%). Characterization data matched those previously reported.²²³ ^1H NMR (400 MHz, CDCl_3) δ 7.81 (d, $J = 7.2$ Hz, 2H), 7.59 (t, $J = 7.4$ Hz, 1H), 7.49 (t, $J = 7.6$ Hz, 2H), 7.41 (s, 2H), 7.21 (s, 1H), 2.39 (s, 6H). ^{13}C NMR (CDCl_3 , 100 MHz) δ 197.50, 138.27, 138.06, 134.41, 132.58, 130.36, 128.54, 128.15, 21.57.



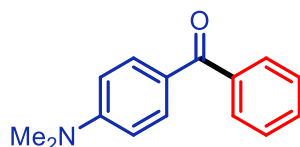
(4-fluorophenyl)(phenyl)methanone (68.6Ea) was prepared according to the general procedure. Purification was done by column chromatography. The first 5 fractions were collected using 20% DCM in hexane, followed by a gradient of 5% \rightarrow 10% EtOAc in hexane to afford **68.6Ea** as a white solid, (37.4 mg, 94%). Characterization data matched those previously reported.²²⁴ ^1H NMR (400 MHz, CDCl_3) δ 7.86 (dd, $J = 8.9, 5.4$ Hz, 2H), 7.78 (dt, $J = 8.4, 1.6$ Hz, 2H), 7.60 (t,

²²² Kuang, Y.; Wang, Y., *Eur. J. Org. Chem.* **2014**, 2014, 1163.

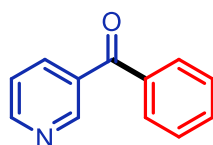
²²³ Zhou, Q.; Wei, S.; Han, W., *J. Org. Chem.* **2014**, 79, 1454.

²²⁴ Wang, G.-Z.; Li, X.-L.; Dai, J.-J.; Xu, H.-J., *J. Org. Chem.* **2014**, 79, 7220.

$J = 7.4$ Hz, 1H), 7.50 (t, $J = 7.5$ Hz, 2H), 7.17 (t, $J = 8.7$ Hz, 2H). ^{13}C NMR (CDCl_3 , 100 MHz) δ 195.58, 165.4 (d, $J=260.5$ Hz), 137.85, 134.16 (d, $J=3.1$ Hz), 132.99 (d, $J=9.2$ Hz), 130.80, 130.20, 128.69, 115.78 (d, $J=21.8$).



(4-(dimethylamino)phenyl)(phenyl)methanone (68.6Ia) was prepared according to the general procedure. Purification by column chromatography (gradient of 5% \rightarrow 20% EtOAc in hexane) afforded **68.6Ia** as a yellowish solid. (26.9 mg, 60%) . Characterization data matched those previously reported.²²⁵ ^1H NMR (400 MHz, CDCl_3) δ 7.79 (d, $J = 8.9$ Hz, 2H), 7.71 (d, $J = 7.1$ Hz, 2H), 7.51 (d, $J = 7.3$ Hz, 1H), 7.44 (d, $J = 7.4$ Hz, 2H), 6.67 (d, $J = 8.9$ Hz, 2H), 3.06 (s, 6H). ^{13}C NMR (100 MHz, CDCl_3) δ 195.47, 153.60, 139.64, 133.07, 131.43, 129.78, 128.33, 125.17, 110.92, 40.41.

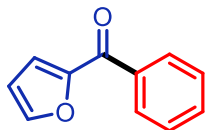


phenyl(pyridin-3-yl)methanone (68.6Ja) was prepared according to the general procedure. Purification by column chromatography (gradient of 10% \rightarrow 40% EtOAc in hexane) afforded **68.6Ja** as yellowish solid (29.2 mg, 83%). Characterization data matched those previously reported.²²⁶ ^1H NMR (400 MHz, CDCl_3) δ 9.00 (d, $J = 1.6$ Hz, 1H), 8.82 (dd, $J = 4.9, 1.6$ Hz, 1H), 8.13 (dt, $J = 7.9, 2.0$ Hz, 1H), 7.82 (dd, $J = 8.1, 1.0$ Hz, 2H), 7.64 (t, $J = 6.8$ Hz, 1H), 7.52 (t,

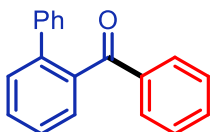
²²⁵ Gooßen, L. J.; Rudolphi, F.; Oppel, C.; Rodríguez, N., *Angew. Chem. Int. Ed.* **2008**, *47*, 3043.

²²⁶ Rieke, R. D.; Suh, Y.; Kim, S.-H., *Tetrahedron Lett.* **2005**, *46*, 5961.

$J = 7.6$ Hz, 2H), 7.43 (dd, $J = 8.2, 4.5$ Hz, 1H). ^{13}C NMR (CDCl_3 , 100 MHz) δ 195.17, 153.11, 151.23, 137.54, 137.03, 133.50, 130.34, 128.95, 123.70.



furan-2-yl(phenyl)methanone (68.6Ka) was prepared according to the general procedure. Purification by column chromatography (gradient of 5% \rightarrow 15% EtOAc in hexane) afforded **68.6Ka** as a colorless oil, (31.6 mg, 92%). Characterization data matched those previously reported.²²⁷ ^1H NMR (400 MHz, CDCl_3) δ 7.98 (dd, $J = 8.3, 1.3$ Hz, 2H), 7.71 (dd, $J = 1.6, 0.7$ Hz, 1H), 7.60 (t, $J = 7.4$ Hz, 1H), 7.50 (t, $J = 7.5$ Hz, 2H), 7.24 (d, $J = 2.9$ Hz, 1H), 6.60 (dd, $J = 3.6, 1.7$ Hz, 1H). ^{13}C NMR (CDCl_3 , 100 MHz) δ 182.89, 152.64, 147.42, 137.60, 132.90, 129.61, 128.79, 120.87, 112.53.

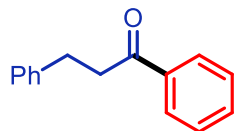


[1,1'-biphenyl]-2-yl(phenyl)methanone (68.6Ma) was prepared according to a modified general procedure with dioxane as the solvent, run for 16 hours at 100 °C. Purification was done by column chromatography. The first 5 fractions were collected using 20% DCM in hexane, followed by a gradient of 5% \rightarrow 10% EtOAc in hexane. The material was then recrystallized in hexanes to afford **68.6Ma** as a white solid, (27.6 mg, 56%). Characterization data matched those previously reported.²²⁸ ^1H NMR (400 MHz, CDCl_3) δ 7.65 (dd, $J = 8.2, 1.0$ Hz, 2H), 7.59 (t, $J = 8.2$ Hz, 1H), 7.54 – 7.45 (m, 3H), 7.41 (t, $J = 7.4$ Hz, 1H), 7.30 – 7.13 (m, 7H). ^{13}C NMR

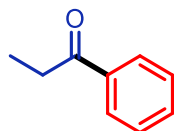
²²⁷ Kuang, Y.; Wang, Y., *Eur. J. Org. Chem.* **2014**, 2014, 1163.

²²⁸ Zeng, J.; Liu, K. M.; Duan, X. F., *Org. Lett.* **2013**, 15, 5342.

(CDCl₃, 100 MHz) 199.12, 141.49, 140.52, 139.31, 137.75, 133.13, 130.69, 130.40, 130.23, 129.34, 129.11, 128.57, 128.40, 127.66, 127.40.



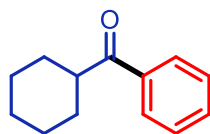
1,3-diphenylpropan-1-one (68.6Na) was prepared according to the general procedure. Purification by column chromatography. The first 5 fractions were collected using 20% DCM in hexane, followed by a gradient of 5% → 10% EtOAc in hexane to afford **68.6Na** as a (27.6mg, 66%). Characterization data matched those previously reported.²²⁹ ¹H NMR (400 MHz, CDCl₃) δ 7.98 (d, *J* = 8.4, Hz, 2H), 7.57 (t, *J* = 7.4 Hz, 1H), 7.47 (t, *J* = 7.6 Hz, 2H), 7.35 – 7.19 (m, 5H), 3.33 (t, *J* = 7.8 Hz, 2H), 3.09 (t, *J* = 6.0 Hz, 2H). ¹³C NMR (100 MHz, CDCl₃) δ 199.55, 141.64, 137.21, 133.39, 128.94, 128.87, 128.77, 128.38, 126.47, 40.79, 30.47.



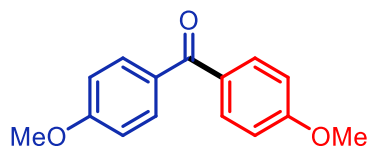
propiophenone (68.6Oa) was prepared according to the general procedure. Purification was done by column chromatography. The first 5 fractions were collected using 20% DCM in hexane, followed by a gradient of 5% → 10% EtOAc in hexane to afford **68.6Oa** as a colourless liquid. (29.6 mg, 74%). Characterization data matched those previously reported.²³⁰ ¹H NMR (400 MHz, CDCl₃) δ 7.95 (d, *J* = 7.1 Hz, 2H), 7.53 (t, *J* = 7.4 Hz, 1H), 7.44 (t, *J* = 7.5 Hz, 2H), 2.98 (t, *J* = 7.2 Hz, 2H), 1.21 (t, *J* = 7.2 Hz, 3H). ¹³C NMR (CDCl₃, 100 MHz) δ 201.14, 137.25, 133.18, 128.85, 128.29, 32.09, 8.55.

²²⁹ Kantam, M. L.; Kishore, R.; Yadav, J.; Sudhakar, M.; Venugopal, A., *Adv. Synth. Catal.* **2012**, 354, 663.

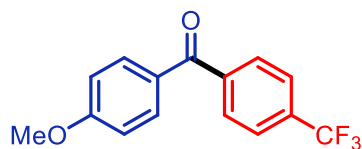
²³⁰ Landers, B.; Berini, C.; Wang, C.; Navarro, O., *J. Org. Chem.* **2011**, 76, 1390.



cyclohexyl(phenyl)methanone (68.6Pa) was prepared according to the general procedure. Purification was done by column chromatography. The first 5 fractions were collected using 20% DCM in hexane, followed by a gradient of 5% \rightarrow 10% EtOAc in hexane to afford **68.6Pa** as a white solid (15.9 mg, 42%). Characterization data matched those previously reported.²³¹ $^1\text{H NMR}$ (400 MHz, CDCl_3) δ 7.95 (dd, $J = 5.2, 3.4$ Hz, 2H), 7.55 (t, $J = 7.3$ Hz, 1H), 7.46 (t, $J = 7.6$ Hz, 2H), 3.27 (tt, $J = 11.5, 3.2$ Hz, 1H), 1.88 (t, $J = 15.4$ Hz, 4H), 1.75 (d, $J = 12.5$ Hz, 1H), 1.57 – 1.20 (m, 5H). $^{13}\text{C NMR}$ (100 MHz, CDCl_3) δ 204.18, 136.70, 133.02, 128.89, 128.57, 77.68, 77.36, 77.04, 45.95, 29.75, 26.29, 26.19.



bis(4-methoxyphenyl)methanone (68.6Fe) was prepared according to the general procedure. Purification by column gradient of 5% \rightarrow 30% EtOAc in hexane afforded **68.6Fe** as a white solid, (38.2 mg, 79%). Characterization data matched those previously reported.²³² $^1\text{H NMR}$ (400 MHz, CDCl_3) δ 7.79 (d, $J=8.7$ Hz, 4H), 6.97 (d, $J=8.7$ Hz, 4H), 3.89 (s, 6H) $^{13}\text{C NMR}$ (100 MHz, CDCl_3) δ 194.77, 163.16, 132.54, 131.09, 113.78, 55.78.

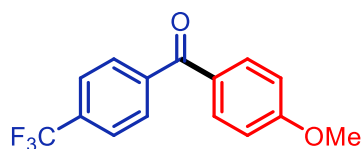


(4-methoxyphenyl)(4-(trifluoromethyl)phenyl)methanone (68.6Fi) was prepared according to the general procedure. Purification was done by column chromatography. The first 5 fractions

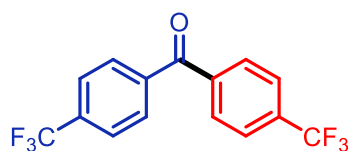
²³¹ Kuang, Y.; Wang, Y., *Eur. J. Org. Chem.* **2014**, 2014, 1163.

²³² Kuang, Y.; Wang, Y., *Eur. J. Org. Chem.* **2014**, 2014, 1163.

were collected using 20% DCM in hexane, followed by a gradient of 5% \rightarrow 10% EtOAc in hexane to afford **68.6Fi** as a white solid, (16.8 mg, 30%). Characterization data matched those previously reported.²³³ $^1\text{H NMR}$ (400 MHz, CDCl_3) δ 7.84 (t, $J = 8.3$ Hz, 4H), 7.75 (d, $J = 8.2$ Hz, 2H), 6.99 (d, $J = 8.8$ Hz, 2H), 3.91 (s, 3H). $^{13}\text{C NMR}$ (100 MHz, CDCl_3) δ 194.26, 163.74, 141.53, 133.30 (q, 32.6 Hz), 132.63, 129.79, 129.37, 125.32 (q, $J = 3.7$ Hz), 122.39 (q, $J = 274$ Hz), 113.82, 55.56.



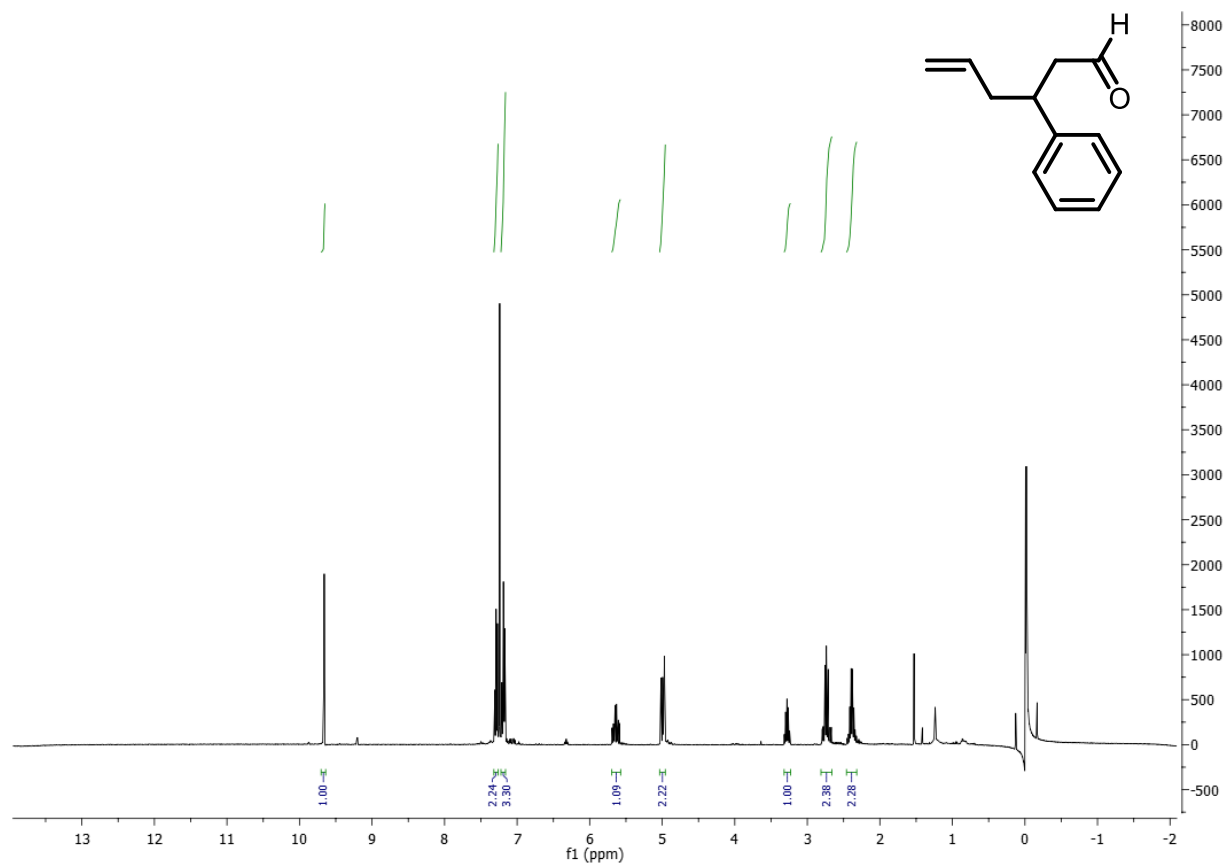
(4-methoxyphenyl)(4-(trifluoromethyl)phenyl)methanone (68.6Ge) was prepared according to the general procedure. Purification was done by column chromatography. The first 5 fractions were collected using 20% DCM in hexane, followed by a gradient of 5% \rightarrow 10% EtOAc in hexane to afford **68.6Ge** as a white solid (54.2 mg, 97%). Characterization data matched that of **68.6Fi**.



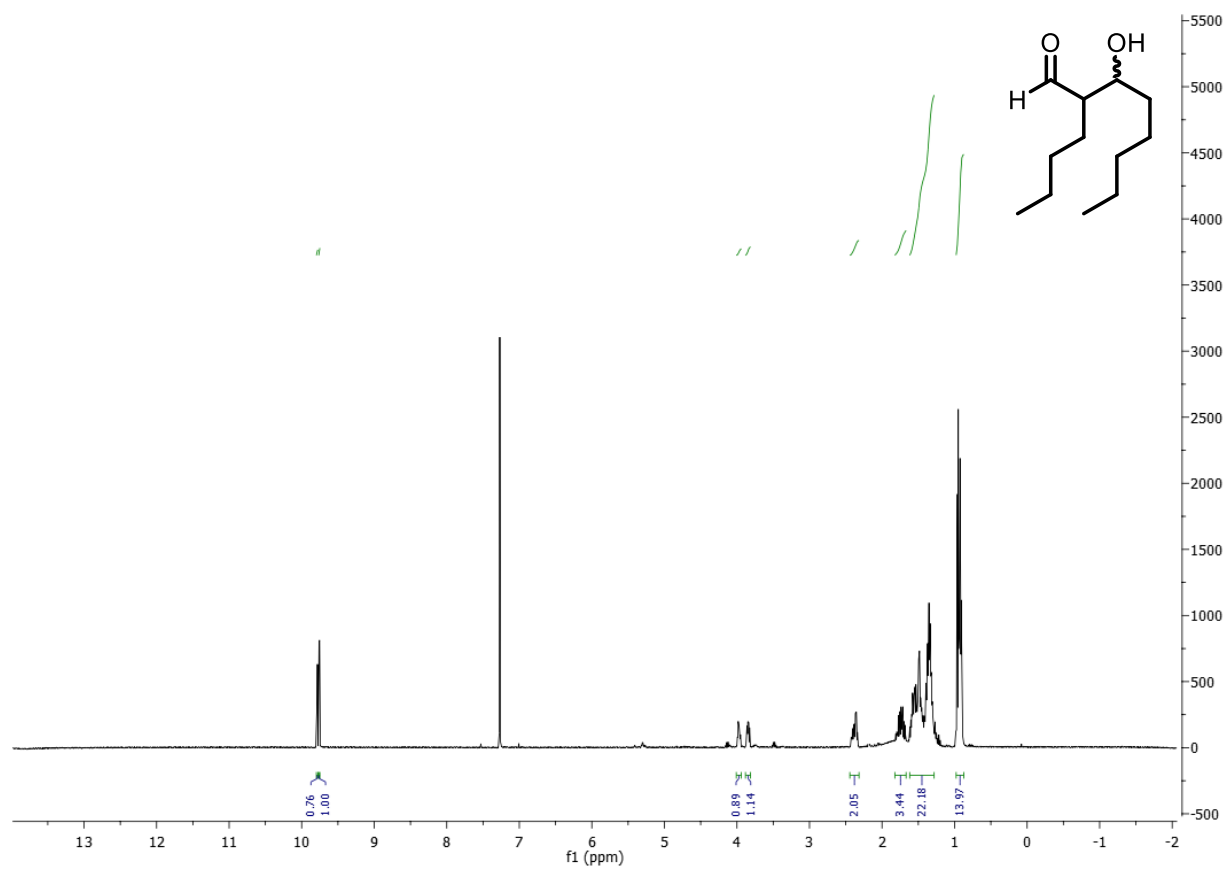
bis(4-(trifluoromethyl)phenyl)methanone (68.6Gi) was prepared according to the general procedure. Purification was done by column chromatography. The first 5 fractions were collected using 20% DCM in hexane, followed by a gradient of 5% \rightarrow 10% EtOAc in hexane to afford **68.6Gi** as a white solid, (39.6 mg, 63%). Characterization data matched those previously reported.²³⁴ $^1\text{H NMR}$ (400 MHz, CDCl_3) δ 7.92 (d, $J = 8.1$ Hz, 4H), 7.79 (d, $J = 8.2$ Hz, 4H). $^{13}\text{C NMR}$ (100 MHz, CDCl_3) δ 194.72, 140.12, 134.75 (q, $J = 33$ Hz), 130.57, 126.02, 125.97 (q, $J = 3.7$ Hz), 123.92 (q, $J = 273.0$ Hz).

²³³ Kuang, Y.; Wang, Y., *Eur. J. Org. Chem.* **2014**, 2014, 1163.

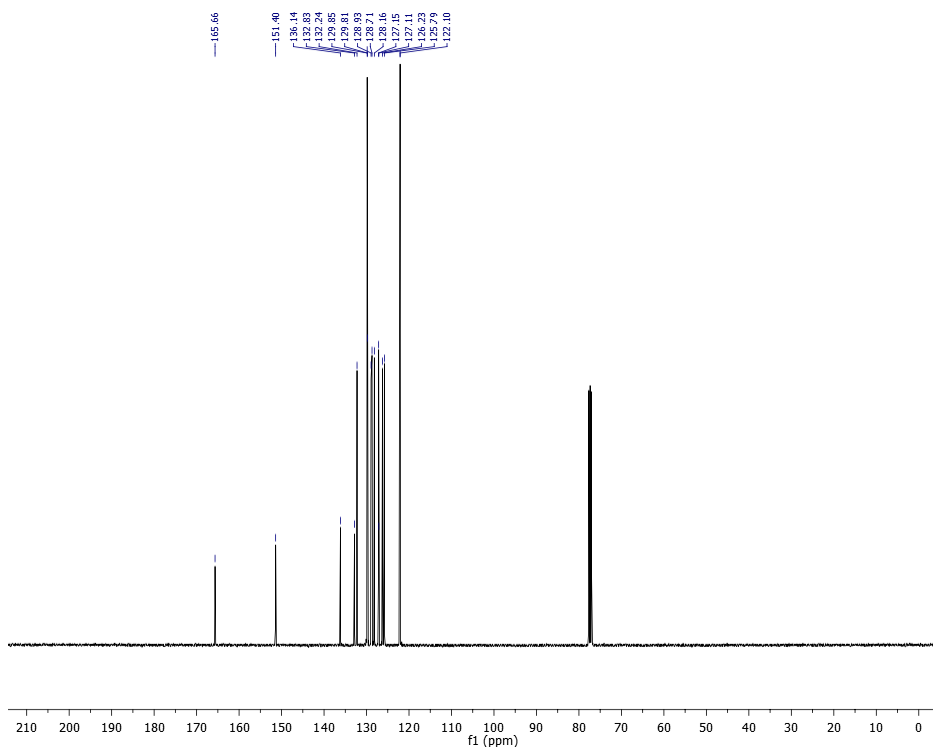
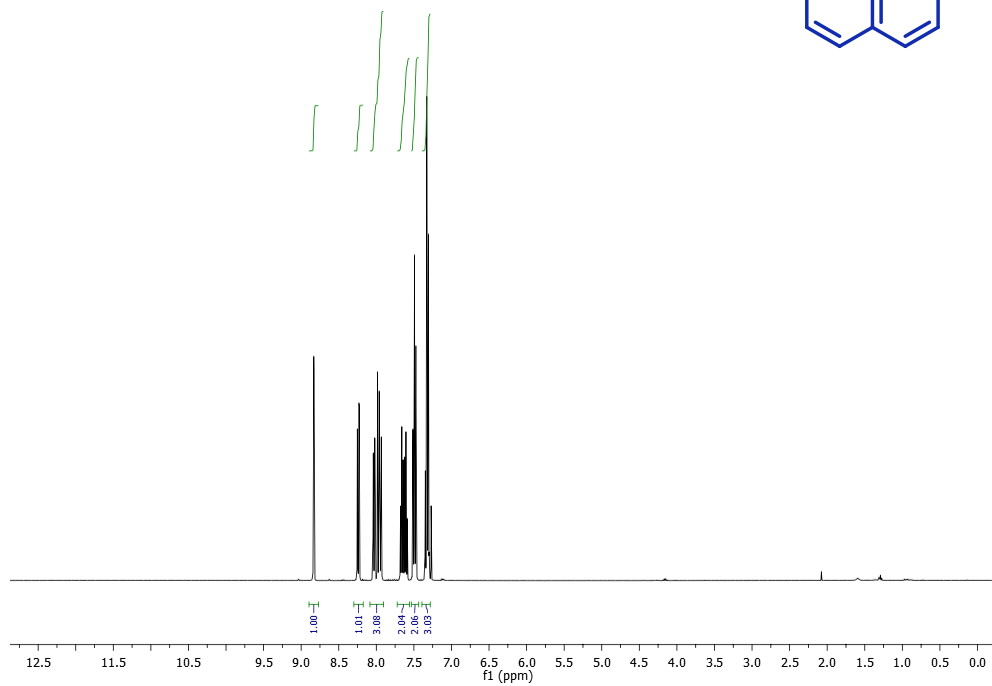
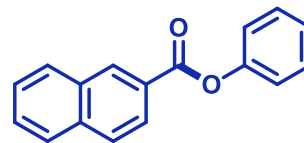
²³⁴ Li, Y.; Lu, W.; Xue, D.; Wang, C.; Liu, Z.-T.; Xiao, J., *Synlett.* **2014**, 25, 1097.

Appendix 1: ^1H and ^{13}C NMR spectra from Chapter 13-phenylhex-5-enal (**23.4**). CDCl_3 , 400 MHz:

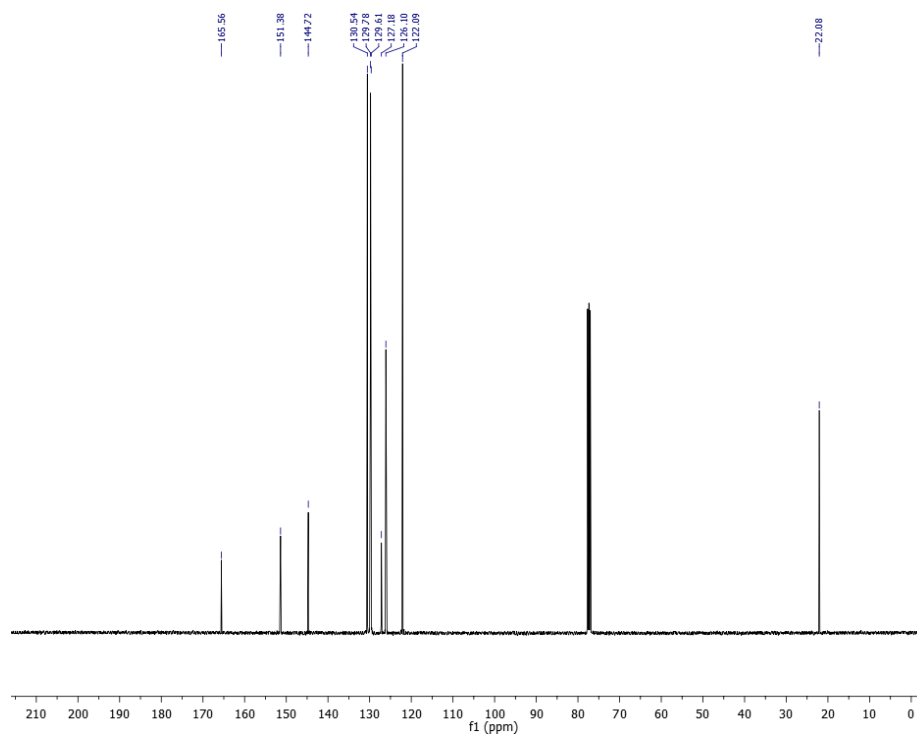
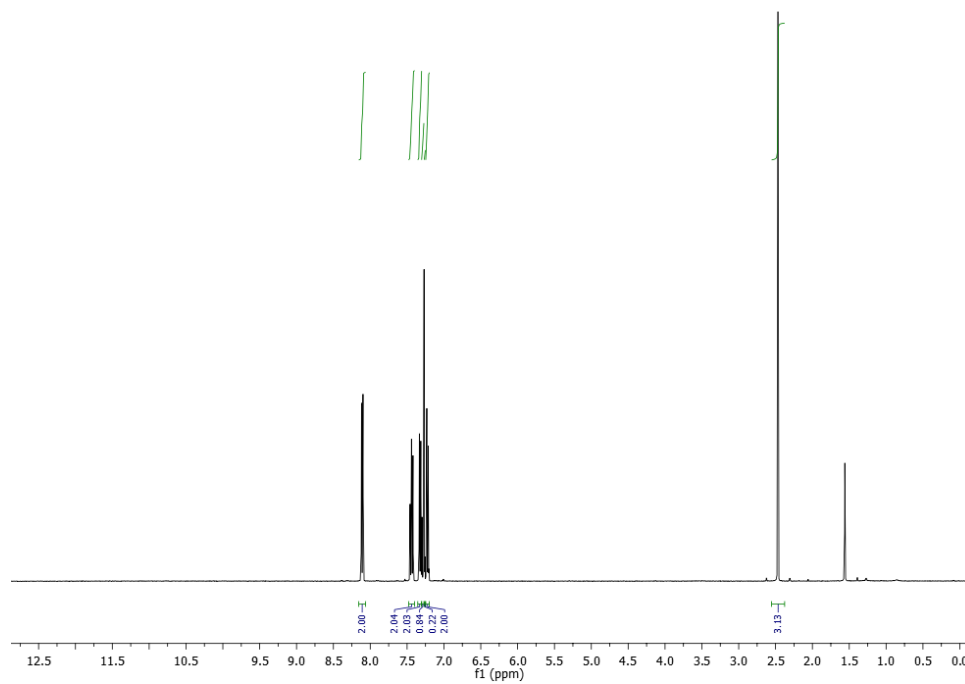
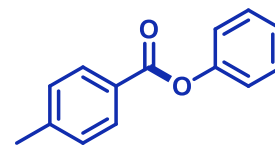
butyl-3-hydroxyoctanal (**29.5**). CDCl₃, 400 MHz:



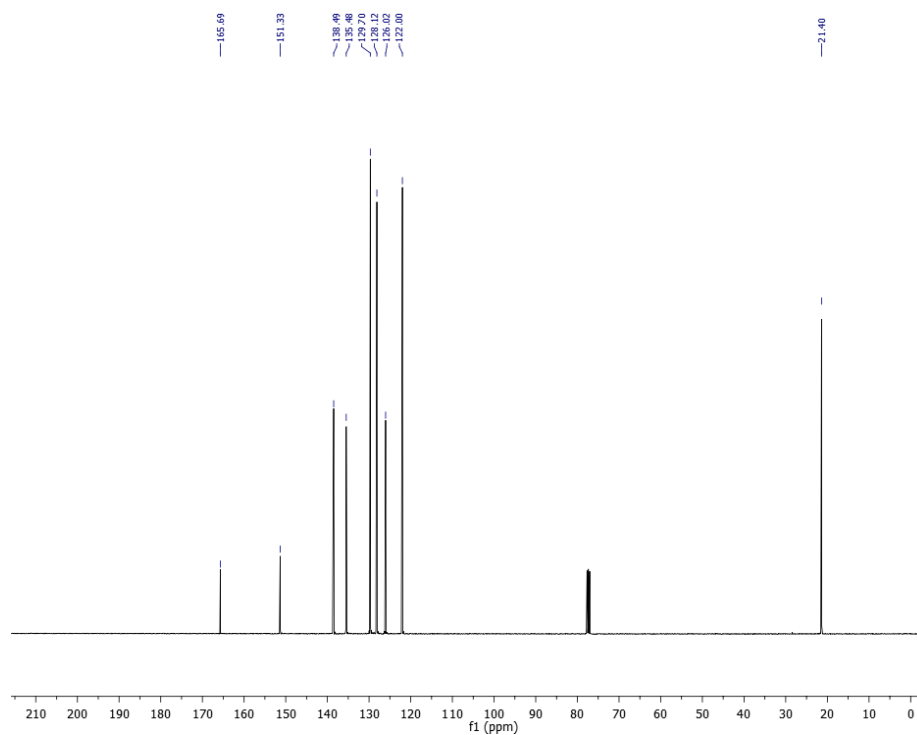
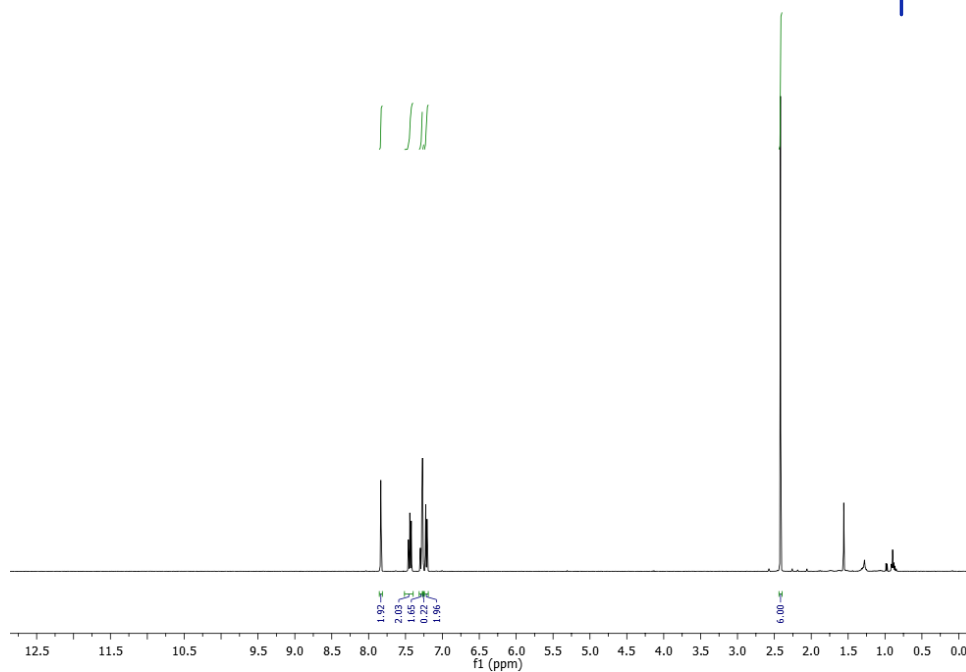
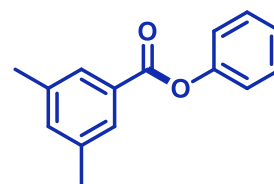
Appendix 2: ^1H and ^{13}C NMR spectra from Chapter 2
phenyl 2-naphthoate (**68.4B**). CDCl_3 , 400MHz:



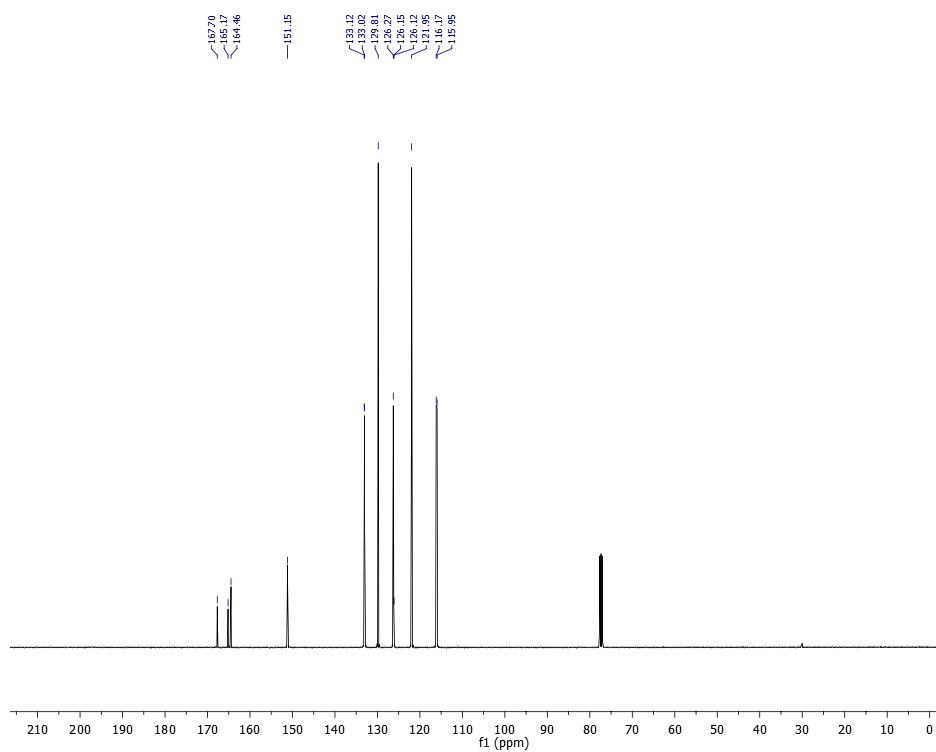
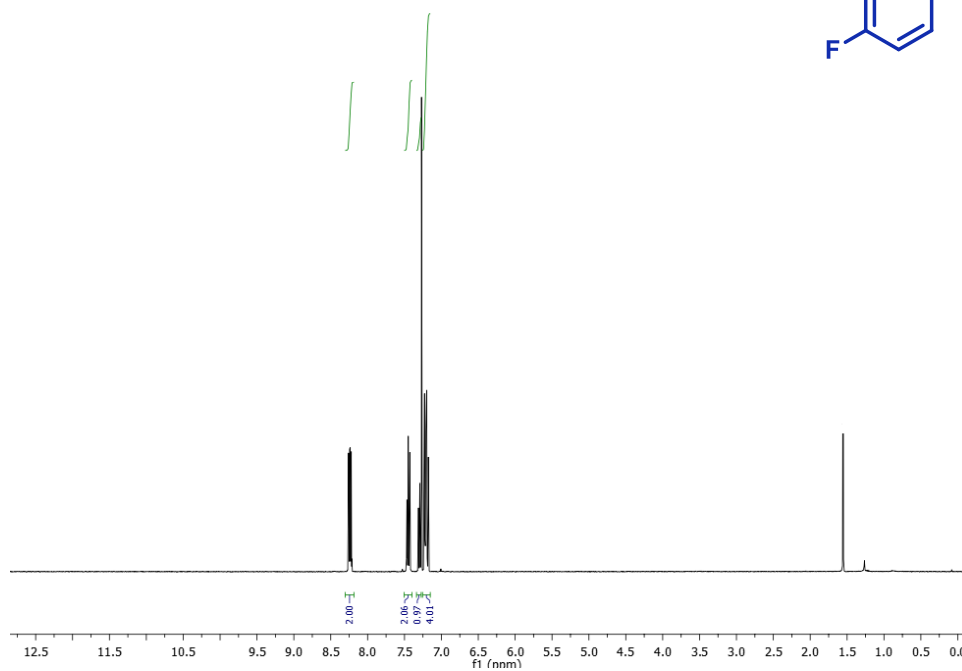
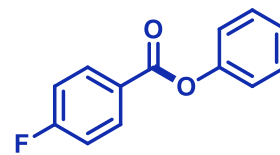
p-methyl benzoic acid phenyl ester (**68.4C**). CDCl₃, 400MHz:



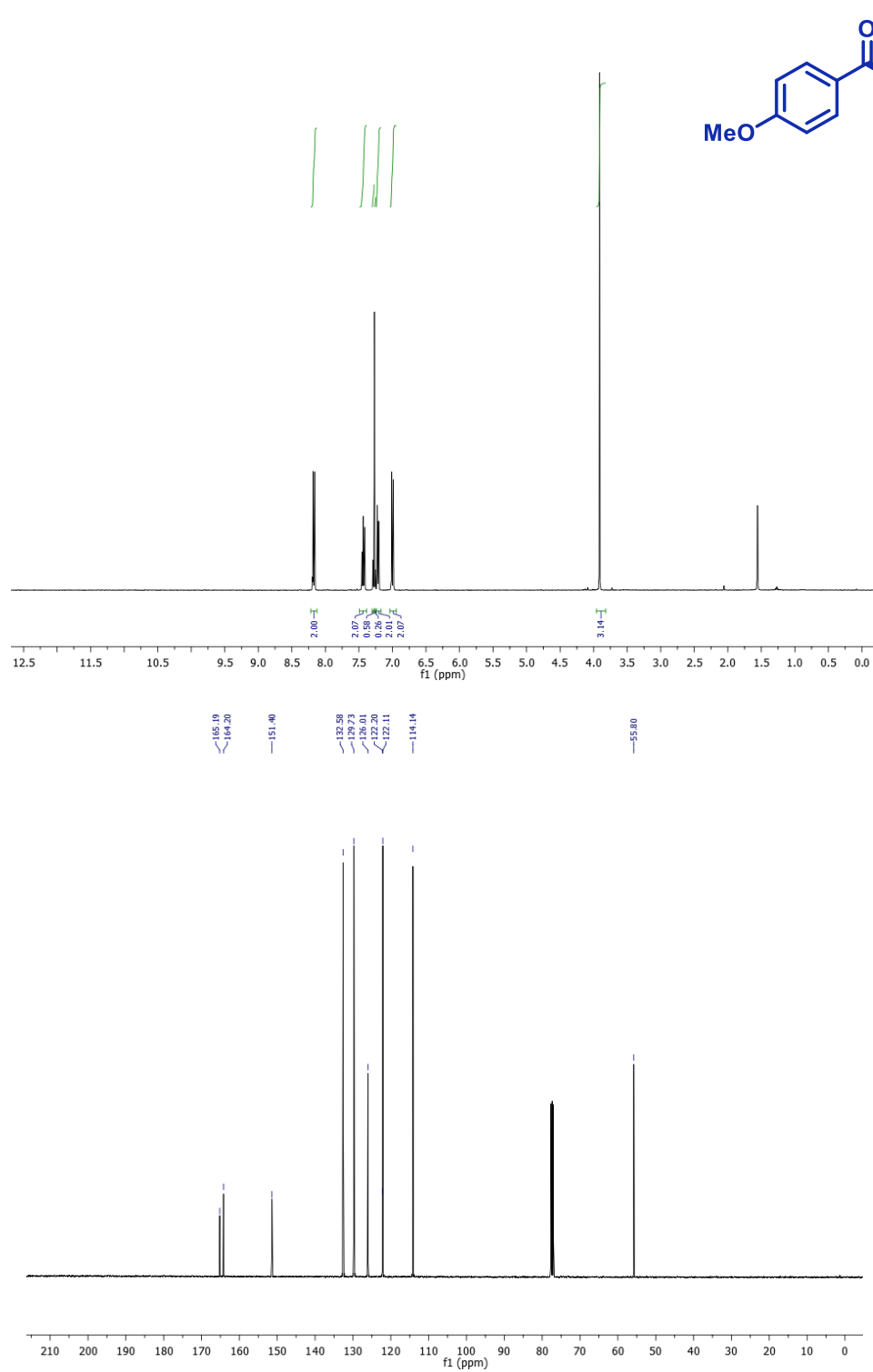
phenyl 3,5-dimethylbenzoate (**68.4D**). CDCl₃, 400 MHz:



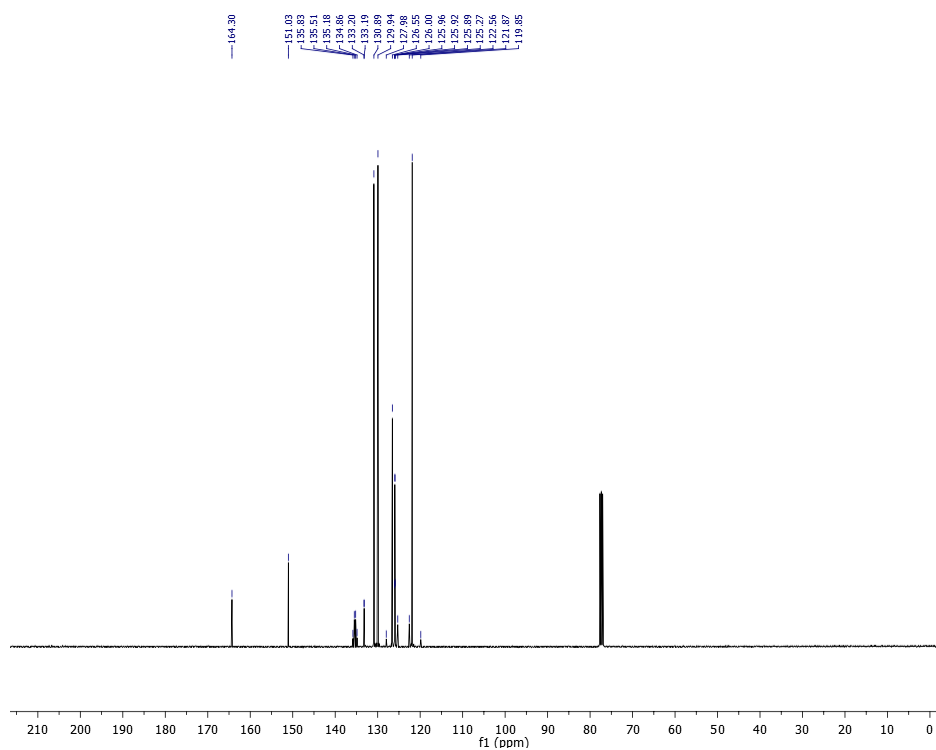
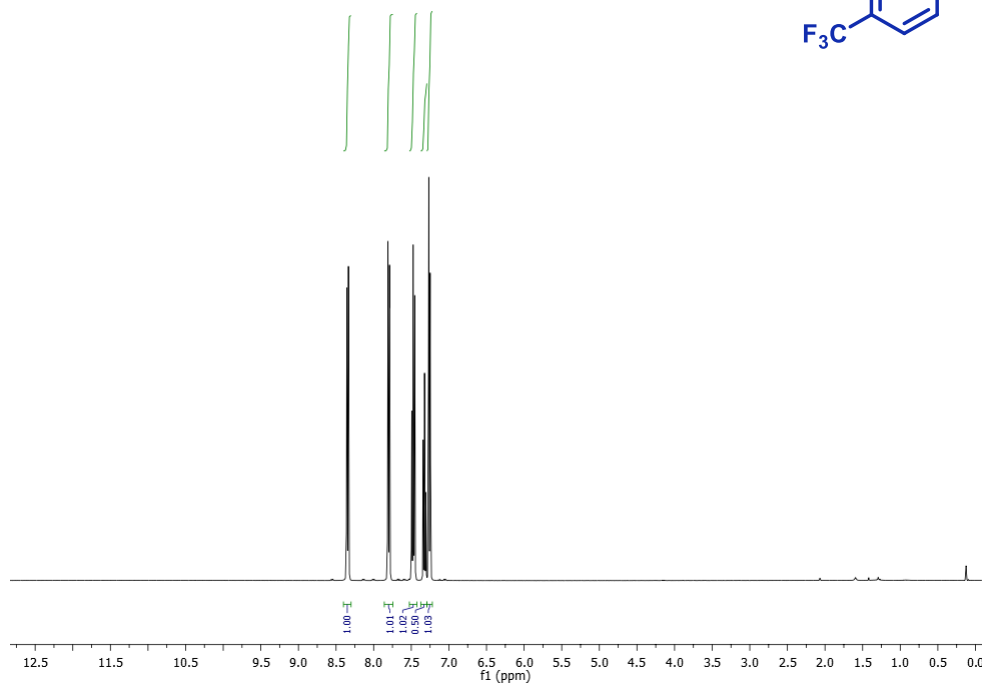
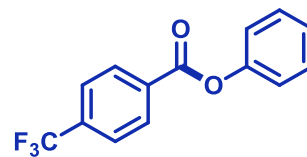
4-fluoro-benzoic acid phenyl ester (**68.4E**). CDCl₃, 400 MHz:



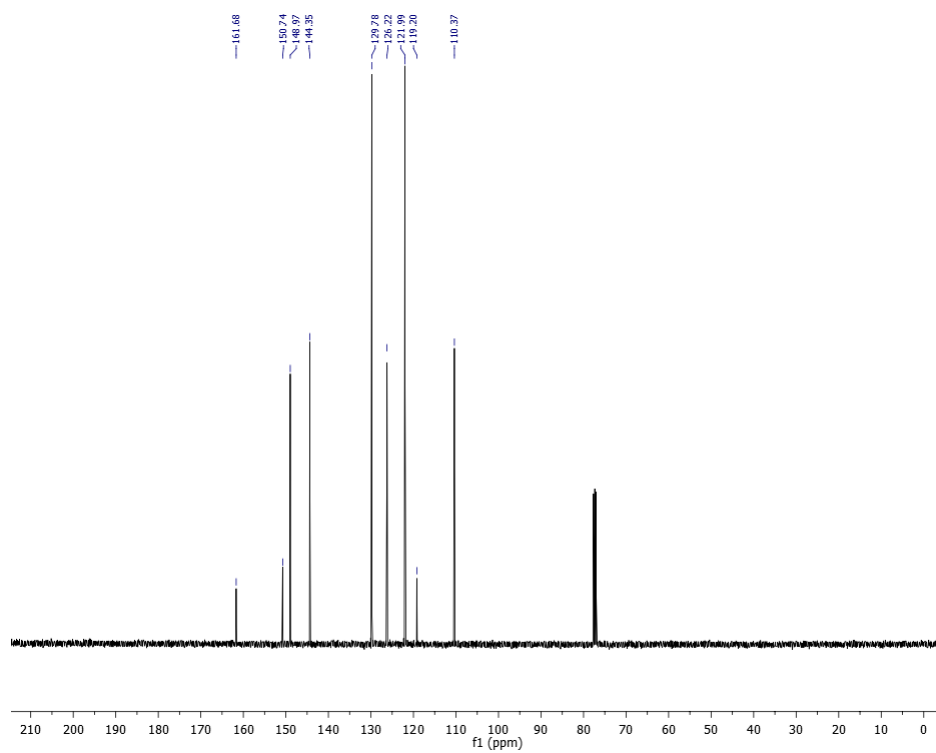
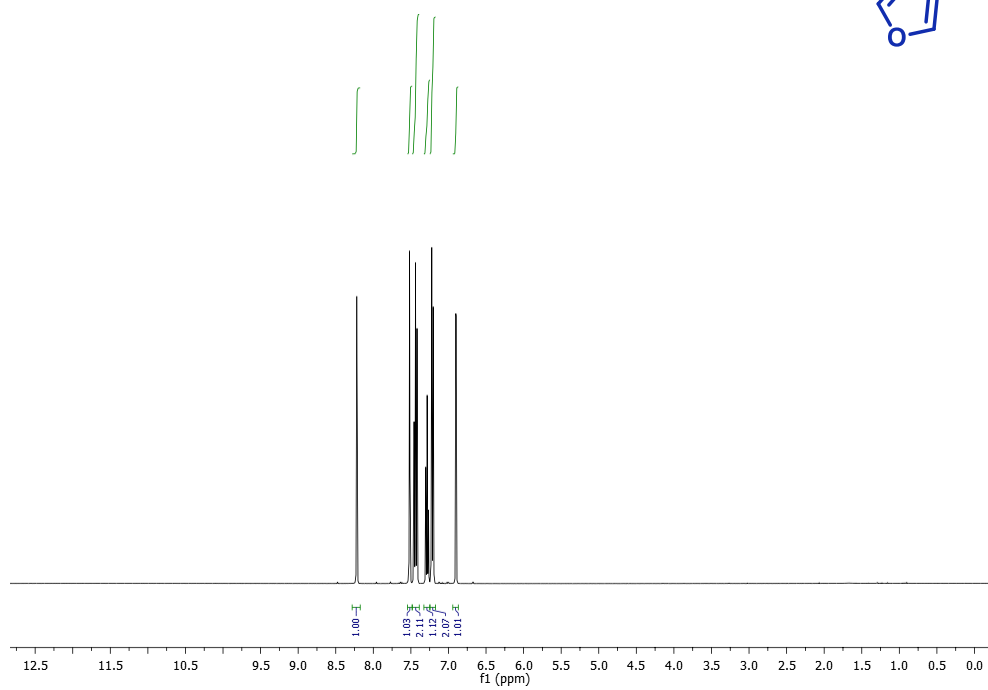
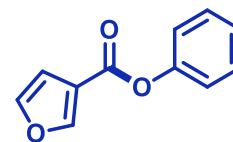
4-methoxy-benzoic acid phenyl ester (**68.4F**). CDCl₃, 400 MHz:



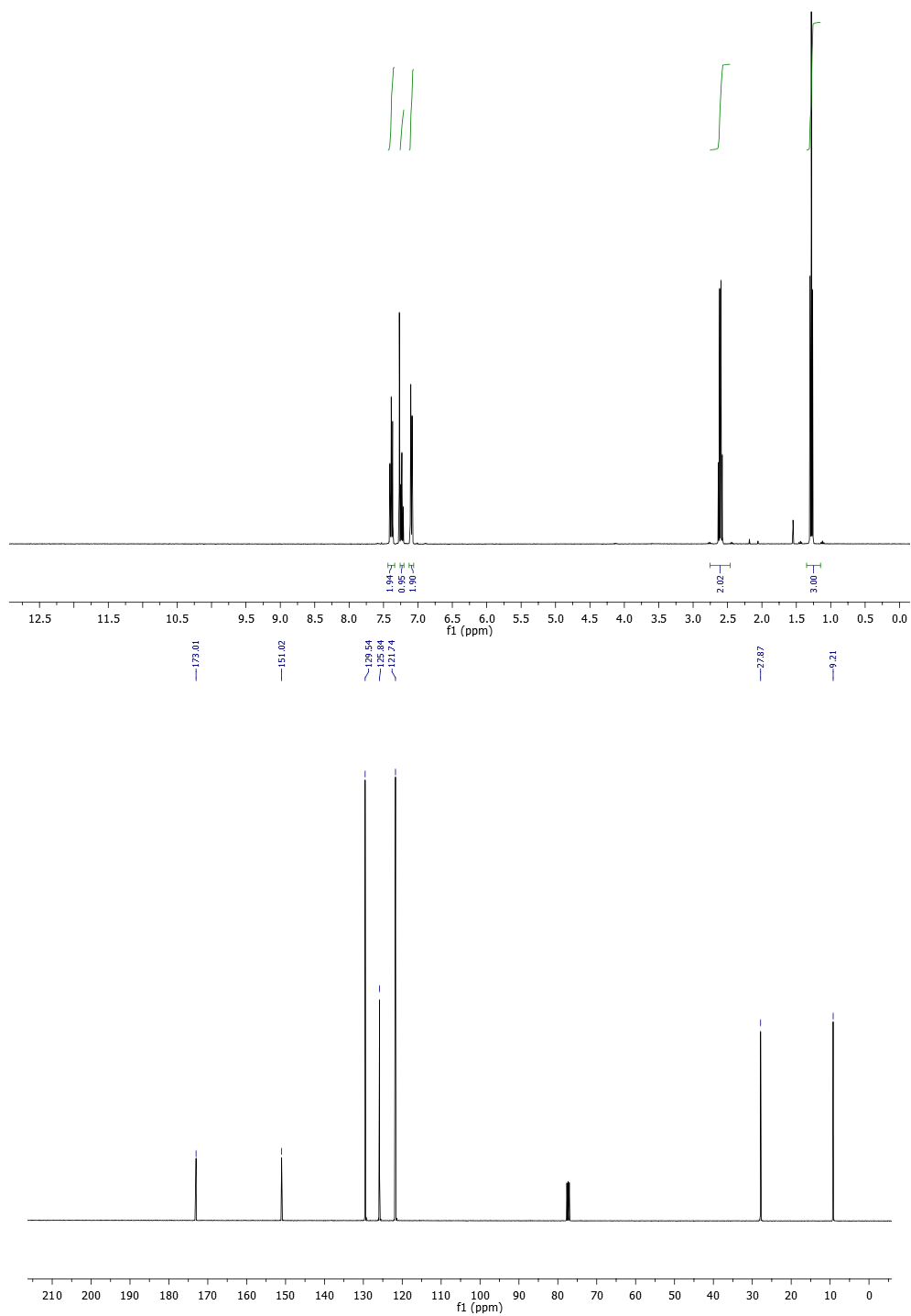
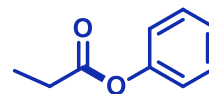
phenyl 4-(trifluoromethyl) benzoate (**68.4G**). CDCl₃, 400 MHz:



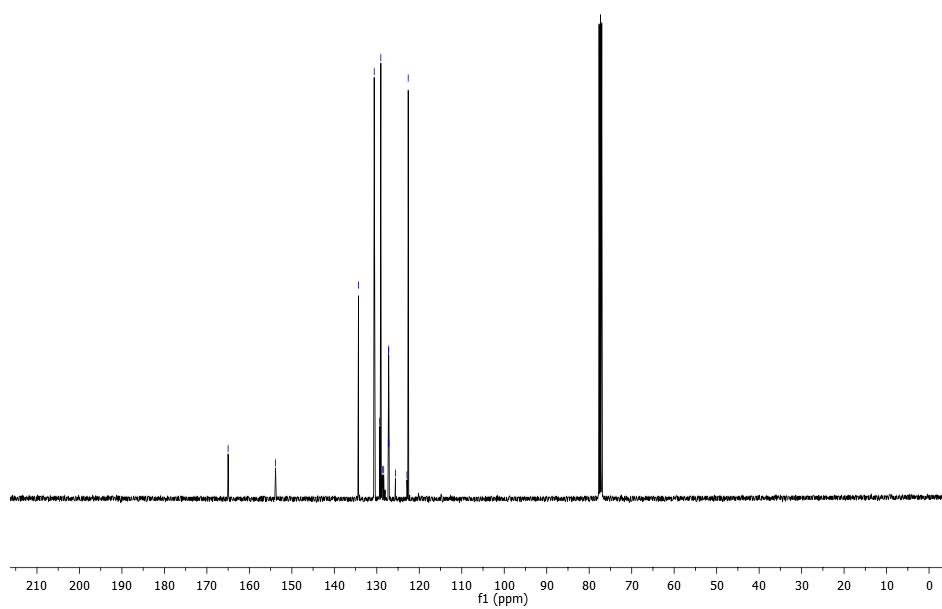
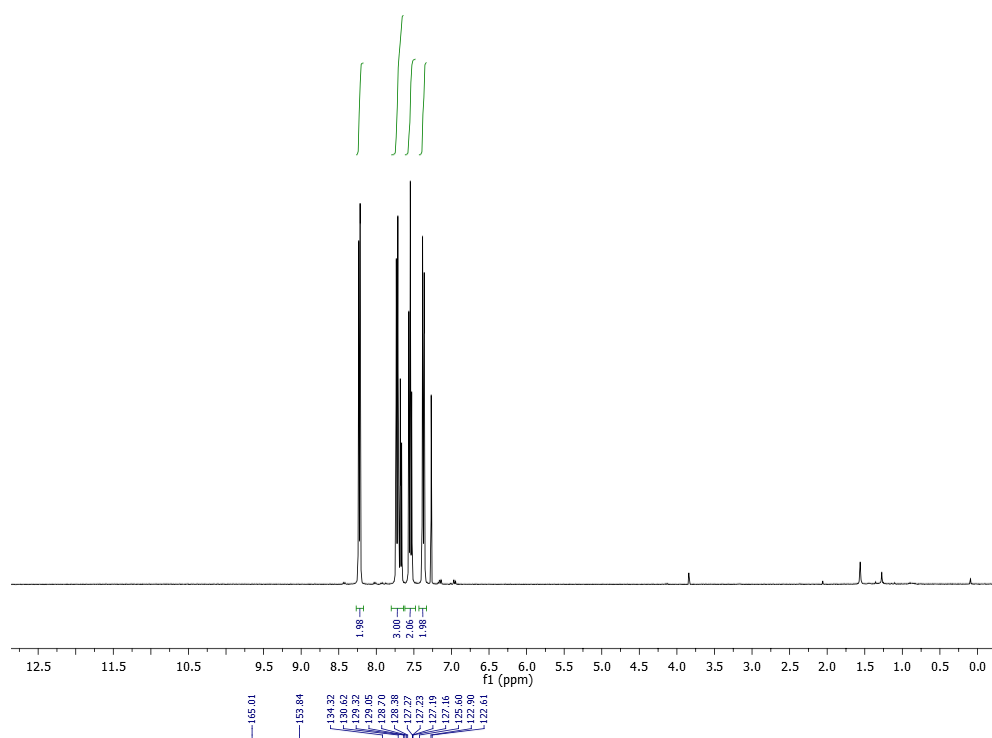
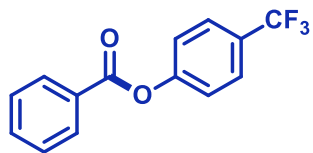
phenyl furan-3-carboxylate (**68.4H**). CDCl₃, 400 MHz:



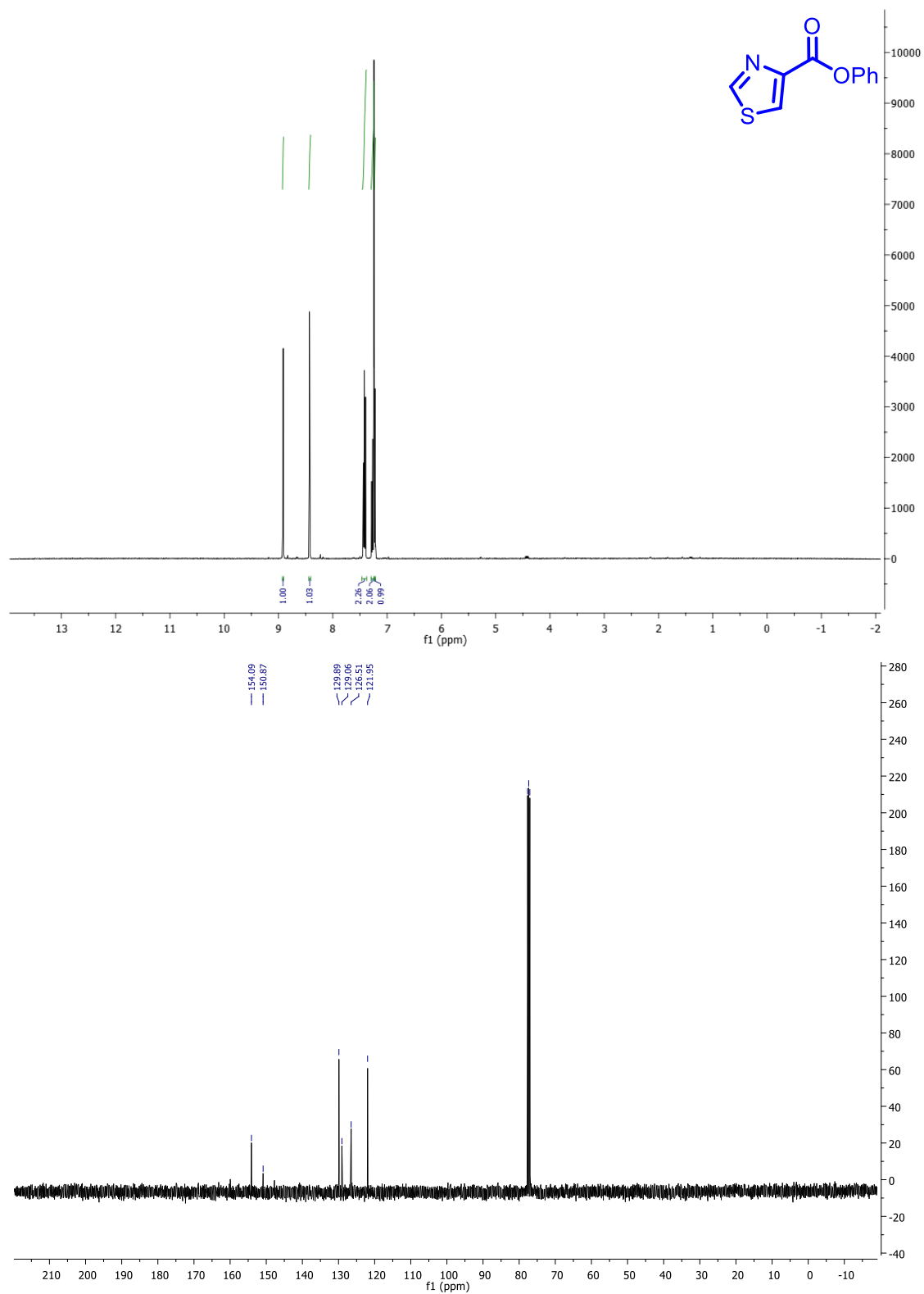
phenyl propionate (**68.40**) CDCl₃, 400 MHz:



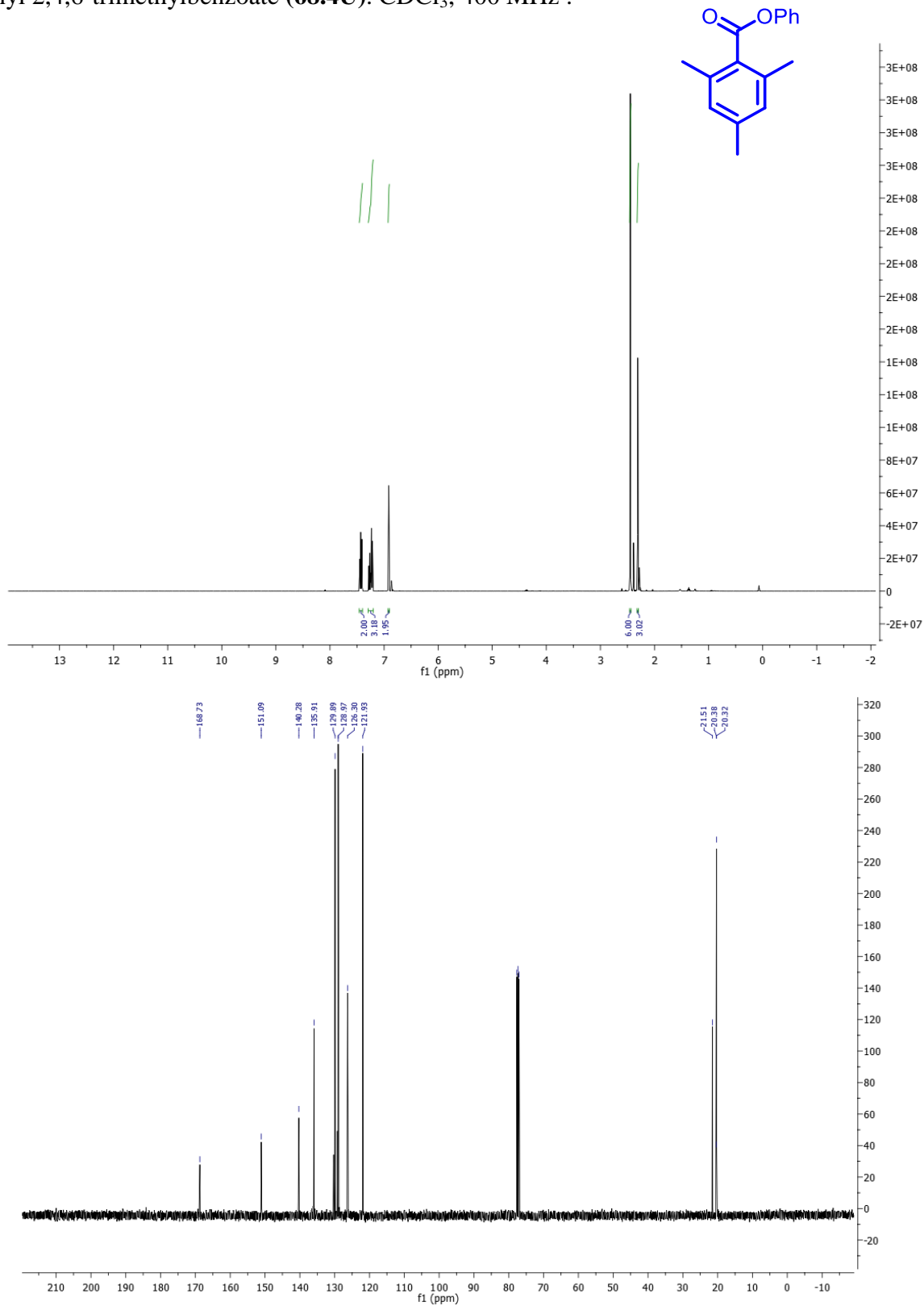
4-(trifluoromethyl) phenyl benzoate (**73.2**). CDCl₃, 400 MHz:



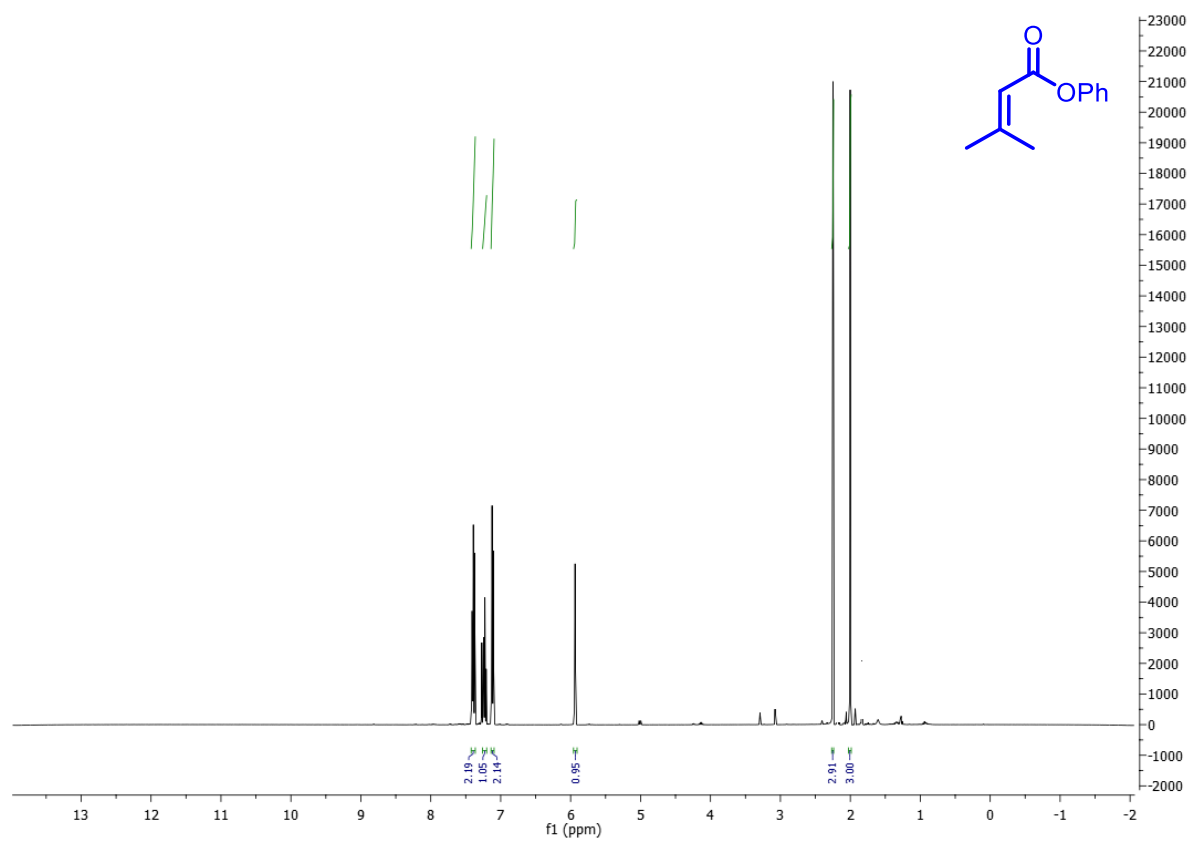
phenyl thiazole-4-carboxylate (**68.4T**). CDCl₃, 400 MHz:



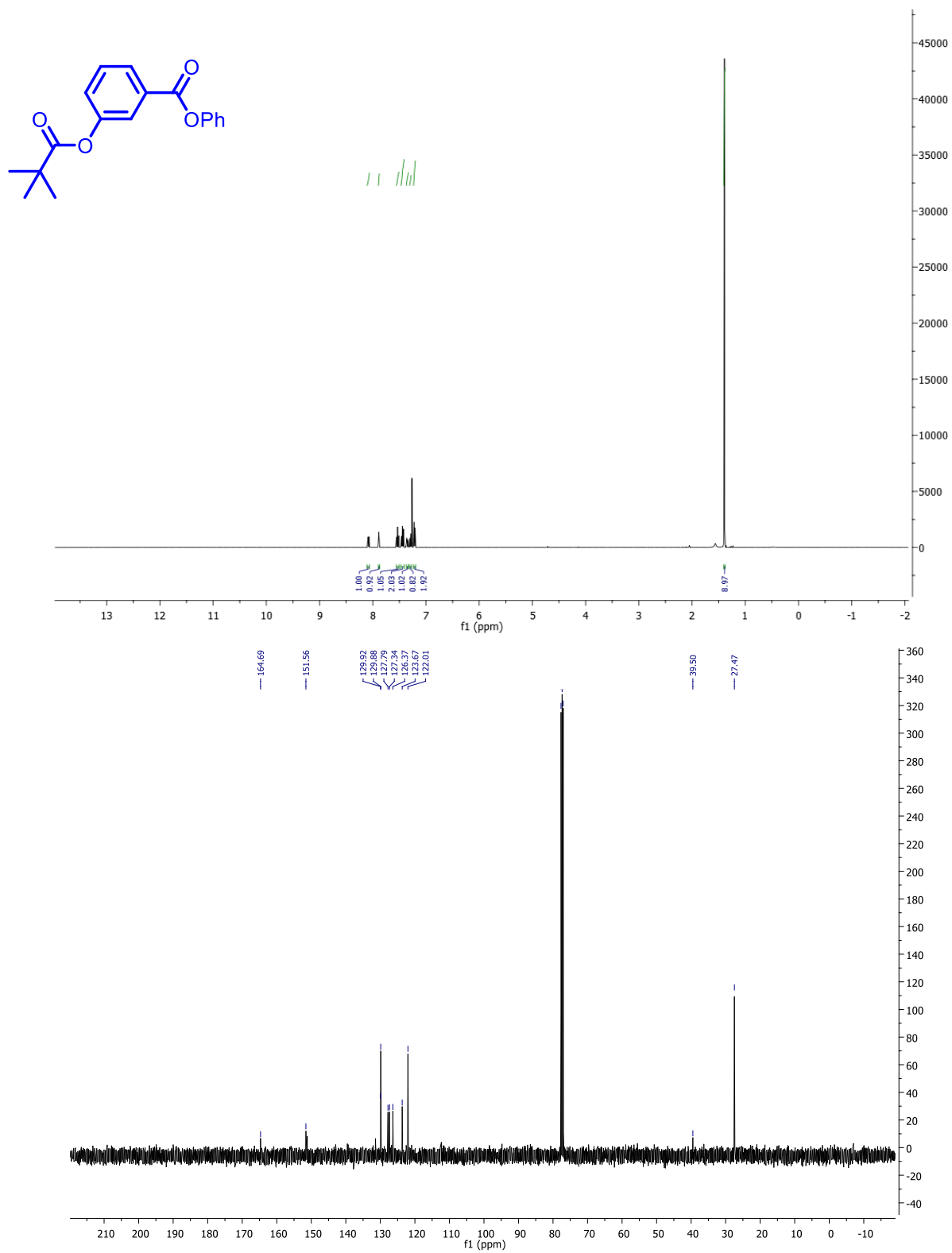
phenyl 2,4,6-trimethylbenzoate (**68.4U**). CDCl₃, 400 MHz :



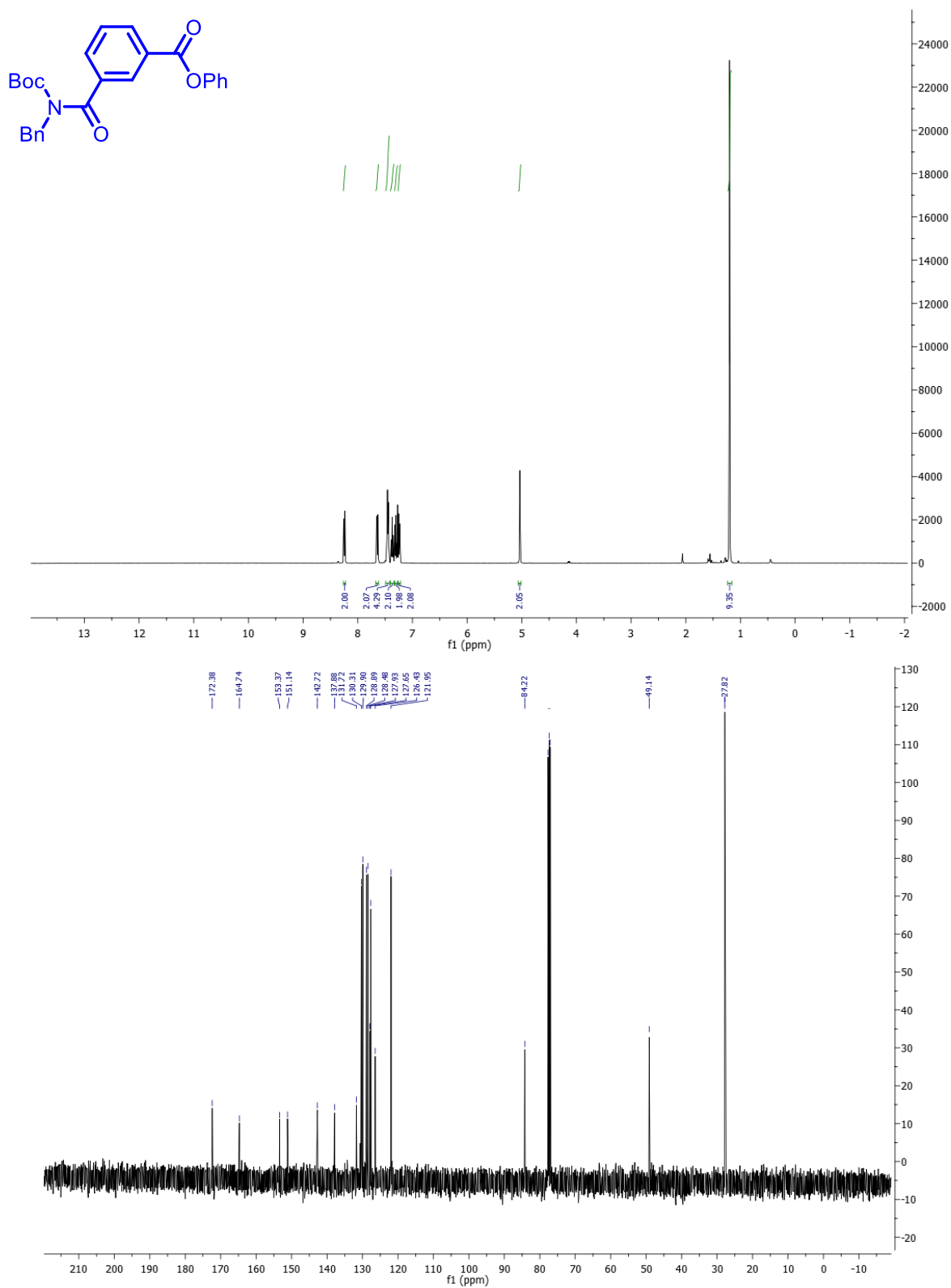
phenyl 3-methylbut-2-enoate (**68.4V**) CDCl_3 , 400 MHz:



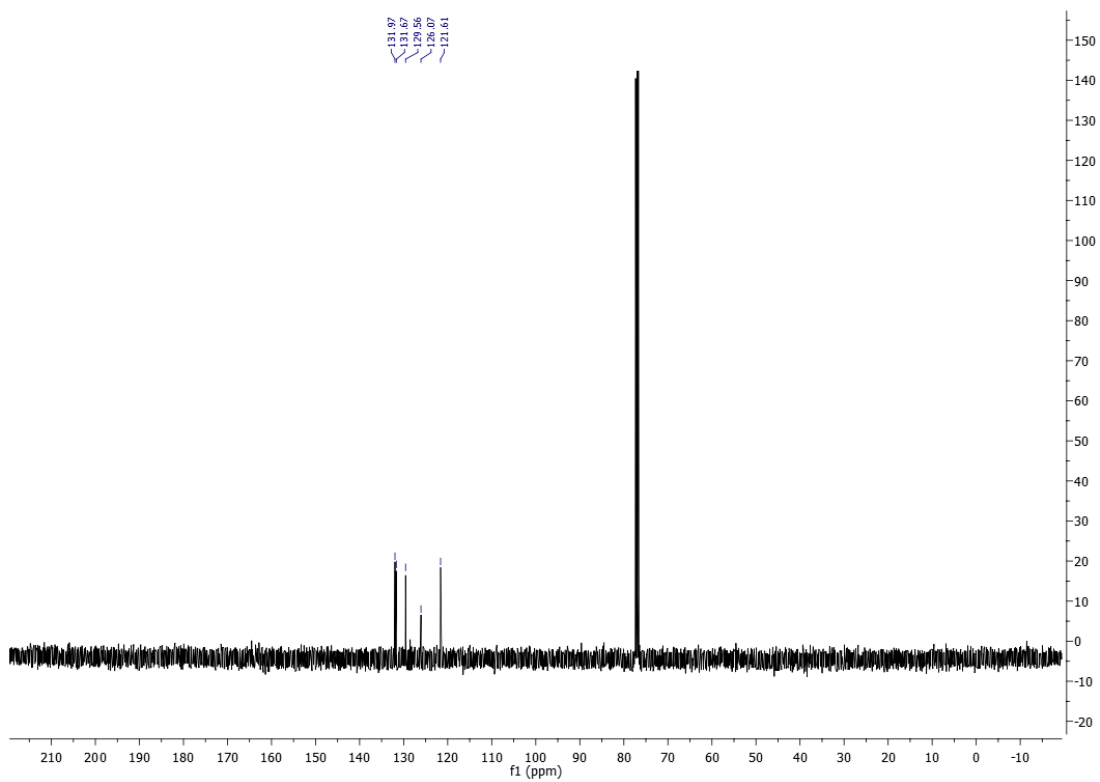
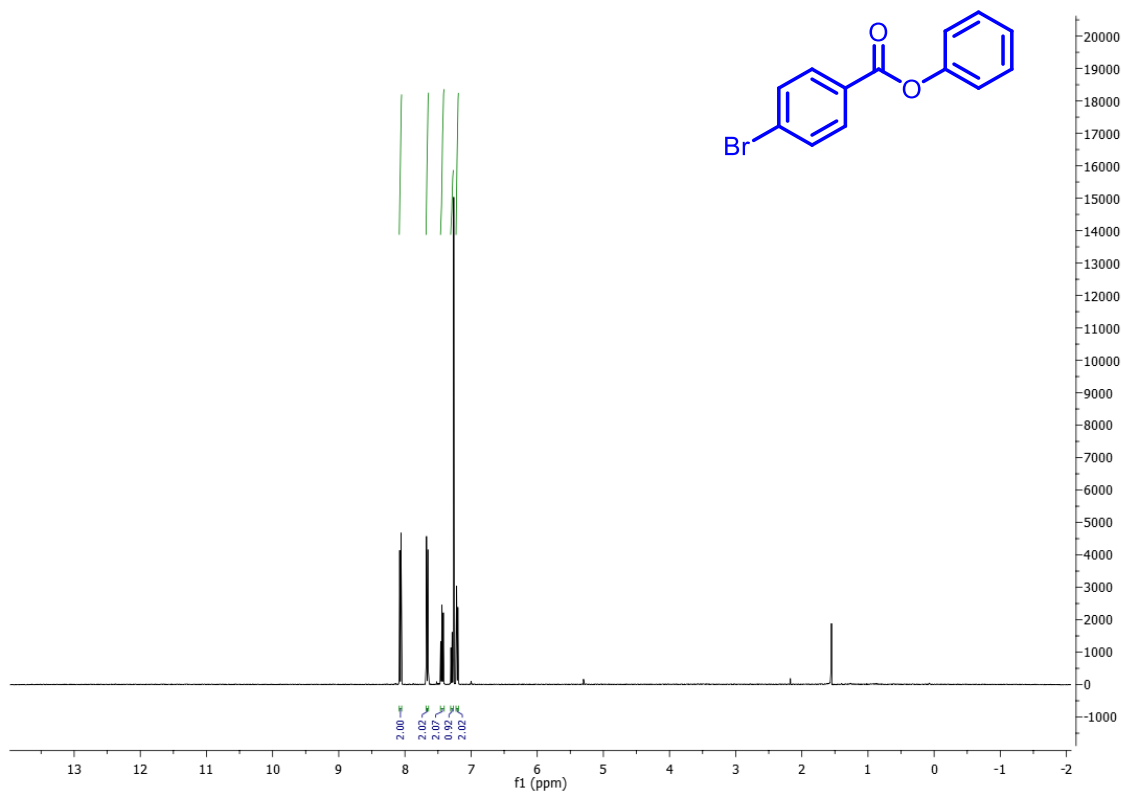
phenyl 3-(pivaloyloxy)benzoate (**68.4W**). CDCl₃, 400 MHz:

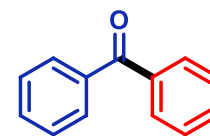


phenyl 3-(benzyl(tert-butoxycarbonyl)carbamoyl)benzoate (**67.3**). CDCl₃, 400 MHz:

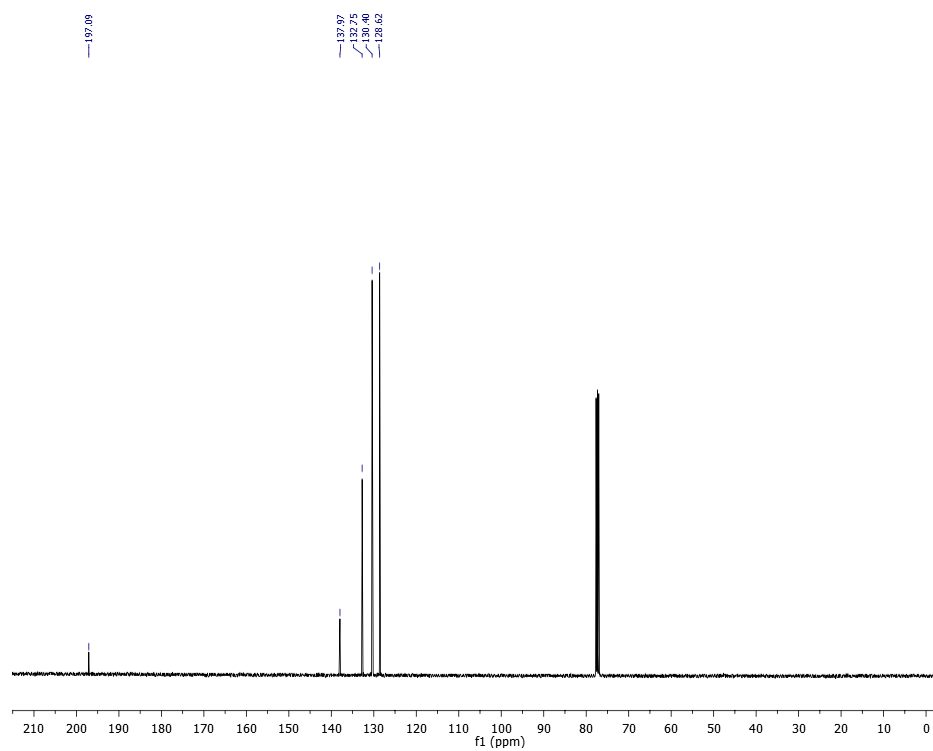
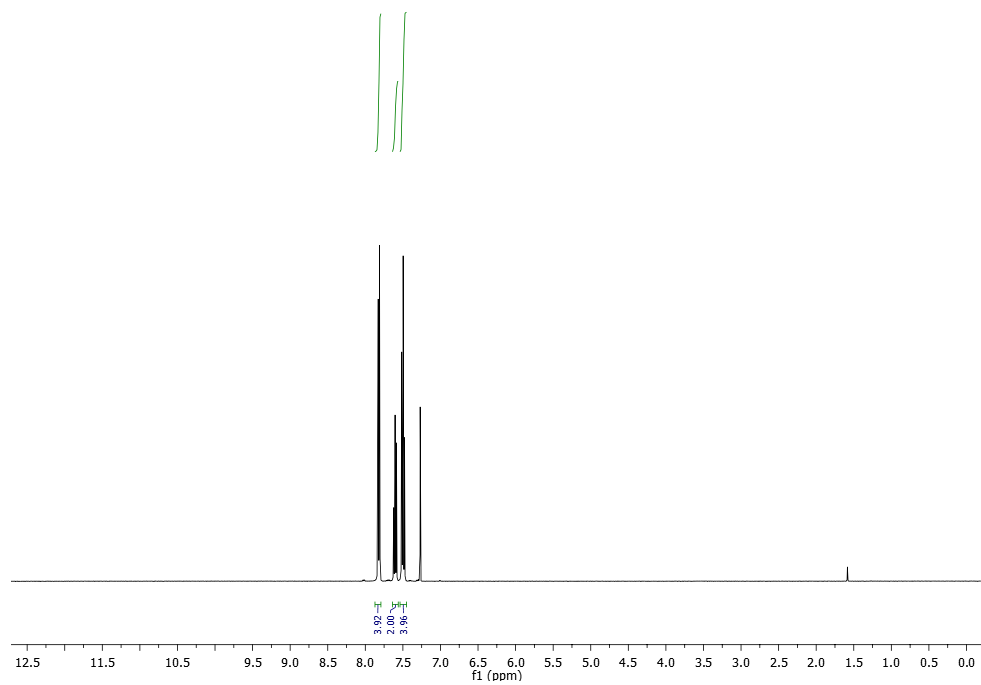


phenyl 4-bromobenzoate (**68.4S**) . CDCl₃, 400 MHz:

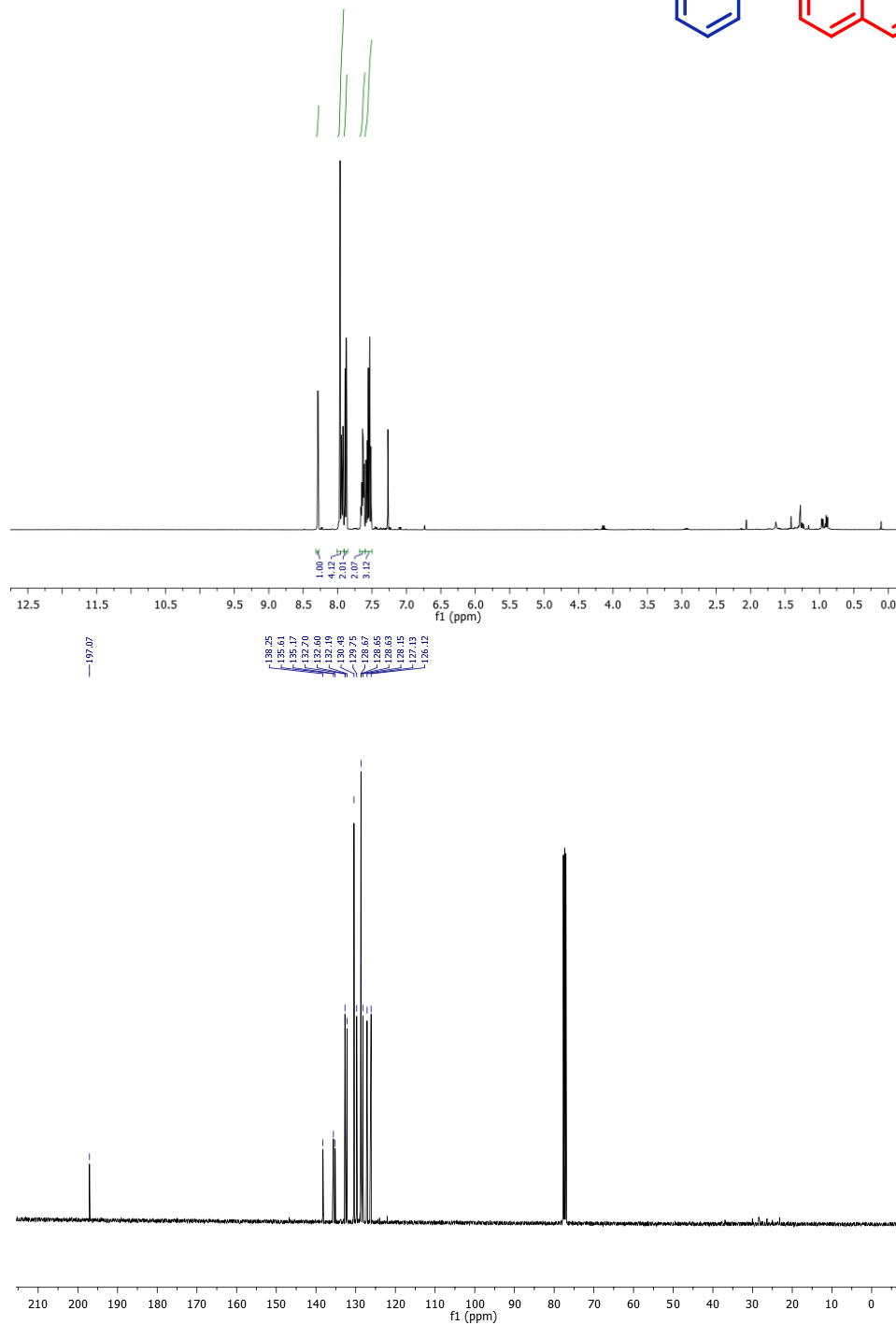
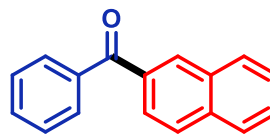




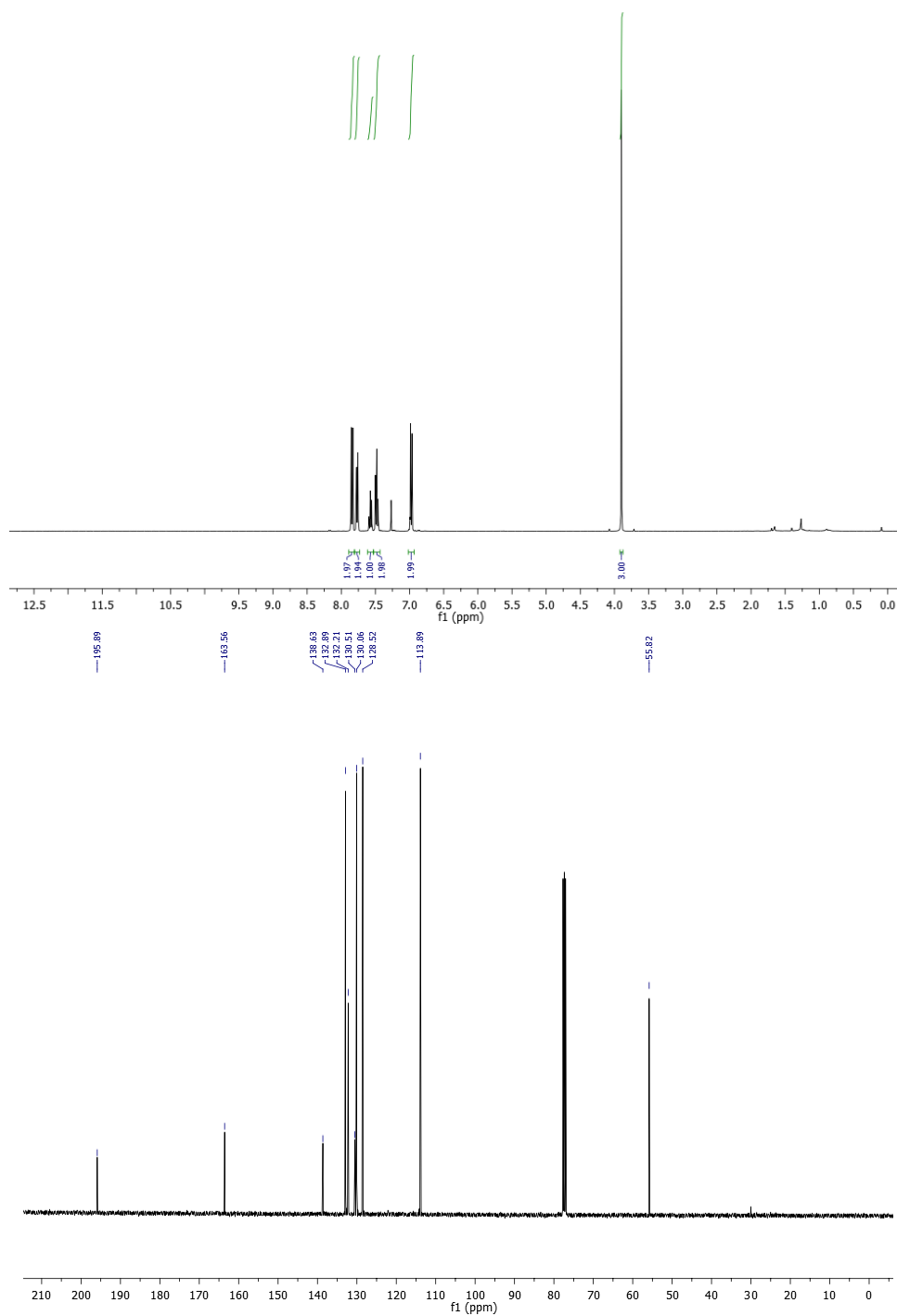
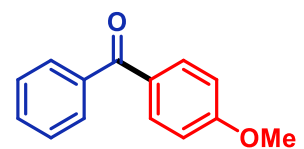
benzophenone (**68.6Aa**). CDCl₃, 400 MHz:



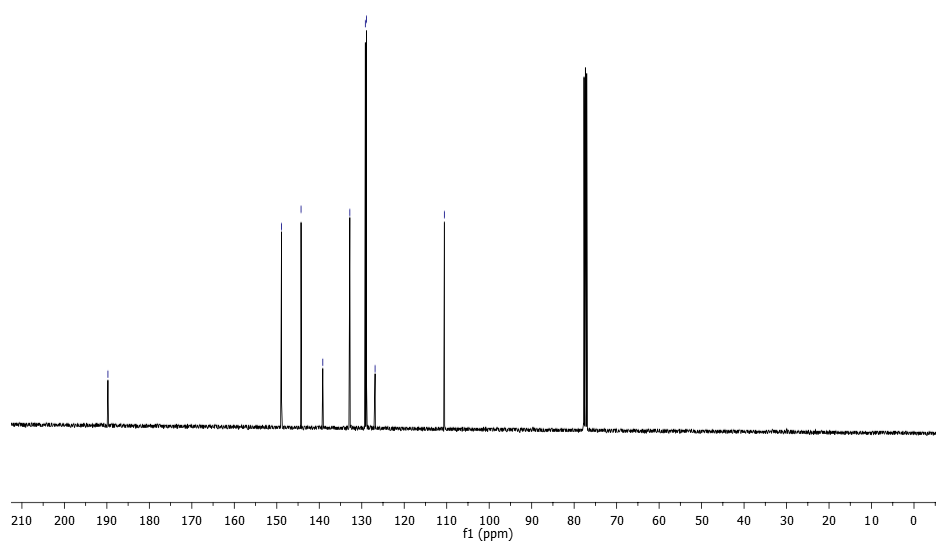
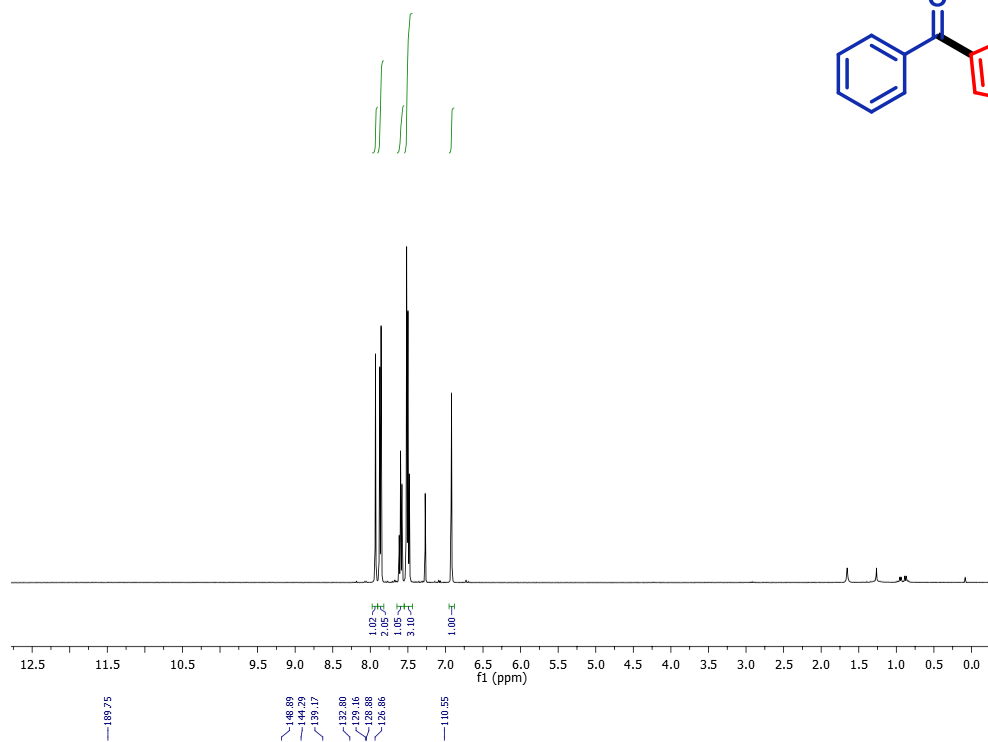
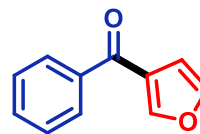
naphthalen-2-yl(phenyl) methanone (**68.6Ab**). CDCl_3 , 400 MHz:

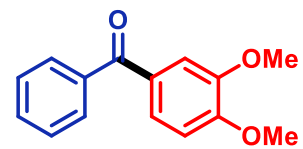


4-methoxyphenyl-(phenyl) methanone (**68.6Ac**). CDCl_3 , 400 MHz:

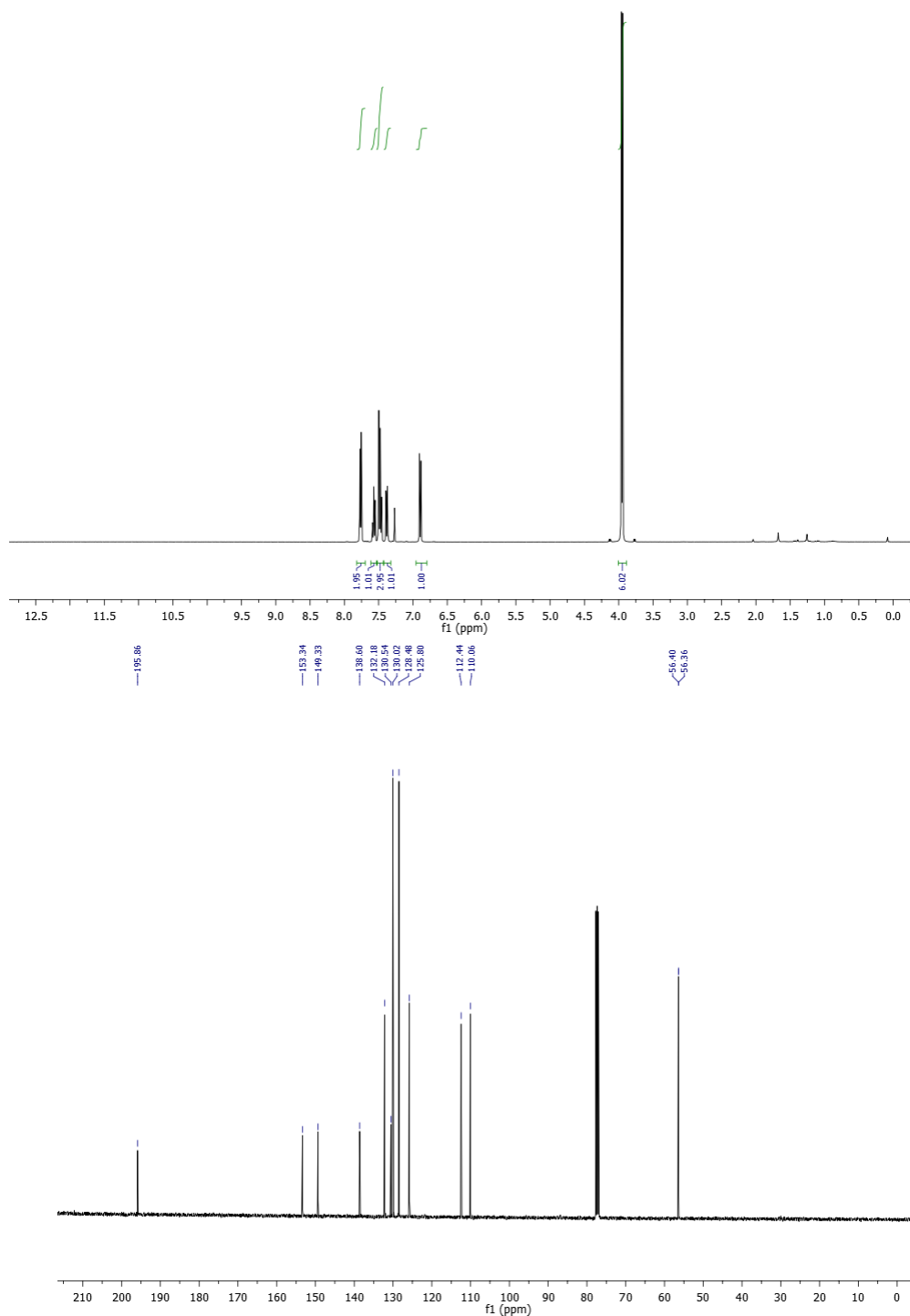


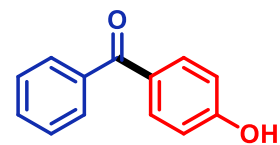
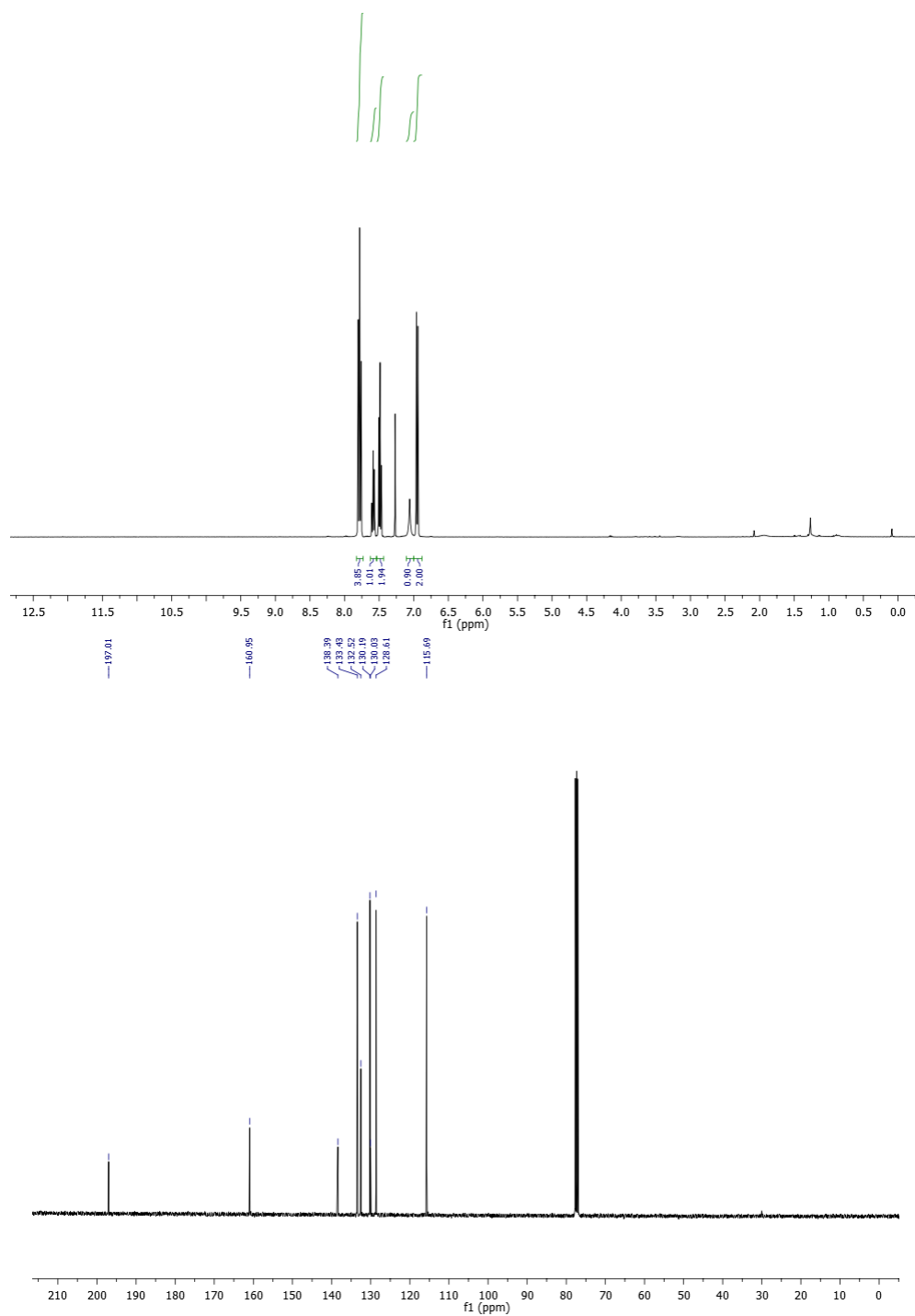
furan-2-yl(phenyl)methanone (**68.6Ad**). CDCl₃, 400 MHz:

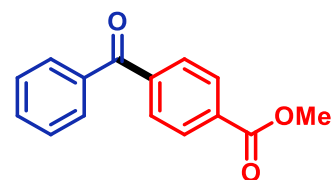




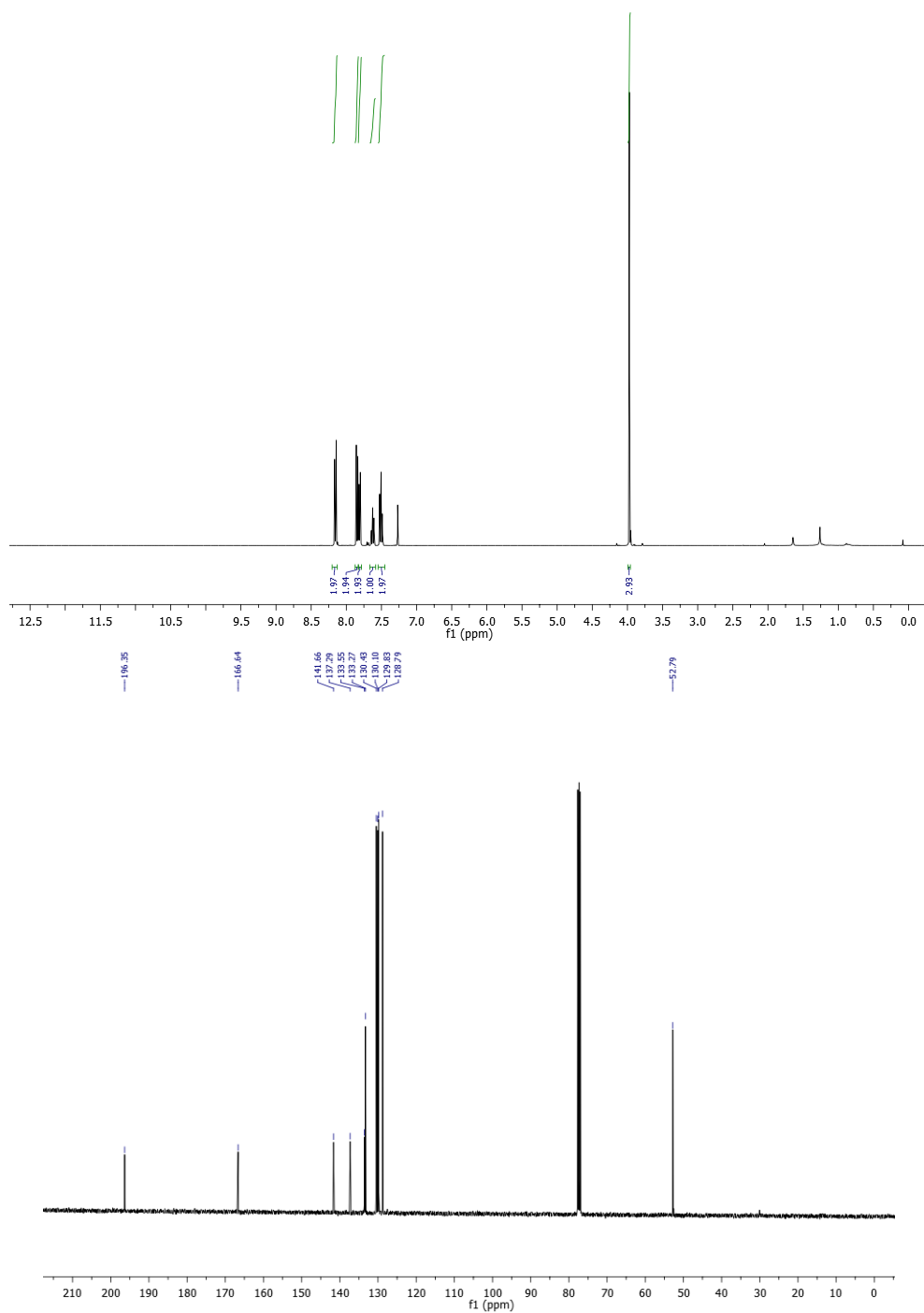
3,4-dimethoxy benzophenone (**68.6Ae**). CDCl_3 , 400 MHz:

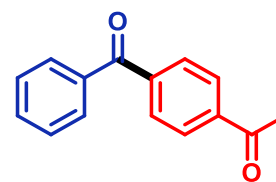


4-hydroxybenzophenone (**68.6Af**). CDCl₃, 400 MHz:

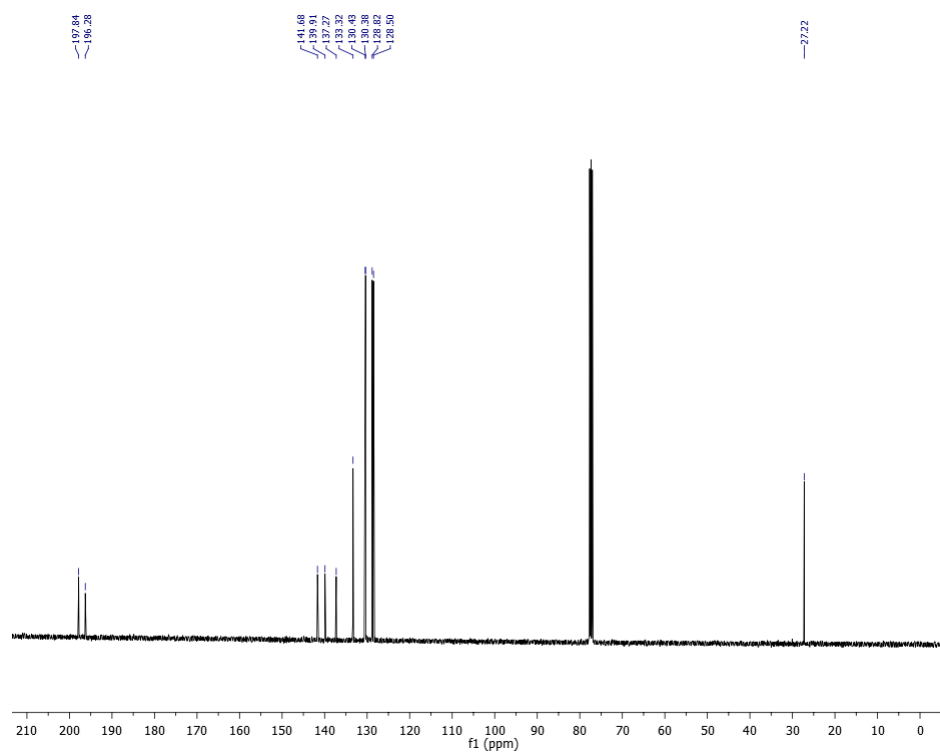
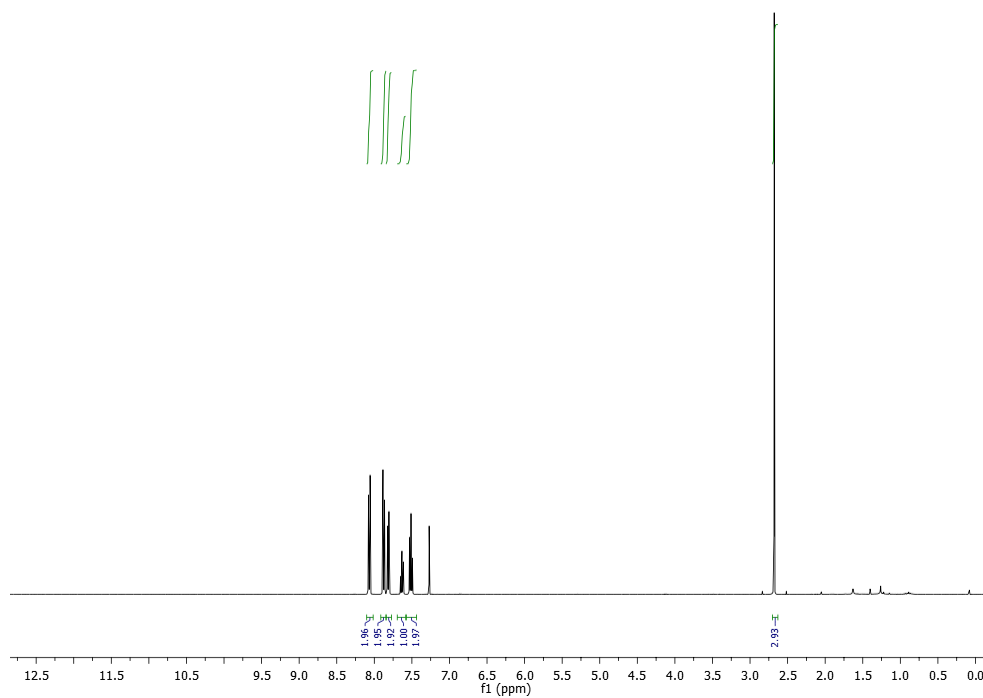


methyl 4-benzoylbenzoate (**68.6Ag**). CDCl_3 , 400 MHz:

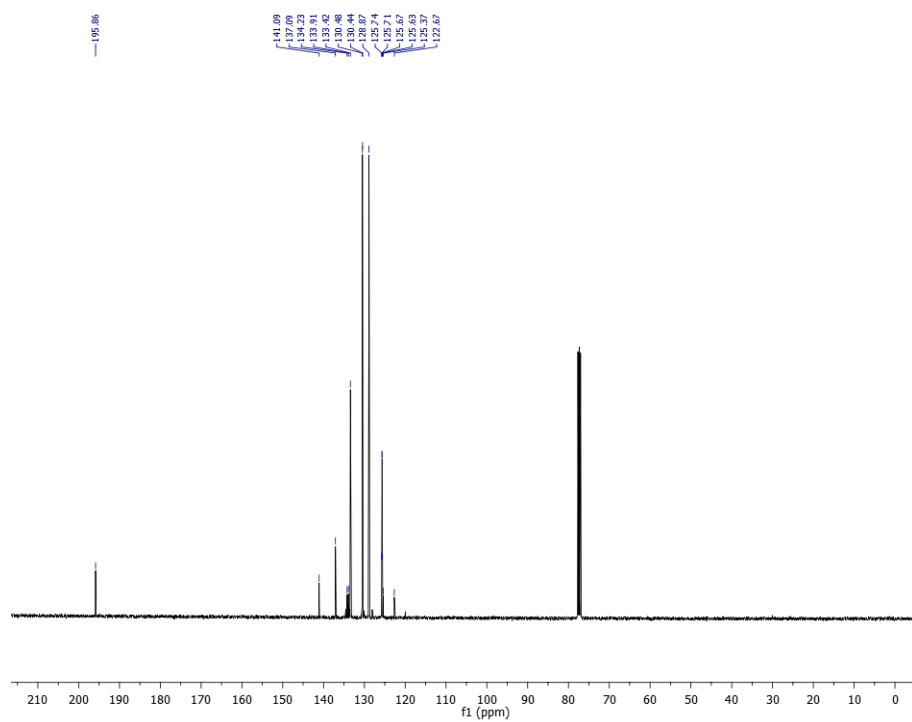
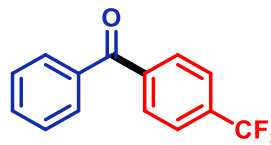
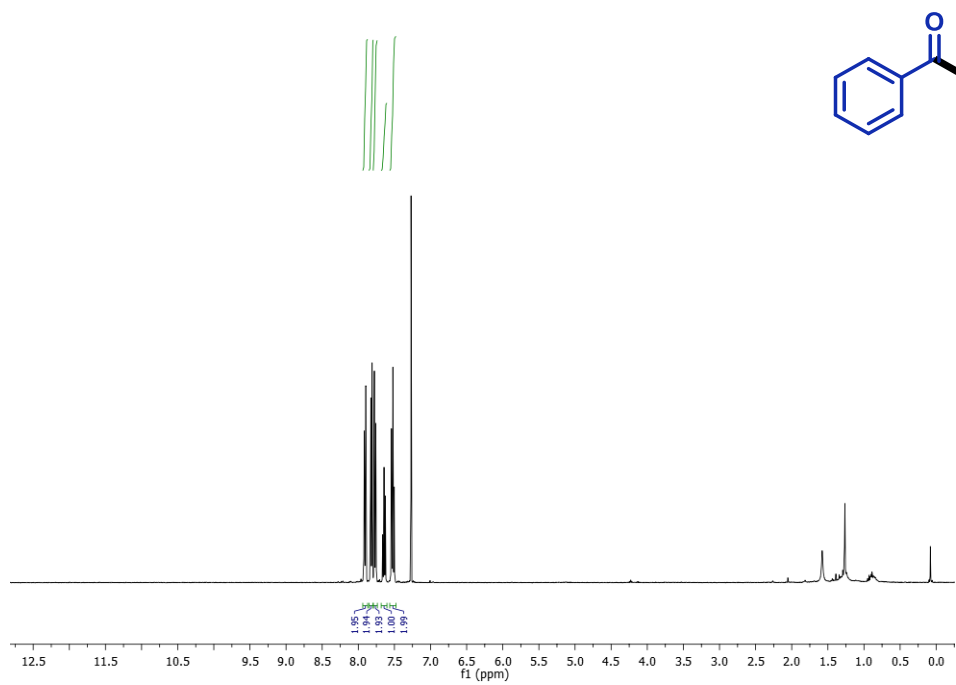




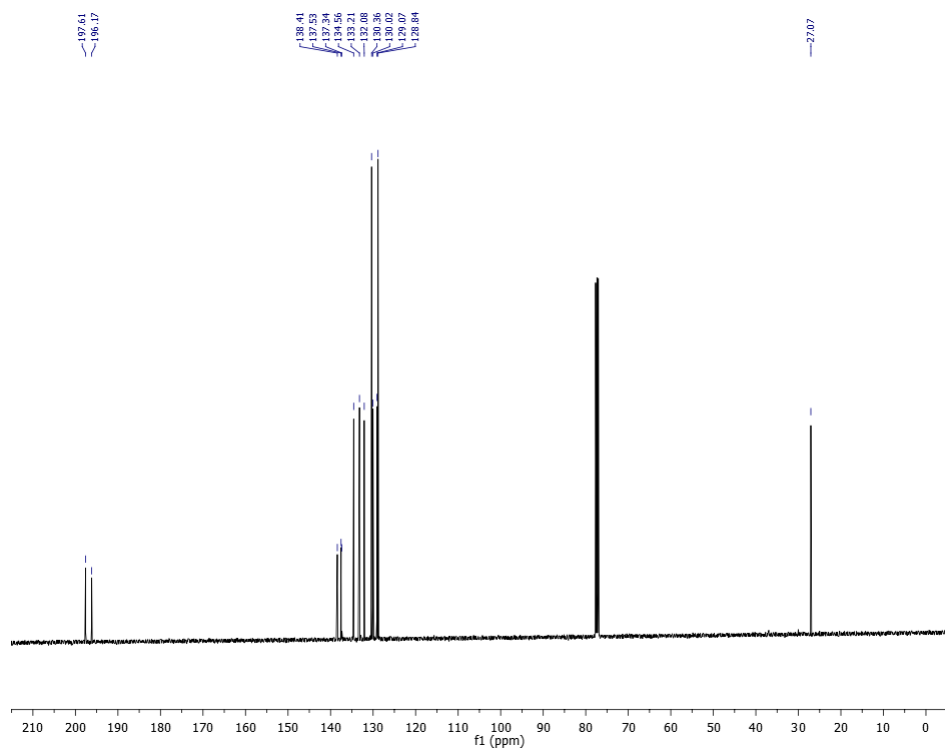
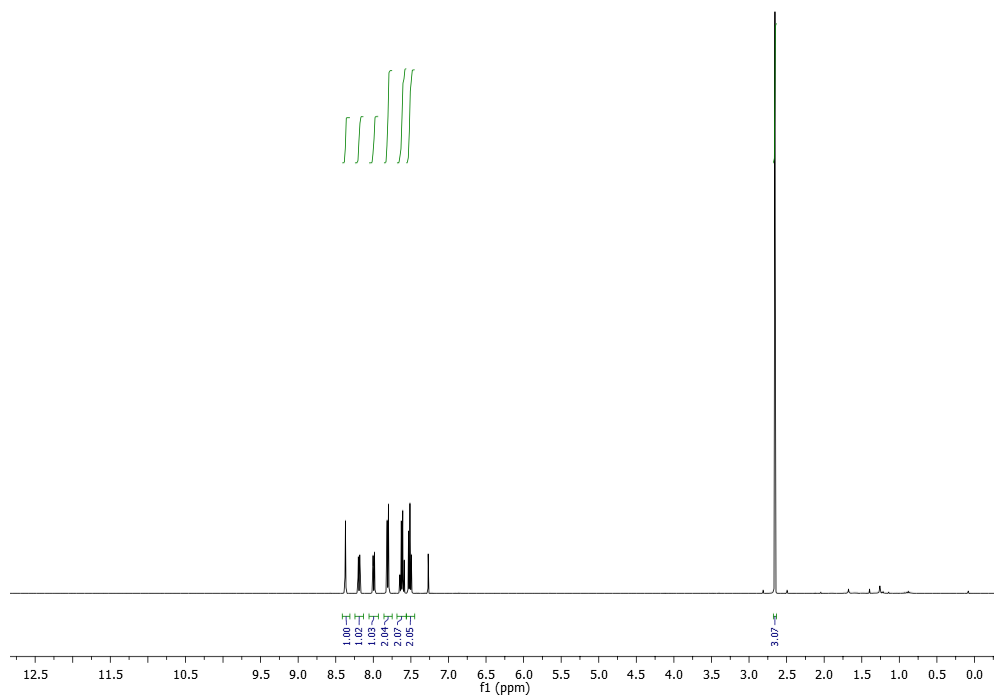
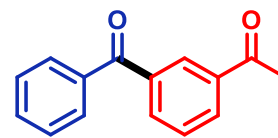
methyl 3-benzoylbenzoate (**68.6Ah**). CDCl₃, 400 MHz:

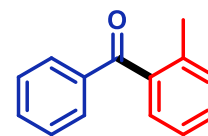


phenyl (4-trifluoromethyl)phenyl methanone (**68.6Ai**). CDCl₃, 400 MHz:

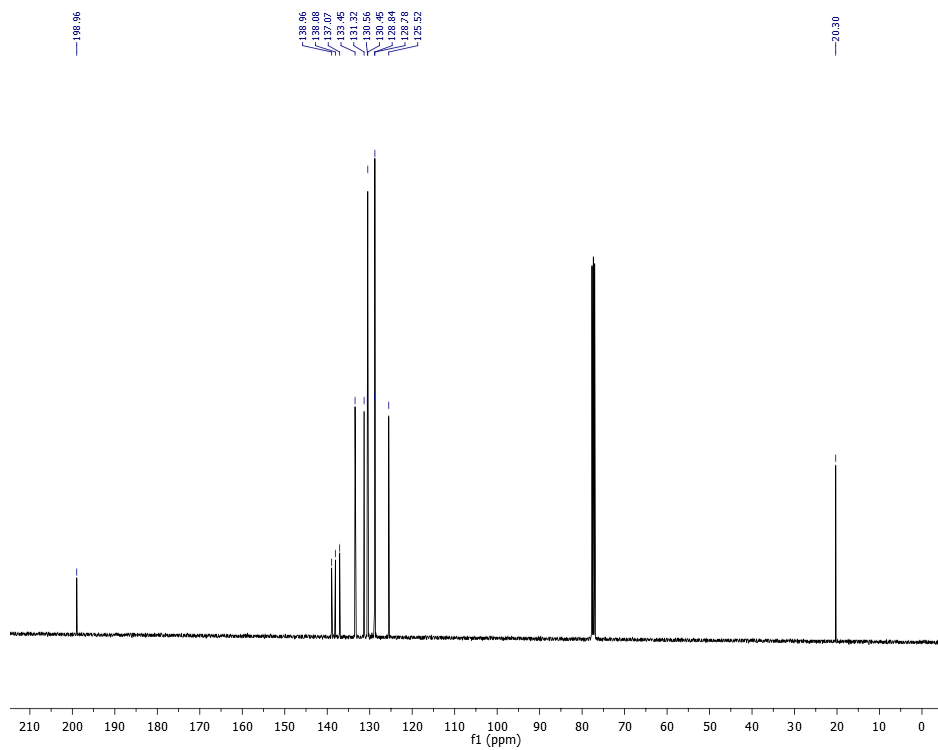
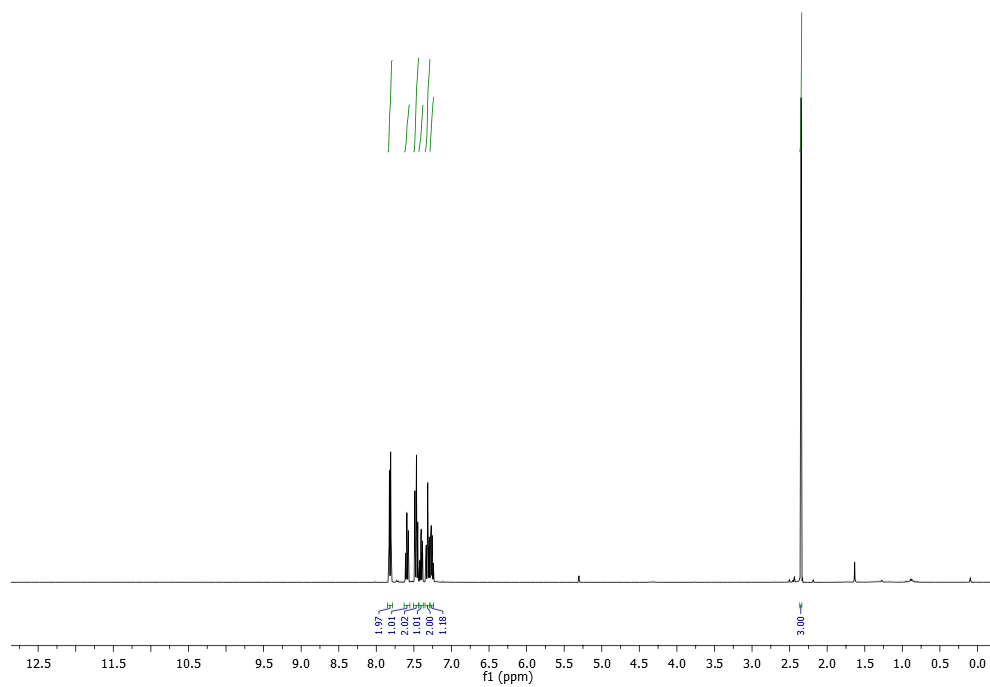


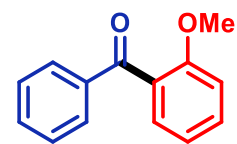
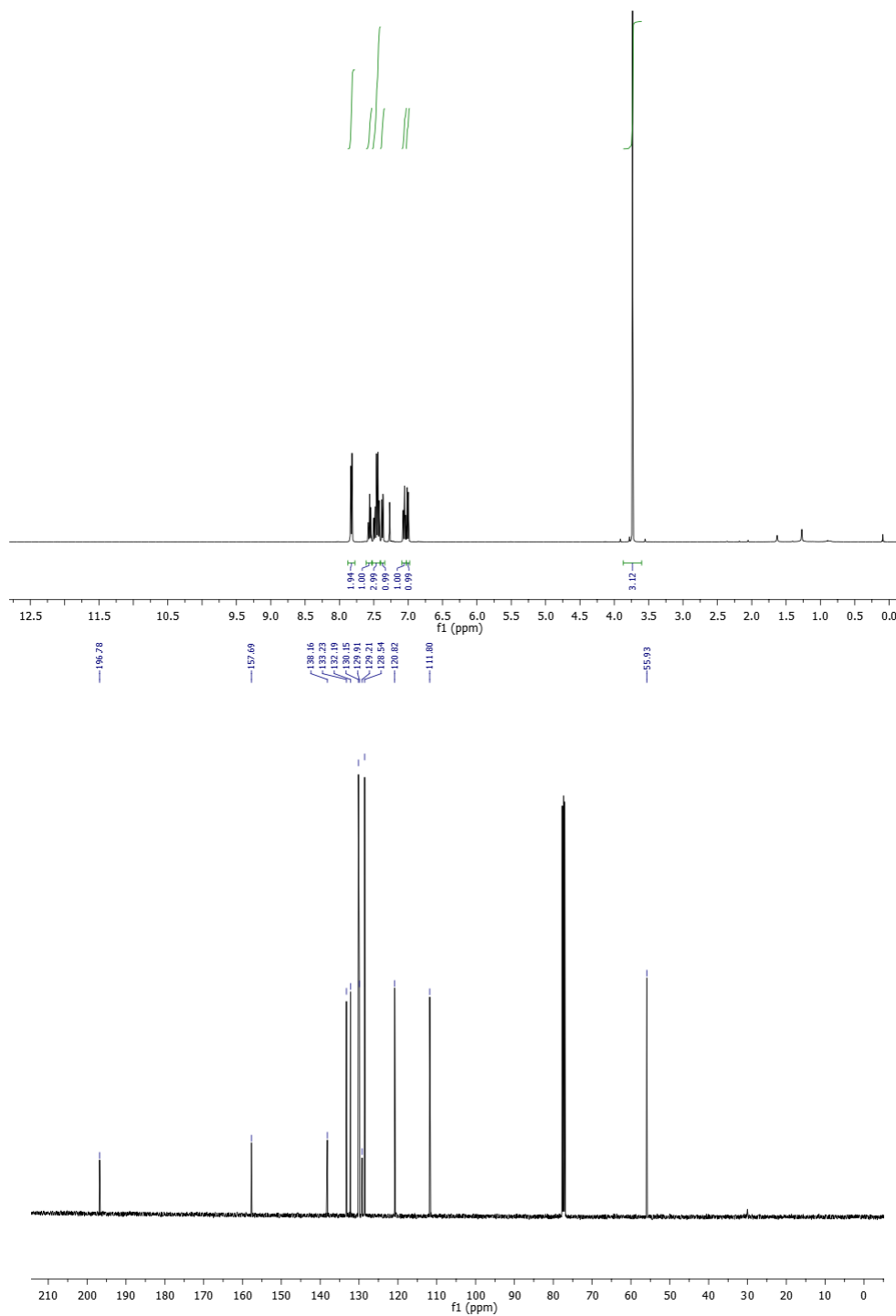
3-acetylphenyl-(phenyl) methanone (**68.6A_j**).CDCl₃, 400 MHz:



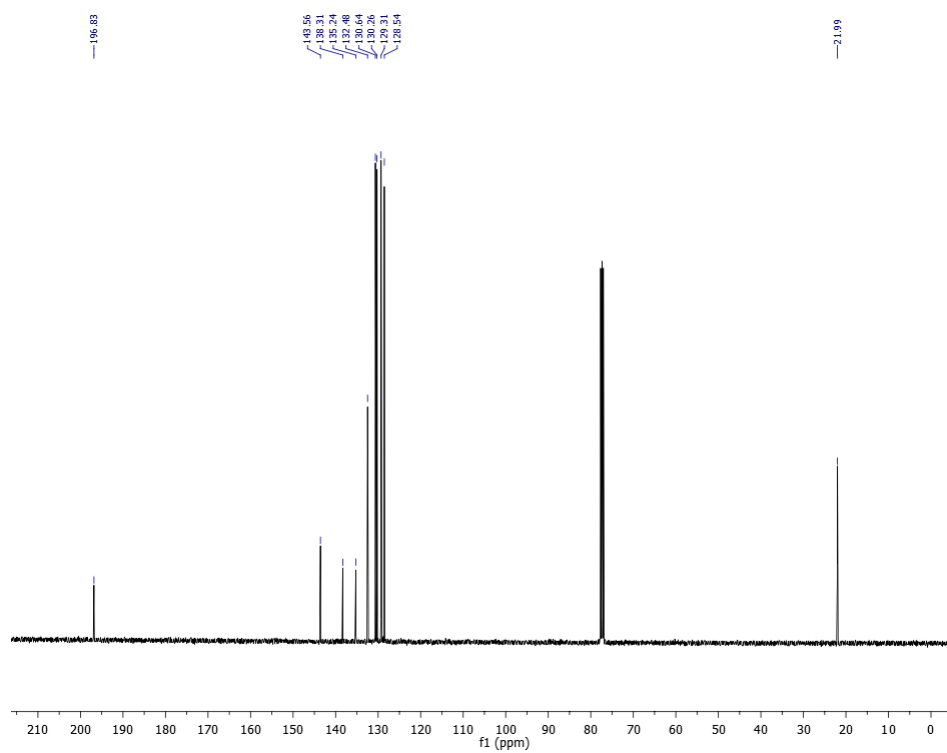
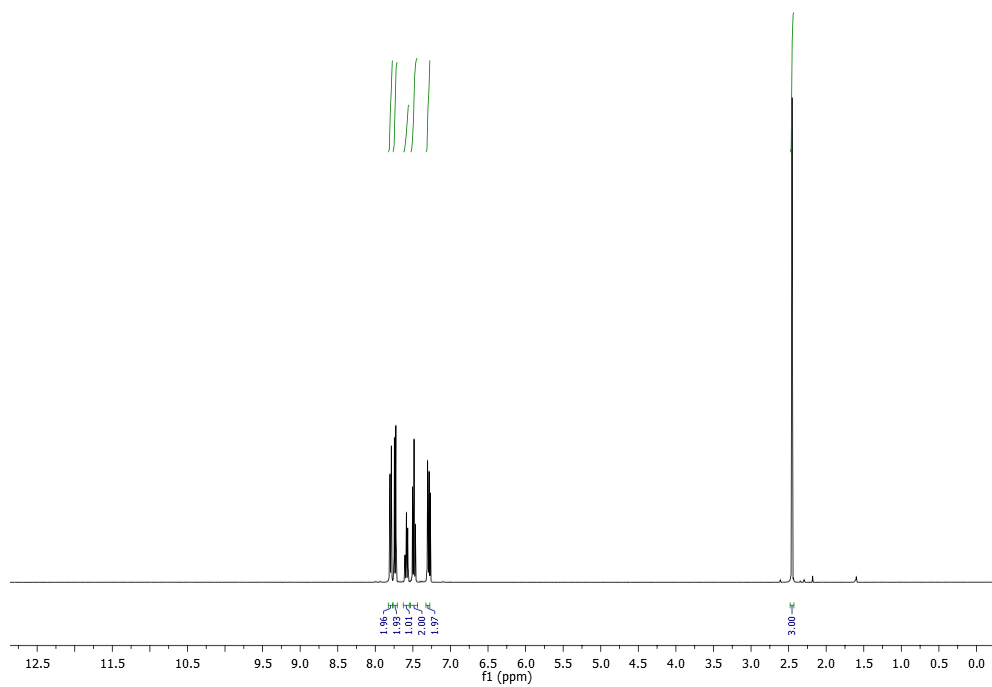
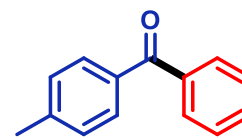


phenyl(o-tolyl) methanone (**68.6Ak**). CDCl₃, 400 MHz:

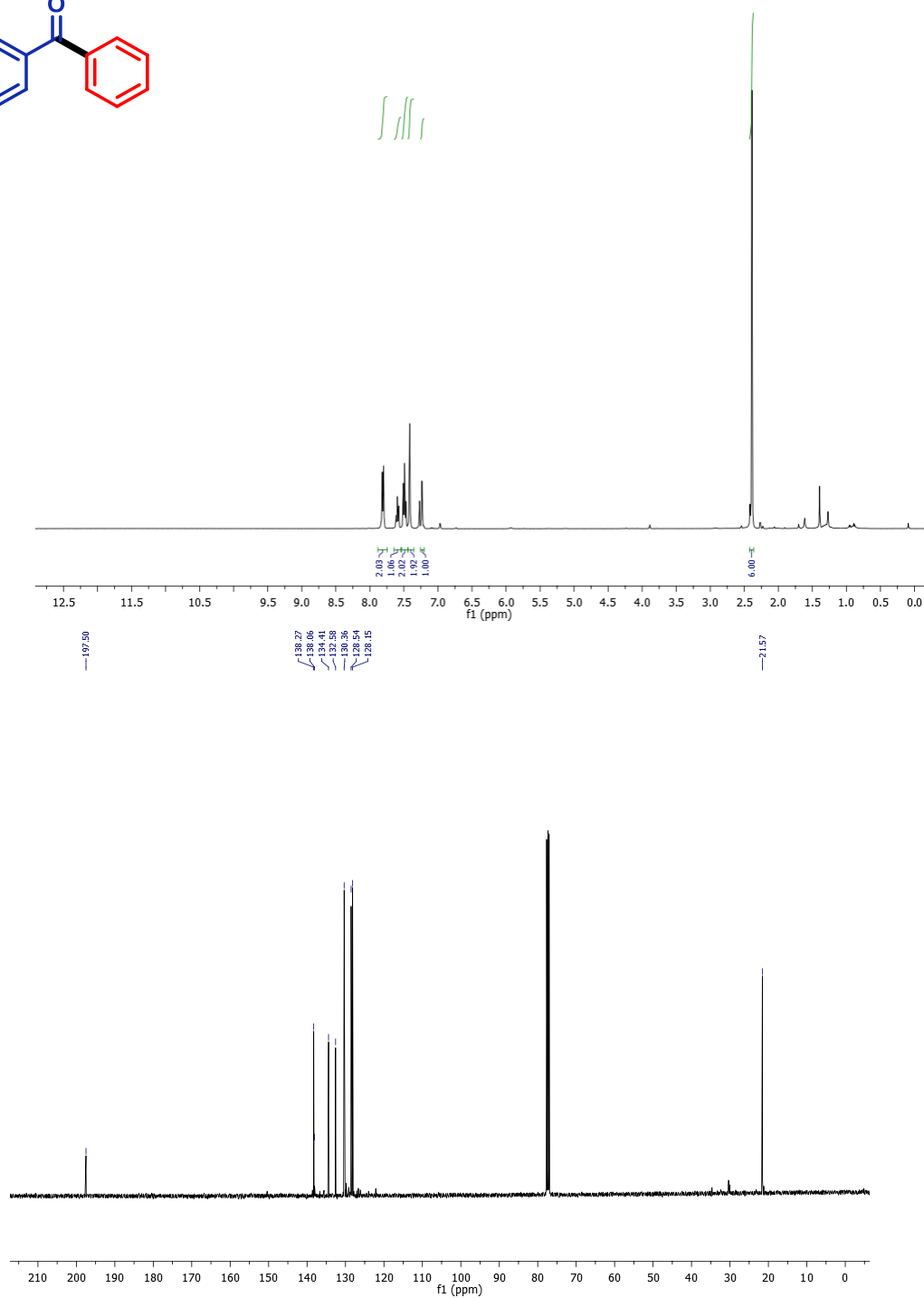
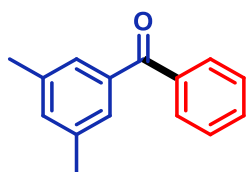


2-methoxy(Phenyl)phenyl methanone (**68.6A1**). CDCl₃, 400 MHz:

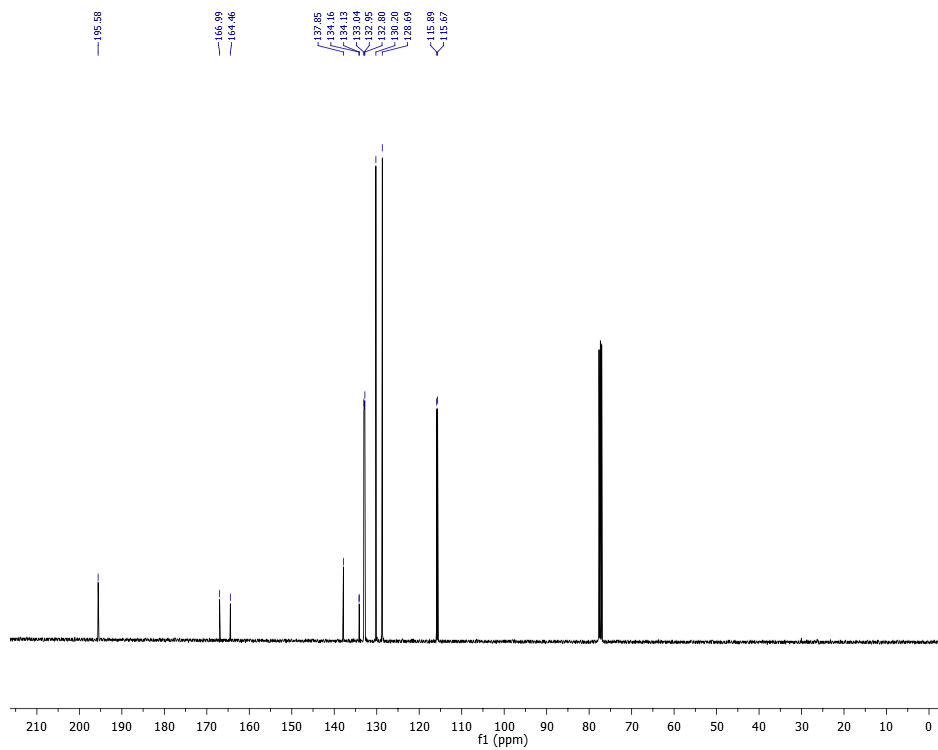
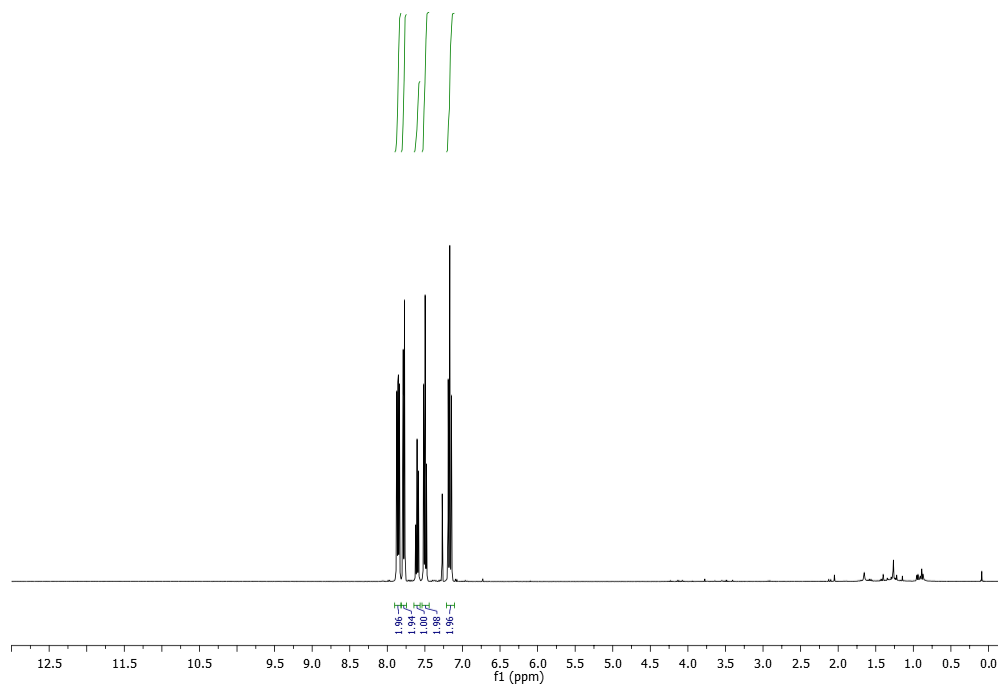
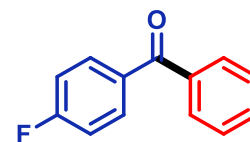
phenyl (p-tolyl) methanone (**68.6Ca**). CDCl₃, 400 MHz:



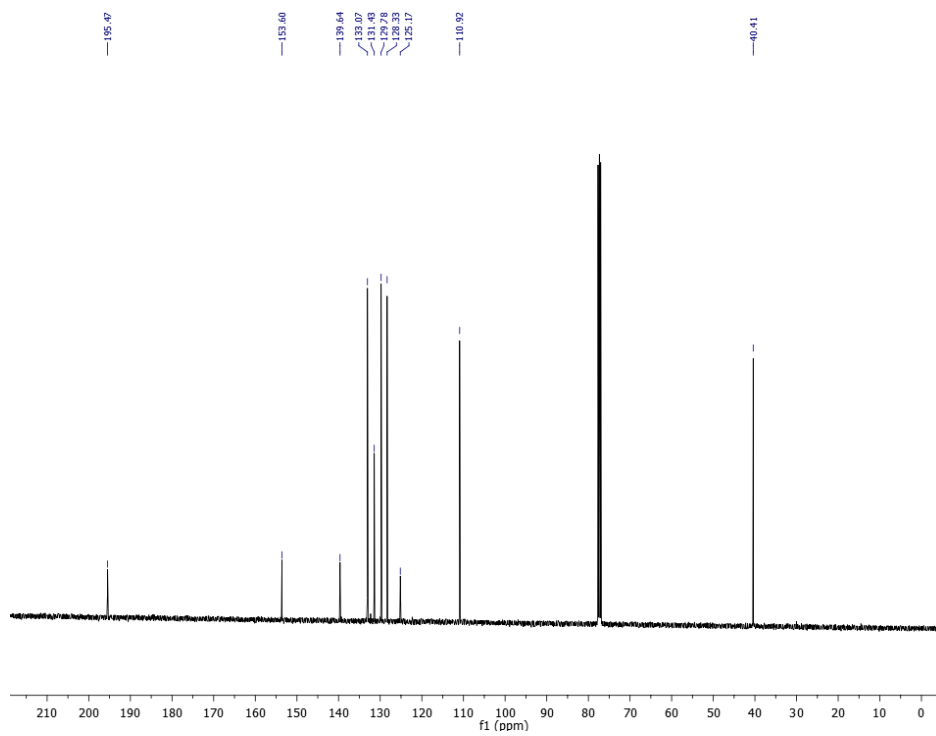
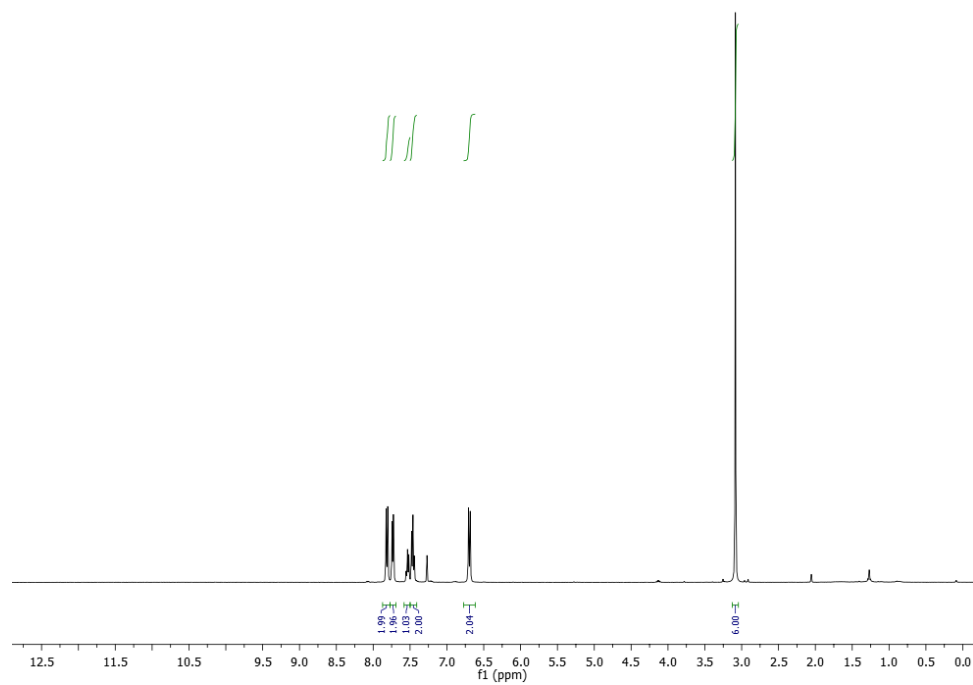
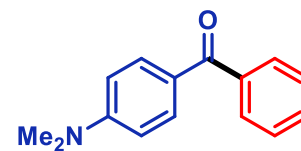
3,5-dimethyl(phenyl) phenyl methanone (**68.6Da**). CDCl₃, 400MHz:

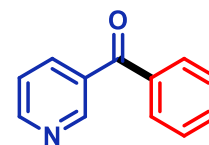
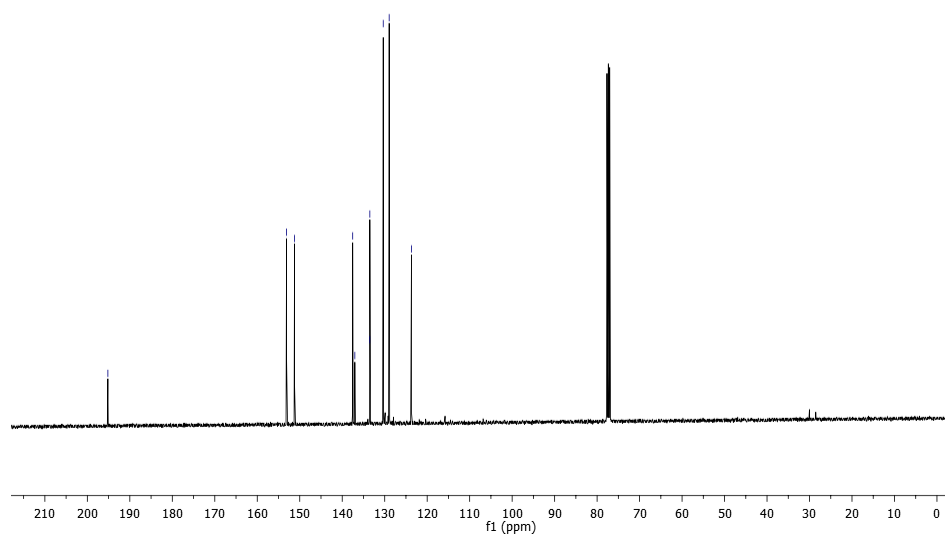
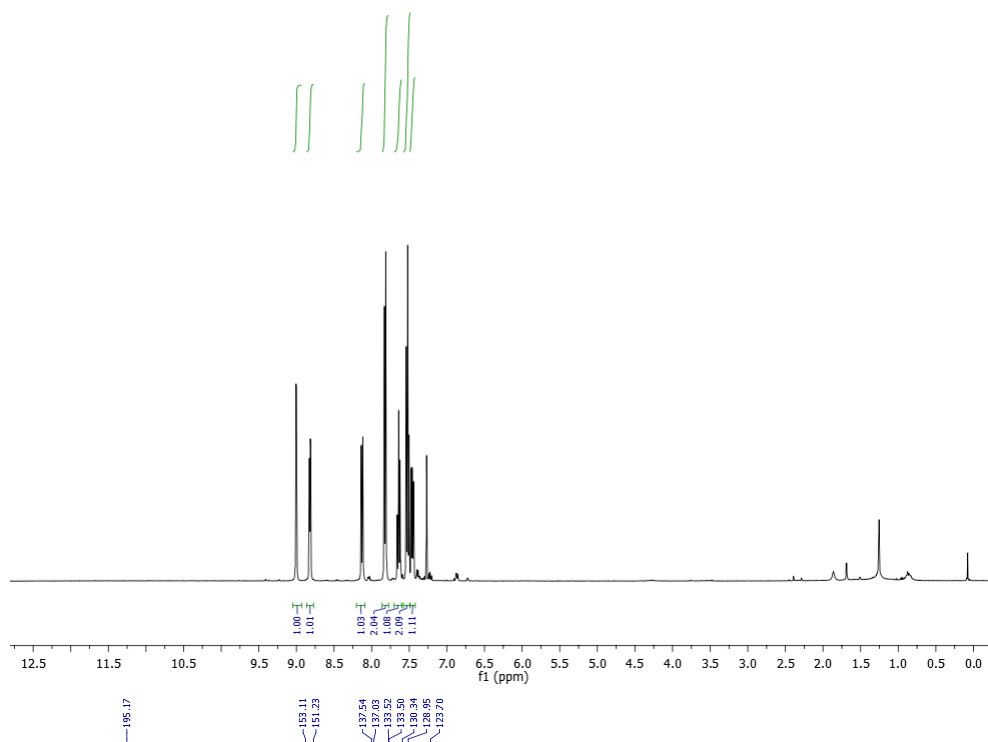


4-fluorophenyl-(phenyl)methanone (**68.6Ea**). CDCl₃, 400 MHz:

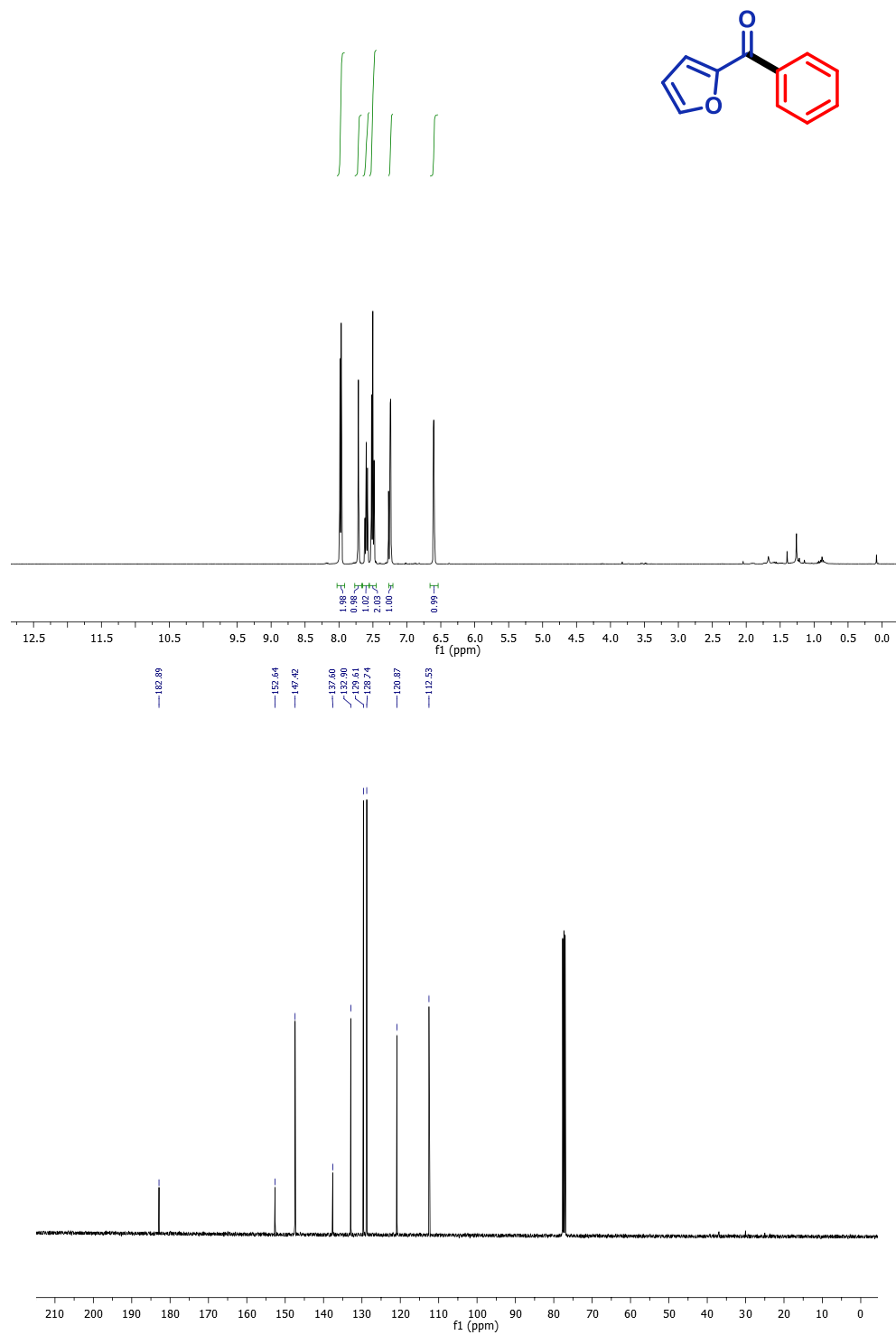


4-(N,N-dimethylamino)benzophenone (**68.61a**).CDCl₃, 400 MHz:

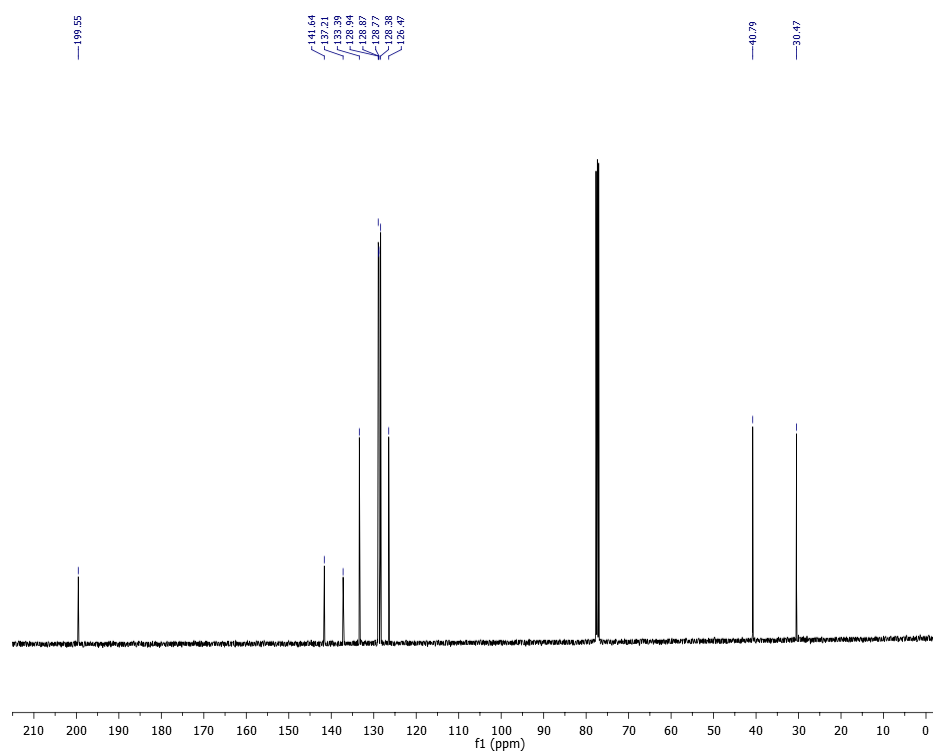
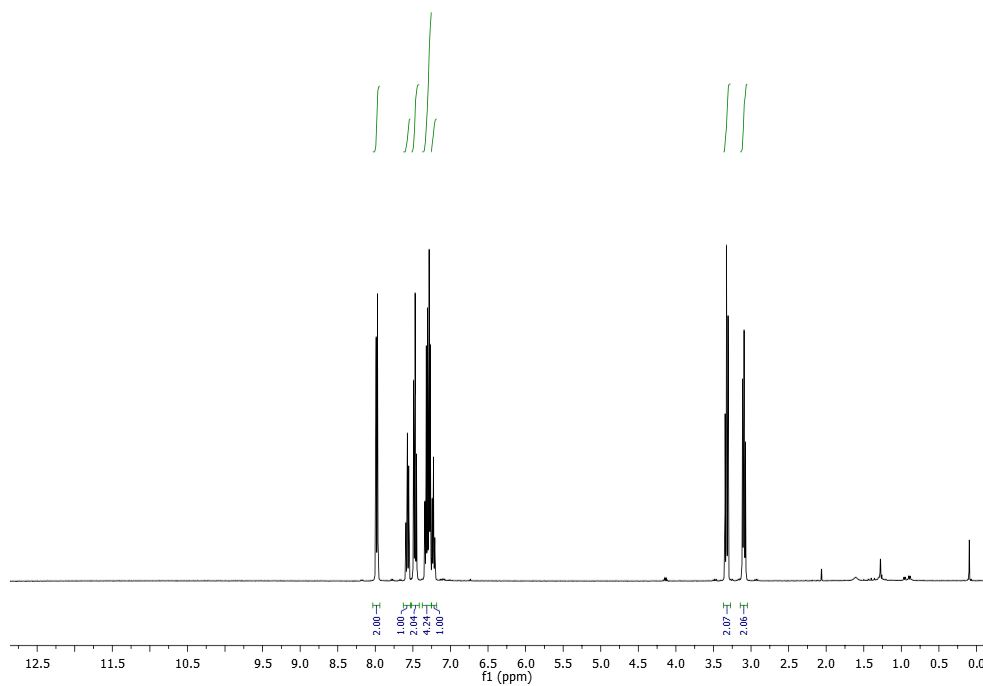
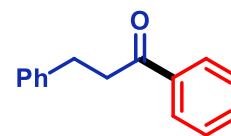


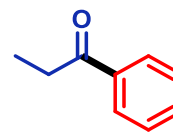
3-benzoyl pyridine (**68.6Ja**). CDCl₃, 400 MHz:

furan-3-yl(phenyl) methanone (**68.6Ka**). CDCl₃, 400 MHz:

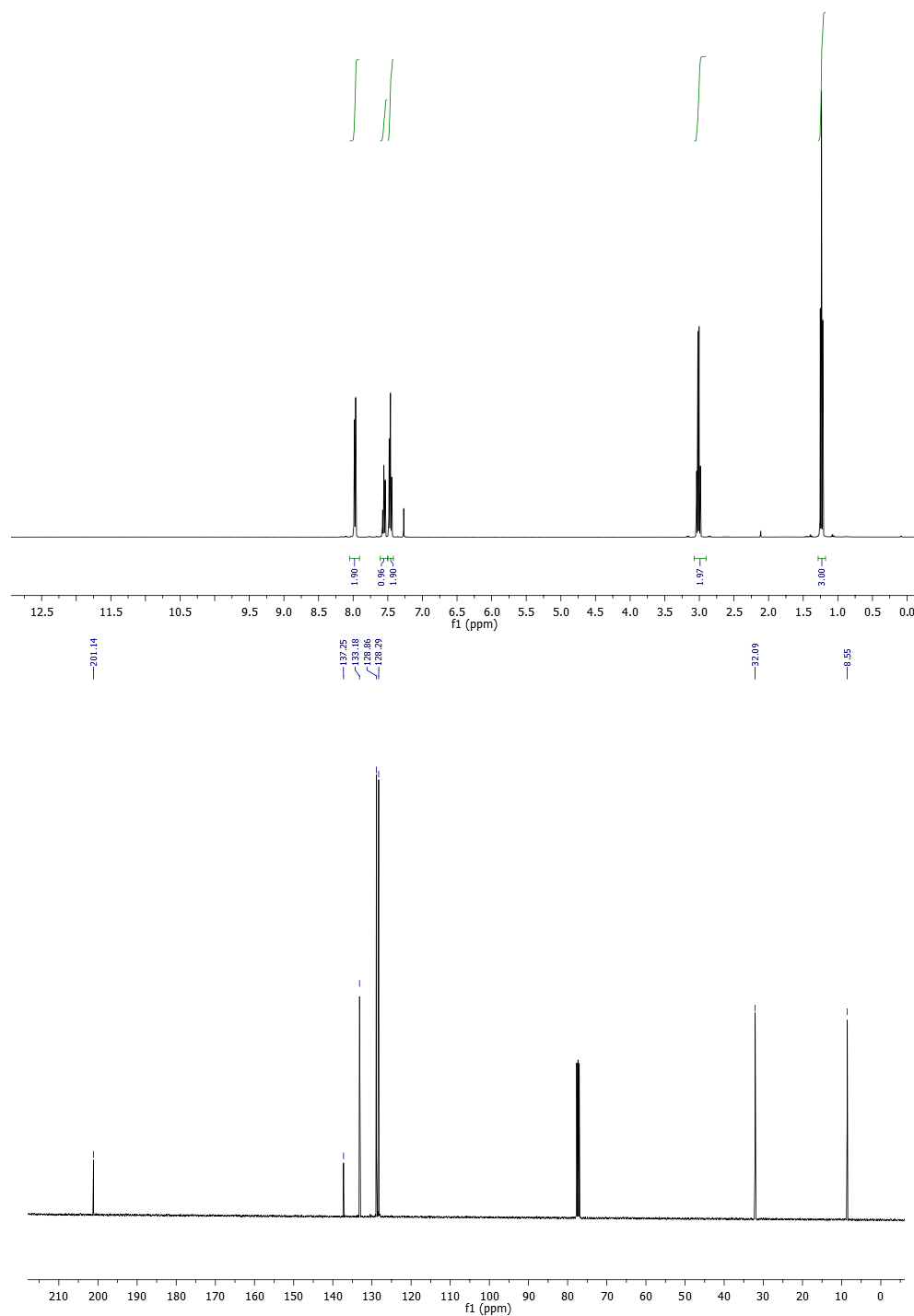


1,3-diphenylpropan-1-one (**68.6Na**). CDCl₃, 400 MHz:

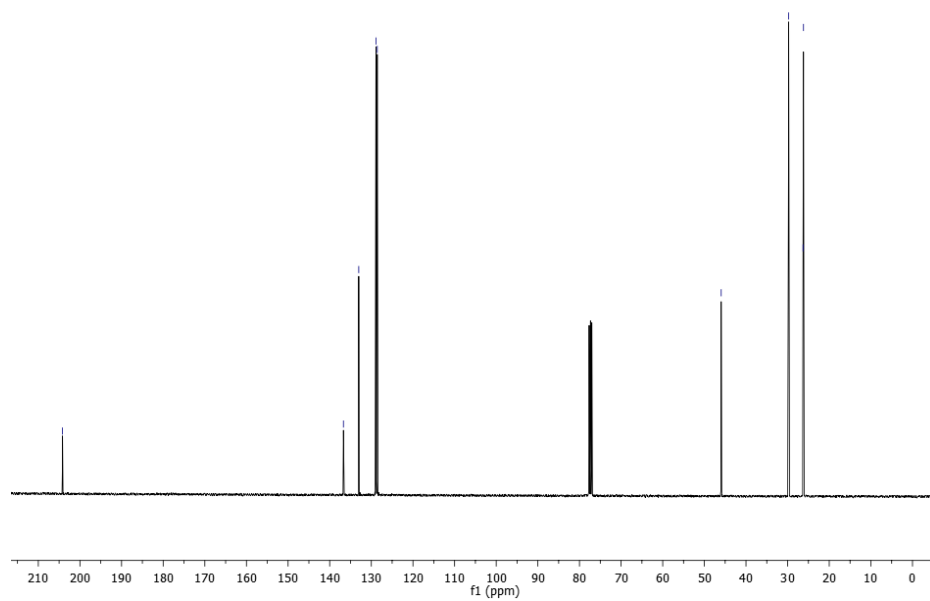
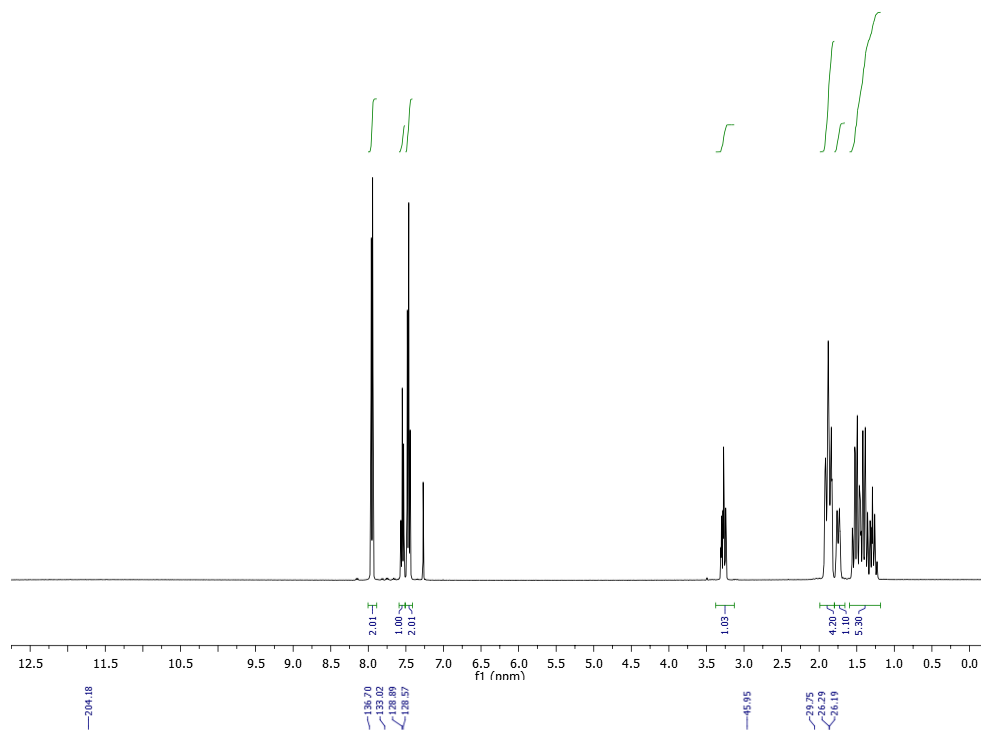
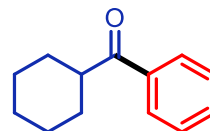




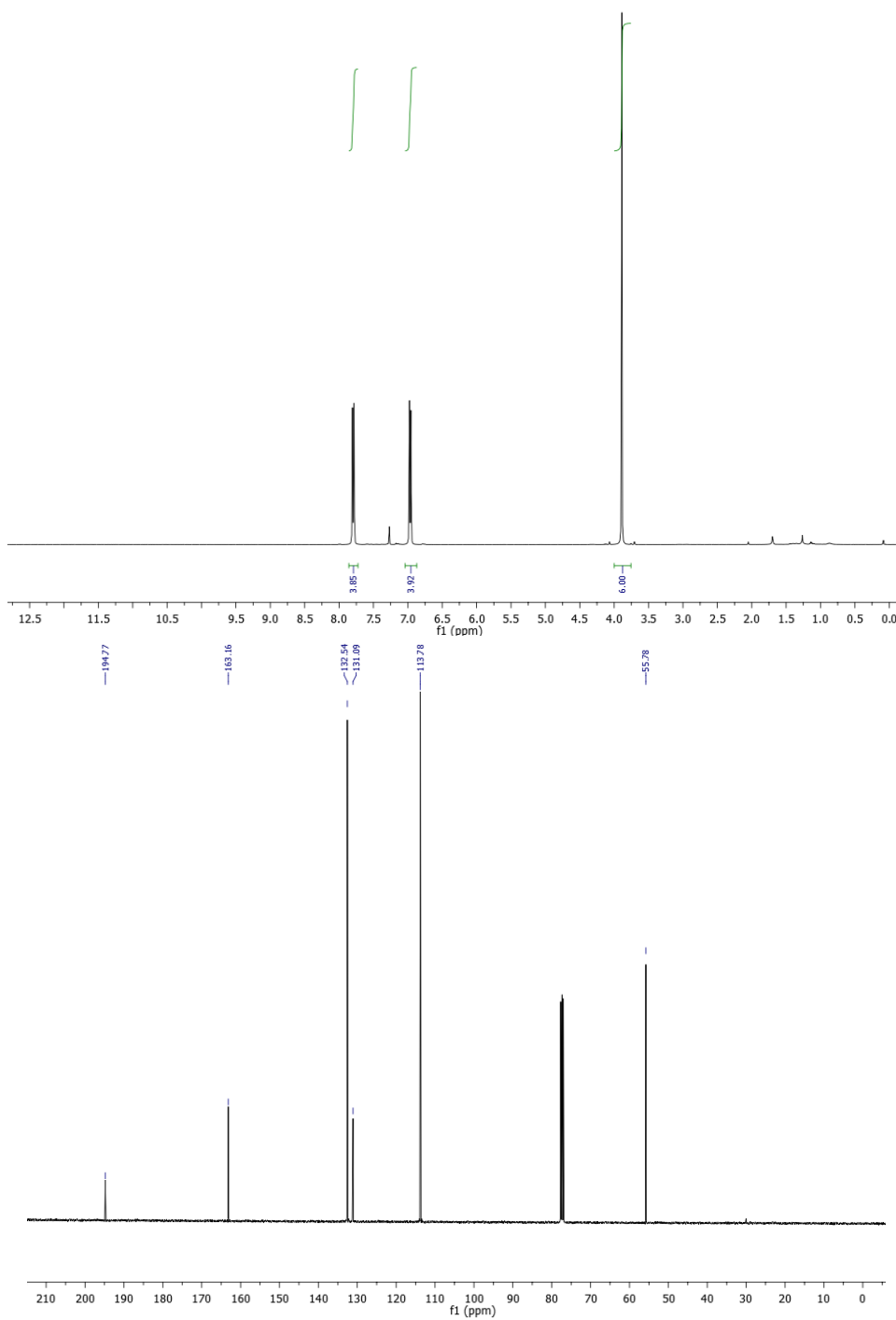
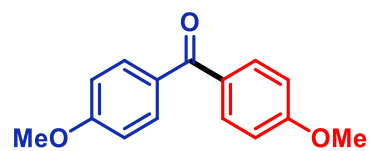
propiophenone (**68.60a**). CDCl₃, 400 MHz:



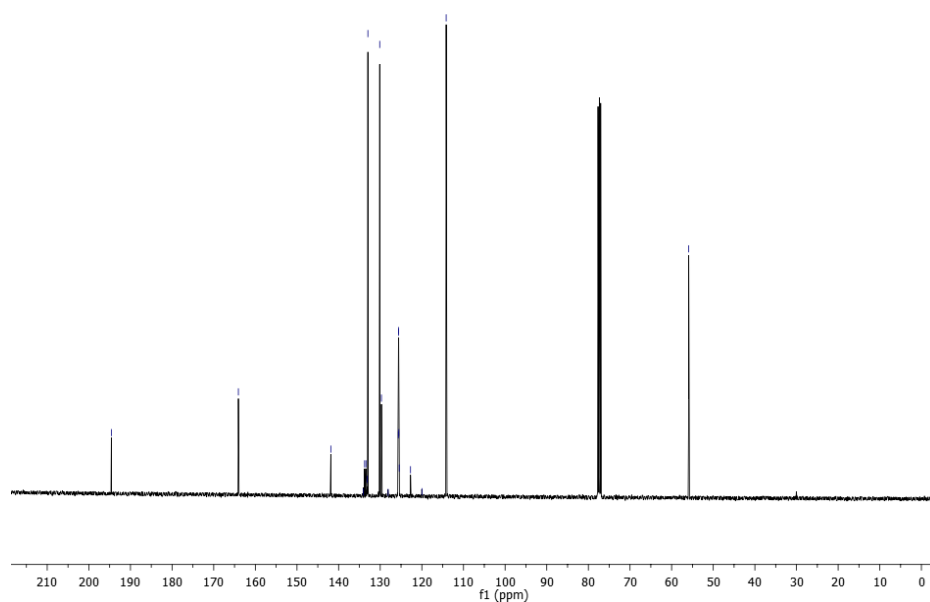
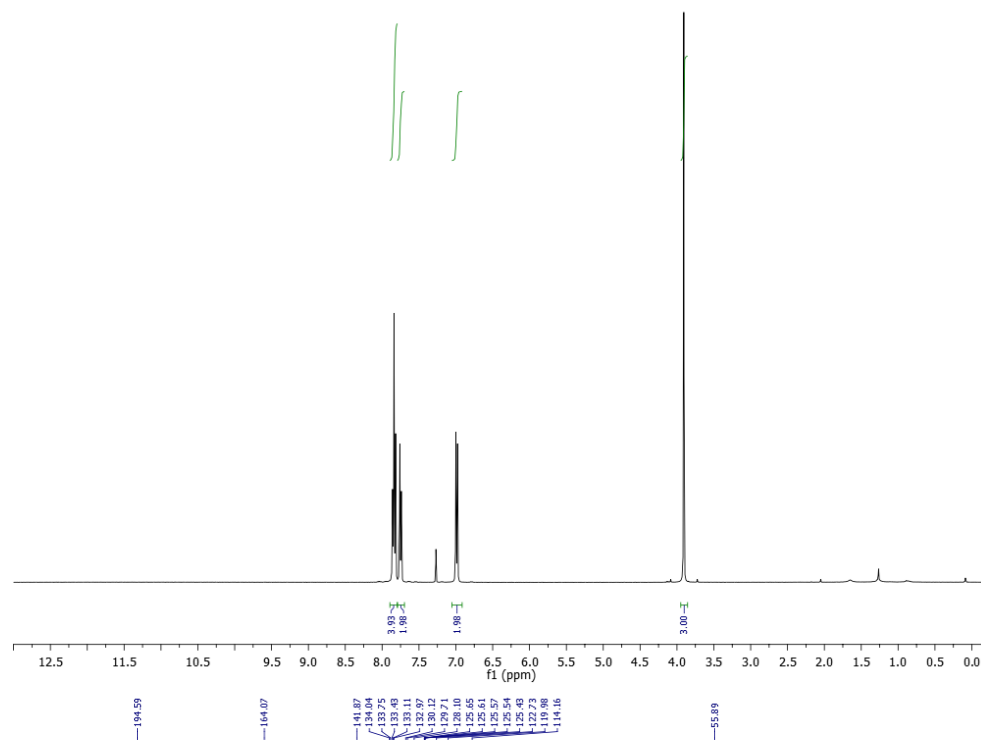
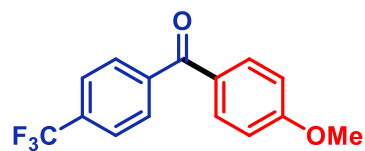
cyclohexyl phenyl methanone (**68.6Pa**). CDCl_3 , 400 MHz:



bis(4-methoxyphenyl)methanone (**68.6Fe**). CDCl₃, 400MHz:



4-methoxyphenyl-(4-(trifluoromethyl)phenyl)methanone (**68.6Ge**). CDCl₃, 400 MHz



bis(4-trifluoromethyl)(phenyl)methanone (**68.6Gi**). CDCl_3 , 400MHz:

